KEEPING THE RHYTHM

–

Cardiac Pacemaker Cell Development

Silja Barbara Burkhard

Cover design by Silja Burkhard. “Cardiac Puppeteer“ - A paper model of a human heart built with instructions from http://torso.amorphous-constructions.com. Photographed by Ina Pohl.

The research presented in this thesis was performed at the Hubrecht Institute, part of the Royal Academy of Arts and Sciences (KNAW), within the framework of the Graduate School of Life Sciences Cancer, Stem Cells and Developmental Biology (CSnD) programme of Utrecht University.

The research described in this thesis was supported by a personal grant from the Netherlands Organisation for Scientific Research (NWO), CGDB Graduate programme 022.001.003.

ISBN: 978-90-393-6892-3

Printed by Gildeprint Drukkerijen, Enschede

KEEPING THE RHYTHM

–

Cardiac pacemaker cell development

In het ritme blijven – Ontwikkeling van pacemakercellen in het hart
(met een samenvatting in het Nederlands)

Im Rhythmus bleiben – Entwicklung der Herzschrittmacherzellen
(mit einer Zusammenfassung in deutscher Sprache)

Proefschrift

ter verkrijging van de graad van doctor aan de Universiteit Utrecht
op gezag van de rector magnificus, prof.dr. G.J. van der Zwaan,
ingevolge het besluit van het college voor promoties
in het openbaar te verdedigen op

dinsdag 28 november 2017
des middags te 12.45 uur

door

Silja Barbara Burkhard

geboren op 4 maart 1986 te Mainz, Duitsland

Promotor: Prof. dr. J.P.W.M. Bakkers

This thesis was (partly) accomplished with financial support from the Netherlands Organisation for Scientific Research (Nederlandse Organisatie voor Wetenschappelijk Onderzoek, NWO; Graduate programme 022.001.003).

Contents

Outline & Scope

In this thesis we aim to identify, describe and characterize the cardiac pacemaker cells that generate the electrical impulse inducing cardiac rhythmicity and determining the basal heart rate in the zebrafish.

In **chapter 1** we summarize and discuss what is currently known about the development of the cardiac pacemaker cells in an evolutionary context in various organisms.

In **chapter 2** we report the initial identification of the pacemaker cells in the adult zebrafish heart. Pacemaker cells in zebrafish, mouse and human expressed the transcription factor Islet-1. Furthermore, we discuss the role of Islet-1 in pacemaker cell function in the embryonic heart. Zebrafish embryos from the isl1K88X mutant line display severe bradycardia and arrhythmia, indicating a pacemaker cell defect.

In **chapter 3** we follow up on the characterization of the Isl1^{+} pacemaker cells and show that the Isl1 expressing cells are still present in the sinoatrial region of the Isl1 mutant heart. Furthermore, we confirmed that Isl1 expression specifically in the pacemaker cells is regulated by several regulatory elements located within a 180kb stretch of genomic DNA downstream of the Isl1 locus.

In **chapter 4** we applied tomo-seq to generate a detailed spatially resolved transcriptome map of the 2 dpf zebrafish heart. We identified over 1100 genes with differential expression patterns in distinct sub-compartments of the heart. Furthermore, we established a novel role for Wnt/β-catenin signalling in controlling heart rate via the parasympathetic nervous system.

In **chapter 5** we introduce CAID (Chronic Atrial and Intestinal Dysrhythmia) syndrome a novel cohesinopathy specifically affecting heart and gut rhythmicity. CAID is caused by a single homozygous mutation in Shugoshin-like 1 (*SGOL1*), a component of the cohesin complex.

In **chapter 6** we discuss the findings described in the previous chapters and place them in a broader context.


Heart
Cell
SAN
Pacemaker
Cardiac
Isl1
System
Express
Develop
Function
Sinus
Factor
Zebrafish
Conduction
Venosus
Initial
Gene
Show
Contract
Mammalian
Nkx2.5
Hcn4
Pattern
Vertebrate
Structure
Side
Tbx18
Tbx3
Shox2
Chamber
Cx40
Cx43
Tube
Myocardium
Pump
Right
Drosophila
Atrial
Study
Mice
Current
Ih
Activity
Early
Form
Gene
Conserved
Molecular
Depolarise
Bilaterian

CHAPTER 1

On the Evolution of the Cardiac Pacemaker

Silja Burkhard [1], Vincent van Eif [2], Laurence Garric [1], Vincent M. Christoffels [2] and Jeroen Bakkers [1,3,*]

[1] Hubrecht Institute-KNAW and University Medical Center Utrecht, 3584 CT, Utrecht, The Netherlands.
[2] Department of Medical Biology, Academic Medical Center Amsterdam, 1105 AZ Amsterdam, The Netherlands.
[3] Department of Medical Physiology, Division of Heart and Lungs, University Medical Center Utrecht, 3584 CT Utrecht, The Netherlands.

J. Cardiovasc. Dev. Dis. **2017**, *4*(2), 4; doi:10.3390/jcdd4020004

1

ABSTRACT

The rhythmic contraction of the heart is initiated and controlled by an intrinsic pacemaker system. Cardiac contractions commence at very early embryonic stages and coordination remains crucial for survival. The underlying molecular mechanisms of pacemaker cell development and function are still not fully understood. Heart form and function show high evolutionary conservation. Even in simple contractile cardiac tubes in primitive invertebrates, cardiac function is controlled by intrinsic, autonomous pacemaker cells. Understanding the evolutionary origin and development of cardiac pacemaker cells will help us outline the important pathways and factors involved. Key patterning factors, such as the homeodomain transcription factors Nkx2.5 and Shox2, and the LIM-homeodomain transcription factor Islet-1, components of the T-box (Tbx), and bone morphogenic protein (Bmp) families are well conserved. Here we compare the dominant pacemaking systems in various organisms with respect to the underlying molecular regulation. Comparative analysis of the pathways involved in patterning the pacemaker domain in an evolutionary context might help us outline a common fundamental pacemaker cell gene programme. Special focus is given to pacemaker development in zebrafish, an extensively used model for vertebrate development. Finally, we conclude with a summary of highly conserved key factors in pacemaker cell development and function.

1

INTRODUCTION

The heart is an evolutionary success story. During the course of evolution, novel structures and functions have been added to the primitive ancient pump. The network of transcription factors regulating mammalian embryonic heart development shows a high degree of evolutionary conservation. Similar signalling pathways controlling muscle growth, patterning, and contractility have been found in animals as distantly related as humans and drosophila (Bishopric, 2005, Boogerd et al., 2009, Burggren and Pinder, 1991, Cripps and Olson, 2002, Fishman and Olson, 1997, Hertel and Pass, 2002, Meijler and Meijler, 2011, Moorman and Christoffels, 2003, Olson, 2006, Satou and Satoh, 2006, Simoes-Costa et al., 2005, Solc, 2007, Xavier-Neto et al., 2010).

Even the most basic heart-like structure shares the common crucial feature of all hearts, the ability to rhythmically contract and pump fluid through the body. Thus, the heart is the motor of a fluid-based transport system for nutrients, metabolites, and oxygen. Even animals with radically different lifestyles and body plans, such as insects, fish, birds, and terrestrial animals show a striking conservation in cardiac function (Bishopric, 2005, Meijler and Meijler, 2011, Simoes-Costa et al., 2005, Solc, 2007, Xavier-Neto et al., 2010) (Figure 1). The cardiac pacemaker and conduction system in the mammalian heart can be considered as an important advancement to increase cardiac efficiency. Mammals possess a sophisticated network of pacemaker nodes, specially coupled cardiomyocytes and a fast conduction system enabling coordinated, sequential contraction of the chambered heart. In comparison, the primitive tubular pumps in invertebrates resemble early mammalian embryonic hearts both in structure (slow-conducting, poorly coupled myocytes, lack of valves and a conduction system) and function (peristaltic contraction pattern) (Boogerd et al., 2009, Greener et al., 2011, Hertel and Pass, 2002, Manner et al., 2010, Tao and Schulz, 2007, Sizarov et al., 2011b, Solc, 2007). It is appealing to hypothesise that these analogies reflect the ancestral background of the mammalian heart. Thus, analysis of heart morphogenesis from an evolutionary perspective might help to understand the mechanisms observed during embryonic development. Many of the morphological changes of the heart have been attributed to physiological adaption of an ancestral cardiac network to an increase in metabolic rate and body size and complexity, and the transition from aquatic to terrestrial habitats. With regard to the pacemaker, it is unclear when exactly the distinct structures evolved.

Pacemaker cells are highly specialized myocardial cells whose intrinsic ability to rhythmically depolarise and initiate an action potential is responsible for the basal heart rate. They are located in the sinoatrial node (SAN) in mammals and the corresponding structures in other vertebrates and several invertebrates (Figure 1). The capacity to

trigger an action potential without external stimulation distinguishes pacemaker cells from the surrounding working myocardium. There have long been two hypotheses addressing the mechanism behind the pacemaker capacity. On the one hand is the expression of Hcn4, a specialized ion channel allowing Na^+/K^+ ion influx (I_f) in response to hyperpolarisation specifically in pacemaker cells (Verkerk et al., 2007, Lei et al., 2001, Liao et al., 2010). On the other hand is an oscillatory release of Ca^{2+} from the sarcoplasmic reticulum (Ca^{2+}-clock) (Maltsev et al., 2006). However, it has recently been proposed that both hypotheses are correct and cooperate in facilitating the rhythmic depolarization (Yaniv et al., 2015, Lakatta et al., 2010). Pacemaker cells are directly coupled to each other as well as to the adjacent working myocardial cells by gap junctions. These allow the exchange of ions from cell to cell, propagating the action potential from the pacemaker cells through the entire myocardium. Gap junctions consist of connexins, transmembrane proteins with different conductive properties (Chandler et al., 2009). The fast conducting subunits Cx43 and Cx40 are the main connexins expressed in the chamber working myocardium. Pacemaker cells express slow-conducting connexins, Cx45 and Cx32 (Vozzi et al., 1999, Desplantez et al., 2007). This ensures the unidirectional propagation of the electrical signal from the pacemaker cells to the working myocardial cells. Congenital or degenerative defects in pacemaker cell function can cause sinus node dysfunction (SND), a major reason for artificial pacemaker implantation (Choudhury et al., 2015, Dobrzynski et al., 2007, Herrmann et al., 2011).

Regarding the evolution of the cardiac pacemaker system, several questions arise. Did the distinct pacemaker evolve out of necessity to accommodate the increasing morphological complexity of the heart in vertebrates to ensure a controlled contraction pattern? Did it evolve to ensure coordinated, unidirectional blood flow in a separated systemic-pulmonary circuit? Was it crucial as a mediator to allow heart regulation by the nervous system?

Origin of the Basic Tubular Heart

The cardiac pacemaker might be described as the specialised, intrinsic structure initiating the cardiac muscular contractions. The first heart-like organ is believed to have evolved in an ancestral bilaterian about 500 million years ago (Figure 1) (Bishopric, 2005, Moorman and Christoffels, 2003, Simoes-Costa et al., 2005). This ancestral “heart” was likely a simple tubular structure, consisting of a single layer of pulsatile cells to force fluid through pericellular interstices without an enclosed vascular system (Bishopric, 2005). The initial appearance of muscle-like cells is not entirely clear, but is proposed to have emerged from the gastrodermis prior to the divergence of Cnidarians and Ctenophora from bilaterians (Olson, 2006, S and Saitou, 1999). Muscle cells are of mesodermal origin and present in all triploblastic animals.

Mesodermal cells specifying into early primitive myocytes arose first in bilaterians (Bishopric, 2005). It remains to be determined at what stage a subset of cells became functionally dominant to coordinate the cellular contractions. Morphologically, it might have resembled the simple tubular heart found in *Amphioxus* (Holland et al., 2003).

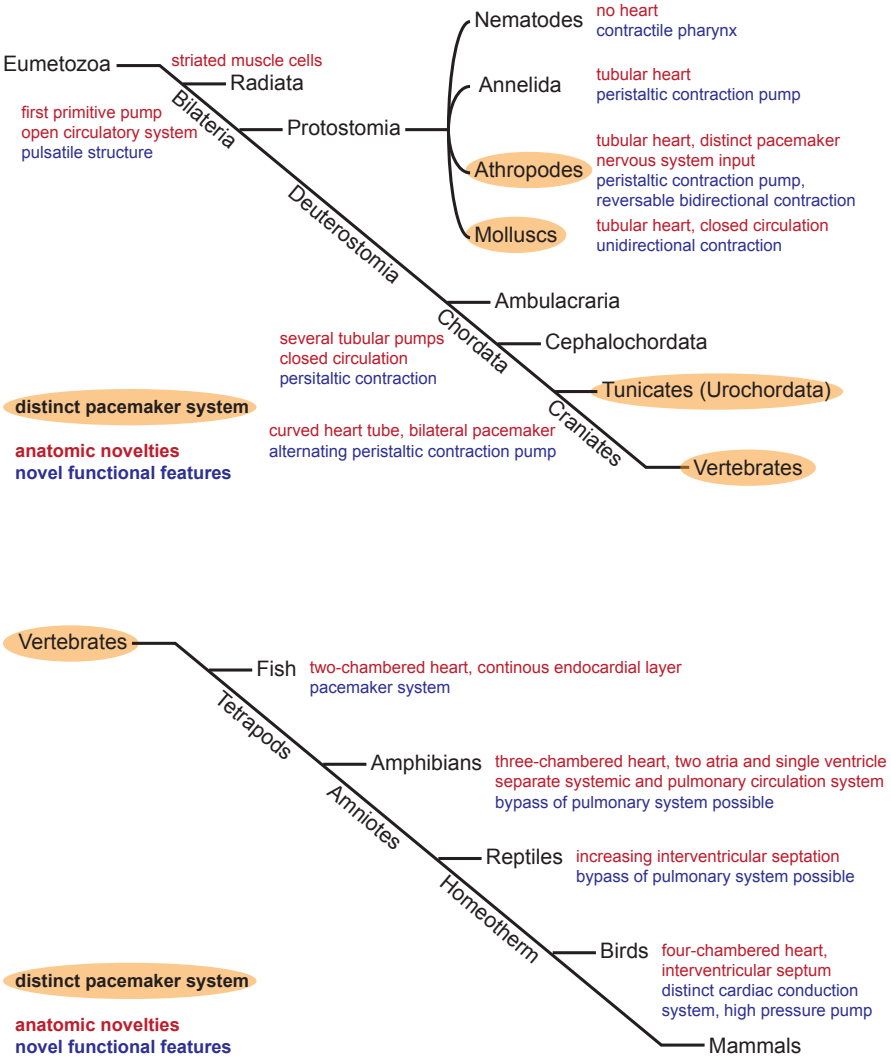

Figure 1.

Evolutionary adaption of the cardiac circulation system, with regard to important morphological (red) and functional (purple) novelties. Heart and pacemaker evolution of existent Eumetazoans, from the presumptive common bilaterian ancestor to vertebrates (top) and within the vertebrate subphylum (bottom). Orange: All groups with an intrinsic pacemaker system, includes all vertebrates.

Bilateral Pacemaker System in Drosophila Melanogaster

Despite the large evolutionary distance between arthropods and mammals, there is compelling evidence supporting a close structural relationship between cardiac systems. This indicates that a basic tubular heart has been present in the common bilaterian ancestor. Although gene regulatory modifications to accommodate the growing organism lead to morphologically distinct structures, common basic mechanisms are still conserved (Bishopric, 2005).

Heart formation in arthropods has been widely studied in the most prominent model organism, the fruit fly *Drosophila melanogaster.* The drosophila heart (also referred to as the dorsal vessel) is a tubular organ consisting of a single layer of contractile mesodermal cardioblasts and an overlying pericardial cell layer (Bishopric, 2005, Tao and Schulz, 2007). As generally found in arthropods, drosophila has an open circulatory system with a dorsally positioned heart able to pump haemolymph through the body (Bodmer and Frasch, 2010). The heart functions as a linear peristaltic pump and develops in several repetitive segments (Medioni et al., 2009, Tao and Schulz, 2007). There are no distinct chambers, but an aortic valve structure at the anterior opening supports fluid flow direction (Bishopric, 2005, Olson, 2006, Bodmer and Frasch, 2010). On the posterior side, there are three (larval) or four (adult) pairs of ostia with a valve-like structure (Bodmer and Frasch, 2010, Wasserthal, 2007, Tao and Schulz, 2007, Molina and Cripps, 2001). Ostia are thought to be the drosophila analogues to vertebrate inflow tract structures. Their formation depends on a distinct gene expression programme, similar to the differential development of sinus venosus structures versus chamber myocardium in vertebrates (Molina and Cripps, 2001). The primary pacemaker is situated at the posterior end of the heart and peristaltic contractions move anteriorly to expel haemolymph into the aorta (Curtis et al., 1999). At the anterior side a secondary site of contraction initiation has been observed. This allows for a reversal in haemolymph flow (Wasserthal, 2007).

Molecularly, the cardiac muscle cells in drosophila and mammalian species show a striking degree of similarity. Transcription factor *tinman*, the drosophila homologue of *Nkx2.5*, is the determining factor underlying cardiomyocyte differentiation (Bodmer and Frasch, 2010, Bodmer, 1993, Azpiazu and Frasch, 1993). Its expression is observed in all cardiac cells. Notably, a subset of cardioblast at the posterior portion of the cardiac vessel lack *tinman* expression (Lo et al., 2002). *Seven-up*, the homologue of vertebrate *NR2F1 and -2* (Coup-TFI, -TFII), is specifically expressed in the posterior part of the dorsal vessel (Bodmer and Frasch, 2010, Molina and Cripps, 2001, Lo and Frasch, 2001). These cells will form the ostia and can be distinguished by re-expression of *dorsocross* genes (Tbx) and expression of *wingless* (Wnt1) (Molina and Cripps, 2001, Lo et al., 2002, Reim and Frasch, 2005). Furthermore, homologues of important mammalian cardiac factors also partaking in

drosophila cardiogenesis are *tailup* (Isl1), *pannier* (Gata4), *mid* (Tbx20), and *Dpp* (Bmp2) (Mann et al., 2009, Reim and Frasch, 2005, Gajewski et al., 2001, Reim et al., 2005, Zaffran et al., 2002).
Since larvae lack nervous innervation of the heart, only an intrinsic pacemaker potential can initiate the peristaltic contractions (Dowse et al., 1995, Gu and Singh, 1995, Dulcis and Levine, 2005). After metamorphosis, the heart is innervated and receives neuronal input (Dulcis and Levine, 2003, Dulcis and Levine, 2005). It therefore combines two established mechanisms of rhythmic contraction, external input from the central nervous system and intrinsic control by an independent myogenic pacemaker. Pharmacological studies showed that the important ion-channels found in mammalian myocytes are also present in drosophila (Johnson et al., 1998). The only major difference was the substitution of the inward sodium current with an inward calcium current as the main depolarization current (Johnson et al., 1998, Bodmer and Frasch, 2010). The mechanism underlying the pacemaker potential in drosophila has not been identified. Drosophila melanogaster I_h (DMIH), a homolog of the pacemaker-specific hyperpolarization activated cyclic nucleotide gated potassium channel 4 (HCN4) is present. It similarly encodes a subunit of the slow inward hyperpolarisation-activated potassium channel (I_h-channels) (Gisselmann et al., 2005). However, whether I_h- is present in the drosophila pacemaker remains to be determined. The *Ork1* gene, encoding a two-pore domain potassium channel facilitating an open rectifier K^+-current, is a critical component of the drosophila pacemaker system. Ork1 regulates the duration of the slow diastolic depolarisation without influencing basal cardiac automaticity (Lalevee et al., 2006). Whether pacemaker depolarisation in drosophila relies on a mechanism similar to the funny current I_f or a calcium clock mechanism as described in mammals remains to be determined.

Basic Circulation System in Early Deuterostomia

A basic, but well-studied organism is the tunicate *Ciona intestinalis* (ascidia, urochordata). *C. intestinalis* has an open circulatory system with a curved, V-shaped heart (Chiba et al., 2004). The tube consists of cardiac myoepithelium containing striated myofilaments and an outer pericardial lining, but lacks an endocardial cell layer (Davidson, 2007). Deuterostome evolution coincided with a multiplication and functional divergence of contractile proteins (Bishopric, 2005). There are no chambers or valves discernible and the tube itself does not show morphological polarity (Simoes-Costa et al., 2005). The heart tube is situated on the ventral side of the body, close to the stomach. It opens into single vessels at the posterior end connecting to the endostyle. At the anterior end, it is connected to the dorsal part of the pharynx (Davidson, 2007, Anderson, 1968). A series of studies by Kriebel et

al. in the 1960s morphologically and physiologically characterised the pacemaker system in tunicates (Kriebel, 1967, Kriebel, 1968c, Kriebel, 1968d, Kriebel, 1968b, Kriebel, 1968a). Early electrophysiology and microscopy studies could localise two independent myogenic pacemakers, one at the posterior and one at the anterior opening of the ciona heart tube generating rhythmic peristaltic contractions (Bishopric, 2005, Anderson, 1968). It is unclear whether one of the pacemakers has a dominant function. The contractions show an alternating pattern and velocity is independent of direction (Kriebel, 1967, Perez-Pomares et al., 2009, Kriebel, 1968d). The reversal of the pumping direction might be a compensating mechanism for inefficiency of the unidirectional fluid flow or a reaction to external stimuli (Davidson and Levine, 2003, Xavier-Neto et al., 2010, Anderson, 1968, Simoes-Costa et al., 2005, Kriebel, 1968d). Nervous system innervation of the heart appears to be absent (Kriebel, 1968d, Pope and Rowley, 2002). Humoral modulation and pharmacological alterations of pacemaker frequencies have been reported. However, whether a similar mechanism of control as in higher vertebrates exists remains unclear (Keefner and Akers, 1971, Kriebel, 1968a).

Several factors important during mammalian heart development are also conserved in ciona, which possesses orthologues of NK homeobox (NKX), GATA binding protein (GATA), T-box (TBX), and heart and neural crest derivatives expressed (HAND) factors (Davidson and Levine, 2003, Di Gregorio, 2017). Recently, Stolfi et al. identified *Islet*-expressing migratory cells in developing ciona embryos, which follow mechanisms homologous to the second heart field (SHF) in vertebrates (Stolfi et al., 2010). However, these cells did not contribute to the heart, but to the adjacent pharyngeal structure. It can be speculated that further evolutionary progress in cardiac differentiation factors lead to a reallocation of Isl^+ cells (Stolfi et al., 2010). This indicates that an *Islet*-expressing precursor population is highly conserved and might have already been present in the early bilaterian ancestor. Evidence for a distinct cardiac conduction system has not been found in the ciona heart. Electrical coupling is believed to be facilitated by tight junctions between adjacent myocardial cells without a preferred conduction pathway or direction (Kriebel, 1968c, Davidson and Levine, 2003, Kriebel, 1967, Kriebel, 1968d).

Transition to a Sequential Contraction Pattern in Lower Vertebrates

The evolutionary step from invertebrates to vertebrates includes significant remodelling of the cardiac and circulatory system. The transition from a linear tube to a chambered heart is still not fully understood. Therefore, it is also not clear whether the positioning and function of the primary pacemaker in the complex vertebrate heart is a vertebrate-specific evolutionary novelty or secondary to the major morphological remodelling of the heart tube.

With the evolution of the early chordates came a rapid structural and functional diversification of the cardiac system, such as a looped heart with separate chambers, functional valves, and trabeculae, facilitating unidirectional blood flow. In higher vertebrates, heart function is eventually controlled by a coordinated pacemaker and conduction system (Perez-Pomares et al., 2009, Simoes-Costa et al., 2005, Bishopric, 2005, Meijler and Meijler, 2011, Moorman and Christoffels, 2003, Olson, 2006, Fishman and Chien, 1997).

All vertebrates have a closed circulatory system with an endocardial layer lining the heart (Simoes-Costa et al., 2005). This also abolishes the possibility to supply the myocardium by direct perfusion. Instead, an epicardial layer and coronary artery system is established to serve the thickening myocardial layer (Simoes-Costa et al., 2005). A basic configuration of alternating slow-conducting and poorly contracting pacemaker components with fast-conducting myocardium appears to be conserved in all higher vertebrates with multi-chambered hearts (Christoffels et al., 2010).

Two-Chambered Heart in Zebrafish

Fish have a single circuit circulation system. The heart is positioned upstream of the gills, rendering a single pumping system sufficient. The best-studied representative is the teleost zebrafish (*Danio rerio*) (Stainier, 2001, Bakkers, 2011). The adult zebrafish heart consists of two contractile chambers, a single atrium, and a single ventricle delimited by valves at the atrioventricular junction. The ventricle of mature zebrafish hearts is a thick muscular pump and is highly trabeculated. Furthermore, it has an enlarged outflow tract, the bulbus arteriosus, and a non-muscular inflow reservoir, the sinus venosus (Figure 2) (Sedmera et al., 2003, Christoffels and Moorman, 2009).

The onset of myocardial contractions is observed early during embryonic development, shortly after formation of the linear heart tube. It originates from the venous pole and initially has a peristaltic contraction pattern (Bakkers, 2011). The embryonic fish heart resembles the dynamic suction pump mechanism seen in invertebrate hearts (Forouhar et al., 2006). During cardiac looping, the onset of a conduction delay at the atrioventricular (AV) canal leads to a sequential atrial-ventricular contraction pattern (Chi et al., 2008). An optogenetic study localised the functional pacemaker in the embryonic zebrafish heart at the inner curvature of the atrium, immediately adjacent to the venous pole and restricted to a small number of cells (Arrenberg et al., 2010). Voltage dynamics visualisation showed that depolarisation originates from the sinoatrial (SA) region (Chi et al., 2008, Tsutsui et al., 2010). This location is considered to be similar to the SAN in mammalian hearts. Interestingly, temperature acclimation studies in another teleostei, the rainbow trout, also located the primary pacemaker at the sinoatrial junction (Haverinen and Vornanen, 2007).

Information on the molecular regulation of the pacemaker domain in the zebrafish has long been sparse, largely due to the lack of a pacemaker specific marker. The LIM-homeodomain transcription factor Islet-1 (Isl1), an important factor in the development of cardiomyocyte precursors of the second heart field, was identified as the first pacemaker specific molecular marker (Tessadori et al., 2012). Zebrafish embryos lacking Isl1 display a bradyarrhythmic and progressive sinus block phenotype reminiscent of pacemaker function defects (de Pater et al., 2009, Tessadori et al., 2012). Isl1 expression marks cardiac pacemaker cells from 48 hours post fertilisation (hpf) to adulthood. Its expression remains highly restricted to a small number of cardiomyocytes at the sinoatrial junction. The cardiac pacemaker cell domain in zebrafish is organised in a ring structure around the sinoatrial junction, rather than a compact node (Tessadori et al., 2012). The initiation of depolarisation at the inner curvature side of the sinoatrial junction might reflect an intrinsic hierarchy between the pacemaker cells in the ring with the dominant cells dictating the heart rhythm. Electrophysiological analyses of isolated adult Isl1-expressing cardiomyocytes show the characteristic pacemaker cell properties such as spontaneous independent depolarisation (Tessadori et al., 2012). Furthermore, the adult pacemaker domain shows expression of *hcn4*, *tbx2b*, and *bmp4*, and is devoid of *nppa* expression (Tessadori et al., 2012, Stoyek et al., 2015). Bmp signalling is essential for atrial formation and inhibits cardiomyocyte differentiation (de Pater et al., 2012, Chocron et al., 2007). Bmp4 is acting downstream of Isl1 since the expression of *bmp4* is lost specifically at the sinoatrial junction of Isl1 knockout mutant embryos (de Pater et al., 2009).

Shox2 is expressed in the embryonic pacemaker domain in zebrafish. Antisense morpholino knock-down of *shox2* in zebrafish embryos results in bradycardia suggesting that Shox2 plays a role in SAN development in fish, as it does in mice (Hoffmann et al., 2013). Both the zebrafish and human genome contain *shox*, a homologue of *shox2*. In Human, *SHOX* and *SHOX2* are very similar in sequence, have a common homeodomain and appear to be redundant in function (Liu et al., 2011). In zebrafish, *shox* expression has been identified in the putative heart (Kenyon et al., 2011). The absence of *Shox* in the mouse genome might explain the severe developmental cardiovascular defects in *Shox2*$^{-/-}$ mice.

In the AV canal of the adult zebrafish heart, a secondary pacemaker has been identified. After resection of the atrium, the pacemaker activity in the AV canal is sufficient to initiate ventricular contraction (Stoyek et al., 2016). In the developing heart, the T-box transcription factor Tbx2b is expressed in the AV canal, whereas the working myocardial marker Nppa is expressed in the chamber myocardium and is absent from the AV canal (Jensen et al., 2012). The mature electrophysiological properties and electrocardiography (ECG) pattern in zebrafish are comparable to the

mammalian heart (Christoffels and Moorman, 2009, Brette et al., 2008, Nemtsas et al., 2010, Alday et al., 2014). The important ion currents for depolarisation, plateau phase, and repolarisation (I_{Na}, $I_{Ca,L}$ and I_{Kr}) are similarly distributed as in mammalian hearts. $I_{Ca,T}$, which has a prominent role in mammalian pacemaker cell depolarisation was expressed in all cardiomyocytes of the zebrafish heart. Unlike the mammalian situation, expression persists in mature cardiomyocytes (Nemtsas et al., 2010).
In mammals, molecular and electrophysiological properties of pacemaker cells have been characterised extensively. The expression of a hyperpolarisation-activated slow rectifier potassium channel is considered the inherent property of mammalian pacemaker cells. Characterisation studies of the zebrafish mutant *slow-mo* argued for the existence of a hyperpolarisation-activated inward potassium current I_h. The mutant presents with bradycardia persisting into adulthood (Warren et al., 2001, Baker et al., 1997, Stainier et al., 1996). However, unlike the funny current (I_f) in mammalian pacemakers, I_h was found in all cardiomyocytes and the underlying genetic components have not been identified, rendering it unsuitable as a pacemaker cell marker (Warren et al., 2001, Baker et al., 1997).
Expression data for homologues of the mammalian cardiac connexins (Cx30.2, Cx40, Cx43, Cx45) is sparse in zebrafish (Chi et al., 2010). *Cx43* (homologue of Cx43) expression has been observed in the embryonic heart (Chi et al., 2008, Chatterjee et al., 2005). *Cx45.6* (homologue of Cx40) is expressed in the chamber myocardium of the ventricle and atrium, similar to the mammalian expression pattern (Chi et al., 2008, Christie et al., 2004). Both pacemaker-specific mammalian connexins (Cx30.2, Cx45) have not been described in zebrafish so far.
The adult zebrafish heart shows profound neuronal innervation, including innervation of the SA junction near *hcn4* and *isl1* expressing pacemaker cells. The neuronal plexus at the SA junction contains cholinergic, adrenergic, and nitrergic axons (Stoyek et al., 2015). Furthermore, zebrafish embryonic hearts express muscarinic acetyl choline and β-adrenergic receptors and the cholinergic agonist carbachol causes a decrease in heart rate (i.e., bradycardia) (Hsieh and Liao, 2002, Stoyek et al., 2016). This indicates a neuronal control of the pacemaker domain possibly similar to the neuronal crosstalk reported in the mammalian SAN (Stoyek et al., 2015).

Septation and Conduction System Development in Amphibians

Contrary to zebrafish, amphibians and reptiles are not well studied on a molecular level. Gene expression information remains sparse. A common amphibian model organism is the clawed frog *Xenopus laevis* (Mercola et al., 2010). Heart rate measurements in Xenopus larvae (Bartlett et al., 2004) and adults (Bartlett et al., 2010) showed that the ECG pattern is comparable to mammals and contractions showed sequential atrial-ventricular contraction with a delay at the AV junction.

Furthermore, drug sensitivity studies showed that the pacemaking system in Xenopus interacts with sympathetic and parasympathetic nervous system input (Bartlett et al., 2004). The location of the primary pacemaker was not addressed in this study. It remains unclear whether this pacemaker shows a similar right-sided laterality as the mammalian SAN.

As described for zebrafish, the presence of an organised ventricular conduction system in Xenopus is unclear. Due to the absence of a ventricular septum, it has been hypothesised, that the ventricular trabeculae or discrete conduction pathways in the ventricular wall might constitute a fast pathway to the apex of the ventricle (Sedmera et al., 2003, Arbel et al., 1977).

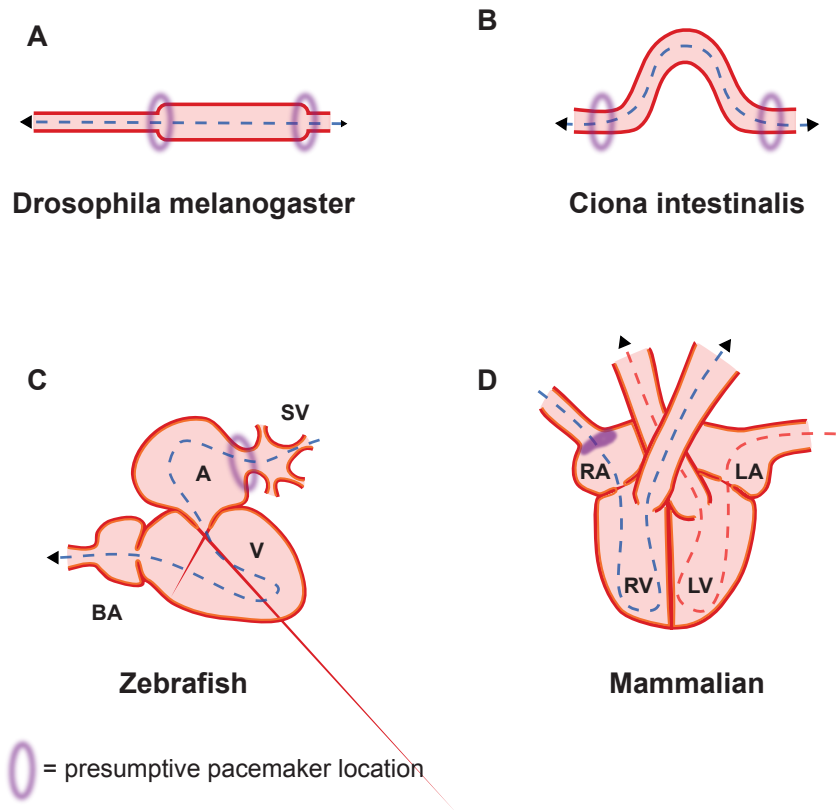

Figure 2.

Illustration of heart evolution. **(A)** Drosophila dorsal vessel and **(B)** Ciona heart with bilateral pacemaker structures. **(C)** two-chambered zebrafish heart with pacemaker ring at sinoatrial junction. **(D)** Four-chambered mammalian heart, primary pacemaker in the sinoatrial node SAN. (A-C: anterior on the left, posterior on the right), Arrows indicate direction of blood flow. Red = myocardial/muscle layer; orange = endocardium; A = atrium; V = ventricle; SV = sinus venosus; BA = bulbus arteriosus.

The reptilian heart on the other hand shows a varied degree of ventricular septation (Koshiba-Takeuchi et al., 2009, Wyneken, 2009, Jensen et al., 2013). The sinus venosus is well developed and the first reservoir to receive blood from the venous system and has been considered to be a fourth chamber (Kik and Mitchell, 2005, Mitchell, 2009, Wyneken, 2009).

Data on the embryonic development of reptilian hearts is sparse. Early morphological development is similar to that of higher vertebrates (Fishman and Chien, 1997, Crossley and Burggren, 2009, Burggren and Crossley, 2002). An initially peristaltic contraction pattern of the early heart tube has been observed in several reptilian species (Crossley and Burggren, 2009). Cardiac contractions in the mature reptile heart originate from the sinus venosus. They result in a characteristic SV wave in ECG measurements that precedes the P wave (atrial depolarisation) (Mitchell, 2009). The pacemaker might be less compact than in mammals, leading to a widespread pacemaker area across the sinus venosus, leading to its referral as a pacemaker chamber (Geddes, 2002). The fully septated, four-chambered crocodilian heart morphologically closely resembles the avian and mammalian heart. A SAN with spontaneously depolarising pacemaker cells has been morphologically outlined in the crocodile heart (Solc, 2007, Koprla, 1987).

Nervous system innervation of the heart has been described for various reptiles and amphibians (Taylor et al., 2010, Seebacher and Franklin, 2005, Taylor et al., 2009, Taylor et al., 1999). Whether these directly interact with the pacemaker structure could not be clarified yet, due to a lack of understanding of the pacemaker system in these animals.

Complex Pacemaker and Cardiac Conduction System in Birds and Mammals

The earliest electrophysiological observations of the primary action potential initiation in the developing chick heart has located the pacemaker site at the left posterior inflow tract of the heart at Hamburger and Hamilton stage 10 (HH10). During the course of heart morphogenesis, a notable shift of the primary pacemaker to the ventral surface of the right inflow tract is accompanied by a RhoA-dependent spatial restriction of a $Tbx18^{+}$ $Isl1^{+}$ $Hcn4^{+}$, and $Nkx2.5^{-}$ myocardial subpopulation (Bressan et al., 2013, Vicente-Steijn et al., 2010). Electrophysiological studies demonstrated impulse initiation in the right atrium (HH29) (Sakai and Kamino, 2015). Through direct cell labelling, Bressan et. al identified a distinct population of pacemaker precursor cells within the right lateral plate mesoderm of the developing chick embryo, favouring a very early pacemaker cell specification (Bressan et al., 2013).

Transcription Factor Network Patterns the Mammalian SAN

The primary pacemaker in the mammalian heart is located in the SAN in the dorsal

wall of the right atrium, at the junction with the superior vena cava (Keith and Flack, 1907). The pacemaker cells in the SAN are automatic and the intercellular conduction velocity is slow. The SAN is surrounded by connective tissue and has a nodal artery (Opthof, 1988).

In mice, the SAN develops within the right sinus horn of the sinus venosus from E9.5 onward, and can be morphologically identified at E10.5 (Challice and Viragh, 1980). Until E9, the transcription factor *Nkx2.5* is expressed in all cardiac cells of the primary heart tube (Reecy et al., 1999, Christoffels et al., 2006). Initially, *Hcn4* is expressed in the early heart tube, highest in the *Nkx2.5*$^{+}$ inflow tract (Mommersteeg et al., 2007, Liang et al., 2013). Between E9 and E12, *Tbx18*$^{+}$ *Nkx2.5*$^{-}$ progenitor cells differentiate into myocardium, are added to the inflow tract, and form the sinus venosus (Christoffels et al., 2006). *Hcn4* is highly expressed in the *Tbx18*$^{+}$ *Nkx2.5*$^{-}$ sinus venosus cells and becomes downregulated in the *Nkx2.5*$^{+}$ cells of the inflow tract, which have moved on to form the *Cx40*$^{+}$ and *Nppa*$^{+}$ atrial myocardium (Wiese et al., 2009, Mommersteeg et al., 2007). A subpopulation of right-sided sinus venosus cells maintains *Isl1* expression and has initiated *Tbx3* expression upon their differentiation (Mommersteeg et al., 2007, Liang et al., 2015). These cells most likely represent the SAN primordium, and form a thickening within the sinus venosus immediately adjacent to the *Cx40*$^{+}$ atrial cardiomyocytes. *Pitx2c* controls right-sided SAN development by suppressing SAN development within its own expression domain at the left side of the atrium and sinus venosus. *Pitx2c* null mice develop a second left-sided SAN primordium as part of right atrial/sinus venosus isomerism (Mommersteeg et al., 2007, Wang et al., 2010).

With further enlargement of the sinus venosus (now comprising the venous side of the venous valves and the common, right, and left sinus horns), the *Nkx2.5*$^{-}$ *Cx40*$^{-}$ *Isl1*$^{+}$ *Tbx3*$^{+}$ *Hcn4*$^{+}$ SAN primordium runs from the thickening in the superior caval vein (*Tbx18*$^{+}$; called ‘head’) to the proximal part of the right venous valve (*Tbx18*$^{+}$ derived; called ‘tail’) (Wiese et al., 2009). During the first stages of development, the size of the SAN mainly increases by addition of cells from the progenitor pool. However, SAN cells divide slowly, which will also contribute to growth of the SAN. During early foetal stages, Hcn4 expression is maintained in the SAN but is downregulated in the remaining cells of the sinus venosus. Cx40 and Cx43, not expressed in the SAN, are upregulated in the remainder of the sinus venosus (referred to as atrialisation of the sinus venosus) (Mommersteeg et al., 2007).

Nkx2.5$^{ires\text{-}Cre,+}$; *R26R*^{lacZ} lineage tracing confirmed that the SAN forms from Nkx2.5^{-} cells (Mommersteeg et al., 2007). Nevertheless, Nkx2.5 is briefly expressed in sinus venosus precursors but is turned off prior to their differentiation (Mommersteeg et al., 2010). *Tbx18* was found to be expressed exclusively in the *Nkx2.5*$^{-}$ sinus venosus, a pattern that is conserved in human, mouse, xenopus, chicken, and zebrafish

(Christoffels et al., 2006, Begemann et al., 2002). Genetic lineage tracing using *Tbx18*$^{cre,+}$/*R26R*^{lacZ} mice revealed that the entire sinus venosus, including the SAN head and tail, are derived from *Tbx18*$^{+}$ precursor cells, although the expression of *Tbx18* becomes downregulated in the tail part during development (Wiese et al., 2009). The critical role of *Tbx18* in SAN and sinus venosus formation was shown in *Tbx18*$^{-/-}$ mice, that form a hypoplastic sinus venosus and SAN head region. In contrast to morphological abnormalities, the small SAN that is formed in *Tbx18*$^{-/-}$ mice does not exhibit an altered SAN gene programme or changes in heart rhythm. However, transduced overexpression of *Tbx18* in neonatal ventricular cardiomyocytes *in vitro* and *in vivo* was sufficient to induce a SAN-specific phenotype and spontaneous depolarization (Kapoor et al., 2013). Moreover, injections with *Tbx18* expressing adenoviral vectors in pig ventricles with complete heart block showed enhanced heart rhythm and decreased expression of *Nkx2.5* and *Cx43* in the injection area, whereas *Hcn4* levels were upregulated. Electroanatomic mapping further showed increased pacemaker activity at the injection site (Hu et al., 2014). In contrast, transgenic misexpression of *Tbx18* in the mouse heart did not result in ectopic pacemaker cell formation (Greulich et al., 2016). Therefore, the extent of *Tbx18* mediated "reprogramming" and the precise mechanism needs to be addressed further.

Tbx3 in the SAN acts as a transcriptional repressor of genes of the working myocardial gene programme, including *Nppa*, *Nppb*, *Scn5a*, *Cx40*, and *Cx43*. In addition, it activates conduction system genes like *Hcn4.* It was shown that ectopic expression of *Tbx3* in developing atrial myocardium reprograms these cells into bona fide functional pacemaker cardiomyocytes (Hoogaars et al., 2007, Bakker et al., 2012). This indicates that *Tbx3* functions as a molecular switch between the genetic programme of working myocardium and SAN.

In the heart tube, *Tbx3* is repressed by *Nkx2.5*. *Nkx2.5*$^{-/-}$ embryos die before E10 due to abnormal heart looping and show increased expression of *Tbx3* and *Hcn4* in the heart tube (Mommersteeg et al., 2007). Ectopic activation of *Nkx2.5* in SAN cells induces expression of working myocardial markers *Nppa* and *Cx40* and repression of *Hcn4,* indicating that *Nkx2.5* activates the working myocardial gene programme and suppresses the pacemaker programme (Espinoza-Lewis et al., 2011). The homeodomain transcription factor *Shox2* is expressed in the SAN and sinus venosus and was shown to repress *Nkx2.5* and control expression of *Bmp4* (Espinoza-Lewis et al., 2011, Ye et al., 2015, Sun et al., 2015). *Shox2*$^{-/-}$ embryos have a reduced SAN size and exhibit increased expression of *Nkx2.5, Cx40,* and *Cx43*, and decreased expression of *Hcn4*, *Tbx3*, and *Isl1* in the SAN primordium and show cardiac arrhythmias and embryonic lethality at day E11.5 (Blaschke et al., 2007). These studies indicate a regulatory function of *Shox2* in repressing the

working myocardial programme via the repression of *Nkx2.5* and induction of Tbx3. Expression of both *Tbx3* and *Shox2* depends on Tbx5 (Mori et al., 2006), a core cardiac transcription factor expressed from early stages in the cardiac progenitors. Shox2 acts upstream of *Isl1* in pacemaker specification (Hoffmann et al., 2013). *Isl1*$^{-/-}$ mice exhibit severe abnormalities with respect to second heart field formation (Cai et al., 2003) but conditional *Isl1* knock-outs in the Hcn4 expression domain show downregulation of *Tbx3*, *Shox2*, *Hcn4*, *Bmp4*, and *Cacna1g* in the developing SAN, whereas *Nppa*, *Gja1*, *Gja5*, and *Scn5a* were upregulated (Vedantham et al., 2015, Liang et al., 2015). Together with the observation that Isl1 is essential for functional pacemaker development in zebrafish, this implies an important role for Isl1 in activating the mammalian pacemaker programme. Interestingly, ISL1 is expressed in the cells of the human SAN of both the embryonic and adult heart suggesting an evolutionary conserved function (Tessadori et al., 2012, Sizarov et al., 2011b, Sizarov et al., 2011a, Weinberger et al., 2012).

In both zebrafish and mice, Bmp signalling is involved in atrioventricular canal (AVC) and atrioventricular conduction system development (Ma et al., 2005, Stefanovic et al., 2014, Verhoeven et al., 2011). Bmp signalling co-operates through Smads with Gata4 and histone acetylases (HATs) and histone deacetylases (HDACs) to activate AVC-specific enhancers in the AVC and inactivate them in the atrial and ventricular chamber myocardium (Stefanovic et al., 2014). The correlation between the HDAC inhibition and conduction system development is further emphasized by knockout experiments, where deletion of *HDAC1* and *HDAC2* in mice resulted in neonatal lethality, bradycardia and increased expression of *Cacna2d2*, a calcium channel that is present in the conduction system (Montgomery et al., 2007). Furthermore, an enhancer region in the first intron of the *Hcn4* locus is activated in the ventricular myocardium after exposure to both transcription factor *Mef2c* and *HDAC* inhibition (Vedantham et al., 2013). Therefore, it is tempting to speculate that SAN gene expression is regulated by a mechanism involving BMP-signalling, core cardiac transcription factors, and HDAC activity.

CONCLUSIONS

The coordinated rhythmic contraction is the fundamental principle of cardiac function. Specialized cardiac pacemaker cells are responsible for initiating the electrical impulse. Despite the vast morphological differences between the simple invertebrate heart and the structurally more complex mammalian heart, there is a striking degree of evolutionary conservation of the fundamental functional and molecular pathways. The presence of specialized pacemaker cells at the inflow pole

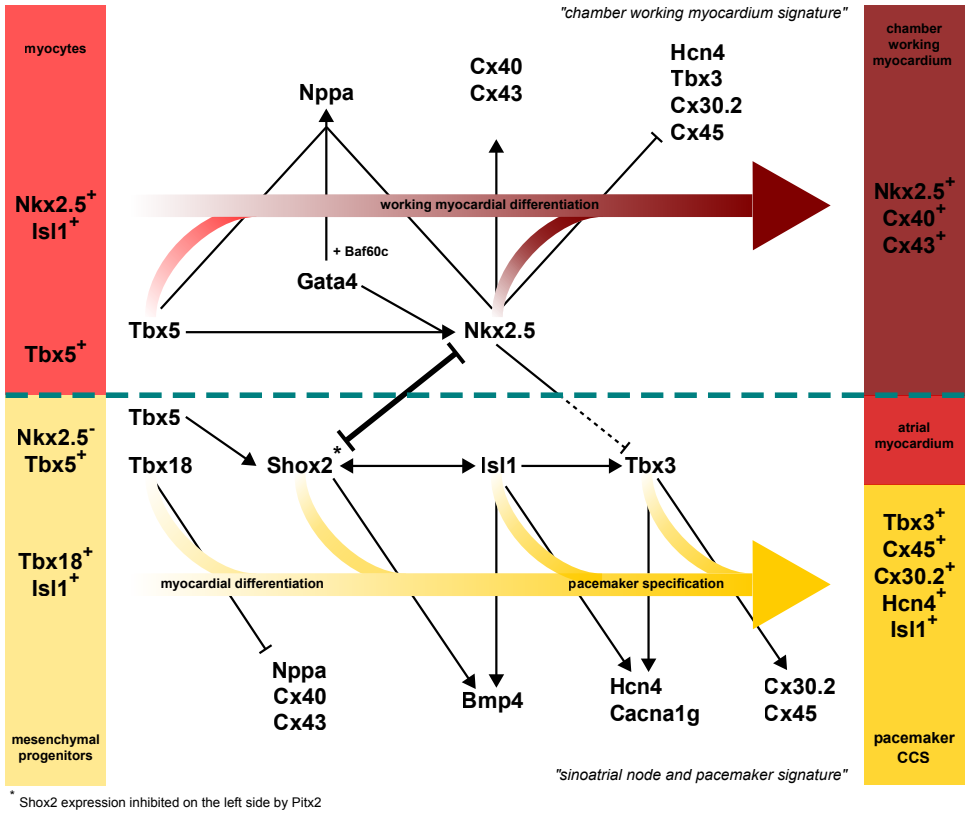

Figure 3.

Important factors in the specification of pacemaker cells in the SAN and atrial working myocardium. SAN cells arise from a *Tbx18*$^{+}$ *Nkx2.5*$^{-}$ mesenchymal progenitor population located adjacent to the *Nkx2.5*$^{+}$ posterior heart tube myocytes. Tbx18 is the main driving factors of myocardial differentiation in the mesenchymal progenitors. It delineates the SAN primordium by competing with Tbx5 and functionally repressing atrial differentiation factors such as Gata4, Nkx2.5, and Nppa. Shox2 inhibits Nkx2.5 expression, activates Tbx3 and interacts with Isl1. Shox2 is a direct target of laterality factor Pitx2 and is inhibited in the left compartments of the developing heart. Tbx3 is the main factor to directly or indirectly activate pacemaker-specific factors. Tbx5 interacts with Gata4 and Nkx2.5 to initiate working myocardial cell differentiation. Tbx5 represses Shox2 in the working myocardium. Nkx2.5 is the main determining factor for chamber myocardial cells and activates working myocardium-specific factors. The transcription factor network leads to the establishment of specific gene expression signatures. The SAN is characterised by the high expression of Tbx3, Shox2, Isl1, Bmp4, Hcn4, Cacna1g, Cx30.2 (mouse), and Cx45, corresponding with the low expression or absence of Cx40, Cx43, and Scn5a in embryos and adults. The working myocardium shows a contrary expression pattern, with the high expression of Cx40, Cx43, Scn5a, and Nppa corresponding to low or absent expression of Cx30.2 (mouse), Cx45, and Hcn4.

of the heart is the common feature of all cardiac systems. In primitive invertebrate species, pacemaker cells are present at several locations, even allowing a reversal of the pumping direction. In contrast, the closed circulatory systems of vertebrates rely on a strictly unidirectional blood flow driven by a single dominant pacemaker structure (Figure 2). When and how this restriction to a single dominant pacemaker structure occurred during evolution remains unclear. During cardiac differentiation, the precursor cells and derived pacemaker cardiomyocytes execute a cascade of patterning factors, driving a pacemaker-specific gene programme. The pacemaker cells remain embedded in and coupled to the surrounding myocardium, requiring a highly-controlled delineation from the working myocardial gene programme (Figure 3). This highlights an ancestral network of gene regulation, which does not seem to have changed dramatically as the heart evolved from a simple suction pump to the complex four-chambered heart in mammals.

The zebrafish is increasingly being used as a model to address pacemaker development and function. Considerable homology between zebrafish and mammalian heart development and physiology and the feasibility of high-throughput genetic or pharmacological manipulation provide promising opportunities for cardiac research. Furthermore, novel gene editing techniques such as the Transcription activator-like effector nucleases (TALEN) and Clustered regularly interspaced short palindromic repeats (CRISPR-Cas9) systems allow for the precise modelling of deleterious human gene mutations (Bakkers, 2011, Nemtsas et al., 2010, Stainier, 2001, Lin et al., 2015, Kessler et al., 2015, Wilkinson et al., 2014, Lodder et al., 2016).

ACKNOWLEDGMENTS

This work was supported by the ZonMW grant 40-00812-98-12086 awarded to V.M.C. and J.B. and an EMBO long-term fellowship (EMBO ALTF 177-2015) awarded to L.G.

AUTHOR CONTRIBUTIONS

All authors contributed to the writing of the manuscript.

CONFLICTS OF INTEREST

The authors declare no conflict of interest.

REFERENCES

ALDAY, A., ALONSO, H., GALLEGO, M., URRUTIA, J., LETAMENDIA, A., CALLOL, C. & CASIS, O. 2014. Ionic channels underlying the ventricular action potential in zebrafish embryo. *Pharmacol Res,* 84**,** 26-31.

ANDERSON, M. 1968. Electrophysiological studies on initiation and reversal of the heart beat in Ciona intestinalis. *J Exp Biol,* 49**,** 363-85.

ARBEL, E. R., LIBERTHSON, R., LANGENDORF, R., PICK, A., LEV, M. & FISHMAN, A. P. 1977. Electrophysiological and anatomical observations on the heart of the African lungfish. *Am J Physiol,* 232**,** H24-34.

ARRENBERG, A. B., STAINIER, D. Y., BAIER, H. & HUISKEN, J. 2010. Optogenetic control of cardiac function. *Science,* 330**,** 971-4.

AZPIAZU, N. & FRASCH, M. 1993. tinman and bagpipe: two homeo box genes that determine cell fates in the dorsal mesoderm of Drosophila. *Genes Dev,* 7**,** 1325-40.

BAKER, K., WARREN, K. S., YELLEN, G. & FISHMAN, M. C. 1997. Defective „pacemaker" current (Ih) in a zebrafish mutant with a slow heart rate. *Proc Natl Acad Sci U S A,* 94**,** 4554-9.

BAKKER, M. L., BOINK, G. J., BOUKENS, B. J., VERKERK, A. O., VAN DEN BOOGAARD, M., DEN HAAN, A. D., HOOGAARS, W. M., BUERMANS, H. P., DE BAKKER, J. M., SEPPEN, J., TAN, H. L., MOORMAN, A. F., T HOEN, P. A. & CHRISTOFFELS, V. M. 2012. T-box transcription factor TBX3 reprogrammes mature cardiac myocytes into pacemaker-like cells. *Cardiovasc Res,* 94**,** 439-49.

BAKKERS, J. 2011. Zebrafish as a model to study cardiac development and human cardiac disease. *Cardiovasc Res,* 91**,** 279-88.

BARTLETT, H. L., ESCALERA, R. B., 2ND, PATEL, S. S., WEDEMEYER, E. W., VOLK, K. A., LOHR, J. L. & REINKING, B. E. 2010. Echocardiographic assessment of cardiac morphology and function in Xenopus. *Comp Med,* 60**,** 107-13.

BARTLETT, H. L., SCHOLZ, T. D., LAMB, F. S. & WEEKS, D. L. 2004. Characterization of embryonic cardiac pacemaker and atrioventricular conduction physiology in Xenopus laevis using noninvasive imaging. *Am J Physiol Heart Circ Physiol,* 286**,** H2035-41.

BEGEMANN, G., GIBERT, Y., MEYER, A. & INGHAM, P. W. 2002. Cloning of zebrafish T-box genes tbx15 and tbx18 and their expression during embryonic development. *Mech Dev,* 114**,** 137-41.

BISHOPRIC, N. H. 2005. Evolution of the heart from bacteria to man. *Ann N Y Acad Sci,* 1047**,** 13-29.

BLASCHKE, R. J., HAHURIJ, N. D., KUIJPER, S., JUST, S., WISSE, L. J., DEISSLER, K., MAXELON, T., ANASTASSIADIS, K., SPITZER, J., HARDT, S. E., SCHOLER, H., FEITSMA, H., ROTTBAUER, W., BLUM, M., MEIJLINK, F., RAPPOLD, G. & GITTENBERGER-DE GROOT, A. C. 2007. Targeted mutation reveals essential functions of the homeodomain transcription factor Shox2 in sinoatrial and pacemaking development. *Circulation,* 115**,** 1830-8.

BODMER, R. 1993. The gene tinman is required for specification of the heart and visceral muscles in Drosophila. *Development,* 118**,** 719-29.

BODMER, R. & FRASCH, M. 2010. Development and Aging of the Drosophila Heart. *In:* ROSENTHAL, N. & HARVEY, R. P. (eds.) *Heart Development and Regeneration.* Elsevier.

BOOGERD, C. J., MOORMAN, A. F. & BARNETT, P. 2009. Protein interactions at the heart of cardiac chamber formation. *Ann Anat,* 191**,** 505-17.

BRESSAN, M., LIU, G. & MIKAWA, T. 2013. Early mesodermal cues assign avian cardiac pacemaker fate potential in a tertiary heart field. *Science,* 340**,** 744-8.

BRETTE, F., LUXAN, G., CROS, C., DIXEY, H., WILSON, C. & SHIELS, H. A. 2008. Characterization of isolated ventricular myocytes from adult zebrafish (Danio rerio). *Biochem Biophys Res Commun,* 374**,** 143-6.

BURGGREN, W. & CROSSLEY, D. A., 2ND 2002. Comparative cardiovascular development: improving the conceptual framework. *Comp Biochem Physiol A Mol Integr Physiol,* 132**,** 661-74.

BURGGREN, W. W. & PINDER, A. W. 1991. Ontogeny of cardiovascular and respiratory physiology in lower vertebrates. *Annu Rev Physiol,* 53**,** 107-35.

CAI, C. L., LIANG, X., SHI, Y., CHU, P. H., PFAFF, S. L., CHEN, J. & EVANS, S. 2003. Isl1 identifies a cardiac progenitor population that proliferates prior to differentiation and contributes a majority of cells to the heart. *Dev Cell,* 5**,** 877-89.

CHALLICE, C. E. & VIRAGH, S. 1980. Origin and early differentiation of the sinus node in the mouse

embryo heart. *Adv Myocardiol,* 1**,** 267-77.
CHANDLER, N. J., GREENER, I. D., TELLEZ, J. O., INADA, S., MUSA, H., MOLENAAR, P., DIFRANCESCO, D., BARUSCOTTI, M., LONGHI, R., ANDERSON, R. H., BILLETER, R., SHARMA, V., SIGG, D. C., BOYETT, M. R. & DOBRZYNSKI, H. 2009. Molecular architecture of the human sinus node: insights into the function of the cardiac pacemaker. *Circulation,* 119**,** 1562-75.
CHATTERJEE, B., CHIN, A. J., VALDIMARSSON, G., FINIS, C., SONNTAG, J. M., CHOI, B. Y., TAO, L., BALASUBRAMANIAN, K., BELL, C., KRUFKA, A., KOZLOWSKI, D. J., JOHNSON, R. G. & LO, C. W. 2005. Developmental regulation and expression of the zebrafish connexin43 gene. *Dev Dyn,* 233**,** 890-906.
CHI, N. C., BUSSEN, M., BRAND-ARZAMENDI, K., DING, C., OLGIN, J. E., SHAW, R. M., MARTIN, G. R. & STAINIER, D. Y. 2010. Cardiac conduction is required to preserve cardiac chamber morphology. *Proc Natl Acad Sci U S A,* 107**,** 14662-7.
CHI, N. C., SHAW, R. M., JUNGBLUT, B., HUISKEN, J., FERRER, T., ARNAOUT, R., SCOTT, I., BEIS, D., XIAO, T., BAIER, H., JAN, L. Y., TRISTANI-FIROUZI, M. & STAINIER, D. Y. 2008. Genetic and physiologic dissection of the vertebrate cardiac conduction system. *PLoS Biol,* 6**,** e109.
CHIBA, S., SASAKI, A., NAKAYAMA, A., TAKAMURA, K. & SATOH, N. 2004. Development of Ciona intestinalis juveniles (through 2nd ascidian stage). *Zoolog Sci,* 21**,** 285-98.
CHOCRON, S., VERHOEVEN, M. C., RENTZSCH, F., HAMMERSCHMIDT, M. & BAKKERS, J. 2007. Zebrafish Bmp4 regulates left-right asymmetry at two distinct developmental time points. *Dev Biol,* 305**,** 577-88.
CHOUDHURY, M., BOYETT, M. R. & MORRIS, G. M. 2015. Biology of the Sinus Node and its Disease. *Arrhythm Electrophysiol Rev,* 4**,** 28-34.
CHRISTIE, T. L., MUI, R., WHITE, T. W. & VALDIMARSSON, G. 2004. Molecular cloning, functional analysis, and RNA expression analysis of connexin45.6: a zebrafish cardiovascular connexin. *Am J Physiol Heart Circ Physiol,* 286**,** H1623-32.
CHRISTOFFELS, V. M., MOMMERSTEEG, M. T., TROWE, M. O., PRALL, O. W., DE GIER-DE VRIES, C., SOUFAN, A. T., BUSSEN, M., SCHUSTER-GOSSLER, K., HARVEY, R. P., MOORMAN, A. F. & KISPERT, A. 2006. Formation of the venous pole of the heart from an Nkx2-5-negative precursor population requires Tbx18. *Circ Res,* 98**,** 1555-63.
CHRISTOFFELS, V. M. & MOORMAN, A. F. 2009. Development of the cardiac conduction system: why are some regions of the heart more arrhythmogenic than others? *Circ Arrhythm Electrophysiol,* 2**,** 195-207.
CHRISTOFFELS, V. M., SMITS, G. J., KISPERT, A. & MOORMAN, A. F. 2010. Development of the pacemaker tissues of the heart. *Circ Res,* 106**,** 240-54.
CRIPPS, R. M. & OLSON, E. N. 2002. Control of cardiac development by an evolutionarily conserved transcriptional network. *Dev Biol,* 246**,** 14-28.
CROSSLEY, D. A., 2ND & BURGGREN, W. W. 2009. Development of cardiac form and function in ectothermic sauropsids. *J Morphol,* 270**,** 1400-12.
CURTIS, N. J., RINGO, J. M. & DOWSE, H. B. 1999. Morphology of the pupal heart, adult heart, and associated tissues in the fruit fly, Drosophila melanogaster. *J Morphol,* 240**,** 225-35.
DAVIDSON, B. 2007. Ciona intestinalis as a model for cardiac development. *Semin Cell Dev Biol,* 18**,** 16-26.
DAVIDSON, B. & LEVINE, M. 2003. Evolutionary origins of the vertebrate heart: Specification of the cardiac lineage in Ciona intestinalis. *Proc Natl Acad Sci U S A,* 100**,** 11469-73.
DE PATER, E., CIAMPRICOTTI, M., PRILLER, F., VEERKAMP, J., STRATE, I., SMITH, K., LAGENDIJK, A. K., SCHILLING, T. F., HERZOG, W., ABDELILAH-SEYFRIED, S., HAMMERSCHMIDT, M. & BAKKERS, J. 2012. Bmp signaling exerts opposite effects on cardiac differentiation. *Circ Res,* 110**,** 578-87.
DE PATER, E., CLIJSTERS, L., MARQUES, S. R., LIN, Y. F., GARAVITO-AGUILAR, Z. V., YELON, D. & BAKKERS, J. 2009. Distinct phases of cardiomyocyte differentiation regulate growth of the zebrafish heart. *Development,* 136**,** 1633-41.
DESPLANTEZ, T., DUPONT, E., SEVERS, N. J. & WEINGART, R. 2007. Gap junction channels and cardiac impulse propagation. *J Membr Biol,* 218**,** 13-28.
DI GREGORIO, A. 2017. T-Box Genes and Developmental Gene Regulatory Networks in Ascidians. *Curr Top Dev Biol,* 122**,** 55-91.

DOBRZYNSKI, H., BOYETT, M. R. & ANDERSON, R. H. 2007. New insights into pacemaker activity: promoting understanding of sick sinus syndrome. *Circulation,* 115**,** 1921-32.

DOWSE, H., RINGO, J., POWER, J., JOHNSON, E., KINNEY, K. & WHITE, L. 1995. A congenital heart defect in Drosophila caused by an action-potential mutation. *J Neurogenet,* 10**,** 153-68.

DULCIS, D. & LEVINE, R. B. 2003. Innervation of the heart of the adult fruit fly, Drosophila melanogaster. *J Comp Neurol,* 465**,** 560-78.

DULCIS, D. & LEVINE, R. B. 2005. Glutamatergic innervation of the heart initiates retrograde contractions in adult Drosophila melanogaster. *J Neurosci,* 25**,** 271-80.

ESPINOZA-LEWIS, R. A., LIU, H., SUN, C., CHEN, C., JIAO, K. & CHEN, Y. 2011. Ectopic expression of Nkx2.5 suppresses the formation of the sinoatrial node in mice. *Dev Biol,* 356**,** 359-69.

FISHMAN, M. C. & CHIEN, K. R. 1997. Fashioning the vertebrate heart: earliest embryonic decisions. *Development,* 124**,** 2099-117.

FISHMAN, M. C. & OLSON, E. N. 1997. Parsing the heart: genetic modules for organ assembly. *Cell,* 91**,** 153-6.

FOROUHAR, A. S., LIEBLING, M., HICKERSON, A., NASIRAEI-MOGHADDAM, A., TSAI, H. J., HOVE, J. R., FRASER, S. E., DICKINSON, M. E. & GHARIB, M. 2006. The embryonic vertebrate heart tube is a dynamic suction pump. *Science,* 312**,** 751-3.

GAJEWSKI, K., ZHANG, Q., CHOI, C. Y., FOSSETT, N., DANG, A., KIM, Y. H., KIM, Y. & SCHULZ, R. A. 2001. Pannier is a transcriptional target and partner of Tinman during Drosophila cardiogenesis. *Dev Biol,* 233**,** 425-36.

GEDDES, L. A. 2002. Electrocardiograms from the turtle to the elephant that illustrate interesting physiological phenomena. *Pacing Clin Electrophysiol,* 25**,** 1762-70.

GISSELMANN, G., GAMERSCHLAG, B., SONNENFELD, R., MARX, T., NEUHAUS, E. M., WETZEL, C. H. & HATT, H. 2005. Variants of the Drosophila melanogaster Ih-channel are generated by different splicing. *Insect Biochem Mol Biol,* 35**,** 505-14.

GREENER, I. D., MONFREDI, O., INADA, S., CHANDLER, N. J., TELLEZ, J. O., ATKINSON, A., TAUBE, M. A., BILLETER, R., ANDERSON, R. H., EFIMOV, I. R., MOLENAAR, P., SIGG, D. C., SHARMA, V., BOYETT, M. R. & DOBRZYNSKI, H. 2011. Molecular architecture of the human specialised atrioventricular conduction axis. *J Mol Cell Cardiol,* 50**,** 642-51.

GREULICH, F., TROWE, M. O., LEFFLER, A., STOETZER, C., FARIN, H. F. & KISPERT, A. 2016. Misexpression of Tbx18 in cardiac chambers of fetal mice interferes with chamber-specific developmental programs but does not induce a pacemaker-like gene signature. *J Mol Cell Cardiol,* 97**,** 140-9.

GU, G. G. & SINGH, S. 1995. Pharmacological analysis of heartbeat in Drosophila. *J Neurobiol,* 28**,** 269-80.

HAVERINEN, J. & VORNANEN, M. 2007. Temperature acclimation modifies sinoatrial pacemaker mechanism of the rainbow trout heart. *Am J Physiol Regul Integr Comp Physiol,* 292**,** R1023-32.

HERRMANN, S., FABRITZ, L., LAYH, B., KIRCHHOF, P. & LUDWIG, A. 2011. Insights into sick sinus syndrome from an inducible mouse model. *Cardiovasc Res,* 90**,** 38-48.

HERTEL, W. & PASS, G. 2002. An evolutionary treatment of the morphology and physiology of circulatory organs in insects. *Comp Biochem Physiol A Mol Integr Physiol,* 133**,** 555-75.

HOFFMANN, S., BERGER, I. M., GLASER, A., BACON, C., LI, L., GRETZ, N., STEINBEISSER, H., ROTTBAUER, W., JUST, S. & RAPPOLD, G. 2013. Islet1 is a direct transcriptional target of the homeodomain transcription factor Shox2 and rescues the Shox2-mediated bradycardia. *Basic Res Cardiol,* 108**,** 339.

HOLLAND, N. D., VENKATESH, T. V., HOLLAND, L. Z., JACOBS, D. K. & BODMER, R. 2003. AmphiNk2-tin, an amphioxus homeobox gene expressed in myocardial progenitors: insights into evolution of the vertebrate heart. *Dev Biol,* 255**,** 128-37.

HOOGAARS, W. M., ENGEL, A., BRONS, J. F., VERKERK, A. O., DE LANGE, F. J., WONG, L. Y., BAKKER, M. L., CLOUT, D. E., WAKKER, V., BARNETT, P., RAVESLOOT, J. H., MOORMAN, A. F., VERHEIJCK, E. E. & CHRISTOFFELS, V. M. 2007. Tbx3 controls the sinoatrial node gene program and imposes pacemaker function on the atria. *Genes Dev,* 21**,** 1098-112.

HSIEH, D. J. & LIAO, C. F. 2002. Zebrafish M2 muscarinic acetylcholine receptor: cloning, pharmacological characterization, expression patterns and roles in embryonic bradycardia. *Br J Pharmacol,* 137**,** 782-92.

HU, Y. F., DAWKINS, J. F., CHO, H. C., MARBAN, E. & CINGOLANI, E. 2014. Biological pacemaker created by minimally invasive somatic reprogramming in pigs with complete heart block. *Sci Transl Med,* 6**,** 245ra94.

JENSEN, B., BOUKENS, B. J., POSTMA, A. V., GUNST, Q. D., VAN DEN HOFF, M. J., MOORMAN, A. F., WANG, T. & CHRISTOFFELS, V. M. 2012. Identifying the evolutionary building blocks of the cardiac conduction system. *PLoS One,* 7**,** e44231.

JENSEN, B., VAN DEN BERG, G., VAN DEN DOEL, R., OOSTRA, R. J., WANG, T. & MOORMAN, A. F. 2013. Development of the hearts of lizards and snakes and perspectives to cardiac evolution. *PLoS One,* 8**,** e63651.

JOHNSON, E., RINGO, J., BRAY, N. & DOWSE, H. 1998. Genetic and pharmacological identification of ion channels central to the Drosophila cardiac pacemaker. *J Neurogenet,* 12**,** 1-24.

KAPOOR, N., LIANG, W., MARBAN, E. & CHO, H. C. 2013. Direct conversion of quiescent cardiomyocytes to pacemaker cells by expression of Tbx18. *Nat Biotechnol,* 31**,** 54-62.

KEEFNER, K. R. & AKERS, T. K. 1971. Sodium localization in digitalis- and epinephrine-treated tunicate myocardium. *Comp Gen Pharmacol,* 2**,** 415-22.

KEITH, A. & FLACK, M. 1907. The Form and Nature of the Muscular Connections between the Primary Divisions of the Vertebrate Heart. *J Anat Physiol,* 41**,** 172-89.

KENYON, E. J., MCEWEN, G. K., CALLAWAY, H. & ELGAR, G. 2011. Functional analysis of conserved non-coding regions around the short stature hox gene (shox) in whole zebrafish embryos. *PLoS One,* 6**,** e21498.

KESSLER, M., ROTTBAUER, W. & JUST, S. 2015. Recent progress in the use of zebrafish for novel cardiac drug discovery. *Expert Opin Drug Discov,* 10**,** 1231-41.

KIK, M. J. L. & MITCHELL, M. A. 2005. Reptile cardiology: A review of anatomy and physiology, diagnostic approaches, and clinical disease. *Seminars in Avian and Exotic Pet Medicine,* 14**,** 52-60.

KOPRLA, E. C. 1987. The ultrastructure of alligator conductive tissue: an electron microscopic study of the sino-atrial node. *Acta Physiol Hung,* 69**,** 71-84.

KOSHIBA-TAKEUCHI, K., MORI, A. D., KAYNAK, B. L., CEBRA-THOMAS, J., SUKONNIK, T., GEORGES, R. O., LATHAM, S., BECK, L., HENKELMAN, R. M., BLACK, B. L., OLSON, E. N., WADE, J., TAKEUCHI, J. K., NEMER, M., GILBERT, S. F. & BRUNEAU, B. G. 2009. Reptilian heart development and the molecular basis of cardiac chamber evolution. *Nature,* 461**,** 95-8.

KRIEBEL, M. E. 1967. Conduction velocity and intracellular action potentials of the tunicate heart. *J Gen Physiol,* 50**,** 2097-107.

KRIEBEL, M. E. 1968a. Cholinoceptive and adrenoceptive properties of the tunicate heart pacemaker. *Biol Bull,* 135**,** 174-80.

KRIEBEL, M. E. 1968b. Electrical characteristics of tunicate heart cell membranes and nexuses. *J Gen Physiol,* 52**,** 46-59.

KRIEBEL, M. E. 1968c. Pacemaker properties of tunicate heart cells. *Biol Bull,* 135**,** 166-73.

KRIEBEL, M. E. 1968d. Studies on cardiovascular physiology of tunicates. *Biol Bull,* 134**,** 434-55.

LAKATTA, E. G., MALTSEV, V. A. & VINOGRADOVA, T. M. 2010. A coupled SYSTEM of intracellular Ca2+ clocks and surface membrane voltage clocks controls the timekeeping mechanism of the heart‘s pacemaker. *Circ Res,* 106**,** 659-73.

LALEVEE, N., MONIER, B., SENATORE, S., PERRIN, L. & SEMERIVA, M. 2006. Control of cardiac rhythm by ORK1, a Drosophila two-pore domain potassium channel. *Curr Biol,* 16**,** 1502-8.

LEI, M., HONJO, H., KODAMA, I. & BOYETT, M. R. 2001. Heterogeneous expression of the delayed-rectifier K+ currents i(K,r) and i(K,s) in rabbit sinoatrial node cells. *J Physiol,* 535**,** 703-14.

LIANG, X., WANG, G., LIN, L., LOWE, J., ZHANG, Q., BU, L., CHEN, Y., CHEN, J., SUN, Y. & EVANS, S. M. 2013. HCN4 dynamically marks the first heart field and conduction system precursors. *Circ Res,* 113**,** 399-407.

LIANG, X., ZHANG, Q., CATTANEO, P., ZHUANG, S., GONG, X., SPANN, N. J., JIANG, C., CAO, X., ZHAO, X., ZHANG, X., BU, L., WANG, G., CHEN, H. S., ZHUANG, T., YAN, J., GENG, P., LUO, L., BANERJEE, I., CHEN, Y., GLASS, C. K., ZAMBON, A. C., CHEN, J., SUN, Y. & EVANS, S. M. 2015. Transcription factor ISL1 is essential for pacemaker development and function. *J Clin Invest,* 125**,** 3256-68.

LIAO, Z., LOCKHEAD, D., LARSON, E. D. & PROENZA, C. 2010. Phosphorylation and modulation of hyperpolarization-activated HCN4 channels by protein kinase A in the mouse sinoatrial node. *J Gen*

Physiol, 136**,** 247-58.
LIN, E., CRAIG, C., LAMOTHE, M., SARUNIC, M. V., BEG, M. F. & TIBBITS, G. F. 2015. Construction and use of a zebrafish heart voltage and calcium optical mapping system, with integrated electrocardiogram and programmable electrical stimulation. *Am J Physiol Regul Integr Comp Physiol,* 308**,** R755-68.
LIU, H., CHEN, C. H., ESPINOZA-LEWIS, R. A., JIAO, Z., SHEU, I., HU, X., LIN, M., ZHANG, Y. & CHEN, Y. 2011. Functional redundancy between human SHOX and mouse Shox2 genes in the regulation of sinoatrial node formation and pacemaking function. *J Biol Chem,* 286**,** 17029-38.
LO, P. C. & FRASCH, M. 2001. A role for the COUP-TF-related gene seven-up in the diversification of cardioblast identities in the dorsal vessel of Drosophila. *Mech Dev,* 104**,** 49-60.
LO, P. C., SKEATH, J. B., GAJEWSKI, K., SCHULZ, R. A. & FRASCH, M. 2002. Homeotic genes autonomously specify the anteroposterior subdivision of the Drosophila dorsal vessel into aorta and heart. *Dev Biol,* 251**,** 307-19.
LODDER, E. M., DE NITTIS, P., KOOPMAN, C. D., WISZNIEWSKI, W., MOURA DE SOUZA, C. F., LAHROUCHI, N., GUEX, N., NAPOLIONI, V., TESSADORI, F., BEEKMAN, L., NANNENBERG, E. A., BOUALLA, L., BLOM, N. A., DE GRAAFF, W., KAMERMANS, M., COCCIADIFERRO, D., MALERBA, N., MANDRIANI, B., AKDEMIR, Z. H., FISH, R. J., ELDOMERY, M. K., RATBI, I., WILDE, A. A., DE BOER, T., SIMONDS, W. F., NEERMAN-ARBEZ, M., SUTTON, V. R., KOK, F., LUPSKI, J. R., REYMOND, A., BEZZINA, C. R., BAKKERS, J. & MERLA, G. 2016. GNB5 Mutations Cause an Autosomal-Recessive Multisystem Syndrome with Sinus Bradycardia and Cognitive Disability. *Am J Hum Genet,* 99**,** 704-10.
MA, L., LU, M. F., SCHWARTZ, R. J. & MARTIN, J. F. 2005. Bmp2 is essential for cardiac cushion epithelial-mesenchymal transition and myocardial patterning. *Development,* 132**,** 5601-11.
MALTSEV, V. A., VINOGRADOVA, T. M. & LAKATTA, E. G. 2006. The emergence of a general theory of the initiation and strength of the heartbeat. *J Pharmacol Sci,* 100**,** 338-69.
MANN, T., BODMER, R. & PANDUR, P. 2009. The Drosophila homolog of vertebrate Islet1 is a key component in early cardiogenesis. *Development,* 136**,** 317-26.
MANNER, J., WESSEL, A. & YELBUZ, T. M. 2010. How does the tubular embryonic heart work? Looking for the physical mechanism generating unidirectional blood flow in the valveless embryonic heart tube. *Dev Dyn,* 239**,** 1035-46.
MEDIONI, C., SENATORE, S., SALMAND, P. A., LALEVEE, N., PERRIN, L. & SEMERIVA, M. 2009. The fabulous destiny of the Drosophila heart. *Curr Opin Genet Dev,* 19**,** 518-25.
MEIJLER, F. L. & MEIJLER, T. D. 2011. Archetype, adaptation and the mammalian heart. *Neth Heart J,* 19**,** 142-148.
MERCOLA, M., GUZZO, R. M. & FOLEY, A. C. 2010. Cardiac Development in the Frog. *In:* ROSENTHAL, N. & HARVEY, R. P. (eds.) *Heart Development and Regeneration.* Elsevier.
MITCHELL, M. A. 2009. Reptile cardiology. *Vet Clin North Am Exot Anim Pract,* 12**,** 65-79, vi.
MOLINA, M. R. & CRIPPS, R. M. 2001. Ostia, the inflow tracts of the Drosophila heart, develop from a genetically distinct subset of cardial cells. *Mech Dev,* 109**,** 51-9.
MOMMERSTEEG, M. T., DOMINGUEZ, J. N., WIESE, C., NORDEN, J., DE GIER-DE VRIES, C., BURCH, J. B., KISPERT, A., BROWN, N. A., MOORMAN, A. F. & CHRISTOFFELS, V. M. 2010. The sinus venosus progenitors separate and diversify from the first and second heart fields early in development. *Cardiovasc Res,* 87**,** 92-101.
MOMMERSTEEG, M. T., HOOGAARS, W. M., PRALL, O. W., DE GIER-DE VRIES, C., WIESE, C., CLOUT, D. E., PAPAIOANNOU, V. E., BROWN, N. A., HARVEY, R. P., MOORMAN, A. F. & CHRISTOFFELS, V. M. 2007. Molecular pathway for the localized formation of the sinoatrial node. *Circ Res,* 100**,** 354-62.
MONTGOMERY, R. L., DAVIS, C. A., POTTHOFF, M. J., HABERLAND, M., FIELITZ, J., QI, X., HILL, J. A., RICHARDSON, J. A. & OLSON, E. N. 2007. Histone deacetylases 1 and 2 redundantly regulate cardiac morphogenesis, growth, and contractility. *Genes Dev,* 21**,** 1790-802.
MOORMAN, A. F. & CHRISTOFFELS, V. M. 2003. Cardiac chamber formation: development, genes, and evolution. *Physiol Rev,* 83**,** 1223-67.
MORI, A. D., ZHU, Y., VAHORA, I., NIEMAN, B., KOSHIBA-TAKEUCHI, K., DAVIDSON, L., PIZARD, A., SEIDMAN, J. G., SEIDMAN, C. E., CHEN, X. J., HENKELMAN, R. M. & BRUNEAU, B. G. 2006. Tbx5-dependent rheostatic control of cardiac gene expression and morphogenesis. *Dev Biol,* 297**,** 566-86.

NEMTSAS, P., WETTWER, E., CHRIST, T., WEIDINGER, G. & RAVENS, U. 2010. Adult zebrafish heart as a model for human heart? An electrophysiological study. *J Mol Cell Cardiol,* 48**,** 161-71.

OLSON, E. N. 2006. Gene regulatory networks in the evolution and development of the heart. *Science,* 313**,** 1922-7.

OPTHOF, T. 1988. The mammalian sinoatrial node. *Cardiovasc Drugs Ther,* 1**,** 573-97.

PEREZ-POMARES, J. M., GONZALEZ-ROSA, J. M. & MUNOZ-CHAPULI, R. 2009. Building the vertebrate heart - an evolutionary approach to cardiac development. *Int J Dev Biol,* 53**,** 1427-43.

POPE, E. C. & ROWLEY, A. F. 2002. The heart of Ciona intestinalis: eicosanoid-generating capacity and the effects of precursor fatty acids and eicosanoids on heart rate. *J Exp Biol,* 205**,** 1577-83.

REECY, J. M., LI, X., YAMADA, M., DEMAYO, F. J., NEWMAN, C. S., HARVEY, R. P. & SCHWARTZ, R. J. 1999. Identification of upstream regulatory regions in the heart-expressed homeobox gene Nkx2-5. *Development,* 126**,** 839-49.

REIM, I. & FRASCH, M. 2005. The Dorsocross T-box genes are key components of the regulatory network controlling early cardiogenesis in Drosophila. *Development,* 132**,** 4911-25.

REIM, I., MOHLER, J. P. & FRASCH, M. 2005. Tbx20-related genes, mid and H15, are required for tinman expression, proper patterning, and normal differentiation of cardioblasts in Drosophila. *Mech Dev,* 122**,** 1056-69.

S, O. O. & SAITOU, N. 1999. Phylogenetic relationship of muscle tissues deduced from superimposition of gene trees. *Mol Biol Evol,* 16**,** 856-67.

SAKAI, T. & KAMINO, K. 2015. Functiogenesis of cardiac pacemaker activity. *J Physiol Sci*.

SATOU, Y. & SATOH, N. 2006. Gene regulatory networks for the development and evolution of the chordate heart. *Genes Dev,* 20**,** 2634-8.

SEDMERA, D., RECKOVA, M., DEALMEIDA, A., SEDMEROVA, M., BIERMANN, M., VOLEJNIK, J., SARRE, A., RADDATZ, E., MCCARTHY, R. A., GOURDIE, R. G. & THOMPSON, R. P. 2003. Functional and morphological evidence for a ventricular conduction system in zebrafish and Xenopus hearts. *Am J Physiol Heart Circ Physiol,* 284**,** H1152-60.

SEEBACHER, F. & FRANKLIN, C. E. 2005. Physiological mechanisms of thermoregulation in reptiles: a review. *J Comp Physiol B,* 175**,** 533-41.

SIMOES-COSTA, M. S., VASCONCELOS, M., SAMPAIO, A. C., CRAVO, R. M., LINHARES, V. L., HOCHGREB, T., YAN, C. Y., DAVIDSON, B. & XAVIER-NETO, J. 2005. The evolutionary origin of cardiac chambers. *Dev Biol,* 277**,** 1-15.

SIZAROV, A., DEVALLA, H. D., ANDERSON, R. H., PASSIER, R., CHRISTOFFELS, V. M. & MOORMAN, A. F. 2011a. Molecular analysis of patterning of conduction tissues in the developing human heart. *Circ Arrhythm Electrophysiol,* 4**,** 532-42.

SIZAROV, A., YA, J., DE BOER, B. A., LAMERS, W. H., CHRISTOFFELS, V. M. & MOORMAN, A. F. 2011b. Formation of the building plan of the human heart: morphogenesis, growth, and differentiation. *Circulation,* 123**,** 1125-35.

SOLC, D. 2007. The heart and heart conducting system in the kingdom of animals: A comparative approach to its evolution. *Exp Clin Cardiol,* 12**,** 113-8.

STAINIER, D. Y. 2001. Zebrafish genetics and vertebrate heart formation. *Nat Rev Genet,* 2**,** 39-48.

STAINIER, D. Y., FOUQUET, B., CHEN, J. N., WARREN, K. S., WEINSTEIN, B. M., MEILER, S. E., MOHIDEEN, M. A., NEUHAUSS, S. C., SOLNICA-KREZEL, L., SCHIER, A. F., ZWARTKRUIS, F., STEMPLE, D. L., MALICKI, J., DRIEVER, W. & FISHMAN, M. C. 1996. Mutations affecting the formation and function of the cardiovascular system in the zebrafish embryo. *Development,* 123**,** 285-92.

STEFANOVIC, S., BARNETT, P., VAN DUIJVENBODEN, K., WEBER, D., GESSLER, M. & CHRISTOFFELS, V. M. 2014. GATA-dependent regulatory switches establish atrioventricular canal specificity during heart development. *Nat Commun,* 5**,** 3680.

STOLFI, A., GAINOUS, T. B., YOUNG, J. J., MORI, A., LEVINE, M. & CHRISTIAEN, L. 2010. Early chordate origins of the vertebrate second heart field. *Science,* 329**,** 565-8.

STOYEK, M. R., CROLL, R. P. & SMITH, F. M. 2015. Intrinsic and extrinsic innervation of the heart in zebrafish (Danio rerio). *J Comp Neurol,* 523**,** 1683-700.

STOYEK, M. R., QUINN, T. A., CROLL, R. P. & SMITH, F. M. 2016. Zebrafish heart as a model to study the integrative autonomic control of pacemaker function. *Am J Physiol Heart Circ Physiol,* 311**,** H676-88.

SUN, C., YU, D., YE, W., LIU, C., GU, S., SINSHEIMER, N. R., SONG, Z., LI, X., CHEN, C., SONG,

Y., WANG, S., SCHRADER, L. & CHEN, Y. 2015. The short stature homeobox 2 (Shox2)-bone morphogenetic protein (BMP) pathway regulates dorsal mesenchymal protrusion development and its temporary function as a pacemaker during cardiogenesis. *J Biol Chem,* 290**,** 2007-23.

TAO, Y. & SCHULZ, R. A. 2007. Heart development in Drosophila. *Semin Cell Dev Biol,* 18**,** 3-15.

TAYLOR, E. W., JORDAN, D. & COOTE, J. H. 1999. Central control of the cardiovascular and respiratory systems and their interactions in vertebrates. *Physiol Rev,* 79**,** 855-916.

TAYLOR, E. W., LEITE, C. A. & LEVINGS, J. J. 2009. Central control of cardiorespiratory interactions in fish. *Acta Histochem,* 111**,** 257-67.

TAYLOR, E. W., LEITE, C. A. & SKOVGAARD, N. 2010. Autonomic control of cardiorespiratory interactions in fish, amphibians and reptiles. *Braz J Med Biol Res,* 43**,** 600-10.

TESSADORI, F., VAN WEERD, J. H., BURKHARD, S. B., VERKERK, A. O., DE PATER, E., BOUKENS, B. J., VINK, A., CHRISTOFFELS, V. M. & BAKKERS, J. 2012. Identification and functional characterization of cardiac pacemaker cells in zebrafish. *PLoS One,* 7**,** e47644.

TSUTSUI, H., HIGASHIJIMA, S., MIYAWAKI, A. & OKAMURA, Y. 2010. Visualizing voltage dynamics in zebrafish heart. *J Physiol,* 588**,** 2017-21.

VEDANTHAM, V., EVANGELISTA, M., HUANG, Y. & SRIVASTAVA, D. 2013. Spatiotemporal regulation of an Hcn4 enhancer defines a role for Mef2c and HDACs in cardiac electrical patterning. *Dev Biol,* 373**,** 149-62.

VEDANTHAM, V., GALANG, G., EVANGELISTA, M., DEO, R. C. & SRIVASTAVA, D. 2015. RNA sequencing of mouse sinoatrial node reveals an upstream regulatory role for Islet-1 in cardiac pacemaker cells. *Circ Res,* 116**,** 797-803.

VERHOEVEN, M. C., HAASE, C., CHRISTOFFELS, V. M., WEIDINGER, G. & BAKKERS, J. 2011. Wnt signaling regulates atrioventricular canal formation upstream of BMP and Tbx2. *Birth Defects Res A Clin Mol Teratol,* 91**,** 435-40.

VERKERK, A. O., WILDERS, R., VAN BORREN, M. M., PETERS, R. J., BROEKHUIS, E., LAM, K., CORONEL, R., DE BAKKER, J. M. & TAN, H. L. 2007. Pacemaker current (I(f)) in the human sinoatrial node. *Eur Heart J,* 28**,** 2472-8.

VICENTE-STEIJN, R., KOLDITZ, D. P., MAHTAB, E. A., ASKAR, S. F., BAX, N. A., LM, V. D. G., WISSE, L. J., PASSIER, R., PIJNAPPELS, D. A., SCHALIJ, M. J., POELMANN, R. E., GITTENBERGER, D. E. G. A. C. & JONGBLOED, M. R. 2010. Electrical activation of sinus venosus myocardium and expression patterns of RhoA and Isl-1 in the chick embryo. *J Cardiovasc Electrophysiol,* 21**,** 1284-92.

VOZZI, C., DUPONT, E., COPPEN, S. R., YEH, H. I. & SEVERS, N. J. 1999. Chamber-related differences in connexin expression in the human heart. *J Mol Cell Cardiol,* 31**,** 991-1003.

WANG, J., KLYSIK, E., SOOD, S., JOHNSON, R. L., WEHRENS, X. H. & MARTIN, J. F. 2010. Pitx2 prevents susceptibility to atrial arrhythmias by inhibiting left-sided pacemaker specification. *Proc Natl Acad Sci U S A,* 107**,** 9753-8.

WARREN, K. S., BAKER, K. & FISHMAN, M. C. 2001. The slow mo mutation reduces pacemaker current and heart rate in adult zebrafish. *Am J Physiol Heart Circ Physiol,* 281**,** H1711-9.

WASSERTHAL, L. T. 2007. Drosophila flies combine periodic heartbeat reversal with a circulation in the anterior body mediated by a newly discovered anterior pair of ostial valves and ‚venous' channels. *J Exp Biol,* 210**,** 3707-19.

WEINBERGER, F., MEHRKENS, D., FRIEDRICH, F. W., STUBBENDORFF, M., HUA, X., MULLER, J. C., SCHREPFER, S., EVANS, S. M., CARRIER, L. & ESCHENHAGEN, T. 2012. Localization of Islet-1-positive cells in the healthy and infarcted adult murine heart. *Circ Res,* 110**,** 1303-10.

WIESE, C., GRIESKAMP, T., AIRIK, R., MOMMERSTEEG, M. T., GARDIWAL, A., DE GIER-DE VRIES, C., SCHUSTER-GOSSLER, K., MOORMAN, A. F., KISPERT, A. & CHRISTOFFELS, V. M. 2009. Formation of the sinus node head and differentiation of sinus node myocardium are independently regulated by Tbx18 and Tbx3. *Circ Res,* 104**,** 388-97.

WILKINSON, R. N., JOPLING, C. & VAN EEDEN, F. J. 2014. Zebrafish as a model of cardiac disease. *Prog Mol Biol Transl Sci,* 124**,** 65-91.

WYNEKEN, J. 2009. Normal reptile heart morphology and function. *Vet Clin North Am Exot Anim Pract,* 12**,** 51-63, vi.

XAVIER-NETO, J., DAVIDSON, B., SIMOES-COSTA, M. S., CASTRO, R. A., CASTILLO, H. A., COELHO SAMPAIO, A. & AZAMBUJA, A. P. 2010. Evolutionary Origins of Hearts. *In:* ROSENTHAL, N. & HARVEY, R. P. (eds.) *Heart Development and Regeneration.* Elsevier.

YANIV, Y., LAKATTA, E. G. & MALTSEV, V. A. 2015. From two competing oscillators to one coupled-clock pacemaker cell system. *Front Physiol,* 6**,** 28.

YE, W., WANG, J., SONG, Y., YU, D., SUN, C., LIU, C., CHEN, F., ZHANG, Y., WANG, F., HARVEY, R. P., SCHRADER, L., MARTIN, J. F. & CHEN, Y. 2015. A common Shox2-Nkx2-5 antagonistic mechanism primes the pacemaker cell fate in the pulmonary vein myocardium and sinoatrial node. *Development,* 142**,** 2521-32.

ZAFFRAN, S., XU, X., LO, P. C., LEE, H. H. & FRASCH, M. 2002. Cardiogenesis in the Drosophila model: control mechanisms during early induction and diversification of cardiac progenitors. *Cold Spring Harb Symp Quant Biol,* 67**,** 1-12.

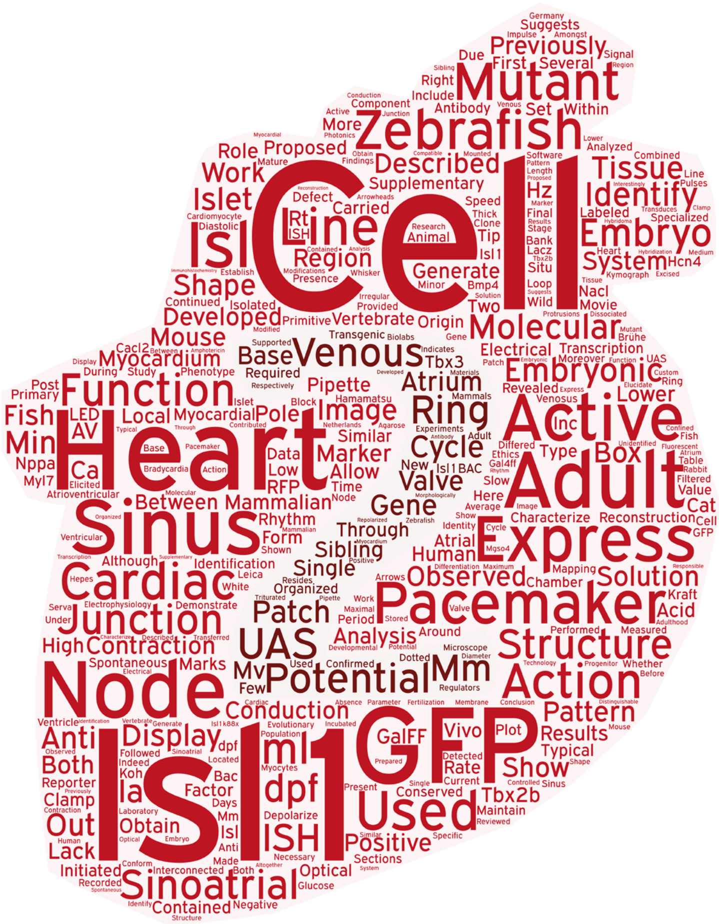
Cell
Isl1
Heart
Node
GFP
Adult
Express
Active
Sinus
Pacemaker
Mutant
Zebrafish
Action
Structure
Junction
Cardiac
Function
Sinoatrial
Potential
UAS
Used
Venous
Molecular
Embryonic
Embryo
Line
Isl
Islet
Tissue
Identify
Previously
Described
Region
Shape
Developed
Mouse
Myocardium
Ring
Atrium
Cycle
Valve
Gene
Patch
Mm
ml
dpf
ISH
GalFF
Vivo
Plot
Results
Show
Pattern
Conduction
Display
Anti
Both
Obtain
Out
Lack
Positive
Contraction
Solution
Observed
Mammalian
Between
Image
Marker
Work
Proposed
Role
Supplementary
Generate
Box
Fish
Min

CHAPTER 2

Identification and Functional Characterization of Cardiac Pacemaker Cells in Zebrafish

Federico Tessadori [1], Jan Hendrik van Weerd [2,*], **Silja B. Burkhard** [1,*], Arie O. Verkerk [2], Emma de Pater [1], Bastiaan J. Boukens [2], Aryan Vink [3], Vincent M. Christoffels [2,#], Jeroen Bakkers [1,4,#]

[1] Hubrecht Institute-KNAW & University Medical Centre Utrecht, The Netherlands.
[2] Department of Anatomy, Embryology and Physiology, Heart Failure Research Center, Academic Medical Center, University of Amsterdam, The Netherlands.
[3] Department of Pathology, University Medical Center Utrecht, The Netherlands.
[4] Interuniversity Cardiology Institute of the Netherlands, 3584CT Utrecht, The Netherlands.

[*] These authors contributed equally.

PLoS One. 2012;7(10) e47644. doi:10.1371/journal.pone.0047644

2

ABSTRACT

In the mammalian heart a conduction system of nodes and conducting cells generates and transduces the electrical signals evoking myocardial contractions. Specialized pacemaker cells initiating and controlling cardiac contraction rhythmicity are localized in an anatomically identifiable structure of myocardial origin, the sinus node. We previously showed that in mammalian embryos sinus node cells originate from cardiac progenitors expressing the transcription factors T-box transcription factor 3 (Tbx3) and Islet-1 (Isl1). Although cardiac development and function are strikingly conserved amongst animal classes, in lower vertebrates neither structural nor molecular distinguishable components of a conduction system have been identified, questioning its evolutionary origin. Here we show that zebrafish embryos lacking the LIM/ homeodomain-containing transcription factor Isl1 display heart rate defects related to pacemaker dysfunction. Moreover, 3D reconstructions of gene expression patterns in the embryonic and adult zebrafish heart led us to uncover a previously unidentified, Isl1-positive and Tbx2b-positive region in the myocardium at the junction of the sinus venosus and atrium. Through their long interconnecting cellular protrusions, the identified Isl1-positive cells form a ring-shaped structure. In vivo labeling of the Isl1-positive cells by transgenic technology allowed their isolation and electrophysiological characterization, revealing their unique pacemaker activity. In conclusion, we demonstrate that Isl1-expressing cells, organized as a ring-shaped structure around the venous pole, hold the pacemaker function in the adult zebrafish heart. We have thereby identified an evolutionary conserved, structural and molecular distinguishable component of the cardiac conduction system in a lower vertebrate.

INTRODUCTION

The cardiac conduction system comprises several components, amongst which the sinus node, the site of electrical impulse generation, and the Purkinje fibers transducing the impulse rapidly through the myocardium (Christoffels et al., 2010). The sinus node harbors specialized pacemaker cells which, due to regular and spontaneous membrane depolarization, generate the electrical signal necessary to induce cardiomyocyte contractions (Mangoni and Nargeot, 2008). Although the sinus node was described histologically and functionally more than a century ago (Flack, 1910), the molecular regulators required for pacemaker cell differentiation and function are not fully understood. Nonetheless, several recent developments have provided new insights. These include identification of the embryonic origins of the sinus- and atrioventricular nodes (Wiese et al., 2009, Christoffels et al., 2006) and of several transcriptional regulators involved in their development (reviewed in (Christoffels et al., 2010)). A major advance for the field was the identification of T-box transcription factor 3 (Tbx3) in pacemaker cells, and the subsequent demonstration that it is required for sinus- and atrioventricular node development and postnatal homeostasis (Frank et al., 2012, Hoogaars et al., 2007). Other transcriptional regulators that have been identified for their role in sinus node development are Nkx2.5, Tbx5, Pitx2 and Shox2 (Dupays et al., 2005, Blaschke et al., 2007, Espinoza-Lewis et al., 2009, Puskaric et al., 2010, Ammirabile et al., 2012, Mommersteeg et al., 2007). The molecular signature of the mouse sinus node primordium has been confirmed in human embryonic hearts, indicating evolutionary conservation of the developmental mechanism (Sizarov et al., 2011). Although the presence of specialized conduction system components in the heart of lower vertebrates has been suggested by functional analysis (Arrenberg et al., 2010, Milan et al., 2006, Chi et al., 2008), their identification has remained elusive due to the lack of morphologically distinctive structures and molecular markers. Our research presented in this manuscript resolved this issue by describing the first molecular and structural identification of specialized cardiac pacemaker cells in the embryonic and adult zebrafish heart, utilizing a combination of *in vivo* microscopic examination, 3D gene expression pattern reconstruction, reporter transgenics and *ex vivo* electrophysiology. Our findings establish that Islet-1 is required for pacemaker activity in the embryonic heart and that Islet-1 marks the pacemaker cells in the adult heart, which represents a previously unappreciated role for Isl1 in the cardiac conduction system.

RESULTS AND DISCUSSION

Cardiac pacemaker activity is affected in Islet-1 mutant hearts

Zebrafish embryos lacking functional Isl1 protein are immobile and display reduced heart rate (bradycardia) at 2 days post fertilization (dpf) (de Pater et al., 2009). Unlike the mouse *Isl1* mutant hearts that fail to loop and lack recognizable chambers (Cai et al., 2003), zebrafish *isl1* mutant hearts loop normally and are morphologically indistinguishable from their wild-type siblings at 2 days post fertilization (dpf), allowing their functional characterization. To identify the primary defect responsible for the observed bradycardia phenotype we further investigated the heart rhythm in *isl1* mutant embryos by high-speed video imaging combined with functional image analysis. Both the *isl1* mutant and wild-type sibling embryos showed initiation of contraction in the inflow region (venous pole) continuing in the atrium, followed by rapid contraction of the ventricle (Supplementary Movies S1 and S2). To quantify heart rhythm, we drew kymographs for atrium and ventricle of sibling and mutant hearts using a 1 pixel-thick collection of lines positioned perpendicularly to the blood flow (Fig. 1A, white dotted lines). The resulting kymographs (Fig.1B) readily confirmed the bradycardia of the *isl1* mutant, as the distance between two dotted lines encompassing a full cardiac cycle (Fig.1B, white double arrows) is much longer in the mutant than in the sibling. Moreover, the kymograph-based quantification of the cardiac cycle (interval necessary for one complete contraction) illustrates the slow and irregular heart rhythm in *isl1* mutant embryos (Fig. 1C). Cardiac cycles of the imaged *isl1* mutants oscillated between about 450 ms and 800 ms, showing not only high variability within a single embryo (Fig. 1C, box-whisker plots for mutants; maximal and minimal values vary of about 200 ms for all mutants analyzed), but also between different individuals (Fig.1C, mutants 1,2 and 3 display average cardiac cycle period times of 586 ms, 661 ms and 494 ms respectively over the recording time). In comparison, siblings displayed a maximal variation in cardiac cycle measured at the atrium of about 20 ms and average cardiac cycle periods of 325 ms (Fig. 1C, Supplementary Movie S1). We never observed uncoupling of the atrial and ventricular contraction, fibrillation or atrioventricular block, as every atrial contraction was followed by a ventricular contraction (Fig. 1B; Supplementary Movie S2).

As development proceeded, the severity of the heart beat phenotype increased. We frequently observed a sinus block in *isl1* mutant hearts at 3-4 dpf resulting in the absence of atrial and ventricular contraction for 10-20 seconds (Fig. 1D). Altogether, the combination of phenotypes displayed by the *isl1* mutant is compatible with defective initiation of contraction, suggesting faulty pacemaker activity.

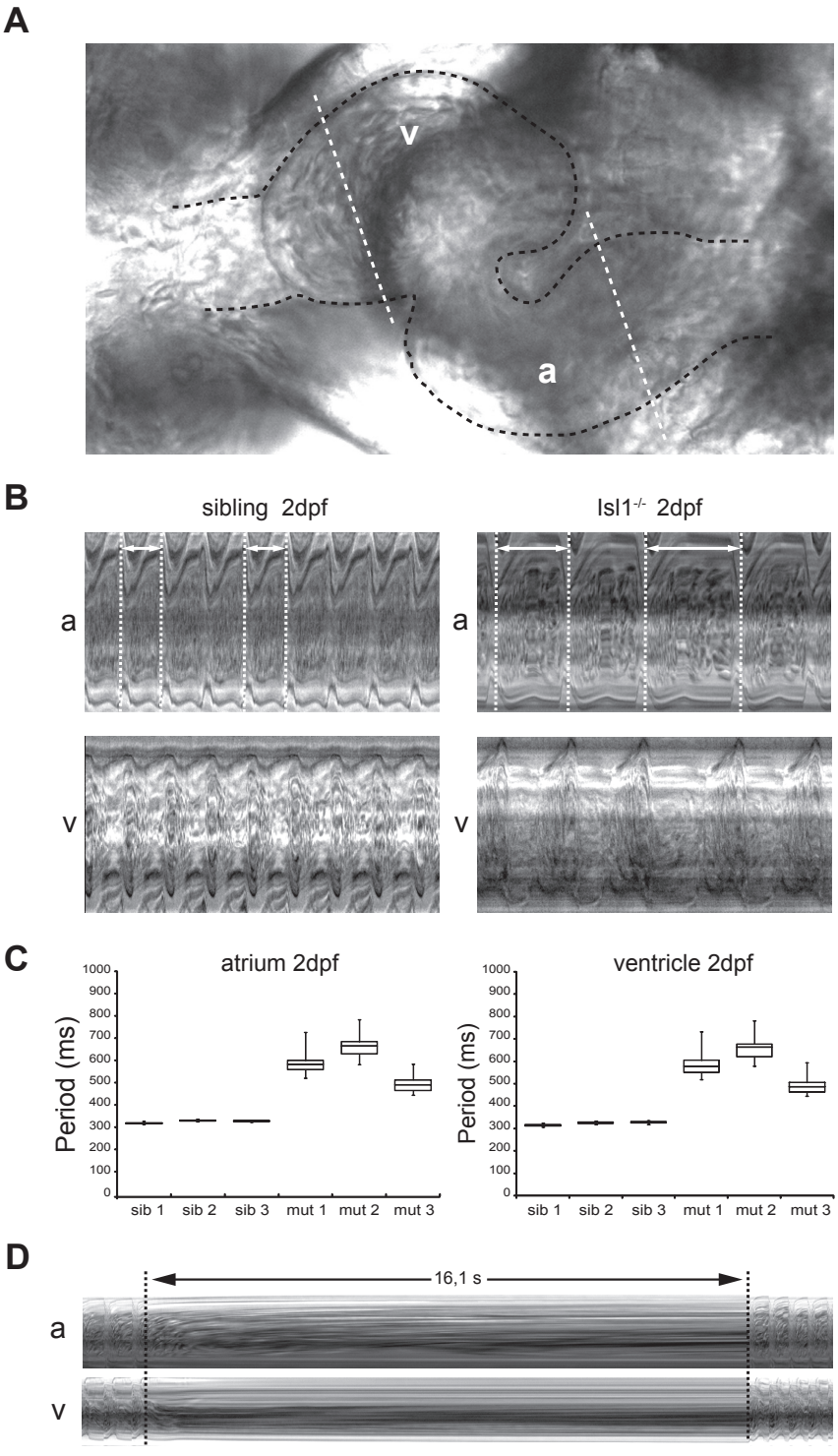
A
v
a
B
sibling 2dpf
Isl1-/- 2dpf
a
a
v
v
C
atrium 2dpf
ventricle 2dpf
Period (ms)
Period (ms)
1000
900
800
700
600
500
400
300
200
100
0
sib 1
sib 2
sib 3
mut 1
mut 2
mut 3
D
16,1 s
a
v

Figure 1: Characterization of the embryonic Isl1$^{-/-}$ cardiac phenotype *in vivo*.

(A) Zebrafish embryonic heart at 2 dpf. The embryonic heart is highlighted in black dotted contour; white dotted lines through the atrium (a) and the ventricle (v) are placed at kymograph positions. **(B)** Atrial (a) and ventricular (v) kymographs from 2 dpf embryonic hearts spanning approximately 2.8 s. Note the much longer period of the Isl$^{-/-}$ heart when compared to the sibling and the irregularity of the period (double arrow and white dotted vertical lines). Movies are available as Movies S1 and S2, respectively. **(C)** Box-whisker plots representation of 20 successive heartbeats of 2 dpf Isl1$^{-/-}$ and sibling embryos. **(D)** Kymograph recorded at 3 dpf covering a period of about 16 s of absent heart contractions. For all panels a: atrium; v: ventricle.

Isl1 is expressed at the putative sinoatrial boundary of the embryonic and adult heart.

In mammals, including humans, the primary pacemaker function is held by the sinus node, which resides at the junction of the superior caval vein and right atrium (Dobrzynski et al., 2005, Glukhov et al., 2010, Sanchez-Quintana et al., 2005, Yamamoto et al., 2006). For example, in mouse, the right sinus venosus was shown to form the sinus node, which includes the venous lining of the right venous valve (Mommersteeg et al., 2007, Wiese et al., 2009). Isl1-expressing cells are found in the developing and mature mammalian sinus node (Weinberger et al., 2012, Sun et al., 2007, Sizarov et al., 2011).

We hypothesized that Isl1 expression marks the pacemaker tissue in the zebrafish heart, as no molecular markers for the zebrafish sinus node or the pacemaker cells within it have been identified to date. Using an antibody recognizing both zebrafish Isl1 and Isl2 (Hutchinson and Eisen, 2006) we observed few Isl-positive cells in both the dorsal and ventral regions of the proposed sinoatrial junction at 2 dpf (Fig. 2A-D), consistent with the proposed pacemaker function at the sinoatrial junction in the zebrafish heart (Arrenberg et al., 2010). The Isl-expressing cells expressed *Tg(myl7:eGFP)*, which marks cardiomyocytes. Isl expression at the sinoatrial junction was detected continuously during development and was maintained in the same region in the adult zebrafish heart (Fig. 2E-H). This indicates that Isl expression in the zebrafish sinoatrial junction is continuous between embryonic stages and adulthood. We continued by molecular characterization of the proposed sinoatrial junction region in the adult heart using in situ hybridization (ISH). Contrary to what has been observed in mammals, the zebrafish sinus venosus did not express the myocardial marker *myl7.* Consequently, the upstream border of myocardium muscle was at the venous valves and atrium (Fig. 3A, B). We observed that *isl1* expression was confined to the myocardium located at the base of the venous valves (Fig. 3C). The zebrafish orthologue of *hcn4* encodes a member of the family of ion channels responsible for the hyperpolarization-activated current, I_f, in pacemaker cells. Its expression is

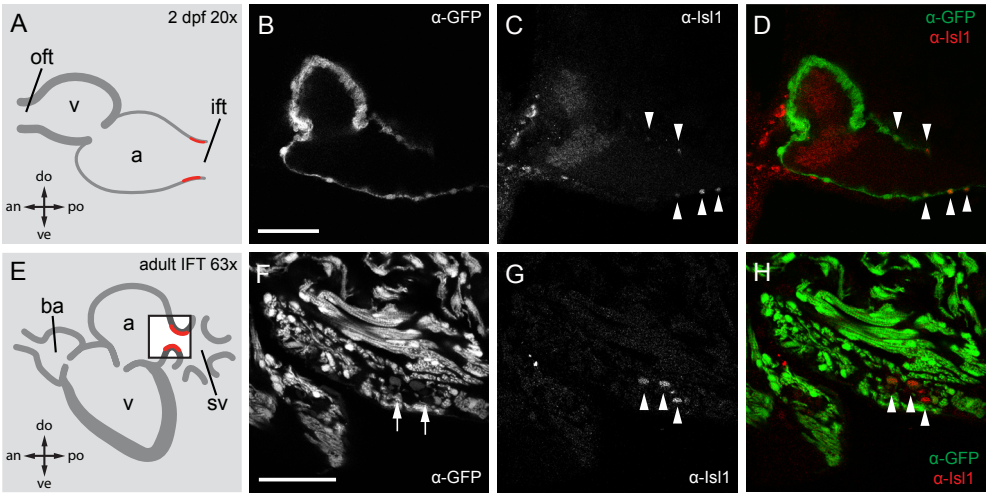

Figure 2: Isl1 expression in the embryonic and adult zebrafish heart.

Single confocal scans of a fluorescent antibody labeling of Isl1 and eGFP in embryonic (2 dpf) **(A–D)** and adult **(E–H)** zebrafish expressing Tg(*myl7*:eGFP) in all cardiomyocytes. GFP$^+$ cardiomyocytes are displayed in grey (B, F) and in green in (D, H). Isl1 is shown in grey (C, G) and in red (D, H). Arrowheads indicate Isl$^+$/GFP$^+$ cells. Illustrations of a lateral view of a 2 dpf (A) and adult (E) zebrafish heart indicate the location of Isl1$^+$ cells (red). The box in panel E represents the area shown in (F–H). **(B–D)** Fluorescent immunolabeling of Isl1 and eGFP in a 2 dpf embryo (sagittal section 100 mm). At this time point Isl1$^+$/GFP$^+$ cells were only found in the IFT of the heart. **(F–H)** Fluorescent immunolabeling of Isl1 and eGFP in an adult zebrafish heart (sagittal section 100 mm). Isl1$^+$/GFP$^+$ cells are located at the junction of the sinus venosus and atrium in the inflow region of the heart (arrowheads). Isl1$^+$ cells showed low expression of *myl7*. v, ventricle; a, atrium; oft, outflow tract; ift, inflow tract; ba, bulbus arteriosus; sv, sinus venosus; a, anterior; p, posterior; d, dorsal; v, ventral. Scale bars represent 50 µm.

enriched in pacemaker tissue of mammalian hearts (Verkerk et al., 2007, Shi et al., 1999, Yamamoto et al., 2006, Baruscotti et al., 2011, Moosmang et al., 2001). In the zebrafish adult heart *hcn4* had a broader expression pattern than *isl1* (Fig. 3D), similar to observations made in the mammalian embryonic heart (Mommersteeg et al., 2007, Sizarov et al., 2011). Expression of the two genes overlapped at the sinoatrial junction, (Fig. 3D). A 3D reconstruction based on a series of ISH on sagittal adult heart sections revealed that *isl1* expression is confined to a ring-like structure within the myocardial tissue at the base of the venous valves, around the proposed sinoatrial junction (Fig. 3F). In the mammalian heart expression of *Nppa* is specific for the fast conducting working myocardium of the atrium and ventricle but is not expressed in the slow conducting primitive myocardium of the pacemaker tissue at the sinoatrial junction (Mommersteeg et al., 2007). We observed a very similar mutually exclusive expression pattern of *nppa* and *isl1* in the sinoatrial junction of

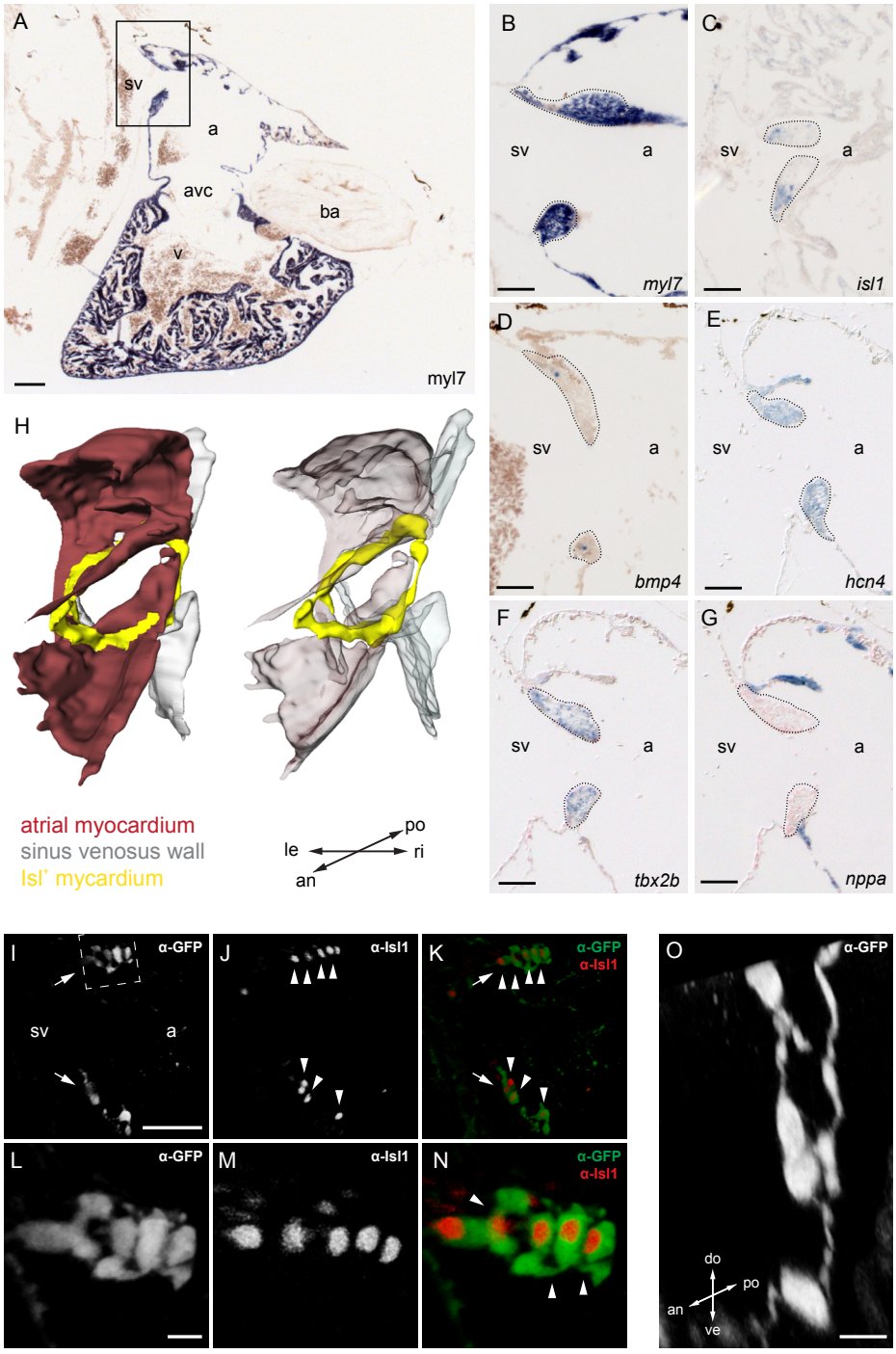
A
sv
a
avc
ba
v
myl7
B
sv
a
myl7
C
sv
a
isl1
D
sv
a
bmp4
E
sv
a
hcn4
F
sv
a
tbx2b
G
sv
a
nppa
H
atrial myocardium
sinus venosus wall
Isl+ mycardium
po
le
ri
an
I
α-GFP
sv
a
J
α-Isl1
K
α-GFP
α-Isl1
L
α-GFP
M
α-Isl1
N
α-GFP
α-Isl1
O
α-GFP
do
po
an
ve

Figure 3: Molecular characterization of the adult isl1 expression domain.

(A–E,G,H) Section in-situ hybridizations on adult wild-type zebrafish hearts. Probes are indicated in the panels. (A) 4-chamber view of a sagittal section through zebrafish heart labeled with the myocardial marker *myl7*. The box indicates the region shown enlarged in panels B–E,G,H. Demarcated areas (C) indicate isl1 expression in the *tbx2b+ hcn4+ nppa-* myocardium at the base of the valves surrounding the sinoatrial junction. BMP4 signal is pointed at in the valves by arrowheads in (H). **(F)** 3D reconstruction of the sinoatrial junction. *isl1* (yellow) is expressed around the entire sinoatrial junction, forming a ring-like structure. **(I–L)** Reconstruction of a confocal scan through a sagittal section of the inflow region of adult Tg(isl1BAC:GalFF; UAS:GFP) transgenic zebrafish heart. Fluorescent antibody labeling for GFP (shown in grey (I, I', L) or green (K, K')) and for Isl1 (shown in grey (J, J') or red (K, K')). GFP+/Isl1+ cells were found in bilateral populations at the sinoatrial junction (arrows). (I'–K') Enlargement of the GFP+/Isl1+ cells at the dorsal rim of the inflow tract (indicated with dashed box in (I)). Nuclei of GFP+ cells were positive for Isl1 (arrowheads). (L) Enlargement of GFP+ cells (transverse section) shows a string of contiguous cells. a, atrium; avc, atrioventricular canal; ba, bulbus arteriosus; sv, sinus venosus; v, ventricle; l, left; r, right; a, anterior; p, posterior; d, dorsal; v, ventral. Scale bars represent 50 µm (A–G, I–K) or 10 µm (I'–K',L).

the zebrafish heart (Fig. 3E). Furthermore, since *bmp4* and *tbx2b* are expressed at the venous pole of the embryonic heart ((de Pater et al., 2009) and Fig. S1) and since the *bmp4-tbx2b* regulatory axis suppresses chamber differentiation and *nppa* expression, we analyzed their expression in the adult heart. Interestingly, expression of *bmp4* and *tbx2b* was maintained in the myocardium of the proposed sinoatrial junction of the adult heart and restricted to the base of the venous valves or the entire venous valve tissue, respectively (Fig. 3G, H). In summary, we identified an *isl1*$^{+}$ cell population in the *hcn4*$^{+}$ *tbx2b*$^{+}$ *nppa*-negative myocardium that is organized in a ring-shape at the proposed sinoatrial junction. Together with the above-described observation that *isl1* mutants display irregular heart rhythms, this suggests that *isl1* expression identifies cardiac pacemaker cells in the zebrafish heart.

Using an Isl1-LacZ knock-in model, Isl1/LacZ activity was observed in the sinus node of the adult mouse heart (Weinberger et al., 2012). Corroborating these findings, we detected endogenous Isl1 expressing cells in the adult sinus node of the mouse heart using an anti-Isl antibody (Supplementary figure S2). Using a similar approach, we also detected Isl1 expressing cells in the sinus node of the adult human heart (Supplementary figure S3). Interestingly, we observed that only a sub-population of sinus node cells expresses Isl1, suggesting that the Isl1 expressing cells have different properties compared to the Isl1-negative sinus node cells.

Isl1 expressing cells display electrical pacemaker activity.

To functionally characterize the Isl1^{+} cells in the zebrafish heart, we generated an Isl1-GFP reporter line using the binary Gal4/UAS expression system (Supplementary figure S4). To validate the reporter line, we additionally confirmed that all GFP^{+} cells were co-labeled by Isl1 immunostaining (Fig. 3I-K' arrowheads). In vibratome sections

GFP$^+$ cells visualized by fluorescent antibody labeling were located in bilateral cell populations at the proposed sinoatrial junction (Fig. 3I-K, arrows), conform the ISH staining. Neighboring GFP+/Isl1+ cells displayed cytoplasmic protrusions, which may connect them between each other (Fig. 3K', arrowheads). 3D reconstruction of confocal image stacks revealed that Isl1+ pacemaker cells are interspersed with Isl-negative cells. However, they form a coherent structure (Fig. 3L). It is known that isolated groups of cells with residual pacemaker activity, such as remnant embryonic nodal atrioventricular canal myocytes, may cause cardiac arrhythmias (reviewed in (Christoffels and Moorman, 2009, Solc, 2007)). The cell-to-cell interconnection could therefore be an essential feature for proper pacemaker function, likely coordinating a synchronous activation of the myocardium. Moreover, the expression of myosin is low in Isl$^+$ cells, which is supportive for a primitive myocardial identity of these cells, typical for pacemaker cells (Supplementary Fig. S5) (Keith and Flack, 1907, Sanchez-Quintana et al., 2005, Viragh and Challice, 1980).

To elucidate whether the GFP$^+$ cells localize to the region in which the electrical activation is initiated, we performed optical mapping of epicardial activation patterns on adult zebrafish hearts. First moment of atrial activation corresponded with the localization of the GFP$^+$ cells (Fig. 4A-C), which is compatible with pacemaker function for *isl1* expressing cells. To unequivocally discriminate whether indeed *isl1* expression marks cells with pacemaker activity, dissociated single GFP$^+$ and GFP$^-$ cells from micro-dissected sinoatrial tissue were patch-clamped (Fig.4D). All measured GFP$^+$ cells (n=6) were spontaneously active, while all measured GFP$^-$ cells (n=8) were typically quiescent. In GFP$^-$ cells, action potentials could be elicited by current pulses through the patch pipette. Figure 4D shows typical spontaneous action potentials of a GFP$^+$ cell as well as typical action potentials recorded from a GFP$^-$ cell that was stimulated at 3 Hz, i.e. with a cycle length similar close to that of the GFP$^+$ cell (Table 1). All parameters, except for action potential duration at 90% repolarization (APD_{90}), differed significantly between both cell types (Table 1). GFP- cells had a stable resting membrane potential of -79.0 ± 1.6 mV, while GFP$^+$ cells showed a spontaneous diastolic depolarization rate (64 ± 17 mV/s) with a maximum diastolic potential of -65.0 ± 3.0 mV. In GFP$^+$ cells, this diastolic depolarization resulted in pacemaker activity with an intrinsic cycle length of 378 ± 58 ms. In GFP$^+$ cells, the maximum upstroke velocity was typically low (7.4 ± 2.6 V/s) as opposed to GFP$^-$ cells (112 ± 14 V/s). In both cell types, action potentials overshot the zero-potential value, but the action potential amplitude was higher in GFP$^-$ cells. Action potentials of GFP$^-$ cells repolarized earlier and faster, resulting in shorter APD_{20} and APD_{50}. Thus, the results obtained on the optical mapping and patch-clamp experiments revealed that while GFP$^-$ cells display characteristics specific to cardiac chamber myocytes, pacemaker activity resides in Isl$^+$/GFP$^+$ cells.

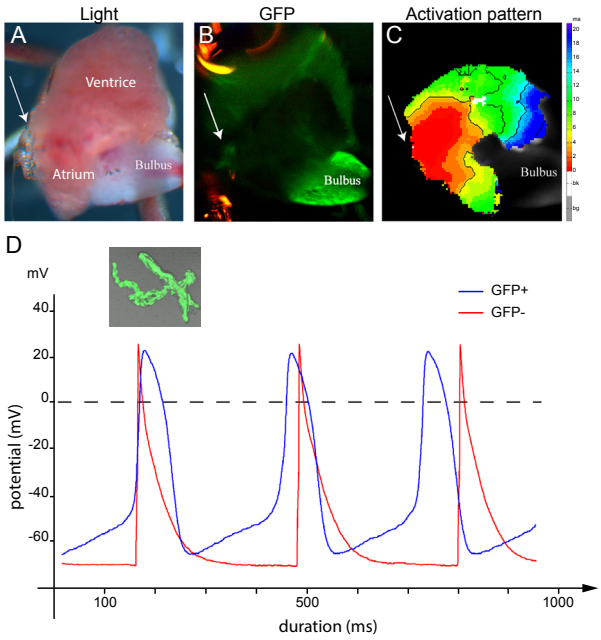

Figure 4: Isl1 cells have pacemaker activity.

(A–C) Optical mapping on an explanted, contracting adult zebrafish tg(isl1BAC:GalFF; UAS:GFP) heart. Arrow indicates the sinus venosus in all panels. (A) Explanted adult zebrafish heart. (B) GFP-fluorescent cells reporting Isl1 expression are situated at the sinus venosus. (C) The activation pattern measured by di-4-ANEPPS fluorescence shows that the GFP^+ myocytes are situated in the area of earliest activation. **(D)** Typical action potentials of freshly isolated GFP^+ and GFP^- myocytes. The GFP^- cell was stimulated at 3 Hz. The inset displays a representative example of a GFP^+ myocyte.

Table 1: Action potential characteristics of single GFP^+ and GFP^- cells.

	GFP^+ cells (n = 6)	GFP^- cells (n = 8)
cycle length (ms)	377±58	–
MDP (mV)	−65.0±3.0	−79.0±1.6*
DDR_{50} (mV/s)	63.4±16.8	–
dV/dt_{max} (V/s)	7.3±2.6	112±14*
APA (mV)	78.5±7.5	98.2±3.5*
APD_{20} (ms)	48.1±6.5	12.5±2.6*
APD_{50} (ms)	71.1±8.6	35.8±2.8*
APD_{90} (ms)	100.0±13.3	82.5±10.7

Data are mean±SEM; n = number of cells, MDP = maximal diastolic potential, DDR_{50} = diastolic depolarization rate over the 50-ms time interval starting at MDP+1 mV, dV/dt_{max} = maximal upstroke velocity, APA = action potential amplitude, APD_{20}, APD_{50}, and APD_{90} = action potential duration at 20, 50, and 90% repolarization. *$p<0.05$.

doi:10.1371/journal.pone.0047644.t001

CONCLUSIONS

We present here the molecular and functional identification of cardiac pacemaker cells in the embryonic and adult zebrafish heart. The embryonic cardiac expression pattern (Fig.2) and knockout phenotype of Isl1 in zebrafish (Fig.1) hinted at a role for this gene in pacemaker function. Indeed, analysis of 3D reconstructions of expression pattern and reporter transgenics in adult fish showed a previously unidentified ring-shaped region of *isl1* expression within the myocardium at the proposed sinoatrial junction of the mature zebrafish heart (Fig.3). Optical mapping of the activation sequence and electrophysiological characterization of single Isl1^{+} myocytes demonstrated the presence of pacemaker activity in the *isl1*-expressing cells (Fig. 4). Altogether, our data allow us to establish that (1) Isl1 is the first identified molecular marker for pacemaker cells in the zebrafish heart, (2) the functional pacemaker of the adult zebrafish heart is organized as a ring around the venous pole and (3) expression of Isl1 in the pacemaker cells of the adult heart is conserved from fish to human.

Cells pertaining to the primary pacemaker structure in zebrafish and mammals share a number of molecular markers, relative position in the heart, and functional identity. However, while in zebrafish the *isl1*-expressing pacemaker cells are few and organized in a ring-shaped structure of interconnected cells in the venous valves, the mammalian sinus node is a more compact, spindle-shaped (also referred to as comma-shaped) clearly demarcated structure. Although at this stage we do not know whether the ring-shaped pacemaker can be extended to other lower vertebrates, the diverging and unpronounced structure of the zebrafish sinus node and the absence of molecular markers until now may explain why a pacemaker structure in lower vertebrates has not previously been identified.

Finally, the 'primitive' myocardial identity of Isl1^{+} cells in adult zebrafish is intriguingly accompanied by a capacity to spontaneously depolarize, which is absent in working cardiomyocytes. Future work focusing on Isl1 and its gene targets will help to elucidate whether *isl1* expression in the pacemaker cells is necessary to maintain the primitive myocardial fate of these cells, similarly to its suggested role in cardiac progenitor cells (Ma et al., 2008, Cai et al., 2003, Prall et al., 2007, Bu et al., 2009). Alternatively, Isl1 could be required to drive a pacemaker gene program, in a similar fashion to what was shown for Tbx3 (Hoogaars et al., 2007).

ACKNOWLEDGEMENTS

We would like to thank K. Kawakami for providing the *galFF* plasmid and the *Tg(UAS:GFP)* and *Tg(UAS:RFP)* fish. The Islet-1 homeobox monoclonal antibody 39.4D5 developed by Jessell, T.M. / Brenner-Morton, S. was obtained from the Developmental Studies Hybridoma Bank developed under the auspices of the NICHD and maintained by The University of Iowa, Department of Biology, Iowa City, IA 52242. Work in J.Bakkers' laboratory was supported by the Royal Dutch Academy of Arts and Sciences (KNAW) and the Netherlands Organization for Scientific Research (NWO/ALW) grant 864.08.009. Work in V. Christoffels' laboratory was supported by the European Commission under the FP7 Integrated Project CardioGeNet (HEALTH-2007-B-223463) and by the Rembrandt Institute.

AUTHOR CONTRIBUTIONS

Conceived and designed the experiments: FT JHvW SBB AOV EdP VMC JB. Performed the experiments: FT JHvW SBB AOV EdP BJB AV. Analyzed the data: FT JHvW SBB AOV EdP BJB AV VMC JB. Contributed reagents/materials/analysis tools: AOV AV. Wrote the paper: FT SBB JHvW VMC JB

MATERIALS AND METHODS

Zebrafish lines

Fish used in this study were kept in standard conditions as previously described (Westerfield, 1995). The *Tg(myl7:gfp)* and isl1 mutant line *isl1K88X (isl1*^{SA0029}*)* were described previously (de Pater et al., 2009, Huang et al., 2003). Generation of the *Tg(Isl1BAC:GalFF; UAS:GFP)* is described in more detail below. All animal and human work conformed to ethical guidelines and was approved by the relevant local animal ethics committees.

Generation of the tg(isl1BAC:Gal4ff) transgenic line

Recombineering of BAC clone CH211-219F7 was performed following the manufacturer's protocol with minor modifications, as described in (Bussmann and Schulte-Merker, 2011). Primers used were: isl1_Gal4FF_F 5′-gggccttctgtccg gttttaaaagtggacctaacaccgccttactttcttaccATGAAGCTACTGTCTTCTATCGAAC-3′ and isl1_KanR_R 5′-aaataaacaataaagcttaacttacttttcggtggatcccccatgtctccT CAGAAGAACTCGTCAAGAAGGCG-3'. BAC DNA was injected at 300 ng/µl in the presence of 0.75U PI-SceI meganuclease (New England Biolabs) into *Tg(UAS:GFP)* embryos (Asakawa et al., 2008). Healthy embryos displaying robust isl1-specific fluorescence were grown to adulthood. *Tg(Isl1BAC:GalFF; UAS:RFP)* were obtained by outcross to a *tg(UAS:RFP)* line (Asakawa et al., 2008).

High-speed imaging and analysis

2 dpf and 4 dpf *isl1K88X* mutant and sibling embryos were mounted in 0.25% agarose (Life Technologies BV) prepared in E3 medium embryonic medium with 16 mg/ml 3-amino benzoic acid ethylester. Embryonic hearts were imaged with a Hamamatsu C9300-221 high speed CCD camera (Hamamatsu Photonics, Hamamatsu City, Japan) at 150 fps mounted on a Leica AF7000 microscope (Leica Microsystems GmbH, Wetzlar, Germany) in a controlled temperature chamber (28.5°C) using Hokawo 2.1 imaging software (Hamamatsu Photonics GmbH, Herrsching am Ammersee, Germany). Image analysis was carried out with ImageJ (http://rsbweb.nih.gov/ij/). Statistical analysis and drawing of the box-whisker plot were carried out in Excel 2007 (Microsoft, Redmond, WA, USA).

In situ hybridization and immunohistochemistry

ISH on embryos was carried out as previously described (Westerfield, 1995). ISH on adult heart tissue was carried out as previously described (Moorman et al., 2001) with minor modifications. 3D reconstructions of serial ISH-labeled sections were performed as described in (Sizarov et al., 2010). Immunohistochemistry was

carried out as previously described (de Pater et al., 2009). Embryos and adult hearts for immunocytochemistry were fixed in 2% paraformaldehyde, embedded in 3% agarose / 1% gelatin and sectioned at 100µm thickness. The primary antibodies used were mouse anti-Isl1 (Developmental Studies Hybridoma Bank, Iowa City, IA, USA, clone 39.4D5, 1:100), mouse-anti-tropomyosin (Sigma-Aldrich, Zwijndrecht, the Netherlands, Cat. No. T9283, 1:100), rabbit anti-GFP (Torrey Pines Biolabs Inc., Secaucus, NJ, USA, Cat. No. TP401, 1:200) and rabbit-anti-DsRed (Clontech Laboratories Inc., Mountain View, CA, USA, Cat No. 632496, 1:100).

Optical Mapping

Hearts from adult *tg(isl1:GalFF; UAS:GFP)* fish were excised and incubated in 10 ml Ringer's solution (composition in mM: NaCl 115, Tris 5, NaH_2PO_4 1, KCl 2.5, $MgSO_4$ 1, $CaCl_2$ 1.5, glucose 5, pH adjusted to 7.2 with HCl) containing 15 µM Di-4 ANEPPS for 5 minutes and placed in an inverted microscope. Excitation light was provided by a 5-Watt power LED (filtered 510 ± 20 nm). Fluorescence (filtered > 610nm) was transmitted through a tandem lens system on CMOS sensor (100 x 100 elements, MICAM Ultima, SciMedia, Costa Mesa, CA, USA). Activation patterns were measured during the sinus rhythm. Optical action potentials were then analyzed with custom-made software.

Single cell preparation

Single cells were isolated from the sinoatrial node and atria as described previously (Verkerk et al., 2009). Sinoatrial node regions were excised from 55 adult *tg(Isl1BAC:GalFF; UAS:GFP)* zebrafishes and stored in Tyrode's solution at RT, containing (in mM): NaCl 140, KCl 5.4, $CaCl_2$ 1.8, $MgCl_2$ 1.0, glucose 5.5, and HEPES 5.0; pH was set to 7.4 with NaOH. They were then transferred to Ca^{2+}-free Tyrode's solution (30°C), i.e., Tyrode's solution with 10 µM $CaCl_2$, which was refreshed two times before the addition liberase IV (0.25–0.29 U/ml; Roche, Indianapolis, IN, USA) and elastase (2.4–0.7 U/mL; Serva, Heidelberg, Germany) for 12-15 min. The final 6 min also contained pronase E (0.92 U/mL; Serva). During the incubation period, the tissue was triturated through a pipette (tip diameter: 2.0 mm). The dissociation was stopped by transferring the strips into a modified Kraft-Brühe solution (30°C) containing (in mM KCl 85, K_2HPO_4 30, $MgSO_4$ 5.0, glucose 20, pyruvic acid 5.0, creatine 5.0, taurine 30, β-hydroxybutyric acid 5.0, succinic acid 5.0, BSA 1%, Na_2ATP 2.0; pH was set to 6.9 with KOH. The tissue was triturated (pipette tip diameter: 0.8 mm) in Kraft-Brühe solution (30°C) for 4 min to obtain single cells, which were stored at RT for 30 min in modified Kraft-Brühe solution before patch-clamping. Cells were allowed to adhere for 5 min after which superfusion with Tyrode's solution (28.5±0.2°C) was started.

Patch clamp experiments

Action potentials were recorded by the amphotericin-perforated patch-clamp technique using an Axopatch 200B amplifier (Molecular Devices, Sunnyvale, CA, USA). Action potentials of GFP+ cells were low-pass filtered (cut-off frequency 5 kHz) and digitized at 10 kHz; action potentials of GFP- cells at 5 kHz and 20 kHz, respectively. Potentials were corrected for the estimated liquid junction potential (Barry and Lynch, 1991). Data acquisition and analysis were accomplished using custom software. Patch pipettes (borosilicate glass; resistance 3–4 MΩ) were heat polished and filled with pipette solution containing (in mM): K-gluc 125, KCl 20, NaCl 10, amphotericin-B 0.22, and HEPES 10; pH was set to 7.2 with KOH. Action potentials in GFP-negative cells were elicited at 3 Hz by 3-ms, ≈1.2x threshold current pulses through the patch pipette. Parameter values obtained from 10 consecutive action potentials were averaged.

SUPPLEMENTARY FIGURES

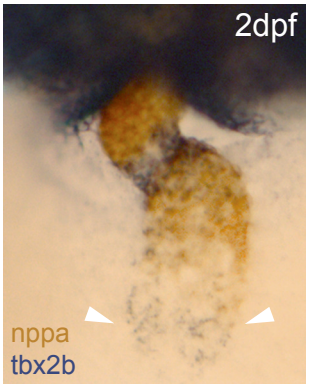

Figure S1: Expression of tbx2b at the venous pole in embryonic heart.

Expression patterns by mRNA in situ hybridization of *tbx2b* and *nppa* in 2 dpf embryos. Expression of *tbx2b* at the venous pole (blue staining indicated with arrowheads) does not overlap with *nppa* expression (red staining), which is confined to atrium and ventricle chamber myocardium. Pictures shown are ventral views with anterior to the top.

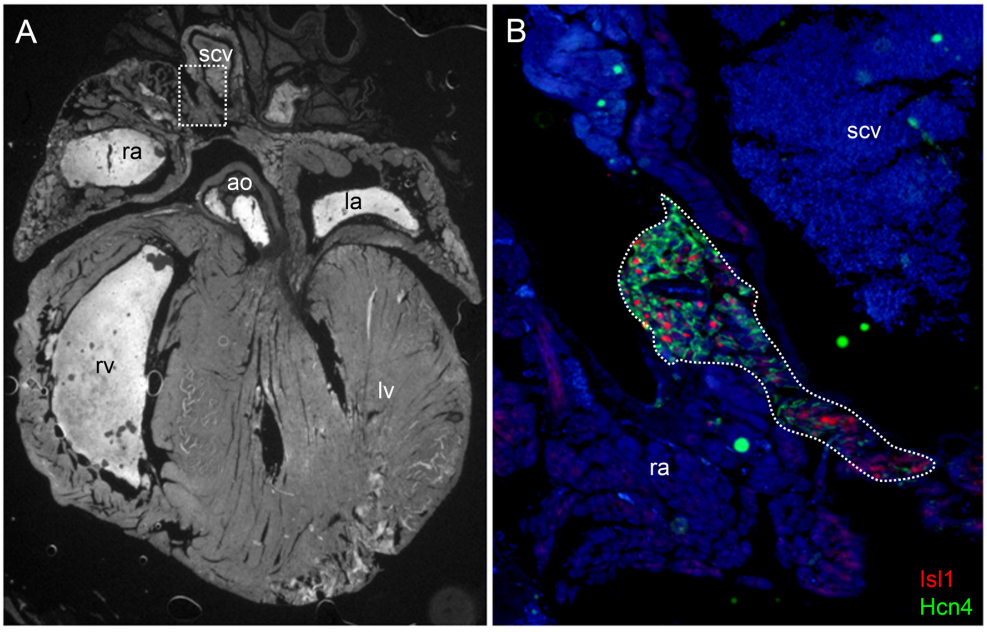

Figure S2: Isl1 expression in the sinus node of the adult mouse heart.

(A) 4-chamber view of section through adult wild-type mouse heart. Boxed region indicates the region shown enlarged in (B). **(B)** Expression of Isl1, depicted in red, colocalizes with the expression of the sinus node marker Hcn4, depicted in green. Dotted line in (B) demarcates the sinus node. ao, aorta; la, left atrium; lv, left ventricle; ra, right atrium; rv, right ventricle; scv, superior caval vein.

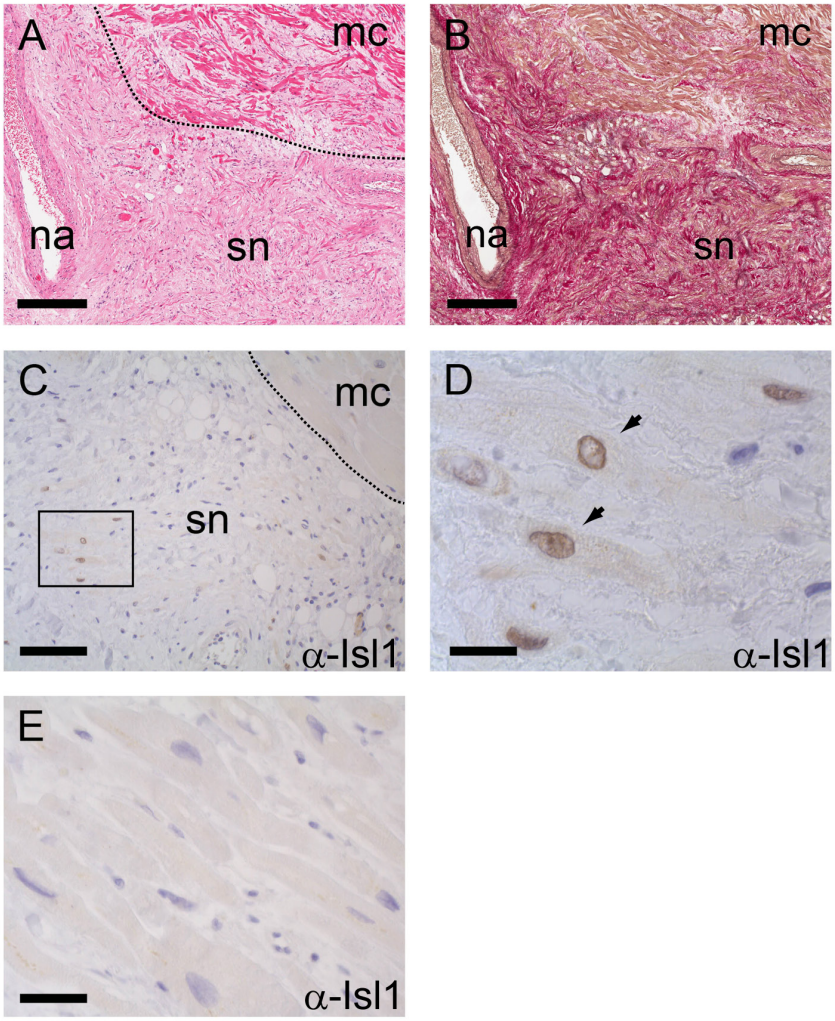

Figure S3: Immunohistochemical detection of Islet-1 in human cardiomyocytes in the sinoatrial node.

(A) Hematoxylin and eosin staining of the sinoatrial node. SN indicates the area of the node showing where the specialized cardiomyocytes are located. MC indicates myocardium adjacent to the node. NA indicates the nodal artery. The boundary between SN and MC is highlighted by the dotted line. Scale bar represents 400 μm. **(B)** Elastic van Giesen stain of a consecutive section of (A) illustrating that the cardiomyocytes are embedded within collagen and elastic tissue. Scale bar represents 400 μm. **(C)** Islet-1 immunostain of sinoatrial node. SN indicates sinoatrial node. MC indicates myocardium adjacent to the node. The boundary between SN and MC is highlighted by the dotted line. Scale bar represents 160 μm. **(D)** Magnification of the boxed region in (C). Islet-1 immunostain with positive brown staining of the nuclei of the cardiomyocytes. On average 5% of the cardiomyocytes in the sinoatrial node revealed a positive signal. Scale bar represents 40 μm. **(E)** Staining is absent in the myocardium next to the sinoatrial node. Scale bar represents 80 μm.

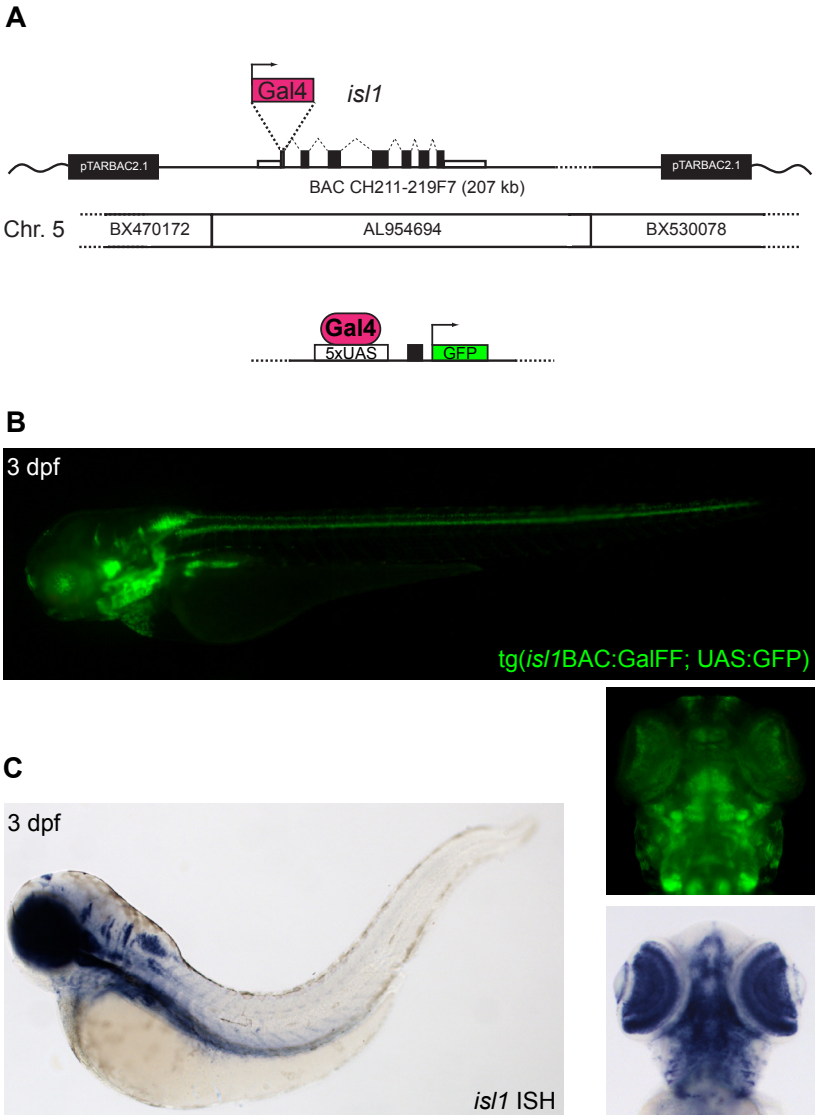

Figure S4: Generation of a reporter transgenic line for isl1.

(A) An expression cassette containing the GalFF gene (Asakawa et al., 2008) and kanamycin resistance gene was inserted by recombineering into BAC CH211-219F7 at the ATG site of the 1st exon of the isl1 gene. The site of recombineering is approximately 40 kb inside the BAC sequence, minimizing any risk of loss of isl1 regulatory sequences. The recombined BAC was then injected in a tg(UAS:GFP) background [1] to obtain the fluorescent Isl1 expression reporter line Tg(Isl1BAC:GalFF; UAS:GFP). (B) GFP expression pattern of the Tg(Isl1BAC:GalFF; UAS:GFP) line at 3 dpf. (C) Isl1 ISH on WT embryo at 3 dpf. The expression pattern of GFP, reporting for isl1 expression, in the Tg(isl1BAC:GalFF; UAS:GFP) is validated by comparison with the isl1 ISH. Especially visible are the identical expression pattern in the eyes and hindbrain.

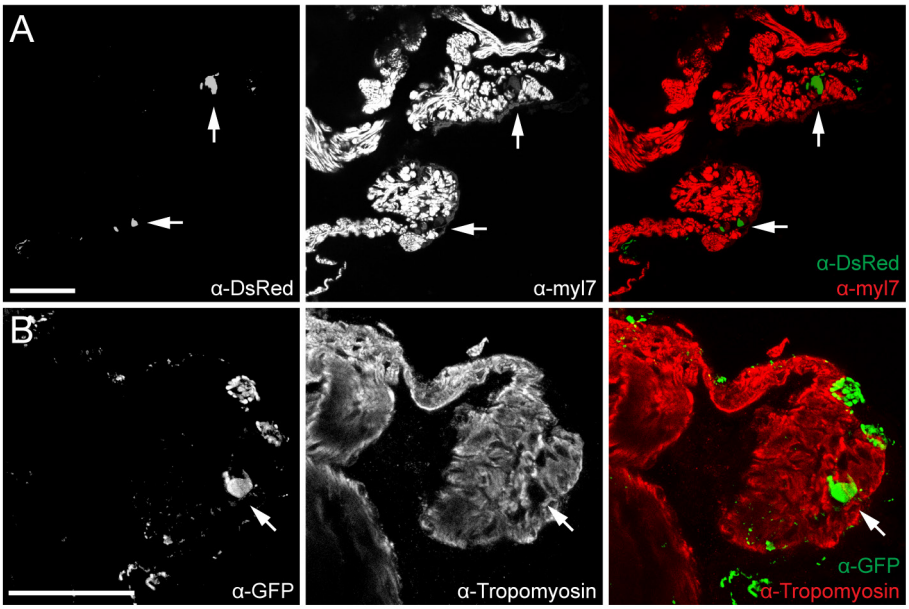

Figure S5: Isl1BAC reporter activity in adult heart.

Confocal images of Tg(isl1BAC:GalFF; UAS:RFP; myl7:eGFP) after immunolabeling with anti-RFP and anti-GFP antibodies **(A)**, or Tg(isl1BAC:GalFF; UAS:GFP) after immunolabeling with anti-GFP and antitropomyosin antibodies **(B)**. Isl1 expressing cells (indicated with arrows) are located at the base of the venous valves and contain much lower levels of myosin light chain or tropomyosin compared to surrounding myocardial cells. Axonal Isl1/GFP+ structures are visible at the outer surface of the myocardium. Scale bars represent 50 µm.

REFERENCES

AMMIRABILE, G., TESSARI, A., PIGNATARO, V., SZUMSKA, D., SUTERA SARDO, F., BENES, J., JR., BALISTRERI, M., BHATTACHARYA, S., SEDMERA, D. & CAMPIONE, M. 2012. Pitx2 confers left morphological, molecular, and functional identity to the sinus venosus myocardium. *Cardiovasc Res,* 93**,** 291-301.

ARRENBERG, A. B., STAINIER, D. Y., BAIER, H. & HUISKEN, J. 2010. Optogenetic control of cardiac function. *Science,* 330**,** 971-4.

ASAKAWA, K., SUSTER, M. L., MIZUSAWA, K., NAGAYOSHI, S., KOTANI, T., URASAKI, A., KISHIMOTO, Y., HIBI, M. & KAWAKAMI, K. 2008. Genetic dissection of neural circuits by Tol2 transposon-mediated Gal4 gene and enhancer trapping in zebrafish. *Proc Natl Acad Sci U S A,* 105**,** 1255-60.

BARRY, P. H. & LYNCH, J. W. 1991. Liquid junction potentials and small cell effects in patch-clamp analysis. *J Membr Biol,* 121**,** 101-17.

BARUSCOTTI, M., BUCCHI, A., VISCOMI, C., MANDELLI, G., CONSALEZ, G., GNECCHI-RUSCONI, T., MONTANO, N., CASALI, K. R., MICHELONI, S., BARBUTI, A. & DIFRANCESCO, D. 2011. Deep bradycardia and heart block caused by inducible cardiac-specific knockout of the pacemaker channel gene Hcn4. *Proc Natl Acad Sci U S A,* 108**,** 1705-10.

BLASCHKE, R. J., HAHURIJ, N. D., KUIJPER, S., JUST, S., WISSE, L. J., DEISSLER, K., MAXELON, T., ANASTASSIADIS, K., SPITZER, J., HARDT, S. E., SCHOLER, H., FEITSMA, H., ROTTBAUER, W., BLUM, M., MEIJLINK, F., RAPPOLD, G. & GITTENBERGER-DE GROOT, A. C. 2007. Targeted mutation reveals essential functions of the homeodomain transcription factor Shox2 in sinoatrial and pacemaking development. *Circulation,* 115**,** 1830-8.

BU, L., JIANG, X., MARTIN-PUIG, S., CARON, L., ZHU, S., SHAO, Y., ROBERTS, D. J., HUANG, P. L., DOMIAN, I. J. & CHIEN, K. R. 2009. Human ISL1 heart progenitors generate diverse multipotent cardiovascular cell lineages. *Nature,* 460**,** 113-7.

BUSSMANN, J. & SCHULTE-MERKER, S. 2011. Rapid BAC selection for tol2-mediated transgenesis in zebrafish. *Development,* 138**,** 4327-32.

CAI, C. L., LIANG, X., SHI, Y., CHU, P. H., PFAFF, S. L., CHEN, J. & EVANS, S. 2003. Isl1 identifies a cardiac progenitor population that proliferates prior to differentiation and contributes a majority of cells to the heart. *Dev Cell,* 5**,** 877-89.

CHI, N. C., SHAW, R. M., JUNGBLUT, B., HUISKEN, J., FERRER, T., ARNAOUT, R., SCOTT, I., BEIS, D., XIAO, T., BAIER, H., JAN, L. Y., TRISTANI-FIROUZI, M. & STAINIER, D. Y. 2008. Genetic and physiologic dissection of the vertebrate cardiac conduction system. *PLoS Biol,* 6**,** e109.

CHRISTOFFELS, V. M., MOMMERSTEEG, M. T., TROWE, M. O., PRALL, O. W., DE GIER-DE VRIES, C., SOUFAN, A. T., BUSSEN, M., SCHUSTER-GOSSLER, K., HARVEY, R. P., MOORMAN, A. F. & KISPERT, A. 2006. Formation of the venous pole of the heart from an Nkx2-5-negative precursor population requires Tbx18. *Circ Res,* 98**,** 1555-63.

CHRISTOFFELS, V. M. & MOORMAN, A. F. 2009. Development of the cardiac conduction system: why are some regions of the heart more arrhythmogenic than others? *Circ Arrhythm Electrophysiol,* 2**,** 195-207.

CHRISTOFFELS, V. M., SMITS, G. J., KISPERT, A. & MOORMAN, A. F. 2010. Development of the pacemaker tissues of the heart. *Circ Res,* 106**,** 240-54.

DE PATER, E., CLIJSTERS, L., MARQUES, S. R., LIN, Y. F., GARAVITO-AGUILAR, Z. V., YELON, D. & BAKKERS, J. 2009. Distinct phases of cardiomyocyte differentiation regulate growth of the zebrafish heart. *Development,* 136**,** 1633-41.

DOBRZYNSKI, H., LI, J., TELLEZ, J., GREENER, I. D., NIKOLSKI, V. P., WRIGHT, S. E., PARSON, S. H., JONES, S. A., LANCASTER, M. K., YAMAMOTO, M., HONJO, H., TAKAGISHI, Y., KODAMA, I., EFIMOV, I. R., BILLETER, R. & BOYETT, M. R. 2005. Computer three-dimensional reconstruction of the sinoatrial node. *Circulation,* 111**,** 846-54.

DUPAYS, L., JARRY-GUICHARD, T., MAZURAIS, D., CALMELS, T., IZUMO, S., GROS, D. & THEVENIAU-RUISSY, M. 2005. Dysregulation of connexins and inactivation of NFATc1 in the cardiovascular system of Nkx2-5 null mutants. *J Mol Cell Cardiol,* 38**,** 787-98.

ESPINOZA-LEWIS, R. A., YU, L., HE, F., LIU, H., TANG, R., SHI, J., SUN, X., MARTIN, J. F., WANG, D., YANG, J. & CHEN, Y. 2009. Shox2 is essential for the differentiation of cardiac pacemaker cells by repressing Nkx2-5. *Dev Biol,* 327**,** 376-85.

FLACK, M. 1910. An investigation of the sino-auricular node of the mammalian heart. *J Physiol,* 41**,** 64-77.
FRANK, D. U., CARTER, K. L., THOMAS, K. R., BURR, R. M., BAKKER, M. L., COETZEE, W. A., TRISTANI-FIROUZI, M., BAMSHAD, M. J., CHRISTOFFELS, V. M. & MOON, A. M. 2012. Lethal arrhythmias in Tbx3-deficient mice reveal extreme dosage sensitivity of cardiac conduction system function and homeostasis. *Proc Natl Acad Sci U S A,* 109**,** E154-63.
GLUKHOV, A. V., FEDOROV, V. V., ANDERSON, M. E., MOHLER, P. J. & EFIMOV, I. R. 2010. Functional anatomy of the murine sinus node: high-resolution optical mapping of ankyrin-B heterozygous mice. *Am J Physiol Heart Circ Physiol,* 299**,** H482-91.
HOOGAARS, W. M., ENGEL, A., BRONS, J. F., VERKERK, A. O., DE LANGE, F. J., WONG, L. Y., BAKKER, M. L., CLOUT, D. E., WAKKER, V., BARNETT, P., RAVESLOOT, J. H., MOORMAN, A. F., VERHEIJCK, E. E. & CHRISTOFFELS, V. M. 2007. Tbx3 controls the sinoatrial node gene program and imposes pacemaker function on the atria. *Genes Dev,* 21**,** 1098-112.
HUANG, C. J., TU, C. T., HSIAO, C. D., HSIEH, F. J. & TSAI, H. J. 2003. Germ-line transmission of a myocardium-specific GFP transgene reveals critical regulatory elements in the cardiac myosin light chain 2 promoter of zebrafish. *Developmental dynamics : an official publication of the American Association of Anatomists,* 228**,** 30-40.
HUTCHINSON, S. A. & EISEN, J. S. 2006. Islet1 and Islet2 have equivalent abilities to promote motoneuron formation and to specify motoneuron subtype identity. *Development,* 133**,** 2137-47.
KEITH, A. & FLACK, M. 1907. The Form and Nature of the Muscular Connections between the Primary Divisions of the Vertebrate Heart. *J Anat Physiol,* 41**,** 172-89.
MA, Q., ZHOU, B. & PU, W. T. 2008. Reassessment of Isl1 and Nkx2-5 cardiac fate maps using a Gata4-based reporter of Cre activity. *Dev Biol,* 323**,** 98-104.
MANGONI, M. E. & NARGEOT, J. 2008. Genesis and regulation of the heart automaticity. *Physiol Rev,* 88**,** 919-82.
MILAN, D. J., GIOKAS, A. C., SERLUCA, F. C., PETERSON, R. T. & MACRAE, C. A. 2006. Notch1b and neuregulin are required for specification of central cardiac conduction tissue. *Development,* 133**,** 1125-32.
MOMMERSTEEG, M. T., HOOGAARS, W. M., PRALL, O. W., DE GIER-DE VRIES, C., WIESE, C., CLOUT, D. E., PAPAIOANNOU, V. E., BROWN, N. A., HARVEY, R. P., MOORMAN, A. F. & CHRISTOFFELS, V. M. 2007. Molecular pathway for the localized formation of the sinoatrial node. *Circ Res,* 100**,** 354-62.
MOORMAN, A. F., HOUWELING, A. C., DE BOER, P. A. & CHRISTOFFELS, V. M. 2001. Sensitive nonradioactive detection of mRNA in tissue sections: novel application of the whole-mount in situ hybridization protocol. *The journal of histochemistry and cytochemistry : official journal of the Histochemistry Society,* 49**,** 1-8.
MOOSMANG, S., STIEBER, J., ZONG, X., BIEL, M., HOFMANN, F. & LUDWIG, A. 2001. Cellular expression and functional characterization of four hyperpolarization-activated pacemaker channels in cardiac and neuronal tissues. *European journal of biochemistry / FEBS,* 268**,** 1646-52.
PRALL, O. W., MENON, M. K., SOLLOWAY, M. J., WATANABE, Y., ZAFFRAN, S., BAJOLLE, F., BIBEN, C., MCBRIDE, J. J., ROBERTSON, B. R., CHAULET, H., STENNARD, F. A., WISE, N., SCHAFT, D., WOLSTEIN, O., FURTADO, M. B., SHIRATORI, H., CHIEN, K. R., HAMADA, H., BLACK, B. L., SAGA, Y., ROBERTSON, E. J., BUCKINGHAM, M. E. & HARVEY, R. P. 2007. An Nkx2-5/Bmp2/Smad1 negative feedback loop controls heart progenitor specification and proliferation. *Cell,* 128**,** 947-59.
PUSKARIC, S., SCHMITTECKERT, S., MORI, A. D., GLASER, A., SCHNEIDER, K. U., BRUNEAU, B. G., BLASCHKE, R. J., STEINBEISSER, H. & RAPPOLD, G. 2010. Shox2 mediates Tbx5 activity by regulating Bmp4 in the pacemaker region of the developing heart. *Hum Mol Genet,* 19**,** 4625-33.
SANCHEZ-QUINTANA, D., CABRERA, J. A., FARRE, J., CLIMENT, V., ANDERSON, R. H. & HO, S. Y. 2005. Sinus node revisited in the era of electroanatomical mapping and catheter ablation. *Heart,* 91**,** 189-94.
SHI, W., WYMORE, R., YU, H., WU, J., WYMORE, R. T., PAN, Z., ROBINSON, R. B., DIXON, J. E., MCKINNON, D. & COHEN, I. S. 1999. Distribution and prevalence of hyperpolarization-activated cation channel (HCN) mRNA expression in cardiac tissues. *Circulation research,* 85**,** e1-6.
SIZAROV, A., ANDERSON, R. H., CHRISTOFFELS, V. M. & MOORMAN, A. F. 2010. Three-dimensional and molecular analysis of the venous pole of the developing human heart. *Circulation,* 122**,** 798-807.

SIZAROV, A., DEVALLA, H. D., ANDERSON, R. H., PASSIER, R., CHRISTOFFELS, V. M. & MOORMAN, A. F. 2011. Molecular analysis of patterning of conduction tissues in the developing human heart. *Circ Arrhythm Electrophysiol,* 4**,** 532-42.

SOLC, D. 2007. The heart and heart conducting system in the kingdom of animals: A comparative approach to its evolution. *Exp Clin Cardiol,* 12**,** 113-8.

SUN, Y., LIANG, X., NAJAFI, N., CASS, M., LIN, L., CAI, C. L., CHEN, J. & EVANS, S. M. 2007. Islet 1 is expressed in distinct cardiovascular lineages, including pacemaker and coronary vascular cells. *Dev Biol,* 304**,** 286-96.

VERKERK, A. O., DEN RUIJTER, H. M., BOURIER, J., BOUKENS, B. J., BROUWER, I. A., WILDERS, R. & CORONEL, R. 2009. Dietary fish oil reduces pacemaker current and heart rate in rabbit. *Heart Rhythm,* 6**,** 1485-92.

VERKERK, A. O., WILDERS, R., VAN BORREN, M. M., PETERS, R. J., BROEKHUIS, E., LAM, K., CORONEL, R., DE BAKKER, J. M. & TAN, H. L. 2007. Pacemaker current (I(f)) in the human sinoatrial node. *Eur Heart J,* 28**,** 2472-8.

VIRAGH, S. & CHALLICE, C. E. 1980. The development of the conduction system in the mouse embryo heart. *Dev Biol,* 80**,** 28-45.

WEINBERGER, F., MEHRKENS, D., FRIEDRICH, F. W., STUBBENDORFF, M., HUA, X., MULLER, J. C., SCHREPFER, S., EVANS, S., CARRIER, L. & ESCHENHAGEN, T. 2012. Localization of Islet-1-Positive Cells in the Healthy and Infarcted Adult Murine Heart. *Circ Res*.

WESTERFIELD, M. 1995. *The Zebrafish Book – A Guide for Laboratory Use of Zebrafish (Brachydanio rerio),* Eugene, Oregon, USA, University of Oregon Press.

WIESE, C., GRIESKAMP, T., AIRIK, R., MOMMERSTEEG, M. T., GARDIWAL, A., DE GIER-DE VRIES, C., SCHUSTER-GOSSLER, K., MOORMAN, A. F., KISPERT, A. & CHRISTOFFELS, V. M. 2009. Formation of the sinus node head and differentiation of sinus node myocardium are independently regulated by Tbx18 and Tbx3. *Circ Res,* 104**,** 388-97.

YAMAMOTO, M., DOBRZYNSKI, H., TELLEZ, J., NIWA, R., BILLETER, R., HONJO, H., KODAMA, I. & BOYETT, M. R. 2006. Extended atrial conduction system characterised by the expression of the HCN4 channel and connexin45. *Cardiovasc Res,* 72**,** 271-81.

Isl1
Tg
Line
Cell
Express
Heart
Region
GFP
Pacemaker
Used
Genome
Sinoatrial
Locus
Element
Mutant
AV
BAC
Develop
Reported
Embryo
Zebrafish
Gene
Enhancer
UAS
Adult
DNA
Rate
Specific
Function
Cardiac
Work
Tube
Active
Canal
Observe
Clone
Target
Located
System
Loss
Role
Stage
Inner
Axons
Transgene
Cardiomyocyte
Factor
Regulatory
Initial
Data
Well
Sequence
Generated
Downstream
Severe
Junction
Remain
Addition
Population
Promoter
Neurons
Structure
Part
Due
Show
Acts
Both
Including
Islet
One
Thus
Mice
gRNA
During
Previously
Injected
Induce
Integrated
Embryonic
Crucial
Pattern
Curvature
Present
Contains
Site
Defect
Such
Crispr
Tissue
PCR
Atrium
Field
Extends
Indicate
Known
Recapitulate
Establish
Lose
Myocardial
Node
Fire
Inflow
Knockout
Form

CHAPTER 3

Regulation of Isl1 expression in pacemaker cell development and function

Silja Burkhard [1] and Jeroen Bakkers [1,2]

[1] Hubrecht Institute-KNAW and University Medical Center Utrecht, 3584 CT, Utrecht, The Netherlands.
[2] Department of Medical Physiology, Division of Heart and Lungs, University Medical Center Utrecht, 3584 CT Utrecht, The Netherlands.

In preparation

ABSTRACT

The vertebrate heart rate is driven and controlled by an innate pacemaker. Within the cardiac pacemaker highly specialized cardiomyocytes, henceforth referred to as cardiac pacemaker cells, are able to rhythmically depolarize and fire an action potential without the need of external stimulation. Since the pacemaker cells and other cardiomyocytes are coupled, they trigger the neighboring working cardiomyocytes to contract. The continuous rhythmical depolarization of the pacemaker cells is responsible for the basic heart rate. The LIM-homeodomain transcription factor Islet-1 (Isl1) is crucial for the development and maintenance of pacemaker cell function in the vertebrate heart. Isl1- expressing cells are located in the sinoatrial region of the heart from early embryonic stages onwards. In the adult heart, the interconnected Isl1^{+} pacemaker cells form a ring around the sinoatrial junction. They are in close proximity with Isl1^{+} axons entering the heart at the sinoatrial junction and extending to the AV canal (AVC). Expression of *isl1* specifically in the sinoatrial region depends on as yet unidentified regulatory enhancer elements located in the genomic region downstream of the Isl1 locus. Loss of Isl1 in the zebrafish embryo causes severe, rapidly progressing bradycardia (slow heart rate) and arrhythmia from 2 days post fertilization onwards. However, this phenotype is not caused by a loss of the pacemaker cells but rather their functional inability to maintain the pacemaker function. The Isl1-expressing pacemaker cells are still present in the mutant heart. Elucidation of the role and regulation of Isl1 remains a pivotal task when investigating pacemaker cell development and function.

INTRODUCTION

The continuous rhythmical contractions of the heart facilitate the transport of oxygen and nutrients through the body. The pumping force is generated by the myocardium, made up of highly efficient muscle cells contracting in a coordinated manner. Cardiomyocytes lose the ability to contract spontaneously during early embryonic development. After cardiomyocyte differentiation, they need an external electrical trigger to depolarize and contract. Only a small number of highly specialized cardiomyocytes, the pacemaker cells, have the intrinsic capacity to initiate rhythmic membrane depolarization without an external stimulus. Pacemaker cells are myocardial cells embedded in the surrounding myocardium located at the sinoatrial region of the vertebrate heart. The spontaneous and cyclic membrane depolarizations are achieved by a specific set of ion channels that cause an influx of positive ions into the pacemaker cell. Through direct cell-cell connections, pacemaker cells trigger neighboring working myocardial cells to depolarize, fire an action potential and contract. Therefore, the firing rate of the sinoatrial pacemaker defines the basic heart rate and rhythm. (Baruscotti and Robinson, 2007)

On a molecular level, pacemaker cells are distinguished by a specific gene regulatory network inhibiting chamber myocardium differentiation and initiating pacemaker cell development (Burkhard et al., 2017). Apart from a few known factors, it remains largely unclear how the pacemaker cells differentiate and little is known about the underlying genetic network.

The pacemaker cells are solely responsible for the initiation of the heartbeat and ensure its rhythmicity. Any aberrations in pacemaker cell function leads to abnormal heart rates and even cardiac arrest (Dobrzynski et al., 2007). The pacemaker rhythm can adapt to physical strain on the heart requiring it to beat faster. Direct innervation of the sinoatrial node by neurons of the central nervous system has been documented in various species including the adult zebrafish (Stoyek et al., 2015). Furthermore, pacemaker cells in the sinoatrial region express both the parasympathetic M_2 receptor and the sympathetic b_2A receptor (Stoyek et al., 2016). Thus, input from the autonomic nervous system can adjust the heart rate directly. In humans, pacemaker cell defects are conventionally treated by implanting artificial electrical pacemakers (Silka and Bar-Cohen, 2006). However, this approach lacks the connection to the autonomic nervous system. Much effort has been made to reprogram progenitor- or stem cells in vitro to function as pacemaker cells with the goal to treat patients with these bio-engineered pacemaker cells to replace their own dysfunctional pacemaker cells (Chauveau et al., 2017, Zhang et al., 2017). In order to reprogram these cells, we need a very thorough understanding of the molecular characteristics and pathways that shape the pacemaker cells.

The LIM-homeodomain transcription factor Islet-1 (Isl1) is expressed in the developing and adult cardiac pacemaker cells in the sinoatrial node. Isl1 is a crucial factor for the development and maintenance of pacemaker cell function (Tessadori et al., 2012, Liang et al., 2015, de Pater et al., 2009). It was first identified due to its expression in the endocrine cells of the pancreas (Karlsson et al., 1990). Furthermore, Isl1 is expressed in various other tissues and organs including motor neurons (Ericson et al., 1992), cells of the inner ear (Li et al., 2004, Radde-Gallwitz et al., 2004) and in the pharyngeal and cardiovascular systems (Zhuang et al., 2013). During heart development, Isl1 is expressed in progenitor cells of the second heart field and crucial for their contribution to the developing heart (Cai et al., 2003). Apart from cardiac cells, the $Isl1^{+}$ progenitor cells have the potential to develop into multiple cell types including smooth muscle, endothelial, coronary vascular and pacemaker cells (Moretti et al., 2006, Sun et al., 2007). In mice loss of Isl1 is embryonic lethal (Pfaff et al., 1996). The heart of $Isl1^{-/-}$ knockout mice lack all cardiac structures derived from cells of the second heart field. The outflow tract, right ventricle and part of both atria are absent hearts (Cai et al., 2003). On the contrary, in $Isl1^{-/-}$ zebrafish no morphological abnormalities of the heart have been reported (Tessadori et al., 2012, de Pater et al., 2009). However, *isl1K88X* knockout zebrafish embryos are completely immotile and experience rapidly progressing bradycardia and arrhythmia. Loss of Isl1 is lethal before 5 days post fertilization (Tessadori et al., 2012). Similar cardiac pacemaker phenotypes have been reported in sinoatrial node-specific Isl1 knockout mice (Liang et al., 2015).

In the context of heart and pacemaker cell development, little is known about the molecular role and downstream effectors of Isl1. Only a few targets of the transcription factor have been identified, such as *bone morphogenetic protein 4* (*bmp4)* and t-box 2b (*tbx2b)* (de Pater et al., 2009, Tessadori et al., 2012). Whether Isl1 acts directly on the expression of characteristic pacemaker cell genes, such as *tbx3* or *hcn4* remains uncertain. Using several transgenic reporter lines as well as genetic knockout approaches we analyzed the role of Isl1 in pacemaker development and further characterized the expression pattern of Isl1 in the adult and embryonic zebrafish heart. $Isl1^{+}$ cells were present in the sinoatrial region of the heart tube from 28 hpf onwards.

Isl1 is one of the key factors in the transcriptional network in pacemaker cells (Fig. 1). Its expression in the developing sinoatrial region (SAR) is directly regulated by short stature homeobox 2 (Shox2) (Hoffmann et al., 2013). Shox2 is a major factor in delineating the SAR myocardium against the working chamber myocardium. Adult pacemaker cells, although of myocardial origin, only show primitive cardiomyocyte characteristics. Expression of cardiomyocyte marker genes such as *myosin light chain 7 (myl7)* is reduced and striated muscle fibers are lacking (Tessadori et al.,

2012). Shox2 drives pacemaker cell development by inhibiting nk2 homeobox 5 (Nkx2.5), a key factor in chamber myocardium development (Liu et al., 2012). Ectopic expression of Nkx2.5 in the developing SAR leads to, a loss of expression of Isl1 and other pacemaker marker genes. Furthermore, ectopic expression of Shox2 in working myocardium results in ectopic expression of Isl1 (Ye et al., 2015). This highlights the antagonistic role of Shox2 and Nkx2.5 in regulating Isl1 during SAN development.

Apart from regulation by other factors, gene expression can be modulated by cis-regulatory enhancer elements (for review: (Shlyueva et al., 2014)). These enhancers activate transcription by guiding important factors to the promoter site and reinforce the assembly of the pre-initiation complex and/or the transition from initiation to elongation (Bulger and Groudine, 2011). It is now believed that the regulatory landscape of a given gene extends far beyond the core promoter region and contains a collection of regulatory elements contributing to the expression pattern. Tissue and stage-specific enhancer elements may enable the fine-tuning of gene expression. Their genomic location varies greatly, from intronic enhancers to elements far up/down-stream of the targeted promoter (reviewed in (Calo and Wysocka, 2013, Spitz and Furlong, 2012)). Identification of active enhancer elements acting on the promoter of a gene of interest remains a tedious task using transgenic reporter constructs or bioinformatical approaches. In ChiP-seq data active enhancer loci can be predicted by characteristic histone modifications. Active enhancers are marked by an accumulation of H3K27ac and H3K4me1 (Creyghton et al., 2010, Heintzman et al., 2007).

We assessed whether the loss of

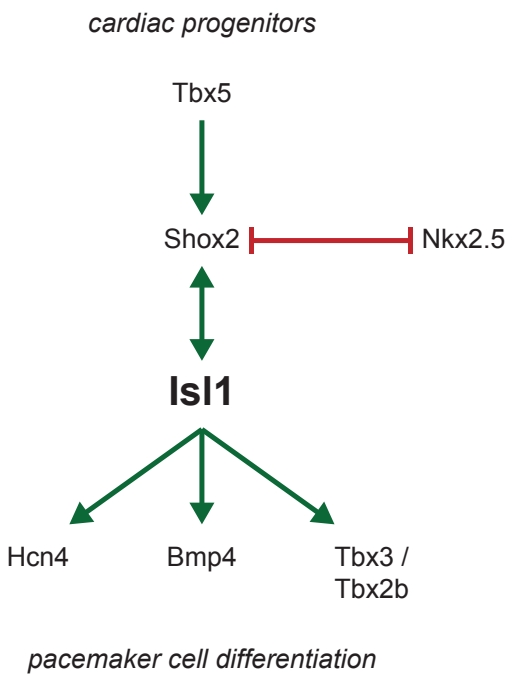

Figure 1: Islet-1 in the transcriptional network inducing pacemaker cell differentiation.

(A) Isl1 has central role in the transcriptional network inducing and controlling pacemaker cell differentiation. Shox2 act upstream of Isl1 and induces its expression. *bmp4*, *hcn4* and *tbx3* (*tbx2b* in zebrafish) are downstream targets of *Isl1*.

putative enhancer elements affects the expression of Isl1 by deleting them from the genome. The CrispR/Cas9 genome editing method is widely used to precisely manipulate the genomic DNA is various species including zebrafish (Fig. 2) (Chang et al., 2013, Hwang et al., 2013, Jinek et al., 2012). Here we applied CrispR/Cas9 to introduce large deletions (>40kb) in the genomic region downstream of the Isl1 locus. Using genome editing techniques to remove large DNA fragments from the genome has been successful in zebrafish (Liu et al., 2013, Xiao and Zhang, 2016).

RESULTS

Islet-1 is expressed in the adult and embryonic sinoatrial region

To visualize *isl1* expression in live zebrafish we previously established a transgenic reporter line, *tg(*Isl1:GalFF^{hu6635Tg}; UAS:GFP^{nkuasgfp1aTg}) (Tessadori et al., 2012). The GFP expression pattern recapitulated the known expression pattern for *isl1* in the adult zebrafish heart (Tessadori et al., 2012). However, expression in the embryonic heart was absent specifically in the sinoatrial region. GFP expression in other parts of the embryo recapitulated the Isl1 antibody labelling. We speculated that the Isl1 reporter line was missing a regulatory element responsible for expression in the pacemaker cells. It is well known that the activity of enhancer elements can be highly tissue specific and regulate the expression of target genes by interacting with their promotor (Spitz and Furlong, 2012). Previously, when generating the published Isl1 reporter line, we used the PI-SceI meganuclease system for genome integration (Thermes et al., 2002, Soroldoni et al., 2009). The endonuclease SceI recognizes an 18bp sequence and cleaves the DNA allowing integration of artificial DNA into the genome. The cleavage can occur anywhere in the genome or BAC clone DNA if the recognition site is present. Thus, we speculate that our initial BAC clone contained an I-SceI recognition site causing the loss of parts of the sequence prior to genome integration. we decided to re-establish the Isl1 reporter line with the same BAC sequence but now using the Tol2 system for genome integration. The Tol2 system requires specific cleavage sites at both ends of the BAC sequence for integration (Kawakami, 2007). This ensures that the entire sequence is integrated into the genome.

The novel Isl1 reporter line *tg(*Isl1:GalFF^{hu10018Tg}; UAS:GFP^{nkuasgfp1aTg}) recapitulated the endogenous *isl1* expression, including in the cardiac sinoatrial region (Fig. 3). Not all cells labelled by the Islet antibody are GFP positive (Fig. 3). This discrepancy could be due to partial silencing frequently reported in the tg(UAS:GFP) line (Akitake et al., 2011). We used the *tg(*Isl1:GalFF^{hu10018Tg}; UAS:GFP^{nkuasgfp1aTg}) reporter line to examine the expression of Isl1 during cardiac development. Isl1^{+} cardiomyocytes

were first observed situated in the cardiac disc at the 22-somites stage prior to tube formation (~20 hpf) (Fig. 4). It remains to be determined whether these Isl1^{+} cells are indeed the developing pacemaker cells. In addition to the cells in the cardiac

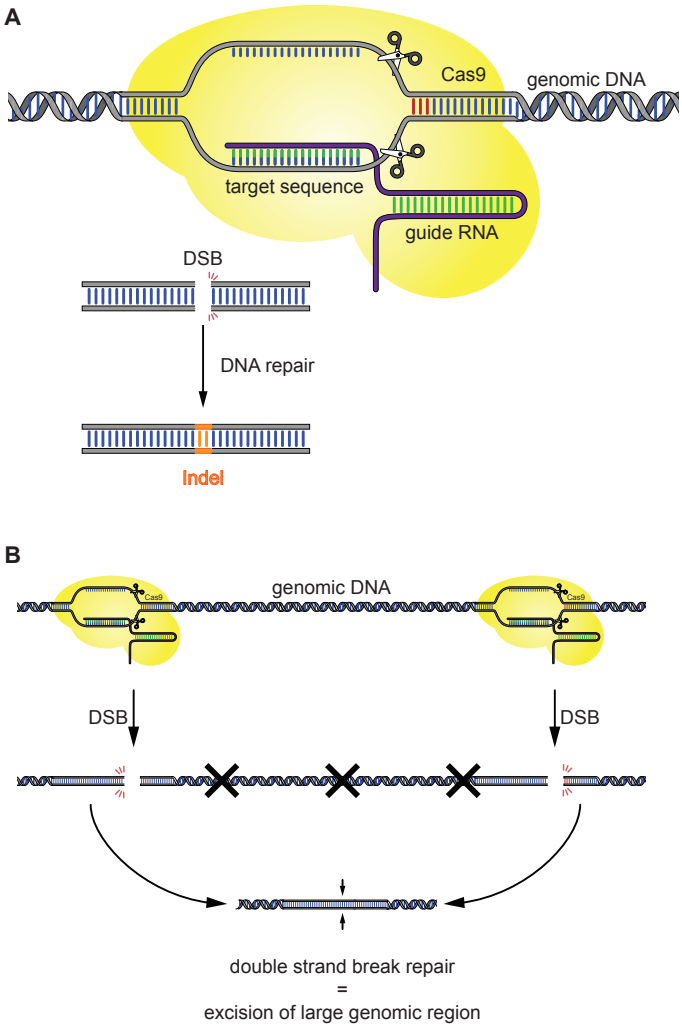

Figure 2: Illustration of the CrispR-Cas9 genome editing method.

(A) GuideRNA (gRNA) constructs were designed complementary to the designated genomic target sequence. The gRNA (purple) recruits a Cas9 endonuclease to the target sequence. Cas9 cleaves both DNA strands inducing a double strand break. During cellular DNA repair mechanisms, small indels cause mutations in the genomic sequence. **(B)** Using 2 gRNA to simultaneously target neighbouring genomic loci. The DSB repair machinery mends the DNA damage by ligating the open ends of the DNA strand back together, regularly resulting in a loss of the genomic region located between the two target loci.

disc, *isl1* is also expressed in other cell types. Isl1^{+} cells are abundant in the lateral plate mesoderm and developing brain, located dorsal and lateral of the cardiac disc extending numerous axons (Fig. 4). Furthermore, cells in the hatching gland are covering the yolk on either side of the head. At 28hpf several Isl1^{+} cells were located at the inflow pole of the heart tube (Fig. 5A-C). As the heart tube undergoes looping, at 32hpf, two clusters of Isl1^{+} cardiomyocytes were observed. One at the posterior rim of the tube and another in the inner curvature of the atrium, reaching towards the AV canal (Fig. 5D-F). At 3 dpf a ring of spindle-shaped Isl1^{+} cells was surrounding the sinoatrial junction. In addition, a second population of Isl1^{+} cells was located in the inner curvature of the atrium (Fig. 5K-M). Both populations of cells expressed the cardiomyocyte-specific myosin *myl7*.

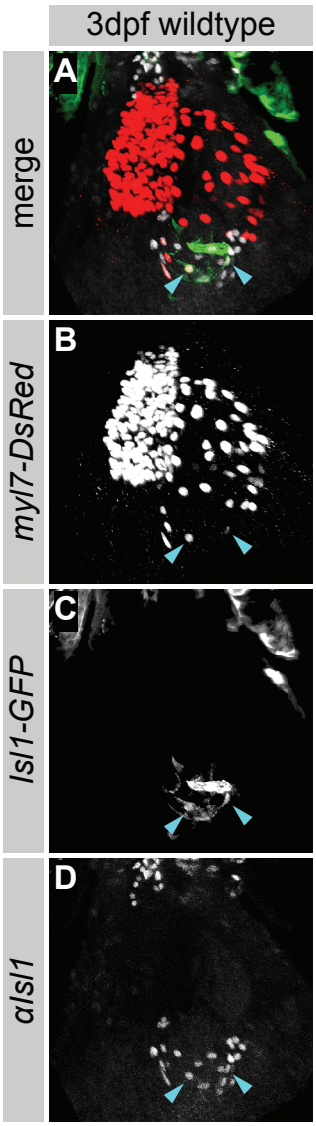

In the adult heart, Isl1 was observed in the pacemaker cells forming a ring around the sinoatrial junction (Fig. 6). They were embedded in the myocardium and showed low expression of *myl7*. The pacemaker cells formed long cellular protrusions connecting them to each other. Using an antibody against Isl1, we could confirm that the Isl1-GFP^{+} cells in the adult heart recapitulate the endogenous *isl1* expression. While endogenous Isl1 was confined to the nucleus, the Isl1::GFF transgenic reporter line induced UAS::GFP expression also in the cytoplasm allowing us to assess the shape of the cells and revealing the various Isl1^{+} axons innervating the heart (Fig. 6).

It has been shown that the adult zebrafish heart is heavily innervated by neurons that enter the heart at the sinoatrial junction where they are in close proximity to Hcn4^{+}/Isl1^{+} pacemaker cells (Stoyek et al., 2015) (Fig. 7). We observed thick Isl1^{+}/Ac-Tubulin^{+}

Figure 3: The tg(Isl1:GalFF^{hu10018Tg}; UAS:GFP^{nkuasgfp1aTg}) transgenic reporter line marks Isl1 expressing cells in the embryonic sinoatrial region.

(A-D) Ventral view of a 3 dpf heart of the tg(Isl1:GalFF^{hu10018Tg}; UAS:GFP^{nkuasgfp1aTg}); *myl7*-DsRed transgenic reporter line. All cardiomyocytes are labelled by *myl7*-DsRed **(B)**. An antibody against Isl1 marks expression in cardiomyocytes in the sinoatrial junction. The transgenic reporter line marks several of the Isl1^{+}/myl7^{+} cardiomyocytes in the sinoatrial region (arrowheads).

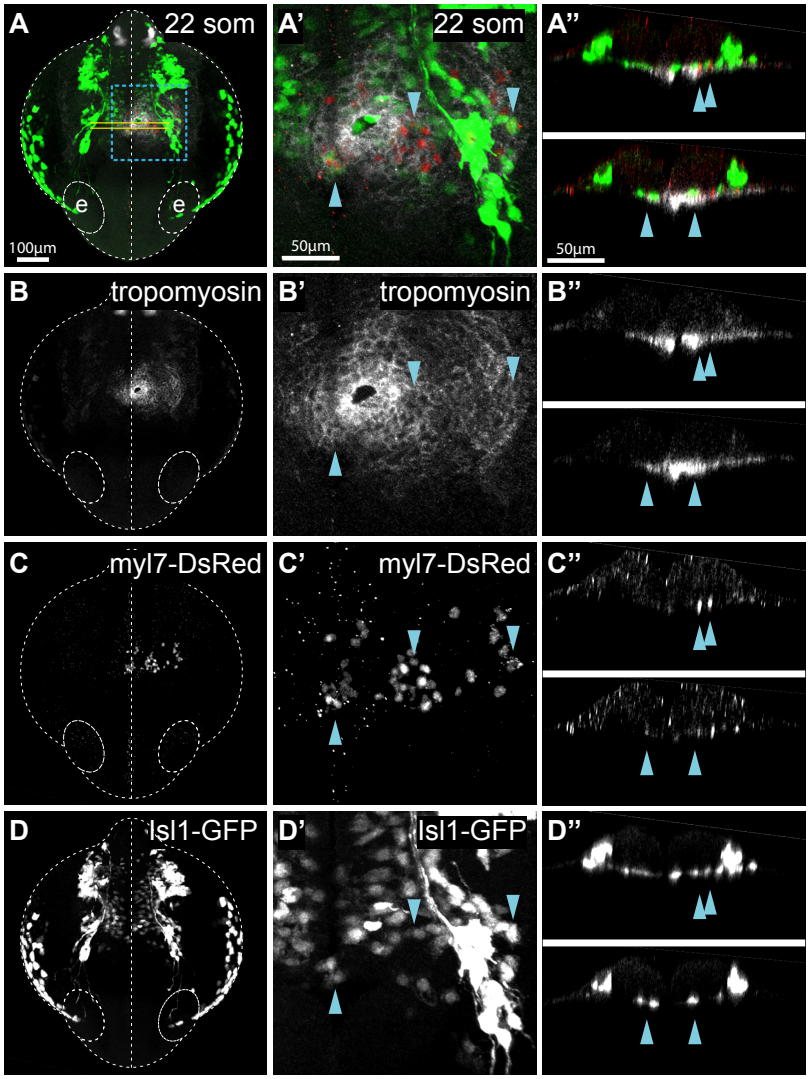

Figure 4: Isl1⁺ cells are integrated in the cardiac disc.

3D reconstruction of a confocal stack of an 22 somite stage embryo from the tg(Isl1:GalFF^{hu10018Tg}; UAS:GFP^{nkuasgfp1aTg}); *myl7*-DsRed transgenic reporter line. Dorsal view on a whole mount embedded embryo. The blue box indicates the region magnified in A'-D'. (A''-D'') shows YZ-cross-sections trough the cardiac disc at locations indicated by yellow lines in (A). **(A/A')** Isl1:GalFF;UAS:GFP in green is expressed in various neurons in the brain, the hatching gland and the lateral plate mesoderm. Several cardiomyocytes in the cardiac disc are GFP⁺ (blue arrowheads). **(B/B')** tropomyosin labels all muscle cells including cardiomyocytes in the cardiac disc. **(C/C')** *myl7*-DsRed labels all cardiomyocytes. **(D/D')** Isl1:GalFF;UAS:GFP labels all Isl1⁺ cells. Isl1 is expressed in cells within the cardiac disc but not restricted to a specific region. White dashed line: outline of whole embryo, highlighting the eyes and midline.

neuronal bundles entering the cardiac tissue at the sinoatrial junction and crossing the atrium towards the AV canal (Fig. 8). We did not observe any Isl1^{+} cells at the AV canal (data not shown). It remains to be determined where the corresponding cell bodies are residing and whether the axons are terminating at a structure within the cardiac tissue. We did not observe any direct contacts between the Isl1^{+} pacemaker cells in the SAR and the innervating Isl1^{+} neurons.

Figure 5: Isl1^{+} cells are already present in the developing heart tube clustering in two distinct cell populations.

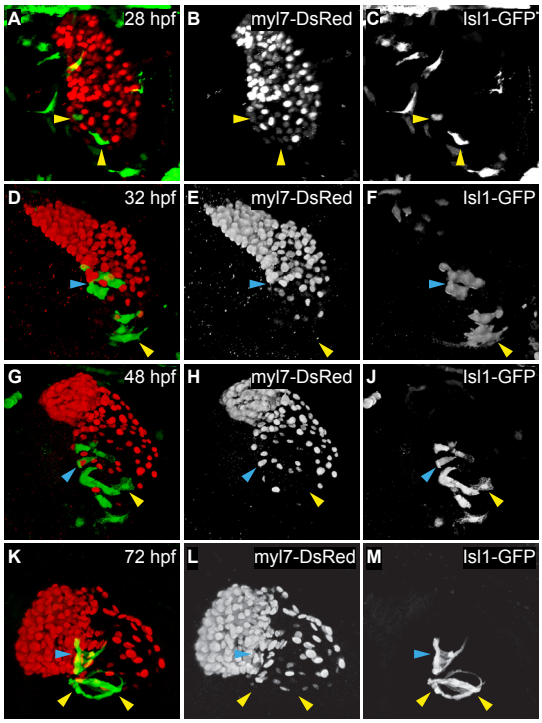

3D reconstruction of a confocal stack of the embryonic heart between 28 and 72hpf from the tg(Isl1:GalFF^{hu10018Tg}; UAS:GFP^{nkuasgfp1aTg}); *myl7*-DsRed transgenic reporter line. *myl7*-DsRed labels all cardiomyocytes (red). **(A-C)** At 28 hpf Isl1 is expressed in cardiomyocytes at the posterior pole of the heart tube (yellow arrowhead). **(D-F)** At 32 hpf two populations of GFP^{+} cells were present. Several cells at the posterior pole (yellow arrowheads) and a cluster of cells in the inner curvature of the atrium (blue arrowheads). **(G-J)** At 48 hpf the two clusters are less well separated, but GFP^{+} cells still stretch from the posterior pole of the heart to the inner curvature of the atrium (blue arrowheads). **(K-M)** At 72 hpf a ring of GFP^{+} cells surrounds the sinoatrial junction at the posterior pole of the heart (yellow arrowheads). The separate second cluster of cells in the inner curvature reaches to the AV canal (blue arrowhead).

Figure 6: Isl1 expressing cells form a ring around the sinoatrial junction (following page).

3D reconstruction of a confocal stack of an adult heart from the tg(Isl1:GalFF^{hu10018Tg}; UAS:GFP^{nkuasgfp1aTg}) transgenic reporter line. Hearts were sectioned at 100µm per section. (A) View onto the sinoatrial junction at the entrance of the atrium. αIsl1^{+} cells (red, 39.4D5 (DSHB)) are located at the base of the inflow valve leaflets, surrounding the sinoatrial junction. Isl1:GalFF-UAS:GFP (green) marks the pacemaker cells at the sinoatrial junction. All GFP^{+} cells are also αIsl1^{+} (blue arrowheads). GFP^{+} axons form a dense network covering the chamber wall and valves. Thick GFP^{+} bundles of axons extend into the sinoatrial region, bifurcate and surround the sinoatrial opening (white arrows). Inset: Illustration of an adult heart. Yellow arrow indicates the viewpoint of the image. In red, the area of the sinoatrial junction. a: atrium, v: ventricle, ba: bulbus arteriosus, sv: sinus venosus, an: anterior, po: posterior, ve: ventral, do: dorsal

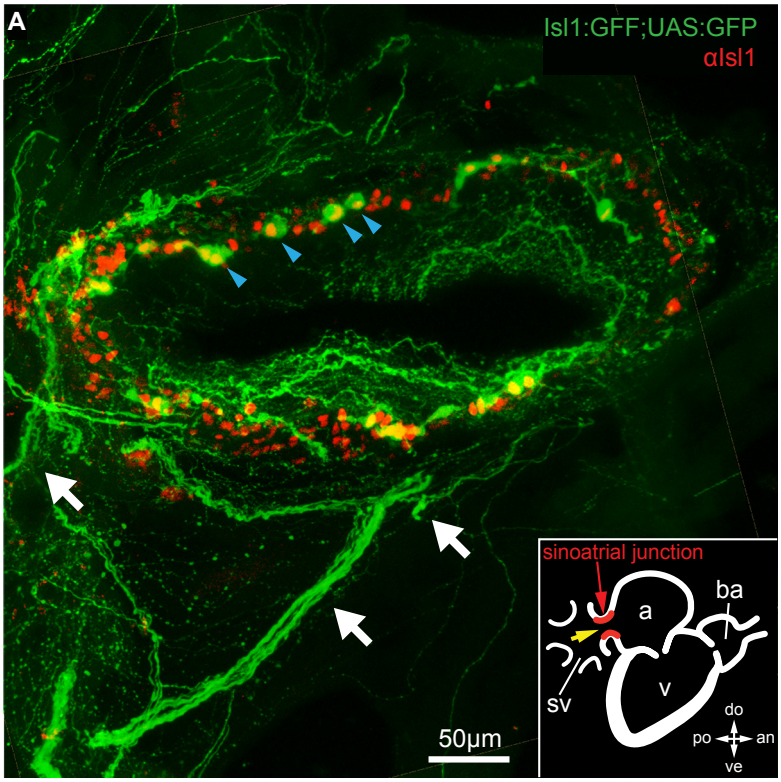

Figure 7: Isl1⁺ neurons innervate the adult zebrafish heart.

3D reconstruction of a confocal stack of the sinoatrial region of an adult heart from the tg(Isl1:GalFF^{hu10018Tg}; UAS:GFP^{nkuasgfp1aTg}) transgenic reporter line (green). All neurons are labelled with αacetylated tubulin (red). Hearts were sectioned at 100μm per section. White dashed box indicates area of zoom-in in A'-C'. **(A-C)** Numerous axons are innervating the heart at the sinoatrial junction (white arrow). The axons are GFP⁺ **(B)** and positive for the neuronal cell marker acetylated tubulin **(C)**. **(A'-C')** Zoom-in image of **(A-C)**. Three interconnected GFP⁺ pacemaker cells (blue arrowheads) surrounded by GFP⁺/αacTubulin⁺ axons. The pacemaker cells are negative for the αacetylated tubulin antibody.

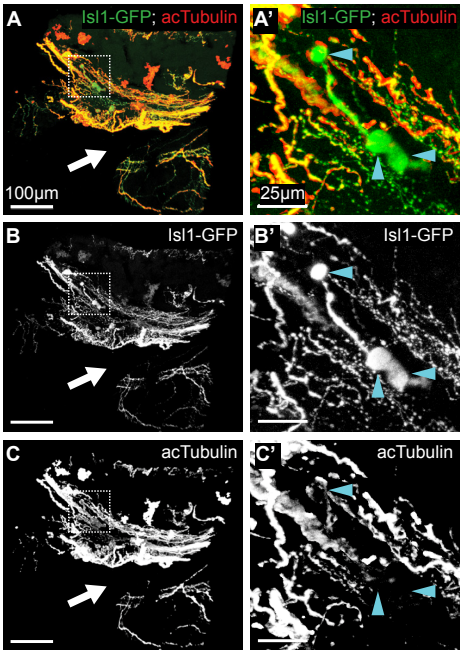

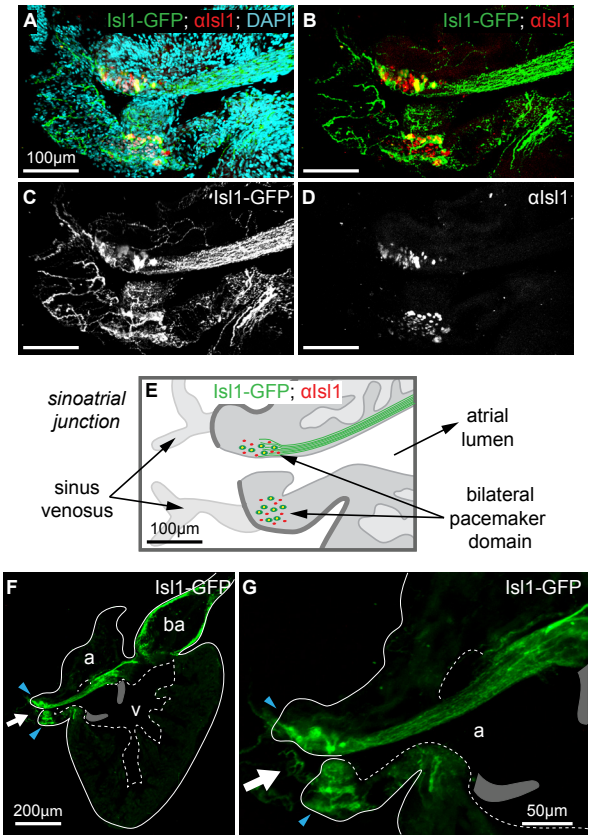

Figure 8: Sinoatrial Isl1 expressing pacemaker cell population is entwined with Isl1:GalFF-UAS:GFP+ axons.

(A-D) 3D reconstruction of a confocal stack of the sinoatrial region of an adult heart from the tg(Isl1:GalFF^{hu10018Tg}; UAS:GFP^{nkuasgfp1aTg}) transgenic reporter line (green), labelled with αIsl1 in red (39.4D5, DSHB) and DAPI. Hearts were sectioned at 100µm per section. Bilateral population of Isl1^{+}/ GFP^{+} pacemaker cells are located in the sinoatrial junction. GFP^{+} axons are entering the heart at the sinoatrial junction and innervate the atrial tissue. The innervating axons are intermingled with the pacemaker cells. A thick bundle of axons is running along the inner wall of the atrium extending from the sinoatrial region towards the atrial lumen. **(E)** Illustration of the adult sinoatrial region shown in **(A-D)** highlighting the bilateral pacemaker cell populations and thick bundle of axons extending into the atrial lumen. **(F-G)** GFP^{+} pacemaker cell populations are situated on both sides of the sinoatrial junction (blue arrowheads). GFP^{+} axons enter the heart from the sinus venosus (white arrow). A thick bundle of GFP+ axons extends from the sinoatrial region across the atrium to the AV canal. The bulbus arteriosus (ba) is densely covered in GFP^{+} axons. White line: outline of the heart; White dashed line: outline of heart lumen. In grey: AV valves. a: atrium, v: ventricle, ba: bulbus arteriosus.

Identification of regulatory sequences driving Isl1 expression

Our previously published transgenic Isl1 reporter line recapitulated the Isl1 expression pattern with the exception of the Isl1 expressing cells in the sinoatrial region. We hypothesized that this cell-type specific loss of the transgene expression was due to one or more regulatory elements missing in the BAC construct.

Hence, we analyzed the genomic sequence used in the generation of the reporter line. We had used the BAC clone CH211-219F7 to establish the transgenic reporter line. It contained a 207kb fragment of genomic zebrafish DNA from chromosome 5. This fragment contained the entire *isl1* locus as well as approximately 160kb of the downstream and 40kb of the upstream genomic sequence (Tessadori et al., 2012). We hypothesized that the expression of *isl1* in the different cell types it is expressed in, is affected by regulatory elements in its genomic region.

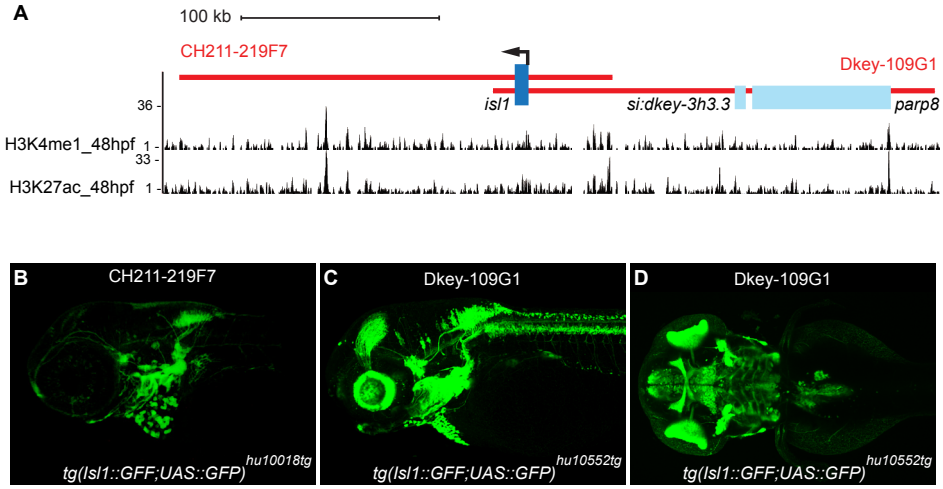

Figure 9: Genomic location of Isl1 on chromosome 5.

(A) ChIP-seq data for H3K4me1 and H3K27ac retrieved form whole embryonic data at the 2 day post fertilisation. Shown is the genomic location of Isl1 on chromosome 5. The Isl1 locus is highlighted in dark blue. Two neighbouring genes *si:dkey-3h3.3* and *parp8* are highlighted in light blue. The genomic regions included in the BAC constructs used to generate the reporter lines are marked in red. **(B)** Lateral view of the GFP expression in a 3dpf embryo of the tg(Isl1:GalFF$^{hu10018Tg;}$ UAS:GFP^{nkuasgfp1aTg}) transgenic reporter line. **(C)** Lateral view and **(D)** dorsal of the GFP expression in a 3dpf embryo of the tg(Isl1:GalFFhu^{10552Tg}; UAS:GFP^{nkuasgfp1aTg}) transgenic reporter line.

To assess the regulatory function of the genomic neighborhood up- and downstream of the Isl1 locus, we established several Isl1 reporter constructs using different BAC clones with different fragments of the genomic DNA around the *isl1* locus. The cloning strategy was similar to the previously described procedure (Tessadori et al., 2012) but using the Tol2 system instead of meganucleases for genome integration. We successfully established two stable lines (Fig. 9). The tg(Isl1:GalFF^{hu10018Tg}) line was made using the aforementioned BAC clone CH211-219F7. For the second line, *tg(*Isl1:GalFF^{hu10552Tg}) we used the BAC clone Dkey-109G1 containing the Isl1 locus as well as approximately 200kb of the upstream, but only 10 kb of the downstream genomic sequence (Fig. 9).

In transgenic embryos, we observed several disparities in the overall GFP expression pattern between the two reporter lines. Most notably was the expression in parts of the mid and forebrain as well as the retina and optic nerve only observed in the Dkey-109G1 derived line (Fig. 9), indicating the presence of specific regulatory elements in the upstream sequence only present in the Dkey-109G1 BAC. At 3 dpf, expression in the sinoatrial region of the embryonic heart was only observed in the CH211-219F7 derived line (Fig. 3) and not in the Dkey-109G1 derived line (Fig. 10).

Figure 10: No GFP^{+} cells in the embryonic sinoatrial region in the tg(Isl1:GalFF^{hu10552Tg}; UAS:GFP^{nkuasgfp1aTg}) transgenic reporter line.

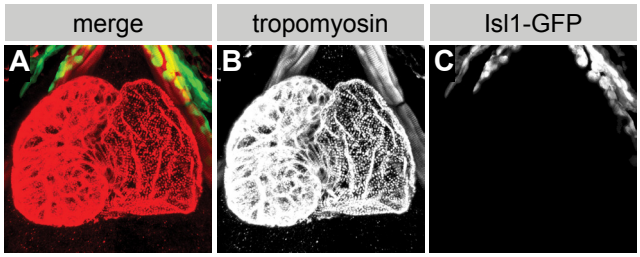

(A-C) Ventral view of a 3 dpf heart of the tg(Isl1:GalFF^{hu10552Tg}; UAS:GFP^{nkuasgfp1aTg}) transgenic reporter line. **(B)** Tropomyosin (red) marks all muscle cells. **(C)** GFP expression was observed in pharyngeal arches anterior to the heart, but not within the cardiac tissue including the sinoatrial region.

This difference in cardiac expression suggested the presence of a cardiac specific enhancer element within the ~180 kb genomic region downstream of the Isl1 locus. Previously published ChIP-seq data from 48 hpf zebrafish embryos for H3K4me1 and H3K27ac samples (L.Kaaij, personal communication; (Kaaij et al., 2016)) revealed multiple peaks indicating the presence of active enhancer elements (Fig. 11). Histone H3 monomethylation at lysine 4 (H3K4me1) and histone H3 acetylation at lysine 27 (H3K27ac) are present on histones flanking active enhancers (Shlyueva et al., 2014). Since enhancers can be located at any given distance from their target gene promoter, their identification remains challenging. To narrow down the genomic region containing the putative pacemaker-specific enhancer, we decided to remove parts of the regulatory region using a CrispR/Cas9 gene editing approach (Fig.2B). We designed several guideRNAs (gRNA) in the 180kb genomic region downstream of the Isl1 locus that could be combined to induce large genomic deletions (Fig. 11). Since the gRNAs can target the genomic DNA as well as the integrated BAC-Isl1-GFP reporter construct in the Isl1 transgenic embryos, we hypothesized that the loss of an enhancer element would result in a loss of GFP reporter expression.

Different combinations of two efficient gRNAs targeting different loci were injected in embryos of the *tg(*Isl1:GalFF^{hu10018Tg}; UAS:GFP^{nkuasgfp1aTg}) line (suppl. Table 1). We assessed successful excision of the targeted genomic region by PCR and by analyzing the GFP expression pattern. Using primers flanking the genomic region to be excised, we validated the deletion by the CrispRs (Fig. 11). While all uninjected control embryos expressed GFP in the sinoatrial region, Expression was lost in 33% of embryos injected with gRNAs 1&2, in 15% of embryos injected with gRNAs 2&4 and in 44% of embryos injected with gRNAs 1&4 (Table 1). All gRNAs targeting locus #3 failed to induce a deletion. This confirmed the importance of the targeted genomic region for the expression of Isl1 in pacemaker cells. Since all combinations of gRNAs had an effect, we concluded that there are several regulatory elements within the region likely acting in a collaborative fashion to induce Isl1 expression.

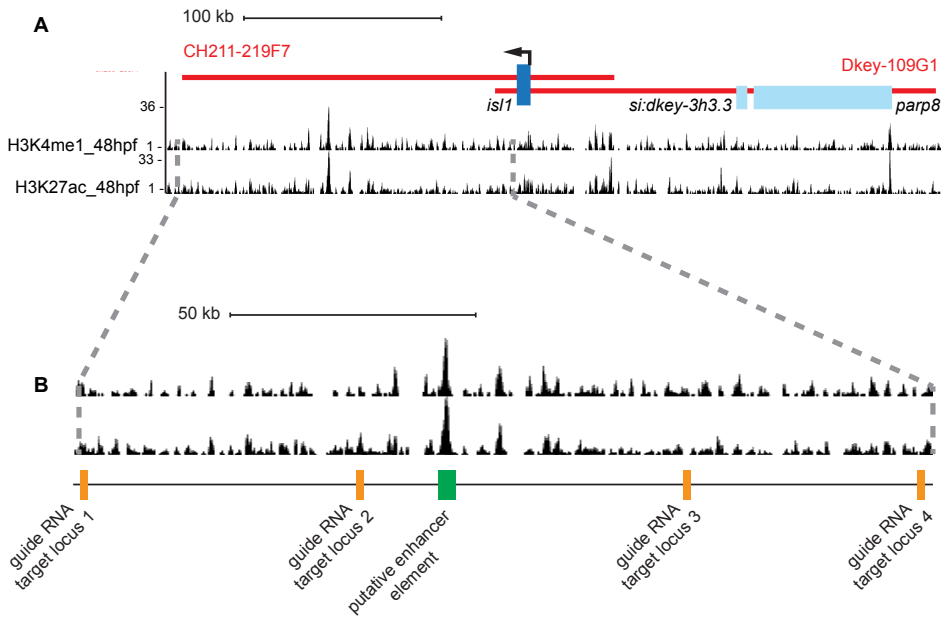

Figure 11: Location of the gRNA target sites in the genomic region downstream of the Isl1 locus.

(B) Zoom in on the ChIP-seq data for the Isl1 genomic region shown in Fig. 3. The gRNA target regions (orange) divide the 180kb region in 3 parts of approximately 40kb each. A putative enhancer locus in highlighted in green.

Table 1

Guide RNA injection	*n*	Isl1-GFP^{+} embryo	Isl1-GFP^{+} SA region	Isl1-GFP^{-} SA region	Isl1-GFP lost in SA region
UIC	237	51	51	0	0%
gRNA1 + gRNA2	54	12	8	4	33%
gRNA2 + gRNA4	104	27	23	4	15%
gRNA1 + gRNA4	100	23	13	10	44%

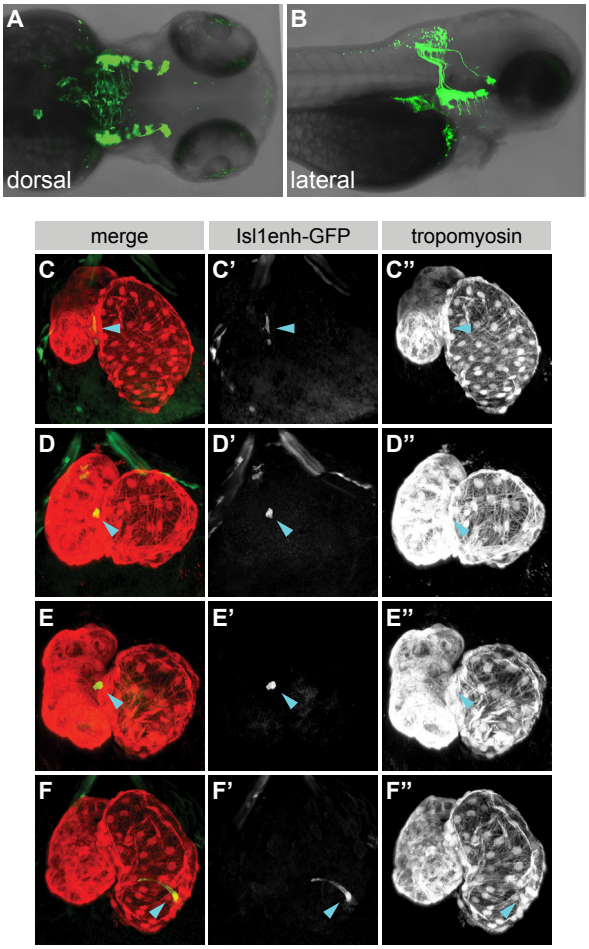

Figure 12: A putative enhancer elements induces GFP reporter expression.

(A) dorsal and lateral **(B)** view of a 3dpf embryo injected with the E1b-GFP reporter construct containing the putative enhancer sequence highlighted in Fig 6B (green). GFP signal superimposed on bright field image. The GFP expression pattern reproduces the Isl1:GalFF-UAS:GFP pattern partly. **(C-F)** Expression of the E1b-GFP-enhancer construct in the embryonic heart at 3dpf. GFP+ cells were present in The AV region **(C-E)** and the sinoatrial region **(F)** of the heart (arrowheads). All cardiomyocytes are labelled by tropomyosin **(C''-F'')**.

In the ChIP-seq data one region located approximately 90 kb downstream of Isl1 showed the most robust signal for the histone modification indicating an active enhancer element (Fig. 11). To test the putative enhancer region, we cloned the 3kb fragment containing the putative enhancer element in the vector containing an *E1b* minimal promotor in front of a GFP reporter gene. Without an enhancer element, the minimal promotor is not able to induce GFP expression. We injected the enhancer reporter construct and examined the GFP expression pattern at 3dpf. GFP expression was detected in various tissues, partly recapitulating the GFP expression pattern in the *tg(*Isl1:GalFF^{hu10018Tg}; UAS:GFP^{nkuasgfp1aTg}) transgenic reporter line. This result indicated that the 3kb enhancer element was active in a subset of Isl1 expressing cells, including cells in the rhombencephalon, pharyngeal arches and anterior intestinal bulb (Fig. 12A-B). GFP^{+} cells in the heart were located in the AV canal and sinoatrial region (Fig. 12C-F'').

In conclusion, the putative enhancer element is active and sufficient to initiate expression on the nearby minimal promotor in a subset of Isl1-expressing cells. The observed expression in the heart shows that the enhancer can induce promotor activity in cardiomyocytes, including the cells in the sinoatrial region.

Supplementary table 1

		Toxicity		Efficiency	
		n	Survival rate	n	Mutation rate
gRNA locus#1	gRNA1	11/55	20.0%	0/10	0.0%
	gRNA2	21/33	63.7%	14/21	66.7%
	gRNA3	*29/32*	*90.6%*	*16/20*	*80%*
	Uninjected	36/37	97.3%	0/30	0.0%
gRNA locus#2	*gRNA1*	*69/77*	*89.6%*	*19/20*	*95.0%*
	gRNA2	58/78	74.4%	12/20	60.0%
	gRNA3	13/20	65.0%	13/13	100%
	Uninjected	60/60	100%	0/9	0.0%
gRNA locus#3	gRNA1	176/225	78.2%	0/40	0.0%
	gRNA2	196/232	84.5%	0/40	0.0%
	gRNA3	54/66	81.8%	0/40	0.0%
	Uninjected	85/86	98.8%	0/16	0.0%
gRNA locus#4	*gRNA1*	*86/96*	*89.6%*	*20/20*	*100%*
	gRNA2	80/86	93.0%	0/20	0.0%
	Uninjected	32/32	100%	0/10	0.0%

Islet-1 expressing cells are still present in the Isl1 KO embryonic mutant heart

The *tg*(Isl1:GalFF^{hu10018Tg}; UAS:GFP^{nkuasgfp1aTg}) reporter line enabled us to highlight the Isl1-expressing cells. In the 3dpf heart several Isl1 expressing cardiomyocytes in the inflow tract are labelled by GFP expression (Fig. 13A-C). In our previous work using a developmental timing assay we observed an effect on differentiation of the cardiomyocytes located at the inflow pole of the *isl1* mutant heart (de Pater et al., 2009). This was suggestive for a defect in the addition of isl1^{+} cells from second heart field. The new *isl1* reporter line now allowed us to assess the fate of the Isl1 positive cells in the Isl1$^{-/-}$ mutant background. Surprisingly, Isl1 expressing cells were still present in the Isl1$^{-/-}$ mutant heart at 3dpf (Fig. 13D-F). In addition, the total number of cardiomyocytes was not decreased in the Isl1$^{-/-}$ mutant hearts (Fig. 13G). These results suggest that Isl1 is not required for the addition of second heart field cells in the zebrafish heart. Furthermore, these results suggest that the bradycardia and arrhythmia observed in the *isl1* mutant is not due to a loss of pacemaker cells but rather a result of a defect in pacemaker function. To further characterize the Isl1-expressing cells in the Isl1$^{-/-}$ mutant, we assessed the expression of several genes that are important during heart and pacemaker cell development (Fig. 14). We speculated that the loss of Isl1 lead to a change in the cells identity and function.

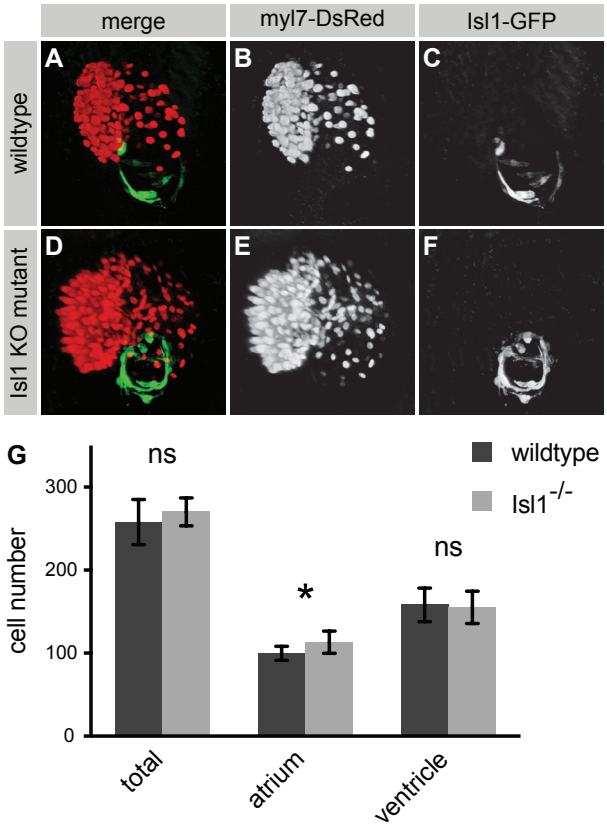

Figure 13: Isl1^{+} cells are still present in the Isl1 mutant heart.

3D reconstructions of 3dpf hearts of the tg(Isl1:GalFF^{hu10018Tg}; UAS:GFP^{nkuasgfp1aTg}); *myl7*-DsRed transgenic reporter line in wildtype **(A-C)** and Isl1K88X mutant **(D-F)** hearts. All cardiomyocytes are marked by *myl7*-DsRed expression. The Isl1^{+} cells form a ring at the sinoatrial junction in wildtype and Isl1 mutants. **(G)** Total and chamber-specific cell number in wildtype and Isl1K88X mutant hearts. wildtype n=9, Isl1 mutant n=8.

The expression domain of the chamber working myocardium marker *natriuretic peptide A* (*nppa)* was expanded in the Isl1$^{-/-}$ mutant. While expression at the IFT was absent in wildtype siblings, the IFT in Isl1$^{-/-}$ mutant showed ectopic expression of *nppa* (Fig. 14B). This indicates that the Isl1$^{-/-}$ pacemaker cells in the sinoatrial region differentiated into working myocardial cells. Furthermore, expression of *bmp4* and *tbx2*, known to be expressed in pacemaker cells (Tessadori et al., 2012), was specifically lost at the IFT (Fig. 14D,F arrowheads). Thus, the cardiomyocytes in the sinoatrial region seem to have adapted a working myocardial identity and lost expression of pacemaker specific genes. Expression of *T-box 20* (*tbx20)*, *T-box 5* (*tbx5a)* and *myocyte enhancer factor 2C* (*mef2c)* was unaffected by the Isl1 mutation (Fig. 14G-M).

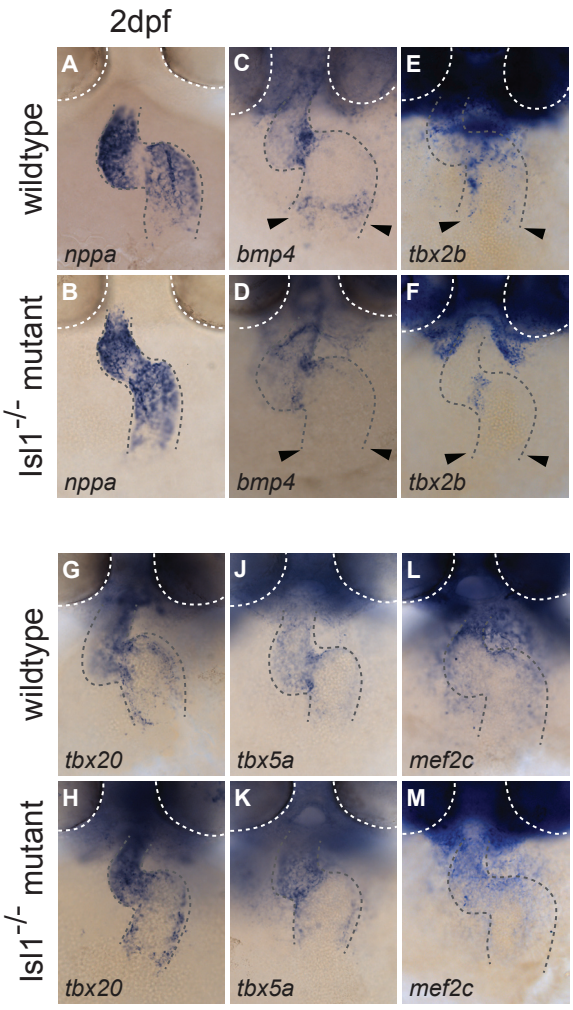

Figure 14: Expression of cardiac marker genes in wildtype and Isl1 mutant hearts.

Whole mount in-situ hybridisation in 2 dpf wildtype and Isl1-/- mutant embryos. **(A,B)** *nppa* expression marks the working myocardium. **(C,D)** *bmp4* and **(E,F)** *tbx2b* are expressed in the AV canal and sinoatrial region (arrowheads). Expression in the sinoatrial region is lost in Isl1$^{-/-}$ mutants. Expression of *tbx20* **(G,H)**, *tbx5* **(J,K)** and *mef2c* **(L,M)** in the heart tube was unchanged in Isl1$^{-/-}$ mutants. White dashed line indicates the position of the eyes.

DISCUSSION

Isl1 is a major factor in pacemaker cell development. Its expression in pacemaker cells is crucial for maintaining the rhythmicity of the heartbeat.
During embryonic heart development, we observed two populations of Isl1$^+$ cells, at the sinoatrial junction and the inner curvature of the atrium. Their location in the inner curvature of the developing atrium did not change between 28 and 72hpf (Fig. 5). It was initially described that the electrical impulse, triggering the wave of cardiomyocyte depolarization in the embryonic heart, originated from cells in the inner curvature of the atrium. Thus, the functional pacemaker was thought to be positioned in this location (Arrenberg et al., 2010). It remains to be determined whether the two populations of Isl1$^+$ cells remain separated and contribute to different structures within the heart. In the adult heart, we only found one population of Isl1$^+$ cells, embedded in the myocardium of the sinoatrial junction (Fig. 8). Possibly, the Isl1$^+$ cell population in the inner curvature joined the Isl1$^+$ cells in the sinoatrial junction. Alternatively, the cells at the inner curvature lose Isl1 expression during later stages of development. The interconnected Isl1$^+$ cells in the sinoatrial junction are functional pacemaker cells as confirmed by electrophysiological analysis (Tessadori et al., 2012). Numerous Isl1$^+$ axons were innervating the heart, entering from the sinoatrial junction and forming a dense network across the chambers and bulbus. In addition, thick bundles of axons were extending from the pacemaker cells at the sinoatrial junction directly to the AV canal (Fig. 8F,G). The axons were positive for acetylated tubulin, confirming their neuronal identity, in contrast to the myocardial Isl1$^+$ pacemaker cells. We could neither detect direct interaction of the Isl1$^+$ axons with the pacemaker cells, nor could we identify the cell bodies extending the axons into the heart. Since the adult heart is heavily innervated by axons from the autonomous nervous system, it is likely that the Isl1$^+$ axons are a part of this neuronal network (Stoyek et al., 2015, Stoyek et al., 2016). Especially the thick cable-like bundle of axons connecting the pacemaker domain directly to the AV canal was an interesting observation. In the developing chick heart Kelder et al. described a continuum of Isl1$^+$ cardiomyocytes extending from the SAN to the AV canal (Kelder et al., 2015). Even though this connection is lost during later development, it could indicate an additional role for Isl1 in early development of cardiac conduction system components such as the AV node on top of its crucial role in pacemaker cell development. The cluster of Isl1$^+$ cells we observed in early stages of heart development in the inner curvature of the atrium close to the AV canal might constitute a similar connection in zebrafish. The existence of a conduction system in the zebrafish heart remains a topic of debate. So far, no distinct structure comparable to the mammalian AV node has been identified. We did not detect any Isl1$^+$ cells at the AV canal. Stoyek et al. described a population of Hcn4$^+$/M_2R^+ cells

embedded in the myocardium at the base of the AV valves (Stoyek et al., 2016). Whether these cells possess the potential to function as independent pacemaker cells remains to be determined. Nevertheless, sustained ventricular contractions in isolated adult hearts after resection of the atrium clearly indicate the ability of cells in the AV canal to induce cardiac contractions independently (data not shown). The neuronal connection might constitute a direct connection between the autonomous nervous system and a secondary pacemaker structure in the AV canal. It could also form a connection between the dominant pacemaker at the sinoatrial junction and a secondary pacemaker in the AV canal. However, the lack of any discernible pacemaker structure or pacemaker-specific molecular markers other than Isl1 has hindered the identification of a secondary pacemaker population.

The first transgenic Isl1 reporter line *tg(*Isl1:GalFF^{hu6635Tg}; UAS:GFP^{nkuasgfp1aTg}) recapitulated the known Isl1 expression pattern with the important exception of the sinoatrial region of the embryonic heart (Tessadori et al., 2012). While the *tg(*Isl1:GalFF^{hu6635Tg}) line was generated using the same BAC clone (CH211-219F7) as for the novel *tg(*Isl1:GalFF^{hu10018Tg}), we used the meganuclease I-Sce1-system instead of the tol2 based system to facilitate genome integration. We speculate that the specific absence of GFP expression in the embryonic sinoatrial region in the initial reporter line was due to the lack of regulatory element(s) crucial for Isl1 expression in developing pacemaker cells. This might have been caused by fragmentation of the BAC sequence prior to genome integration due to unspecific cleavage of the meganuclease.

Little is known about the regulation of Isl1 in pacemaker cells. We concluded that the genomic region downstream of the Isl1 locus contains one or more regulatory elements crucial for Isl1 expression specifically in pacemaker cells. The genomic region upstream of the Isl1 promoter was not sufficient to induce Isl1 expression in pacemaker cells. A comparison of the Isl1 transgenic reporter lines we generated highlighted the importance of regulatory elements around the gene of interest. Hence, it is important to carefully assess whether the reporter gene expression pattern recapitulates the native gene expression pattern. We could not narrow down the exact genomic location of the putative enhancer element(s), but transient loss of the whole 180kb locus or parts of it in the *tg(*Isl1:GalFF^{hu10018Tg}; UAS:GFP^{nkuasgfp1aTg}) transgenic reporter line lead to a reduced number of GFP^{+} pacemaker cells. The variable efficiency in eradicating the expression of GFP in pacemaker cells might be due to a collaborative role of several regulatory elements acting on the Isl1 promoter. Furthermore, we cannot exclude several integrations of the BAC construct, impeding a full loss of GFP expression. A region displaying high accumulation of histone marks indicating an active enhancer element was sufficient to initiate gene expression in cardiomyocytes, including pacemaker cells. However, there are likely several

regulatory elements cooperatively acting on the Isl1 promoter.

Contrary to Isl1 knockout mice, Isl1$^{-/-}$ zebrafish embryonic mutant hearts show no morphological defects. While the mutant mouse heart lacks large parts of the heart, the cell number in zebrafish knockout mutants was equal to wildtype siblings (Fig. 13G). The Isl1-positive pacemaker cells were still present in the Isl1$^{-/-}$ heart. Thus, the bradyarrhythmic phenotype in Isl1 mutants was not caused by a loss of the pacemaker cells, but rather by an inability to maintain pacemaker function. Whereas expression of *tbx2b* and *bmp4* was lost in the Isl1 mutant, the expression domain of *nppa* was expanded posteriorly. We hypothesize that Isl1$^{-/-}$ pacemaker cells fail to fully execute the pacemaker differentiation program and instead adapt a working cardiomyocyte identity. Since working cardiomyocytes lose their ability to initiate action potentials without external stimulation, they cannot function as pacemaker cells. Physiological characterization of the Isl1 expressing cells by comparing the wildtype and Isl1$^{-/-}$ pacemaker cells is needed to confirm the proposed change in cellular identity. The homeobox protein Nkx2.5 in combination with other factors such as Gata4 and Tbx5, acts as an important factor in early cardiac cell development where it induces differentiation of the working chamber cardiomyocytes (Brunskill et al., 2001, Small and Krieg, 2003). Nkx2.5 is not expressed in pacemaker cells and believed to play an antagonistic role to Isl1 and its presumed upstream regulator Shox2 (Dorn et al., 2015, Ye et al., 2015). If the Isl1$^{-/-}$ pacemaker cells indeed adapt a working myocardial identity it could be due to ectopic expression of *nkx2.5* in the absence of Isl1. Expression analysis of both *nkx2.5* and *shox2* in wildtype and Isl1$^{-/-}$ pacemaker cells should clarify their cell identity.

During cardiac development in zebrafish cells from the first heart field (FHF) make up the initial heart tube and cells from the second heart field (SHF) are added to both poles of the tube. The SHF cells contribute to the outflow- and inflow pole structures, including the sinoatrial junction (de Pater et al., 2009). Given the location of the Isl1^{+} pacemaker cells at the sinoatrial junction, it has been speculated that the they originate from the SHF cell population and are added to the tube during the final stages of cell addition. We showed that there are already Isl1^{+} cells in the heart tube at 28hpf, when the addition of SHF cells is still ongoing (de Pater et al., 2009). Thus, the Isl1^{+} cells are not joining the heart in the final stages of cell addition. Furthermore, the pacemaker cells were still present in the Isl1$^{-/-}$ mutant heart and the cardiomyocyte number was not affected. Hence, Isl1 is not required for the addition of cells to the heart tube. This presents a striking difference to the role of Isl1 in mammalian heart development, since Isl1 knockout mice lack the SHF-derived structures of the heart (Cai et al., 2003).

METHODS

Zebrafish lines

Fish used in this study were kept in standard conditions as previously described (Westerfield, 1995). Tupfel long fin (TL) wildtype, *isl1K88X (isl1$^{sa29/sa29}$)* mutant (de Pater et al., 2009), *tg(myl7:EGFP)^{twu26}* (Huang et al., 2003) and *tg(-5.1myl7:nDsRed2-NLS)^{f2}* (Mably et al., 2003) transgenic zebrafish lines were available from ZIRC. The Islet-1 reporter line *tg(Isl1:GalFF^{hu6635Tg}; UAS:GFP^{nkuasgfp1aTg})* was previously described (Tessadori et al., 2012). Details on the generation of the additional Isl1 transgenic reporter lines *tg(Isl1:GalFF^{hu10018Tg})* and *tg(Isl1:GalFF^{hu10552Tg})* in *tg(UAS:GFP^{nkuasgfp1aTg})* embryos (Asakawa et al., 2008) are given below. All studies involving vertebrate animals were performed with institutional approval in compliance with institutional ethical guidelines.

Generation of transgenic E1b-enhancer reporter lines

The putative Isl1 enhancer locus was amplified by PCR (Fwd-primer: 5'-ACCACATTAGCACCACATTAGT-3'; Rev-primer, 5'-GGATAGGGGAAAGGGCAAAG-3'), cloned in the pCR™8/GW/TOPO® TA vector (Life Technologies, Cat. No. K250020) and transformed in One Shot® Top 10 F' Chemically Competent E. coli cells (Life Technologies, Cat. No. C303003) according to the manufacturer's instructions. Next, the locus was cloned into the E1b-GFP-Tol2-Gateway (Addgene, plasmid 37846) vectors using LR Clonase® II Plus (Life Technologies, Cat. No. 12538-120). TL wildtype zebrafish embryos at one-cell stage were injected with 1nl of the E1b-enhancer reporter construct plasmids and 1µl Tol2 RNA (250ng/µl; a kind gift of Chien, C.B., University of Utah Medical Center, Salt Lake City, Utah) GFP expression was assessed at 2-3dpf and GFP^{+} embryos were used for further immunohistochemistry and the establishment of stable zebrafish reporter lines.

In-situ hybridization

For in-situ hybridization (ISH) TL wildtype embryos were fixed in 4% PFA-PBS overnight and dehydrated in methanol. ISH on 3dpf embryos was carried out as previously described (Chocron et al., 2007, Westerfield, 1995).

Generation of the Islet-1 transgenic line

The *tg(Isl1:GalFF^{hu10018tg})* and *tg(Isl1:GalFF^{hu10552Tg})* line was generated essentially as described previously (Tessadori et al., 2012, Bussmann and Schulte-Merker, 2011). An iTOL2_amp cassette for pTarBAC was inserted in the vector sequences of bacterial artificial chromosome (BAC) CH211-219F7 and Dkey-109G1, containing

the full *isl1* locus. An expression cassette containing the GalFF gene (Asakawa et al., 2008) and kanamycin resistance gene was integrated at the ATG site of the 1st exon of the isl1 gene. Primers used were (in lower case sequence homologous to BAC): isl1_Gal4FF_F 5'-gggccttctgtccggttttaaaagtggacctaacaccgccttactttcttaccATGAAGCTACTGT-CTTCTATCGAAC-3' and isl1_KanR_R 5'-aaataaacaataaagcttaacttacttttcggtggatcccccatgtct-ccTCAGAAGAACTCGTCAAGAAGGCG-3'. Red/ET recombination was done following the manufacturer's protocol (Gene Bridges) with minor modifications. BAC-DNA isolation was carried out using a Midiprep kit (Life Technologies). 300 ng/µl of BAC-DNA was injected in *tg(UAS:GFP^{nkuasgfp1aTg})* embryos (Asakawa et al., 2008) in combination with 25ng Tol2 mRNA. To establish the stable transgenic line, healthy embryos displaying robust isl1-specific fluorescence were selected and grown to adulthood.

Immunohistochemistry and image processing

Embryos and adult hearts were fixed in 2% paraformaldehyde-PBS overnight. Adult hearts were embedded in 3% agarose + 1% gelatine and sectioned at 100 µm thickness. Immunohistochemistry was carried out as previously described (de Pater et al., 2009). The primary antibodies used were chicken αGFP (Aves Labs, 1:500), rabbit αDsRed (Clontech, 1:200), mouse αTropomyosin (Sigma Aldrich, 1:200), mouse αIslet-1&2 (DSHB, 1:100), mouse αAcetylated Tubulin clone 6-11B-1 (Sigma Aldrich, 1:100) and DAPI (Life Technologies, 1:2500). All immunohistochemistry images are 3D reconstructions of confocal scans. Image processing was done using the Imaris data visualization software (Bitplane). For image clarity, non-cardiac expression of the TCF-mCherry reporter line was removed (Fig.3).

CRISPR/Cas9 system

CrispR/Cas9 mediated mutagenesis was carried out as previously described (Montague et al., 2014). Four target loci within the 163,588bp stretch of genomic DNA downstream of *isl1* were chosen, dividing the genomic region in three parts. Three guideRNA (gRNA) oligos were designed for each target locus (Supplementary data table 1). For microinjection, 12.5ng/µl gRNA and 150ng/µl Cas9 mRNA were diluted in RNase-free. 1 nl per embryo was manually injected in TL wildtype and *tg(*Isl1:GalFF^{hu10018Tg}; UAS:GFP^{nkuasgfp1aTg}*); myl:DsRed)* embryos at the one-cell stage. Successful deletion of the targeted DNA locus was assessed by PCR.

gRNA locus#1	gRNA1	F	5'-TAGGGCTGGAGATGAAGTGTTG-3'
		R	5'-AAACCAACACTTCATCTCCAGC-3'
	gRNA2	F	5'-TAGGAGGCAAGATAATGGCTCT-3'
		R	5'-AAACAGAGCCATTATCTTGCCT-3'
	gRNA3	F	5'-TAGGAGATGTAAATCCCTCCTC-3'
		R	5'-AAACGAGGAGGGATTTACATCT-3'
gRNA locus#2a	gRNA1	F	5'-TAGGTAACGGAGACTCTCTCAA-3'
		R	5'-AAACTTGAGAGAGTCTCCGTTA-3'
	gRNA2	F	5'-TAGGGCCAGCTTCTTATCAGCC-3'
		R	5'-AAACGGCTGATAAGAAGCTGGC-3'
gRNA locus#2b	gRNA3	F	5'-TAGGATGGCCACCTGCCTCATA-3'
		R	5'-AAACTATGAGGCAGGTGGCCAT-3'
gRNA locus#3a	gRNA1	F	5'-TAGGGCACATATTAGAAGTTAA-3'
		R	5'-AAACTTAACTTCTAATATGTGC-3'
	gRNA2	F	5'-TAGGCAATTTAACAAGTTAAAT-3'
		R	5'-AAACATTTAACTTGTTAAATTG-3'
	gRNA3	F	5'-TAGGCAGGTAATTGTTTGTCTG-3'
		R	5'-AAACCAGACAAACAATTACCTG-3'
gRNA locus#4b	gRNA1	F	5'-TAGGAGGCTTTGTGCTACCCAA-3'
		R	5'-AAACTTGGGTAGCACAAAGCCT-3'
	gRNA2	F	5'-TAGGATTCATTGAATCACAAGT-3'
		R	5'-AAACACTTGTGATTCAATGAAT-3'
enhancer locus#1	gRNA1	F	5'-TAGGGCCTTACAATATTTTCCA-3'
		R	5'-AAACTGGAAAATATTGTAAGGC-3'
	gRNA2	F	5'-TAGGTCTCAGACAAAAAAAGGT-3'
		R	5'-AAACACCTTTTTTTGTCTGAGA-3'
	gRNA3	F	5'-TAGGAAGCTGATTACAGCAGCT-3'
		R	5'-AAACAGCTGCTGTAATCAGCTT-3'
enhancer locus#2b	gRNA1	F	5'-TAGGTTTAGGGCTGCACGATAG-3'
		R	5'-AAACCTATCGTGCAGCCCTAAA-3'
enhancer locus#2a	gRNA2	F	5'-TAGGTATTACACAGGTATTGCA-3'
		R	5'-AAACTGCAATACCTGTGTAATA-3'
	gRNA3	F	5'-TAGGGAAATTATTAGCATATTG-3'
		R	5'-AAACCAATATGCTAATAATTTC-3'

REFERENCES

AKITAKE, C. M., MACURAK, M., HALPERN, M. E. & GOLL, M. G. 2011. Transgenerational analysis of transcriptional silencing in zebrafish. *Dev Biol,* 352**,** 191-201.

ARRENBERG, A. B., STAINIER, D. Y., BAIER, H. & HUISKEN, J. 2010. Optogenetic control of cardiac function. *Science,* 330**,** 971-4.

ASAKAWA, K., SUSTER, M. L., MIZUSAWA, K., NAGAYOSHI, S., KOTANI, T., URASAKI, A., KISHIMOTO, Y., HIBI, M. & KAWAKAMI, K. 2008. Genetic dissection of neural circuits by Tol2 transposon-mediated Gal4 gene and enhancer trapping in zebrafish. *Proc Natl Acad Sci U S A,* 105**,** 1255-60.

BARUSCOTTI, M. & ROBINSON, R. B. 2007. Electrophysiology and pacemaker function of the developing sinoatrial node. *Am J Physiol Heart Circ Physiol,* 293**,** H2613-23.

BRUNSKILL, E. W., WITTE, D. P., YUTZEY, K. E. & POTTER, S. S. 2001. Novel cell lines promote the discovery of genes involved in early heart development. *Dev Biol,* 235**,** 507-20.

BULGER, M. & GROUDINE, M. 2011. Functional and mechanistic diversity of distal transcription enhancers. *Cell,* 144**,** 327-39.

BURKHARD, S., VAN EIF, V., GARRIC, L., CHRISTOFFELS, V. M. & BAKKERS, J. 2017. On the Evolution of the Cardiac Pacemaker. *Journal of Cardiovascular Development and Disease,* 4**,** 4.

BUSSMANN, J. & SCHULTE-MERKER, S. 2011. Rapid BAC selection for tol2-mediated transgenesis in zebrafish. *Development,* 138**,** 4327-32.

CAI, C. L., LIANG, X., SHI, Y., CHU, P. H., PFAFF, S. L., CHEN, J. & EVANS, S. 2003. Isl1 identifies a cardiac progenitor population that proliferates prior to differentiation and contributes a majority of cells to the heart. *Dev Cell,* 5**,** 877-89.

CALO, E. & WYSOCKA, J. 2013. Modification of enhancer chromatin: what, how, and why? *Mol Cell,* 49**,** 825-37.

CHANG, N., SUN, C., GAO, L., ZHU, D., XU, X., ZHU, X., XIONG, J. W. & XI, J. J. 2013. Genome editing with RNA-guided Cas9 nuclease in zebrafish embryos. *Cell Res,* 23**,** 465-72.

CHAUVEAU, S., ANYUKHOVSKY, E. P., BEN-ARI, M., NAOR, S., JIANG, Y. P., DANILO, P., JR., RAHIM, T., BURKE, S., QIU, X., POTAPOVA, I. A., DORONIN, S. V., BRINK, P. R., BINAH, O., COHEN, I. S. & ROSEN, M. R. 2017. Induced Pluripotent Stem Cell-Derived Cardiomyocytes Provide In Vivo Biological Pacemaker Function. *Circ Arrhythm Electrophysiol,* 10**,** e004508.

CHOCRON, S., VERHOEVEN, M. C., RENTZSCH, F., HAMMERSCHMIDT, M. & BAKKERS, J. 2007. Zebrafish Bmp4 regulates left-right asymmetry at two distinct developmental time points. *Dev Biol,* 305**,** 577-88.

CREYGHTON, M. P., CHENG, A. W., WELSTEAD, G. G., KOOISTRA, T., CAREY, B. W., STEINE, E. J., HANNA, J., LODATO, M. A., FRAMPTON, G. M., SHARP, P. A., BOYER, L. A., YOUNG, R. A. & JAENISCH, R. 2010. Histone H3K27ac separates active from poised enhancers and predicts developmental state. *Proc Natl Acad Sci U S A,* 107**,** 21931-6.

DE PATER, E., CLIJSTERS, L., MARQUES, S. R., LIN, Y. F., GARAVITO-AGUILAR, Z. V., YELON, D. & BAKKERS, J. 2009. Distinct phases of cardiomyocyte differentiation regulate growth of the zebrafish heart. *Development,* 136**,** 1633-41.

DOBRZYNSKI, H., BOYETT, M. R. & ANDERSON, R. H. 2007. New insights into pacemaker activity: promoting understanding of sick sinus syndrome. *Circulation,* 115**,** 1921-32.

DORN, T., GOEDEL, A., LAM, J. T., HAAS, J., TIAN, Q., HERRMANN, F., BUNDSCHU, K., DOBREVA, G., SCHIEMANN, M., DIRSCHINGER, R., GUO, Y., KUHL, S. J., SINNECKER, D., LIPP, P., LAUGWITZ, K. L., KUHL, M. & MORETTI, A. 2015. Direct nkx2-5 transcriptional repression of isl1 controls cardiomyocyte subtype identity. *Stem Cells,* 33**,** 1113-29.

ERICSON, J., THOR, S., EDLUND, T., JESSELL, T. M. & YAMADA, T. 1992. Early stages of motor neuron differentiation revealed by expression of homeobox gene Islet-1. *Science,* 256**,** 1555-60.

HEINTZMAN, N. D., STUART, R. K., HON, G., FU, Y., CHING, C. W., HAWKINS, R. D., BARRERA, L. O., VAN CALCAR, S., QU, C., CHING, K. A., WANG, W., WENG, Z., GREEN, R. D., CRAWFORD, G. E. & REN, B. 2007. Distinct and predictive chromatin signatures of transcriptional promoters and enhancers in the human genome. *Nat Genet,* 39**,** 311-8.

HOFFMANN, S., BERGER, I. M., GLASER, A., BACON, C., LI, L., GRETZ, N., STEINBEISSER, H., ROTTBAUER, W., JUST, S. & RAPPOLD, G. 2013. Islet1 is a direct transcriptional target of the homeodomain transcription factor Shox2 and rescues the Shox2-mediated bradycardia. *Basic Res*

Cardiol, 108**,** 339.
HUANG, C. J., TU, C. T., HSIAO, C. D., HSIEH, F. J. & TSAI, H. J. 2003. Germ-line transmission of a myocardium-specific GFP transgene reveals critical regulatory elements in the cardiac myosin light chain 2 promoter of zebrafish. *Dev Dyn,* 228**,** 30-40.
HWANG, W. Y., FU, Y., REYON, D., MAEDER, M. L., TSAI, S. Q., SANDER, J. D., PETERSON, R. T., YEH, J. R. & JOUNG, J. K. 2013. Efficient genome editing in zebrafish using a CRISPR-Cas system. *Nat Biotechnol,* 31**,** 227-9.
JINEK, M., CHYLINSKI, K., FONFARA, I., HAUER, M., DOUDNA, J. A. & CHARPENTIER, E. 2012. A programmable dual-RNA-guided DNA endonuclease in adaptive bacterial immunity. *Science,* 337**,** 816-21.
KAAIJ, L. J., MOKRY, M., ZHOU, M., MUSHEEV, M., GEEVEN, G., MELQUIOND, A. S., DE JESUS DOMINGUES, A. M., DE LAAT, W., NIEHRS, C., SMITH, A. D. & KETTING, R. F. 2016. Enhancers reside in a unique epigenetic environment during early zebrafish development. *Genome Biol,* 17**,** 146.
KARLSSON, O., THOR, S., NORBERG, T., OHLSSON, H. & EDLUND, T. 1990. Insulin gene enhancer binding protein Isl-1 is a member of a novel class of proteins containing both a homeo- and a Cys-His domain. *Nature,* 344**,** 879-82.
KAWAKAMI, K. 2007. Tol2: a versatile gene transfer vector in vertebrates. *Genome Biol,* 8 Suppl 1**,** S7.
KELDER, T. P., VICENTE-STEIJN, R., HARRYVAN, T. J., KOSMIDIS, G., GITTENBERGER-DE GROOT, A. C., POELMANN, R. E., SCHALIJ, M. J., DERUITER, M. C. & JONGBLOED, M. R. 2015. The sinus venosus myocardium contributes to the atrioventricular canal: potential role during atrioventricular node development? *J Cell Mol Med,* 19**,** 1375-89.
LI, H., LIU, H., SAGE, C., HUANG, M., CHEN, Z. Y. & HELLER, S. 2004. Islet-1 expression in the developing chicken inner ear. *J Comp Neurol,* 477**,** 1-10.
LIANG, X., ZHANG, Q., CATTANEO, P., ZHUANG, S., GONG, X., SPANN, N. J., JIANG, C., CAO, X., ZHAO, X., ZHANG, X., BU, L., WANG, G., CHEN, H. S., ZHUANG, T., YAN, J., GENG, P., LUO, L., BANERJEE, I., CHEN, Y., GLASS, C. K., ZAMBON, A. C., CHEN, J., SUN, Y. & EVANS, S. M. 2015. Transcription factor ISL1 is essential for pacemaker development and function. *J Clin Invest,* 125**,** 3256-68.
LIU, H., ESPINOZA-LEWIS, R. A., CHEN, C., HU, X., ZHANG, Y. & CHEN, Y. 2012. The role of Shox2 in SAN development and function. *Pediatr Cardiol,* 33**,** 882-9.
LIU, Y., LUO, D., ZHAO, H., ZHU, Z., HU, W. & CHENG, C. H. 2013. Inheritable and precise large genomic deletions of non-coding RNA genes in zebrafish using TALENs. *PLoS One,* 8**,** e76387.
MABLY, J. D., MOHIDEEN, M. A., BURNS, C. G., CHEN, J. N. & FISHMAN, M. C. 2003. heart of glass regulates the concentric growth of the heart in zebrafish. *Curr Biol,* 13**,** 2138-47.
MONTAGUE, T. G., CRUZ, J. M., GAGNON, J. A., CHURCH, G. M. & VALEN, E. 2014. CHOPCHOP: a CRISPR/Cas9 and TALEN web tool for genome editing. *Nucleic Acids Res,* 42**,** W401-7.
MORETTI, A., CARON, L., NAKANO, A., LAM, J. T., BERNSHAUSEN, A., CHEN, Y., QYANG, Y., BU, L., SASAKI, M., MARTIN-PUIG, S., SUN, Y., EVANS, S. M., LAUGWITZ, K. L. & CHIEN, K. R. 2006. Multipotent embryonic isl1+ progenitor cells lead to cardiac, smooth muscle, and endothelial cell diversification. *Cell,* 127**,** 1151-65.
PFAFF, S. L., MENDELSOHN, M., STEWART, C. L., EDLUND, T. & JESSELL, T. M. 1996. Requirement for LIM homeobox gene Isl1 in motor neuron generation reveals a motor neuron-dependent step in interneuron differentiation. *Cell,* 84**,** 309-20.
RADDE-GALLWITZ, K., PAN, L., GAN, L., LIN, X., SEGIL, N. & CHEN, P. 2004. Expression of Islet1 marks the sensory and neuronal lineages in the mammalian inner ear. *J Comp Neurol,* 477**,** 412-21.
SHLYUEVA, D., STAMPFEL, G. & STARK, A. 2014. Transcriptional enhancers: from properties to genome-wide predictions. *Nat Rev Genet,* 15**,** 272-86.
SILKA, M. J. & BAR-COHEN, Y. 2006. Pacemakers and implantable cardioverter-defibrillators in pediatric patients. *Heart Rhythm,* 3**,** 1360-6.
SMALL, E. M. & KRIEG, P. A. 2003. Transgenic analysis of the atrialnatriuretic factor (ANF) promoter: Nkx2-5 and GATA-4 binding sites are required for atrial specific expression of ANF. *Dev Biol,* 261**,** 116-31.
SOROLDONI, D., HOGAN, B. M. & OATES, A. C. 2009. Simple and efficient transgenesis with meganuclease constructs in zebrafish. *Methods Mol Biol,* 546**,** 117-30.
SPITZ, F. & FURLONG, E. E. 2012. Transcription factors: from enhancer binding to developmental

control. *Nat Rev Genet,* 13**,** 613-26.
STOYEK, M. R., CROLL, R. P. & SMITH, F. M. 2015. Intrinsic and extrinsic innervation of the heart in zebrafish (Danio rerio). *J Comp Neurol,* 523**,** 1683-700.
STOYEK, M. R., QUINN, T. A., CROLL, R. P. & SMITH, F. M. 2016. Zebrafish heart as a model to study the integrative autonomic control of pacemaker function. *Am J Physiol Heart Circ Physiol,* 311**,** H676-88.
SUN, Y., LIANG, X., NAJAFI, N., CASS, M., LIN, L., CAI, C. L., CHEN, J. & EVANS, S. M. 2007. Islet 1 is expressed in distinct cardiovascular lineages, including pacemaker and coronary vascular cells. *Dev Biol,* 304**,** 286-96.
TESSADORI, F., VAN WEERD, J. H., BURKHARD, S. B., VERKERK, A. O., DE PATER, E., BOUKENS, B. J., VINK, A., CHRISTOFFELS, V. M. & BAKKERS, J. 2012. Identification and functional characterization of cardiac pacemaker cells in zebrafish. *PLoS One,* 7**,** e47644.
THERMES, V., GRABHER, C., RISTORATORE, F., BOURRAT, F., CHOULIKA, A., WITTBRODT, J. & JOLY, J. S. 2002. I-SceI meganuclease mediates highly efficient transgenesis in fish. *Mech Dev,* 118**,** 91-8.
WESTERFIELD, M. 1995. A Guide for the Laboratory Use of Zebrafish (Danio rerio). *The Zebrafish Book.* 3rd ed. Eugene, OR: University of Oregon Press.
XIAO, A. & ZHANG, B. 2016. Generation of Targeted Genomic Deletions Through CRISPR/Cas System in Zebrafish. *Methods Mol Biol,* 1451**,** 65-79.
YE, W., WANG, J., SONG, Y., YU, D., SUN, C., LIU, C., CHEN, F., ZHANG, Y., WANG, F., HARVEY, R. P., SCHRADER, L., MARTIN, J. F. & CHEN, Y. 2015. A common Shox2-Nkx2-5 antagonistic mechanism primes the pacemaker cell fate in the pulmonary vein myocardium and sinoatrial node. *Development,* 142**,** 2521-32.
ZHANG, L., LI, X., YU, X., LI, Y., SUN, A., HUANG, C., XU, F., GUO, J., SUN, Y., ZHANG, X., YANG, X. & ZHANG, C. 2017. Construction of vascularized pacemaker tissues by seeding cardiac progenitor cells and endothelial progenitor cells into Matrigel. *Life Sci,* 179**,** 139-146.
ZHUANG, S., ZHANG, Q., ZHUANG, T., EVANS, S. M., LIANG, X. & SUN, Y. 2013. Expression of Isl1 during mouse development. *Gene Expr Patterns,* 13**,** 407-12.

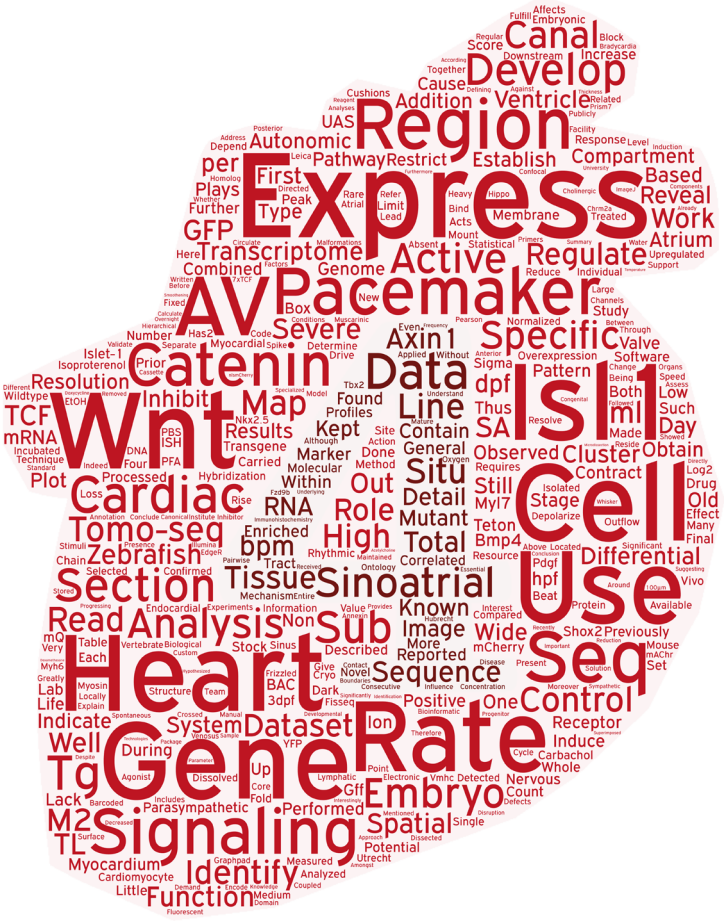
Heart
Gene
Rate
Signaling
Wnt
Cell
Use
Express
Region
Pacemaker
AV
Catenin
Isl1
Data
Develop
Canal
Ventricle
Addition
Cause
Together
Score
Increase
Downstream
Block
Bradycardia
Fulfill
Affects
Embryonic
Cushions
UAS
Autonomic
Depend
Posterior
Address
Facility
Response
Level
Induction
Compartment
Establish
Restrict
Pathway
per
Plays
First
Peak
Type
Further
Rare
Atrial
Refer
Limit
Lead
Heavy
Bind
Acts
Mount
Hippo
Membrane
Based
Reveal
Work
Atrium
GFP
Here
Transcriptome
Active
Regulate
Upregulated
Support
Reduce
Individual
Combined
Genome
Factors
Circulate
Malformations
Absent
Statistical
Primers
Summary
Water
Fixed
Written
Before
Box
New
Large
Channels
Study
Normalized
Pearson
Frequency
Even
Through
Between
Valve
Specific
Severe
Axin1
Number
Has2
Code
Separate
Myocardial
Spike
Determine
Drive
Conditional
Myocardinic
Overexpression
Software
Sigma
Pattern
Change
Being
Speed
Assess
Organs
Both
Low
Such
Day
Made
Showed
Besides
Obtain
Cluster
Observed
Requires
Contract
Log2
Drug
Old
Effect
Many
Final
Vivo
Available
Mouse
mAChr
Set
Previously
Shox2
Wide
Seq
Control
One
Receptor
Induce
Carbachol
Whole
Nervous
Count
Defects
Single
Spatial
Potential
Utrecht
Dissected
Mentioned
Disruption
Embryo
Detected
Vmhc
Electronic
Point
Lymphatic
Gff
Performed
Parasympathetic
Includes
Barcoded
Dissolved
Up
Core
Fold
Aqonist
Tg
Lack
M2
TL
Surface
Myocardium
Cardiomyocyte
Little
Function
Identify
Measured
Analyzed
Coupled
Graphpad
Encode
Medium
Domain
Fluorescent
Demand
Dataset
System
Ion
Positive
Bioinformatic
Progenitor
Therefore
Cycle
Dynamic
Sympathetic
Moreover
Concentration
Influence
Disease
Present
Isolation
Mcherry
Reported
More
Sequence
Novel
Boundaries
Consecutive
Significantly
Laboratories
Give
Cryo
Contact
Dark
Frizzled
BAC
3dpf
Fisseq
Structure
Team
Myosin
Locally
Explain
Lab
Life
Indicate
Spontaneous
Crossed
Manual
Well
During
Packaged
Without
Female
YFP
Aqonist
Dissolved
Up
Core
Fold
Includes
Barcoded
Parasympathetic
Performed
Gff
Lymphatic
Point
Electronic
Vmhc
Detected
Nervous
Count
Defects
Single
Spatial
Potential
Utrecht
Dissected
Mentioned
Disruption
Myocardium
Cardiomyocyte
Little
Function
Identify
Measured
Analyzed
Coupled
Graphpad
Encode
Medium
Domain
Fluorescent
Demand
Read
Analysis
Sub
Image
Wide
Seq
Control
Sinoatrial
Use
Section
Tissue
Tomo-seq
Cardiac
Zebrafish
High
Total
Situ
Detail
Mutant
Role
Out
RNA
Within
Hybridization
Rise
Loss
Processed
Plot
Four
DNA
PFA
Indeed
Incubated
Technique
Standard
PBS
ISH
mRNA
TCF
Wildtype
Different
Resolution
Isoproterenol
Prior
Islet-1
Validate
Inhibit
Map
Results
Transgene
Carried
Nkx2.5
Kept
Found
Profiles
Tbx2
Line
Contain
General
Marker
Done
Method
Molecular
Site
Action
Although
Mature
Understand
Model
Dpf
Thus
SA
Still
Myl7
Teton
Bmp4
Pdgf
hpf
Beat
Stage
Depolarize
Isolated
Whisker
Outflow
Above
Located
Resource
Correlated
Differential
Significant
Enriched
bpm
Rhythmic
Tract
Received
Pairwise
Maintained
Ontology
Essential
Chain
Stimuli
Presence
Selected
Confirmed
Stored
Progressing
Endocardial
Experiments
Information
Mechanism
Entire
Value
Provides
Annexin
Fluorescein
Interest
Compared
Protein
Known
Non
Stock
Sinus
Described
Vertebrate
Biological
Custom
Table
Each
mQ
Very
Myh6
Greatly
Structure
Team
Frizzled
BAC
3dpf
Fisseq
Give
Cryo
Contact
Dark
Novel
Boundaries
Consecutive
Significantly
Laboratories
Sequence
Positive
Bioinformatic
Progenitor
Therefore
Cycle
Dynamic
Sympathetic
Moreover
Concentration
Influence
Disease
Present
Isolation
Mcherry
Reported
More
Receptor
Induce
Carbachol
Whole
Nervous
Count
Defects
Single
Spatial
Potential
Utrecht
Dissected
Mentioned
Disruption
Myocardium
Cardiomyocyte
Little
Function
Identify
Measured
Analyzed
Coupled
Graphpad
Encode
Medium
Domain
Fluorescent
Demand
Lack
M2
TL
Surface
Barcoded
Includes
Parasympathetic
Performed
Gff
Lymphatic
Point
Electronic
Vmhc
Detected
Nervous
Count
Defects
Single
Spatial
Potential
Utrecht
Dissected
Mentioned
Disruption
Tg
Aqonist
Dissolved
Up
Core
Fold
Well
During
Packaged
Without
Female
YFP
Indicate
Spontaneous
Crossed
Manual
Lab
Life
Myosin
Locally
Explain
Structure
Team
Frizzled
BAC
3dpf
Fisseq
Give
Cryo
Contact
Dark
Novel
Boundaries
Consecutive
Significantly
Laboratories
Sequence
Positive
Bioinformatic
Progenitor
Therefore
Cycle
Dynamic
Sympathetic
Moreover
Concentration
Influence
Disease
Present
Isolation
Mcherry
Reported
More
Receptor
Induce
Carbachol
Whole
Nervous
Count
Defects
Single
Spatial
Potential
Utrecht
Dissected
Mentioned
Disruption
Myocardium
Cardiomyocyte
Little
Function
Identify
Measured
Analyzed
Coupled
Graphpad
Encode
Medium
Domain
Fluorescent
Demand
Read
Analysis
Sub
Image
Wide
Seq
Control
Sinoatrial
Use
Section
Tissue
Tomo-seq
Cardiac
Zebrafish
High
Total
Situ
Detail
Mutant
Role
Out
RNA
Within
Hybridization
Rise
Loss
Processed
Plot
Four
DNA
PFA
Indeed
Incubated
Technique
Standard
PBS
ISH
mRNA
TCF
Wildtype
Different
Resolution
Isoproterenol
Prior
Islet-1
Validate
Inhibit
Map
Results
Transgene
Carried
Nkx2.5
Kept
Found
Profiles
Tbx2
Line
Contain
General
Marker
Done
Method
Molecular
Site
Action
Although
Mature
Understand
Model
Dpf
Thus
SA
Still
Myl7
Teton
Bmp4
Pdgf
hpf
Beat
Stage
Depolarize
Isolated
Whisker
Outflow
Above
Located
Resource
Correlated
Differential
Significant
Enriched
bpm
Rhythmic
Tract
Received
Pairwise
Maintained
Ontology
Essential
Chain
Stimuli
Presence
Selected
Confirmed
Stored
Progressing
Endocardial
Experiments
Information
Mechanism
Entire
Value
Provides
Annexin
Fluorescein
Interest
Compared
Protein
Known
Non
Stock
Sinus
Described
Vertebrate
Biological
Custom
Table
Each
mQ
Very
Myh6
Greatly
Structure
Team
Frizzled
BAC
3dpf
Fisseq
Give
Cryo
Contact
Dark
Novel
Boundaries
Consecutive
Significantly
Laboratories
Sequence
Positive
Bioinformatic
Progenitor
Therefore
Cycle
Dynamic
Sympathetic
Moreover
Concentration
Influence
Disease
Present
Isolation
Mcherry
Reported
More
Receptor
Induce
Carbachol
Whole
Nervous
Count
Defects
Single
Spatial
Potential
Utrecht
Dissected
Mentioned
Disruption
Myocardium
Cardiomyocyte
Little
Function
Identify
Measured
Analyzed
Coupled
Graphpad
Encode
Medium
Domain
Fluorescent
Demand
Lack
M2
TL
Surface
Barcoded
Includes
Parasympathetic
Performed
Gff
Lymphatic
Point
Electronic
Vmhc
Detected
Nervous
Count
Defects
Single
Spatial
Potential
Utrecht
Dissected
Mentioned
Disruption
Tg
Aqonist
Dissolved
Up
Core
Fold
Well
During
Packaged
Without
Female
YFP
Indicate
Spontaneous
Crossed
Manual
Lab
Life
Myosin
Locally
Explain
Structure
Team
Frizzled
BAC
3dpf
Fisseq
Give
Cryo
Contact
Dark
Novel
Boundaries
Consecutive
Significantly
Laboratories
Sequence
Positive
Bioinformatic
Progenitor
Therefore
Cycle
Dynamic
Sympathetic
Moreover
Concentration
Influence
Disease
Present
Isolation
Mcherry
Reported
More
Receptor
Induce
Carbachol
Whole
Nervous
Count
Defects
Single
Spatial
Potential
Utrecht
Dissected
Mentioned
Disruption
Myocardium
Cardiomyocyte
Little
Function
Identify
Measured
Analyzed
Coupled
Graphpad
Encode
Medium
Domain
Fluorescent
Demand

CHAPTER 4

Spatially resolved RNA-sequencing of the embryonic heart identifies a role for Wnt/β-catenin signaling in autonomic control of heart rate

Silja Burkhard [1] and Jeroen Bakkers [1,2*]

[1] Hubrecht Institute-KNAW and University Medical Center Utrecht, 3584 CT, Utrecht, The Netherlands.
[2] Department of Medical Physiology, Division of Heart and Lungs, University Medical Center Utrecht, 3584 CT Utrecht, The Netherlands.

submitted

4

SUMMARY

Development of specialized cell types and structures in the vertebrate heart is regulated by spatially-restricted molecular pathways. Disruptions in these pathways can cause severe congenital cardiac malformations or functional defects. To better understand these pathways and how they regulate cardiac development and function we used *tomo*-seq, combining high-throughput RNA sequencing with tissue sectioning, to establish a genome-wide expression dataset with high spatial resolution for the developing zebrafish heart. Analysis of the dataset revealed over 1100 genes differentially expressed in sub-compartments. Pacemaker cells in the sinoatrial region induce heart contractions, but little is known about the mechanisms underlying their development and function. Using our transcriptome map, we identified spatially restricted Wnt/β-catenin signaling activity in pacemaker cells, which was controlled by Islet-1 activity. Moreover, Wnt/β-catenin signaling at a specific developmental stage in the myocardium controls heart rate by regulating pacemaker cellular response to parasympathetic stimuli. Thus, this high-resolution transcriptome map incorporating all cell types in the embryonic heart can expose spatially-restricted molecular pathways critical for specific cardiac functions.

Keywords: heart, pacemaker, Islet-1, *tomo*-seq, transcriptome, wnt, autonomic nervous system, zebrafish, heart rate

INTRODUCTION

The vertebrate heart exerts regular contractions to circulate nutrients and oxygen. Cardiomyocyte contraction is caused by an action potential generated by cardiac pacemaker cells: spontaneous, rhythmic membrane depolarization of the pacemaker cells enables them to trigger the neighboring working myocardium to contract. Heart disease, congenital malformations, aging, or somatic gene defects may cause pacemaker tissue dysfunction, resulting in severely disabling and potentially lethal bradycardia (inappropriately low heart rates) (Dobrzynski et al., 2007, Wolf and Berul, 2006). These conditions can be treated by implantation of an electronic pacemaker. However, this is not ideal as electronic pacemakers can cause cardiac complications, lack autonomic responsiveness, and are unsuitable for pediatric patients. Biological pacemakers, generated in- or ex vivo are thus being explored as alternatives (Rosen et al., 2011, Protze et al., 2017). This however requires exquisite knowledge of the regulatory network driving pacemaker cell differentiation and function.

Although pacemaker cells are situated within, and coupled to, the surrounding cardiomyocytes, they retain a primitive myocardial identity (Bakker et al., 2010). This is established during cardiac development, when a myocardial progenitor cell population ($Shox2^{+}/Tbx18^{+}/Isl1^{+}/Nkx2.5^{-}$) becomes spatially restricted to the region connecting the sinus venosus to the atria (sinoatrial region). These progenitor cells differentiate into $Isl1^{+}/Hcn4^{+}$ pacemaker cells, strictly separated from the $Nkx2.5^{+}$ working cardiomyocytes (Ye et al., 2015, Mommersteeg et al., 2007, Wiese et al., 2009). The pacemaker cells are prevented from differentiating into working myocardium by Shox2, which inhibits Nkx2.5 expression (Espinoza-Lewis et al., 2011, Ye et al., 2015, Sun et al., 2015). Isl1 plays a conserved role in pacemaker cells since zebrafish and mouse embryos lacking Isl1 have severe bradycardia progressing to complete loss of pacemaker function (de Pater et al., 2009, Liang et al., 2015, Tessadori et al., 2012). The etiology of the pacemaker phenotype is unclear and mechanisms acting downstream of Isl1 to control heart rate remain to be determined.

The cardiac pacemaker generates rhythmic action potentials through the combined and oscillating activity of ion channels on the surface membrane and calcium channels on the sarcoplasmic reticulum (Lakatta et al., 2010). Heart rate can vary greatly in response to physiological demand, which is regulated by the autonomic nervous system (Gordan et al., 2015). The autonomic nervous system influences the activity of the ion channels on the surface membrane through G-protein coupled β-adrenergic and cholinergic receptors (Gordan et al., 2015). Developing biological pacemakers that can be controlled by the autonomous nervous system will be a significant improvement from electronic pacemakers used today. Therefore, it is

important to understand how autonomous control is established in pacemaker cells, of which there is very little knowledge.

Identifying novel molecular pathways that regulate the development and specialized functions of individual organs or tissues *in vivo* would be greatly facilitated by genome-wide transcriptome datasets with detailed spatial resolution during development. Several techniques have recently been developed that can resolve the expression of many genes without disruption of tissue organization. FISSEQ is an in-situ sequencing technique based on sequencing on a solid substrate using fluorescent-tagged random hexamers. When combined with confocal imaging, FISSEQ can be applied to tissue sections or whole embryos (Lee et al., 2014). *Tomo*-seq combines standard RNA-sequencing using barcoded primers with histological tissue dissection, and has been used to establish genome-wide transcriptome datasets with high spatial resolution of the whole zebrafish embryo and the injured adult zebrafish heart (Junker et al., 2014, Kruse et al., 2016, Wu et al., 2016). The advantages of the FISSEQ and *tomo*-seq techniques compared to other mRNA-seq related techniques are that: 1) there is no need for prior anatomical annotation of the tissue, 2) it does not rely on tissue dissociation and cell sorting that can influence gene expression, 3) spatial information of the transcripts within the tissue is maintained.

Here we used one of these techniques, *tomo*-seq, to obtain the first genome-wide transcriptome map with high spatial resolution of the developing zebrafish heart. Using *tomo*-seq data, we identified sub-compartment specific gene expression signatures for the ventricle, atrium, AV canal, and the sinoatrial region, where pacemaker cells reside. We found that several members of the Wnt/β-catenin signaling pathway were differentially expressed in the sinoatrial region, resulting in active Wnt/β-catenin signaling in developing pacemaker cells. Functional analysis demonstrated that Wnt/β-catenin signaling acts downstream of Isl1 to establish parasympathetic control of heart rate. Together these results reveal a genetic pathway regulating autonomic control of pacemaker activity.

RESULTS

A genome-wide transcriptome dataset with high spatial resolution of the developing zebrafish heart

At 2 days post fertilization (2 dpf) the zebrafish heart has developed into a looped structure with a recognizable atrium and ventricle that is able to sustain blood circulation in the larvae. At this stage, functional Isl^{+} pacemaker cells are located in the sinoatrial region (Arrenberg et al., 2010, Tessadori et al., 2012). To obtain a transcriptome map of the developing heart at that stage with spatial resolution we

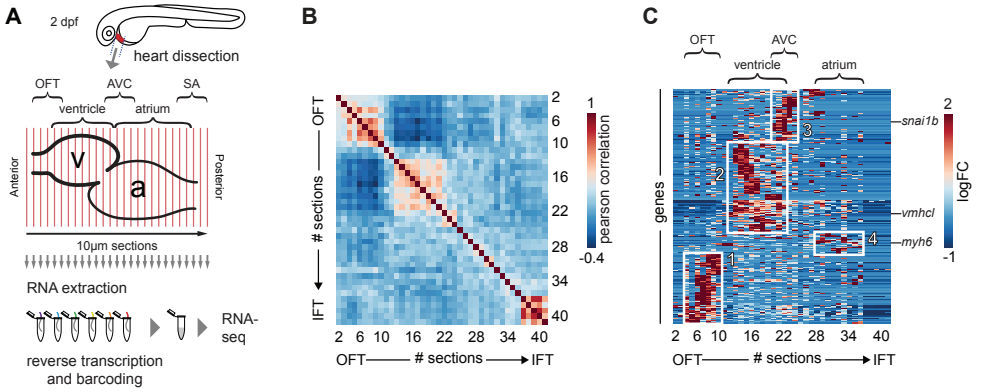

Figure 1: Tomo-seq on isolated embryonic hearts reveals distinct clusters of gene expression.

(A) Hearts were isolated from 2 day old embryos and 10 µm sections were made along the anterior-posterior axis, from outflow to inflow pole. Each section was collected in an individual tube followed by RNA isolation and cDNA transcription using section specific barcodes. After that, samples were pooled for linear amplification and sequence library preparation. **(B)** Pairwise correlation between individual sections across all genes detected at more than 20 reads in at least 2 sections. +1 equals total positive correlation, 0 no correlation, -1 total negative correlation. Blocks of correlating sections can be observed. **(C)** Hierarchical cluster analysis of gene expression per section. Distinct gene expression clusters correspond to different regions of the heart shown in boxed areas: 1. arterial pole/OFT; 2. Ventricle; 3. AV canal; 4. Atrium. RNA sequencing reads per gene were normalized against the total read count per section as well as the total spike-in control RNA read counts. Genes expressed in min 3 sections z-value >1.25. See also Figure S1 and Table S1.

applied the *tomo*-seq method on dissected hearts from 2-day-old zebrafish embryos (Fig. 1A). In short, the isolated cryo-preserved hearts were sectioned into forty 10 µm sections along the anterior-posterior axis. Total RNA was isolated from each section, barcoded and processed for mRNA-sequencing (Hashimshony et al., 2016). We obtained a gene expression dataset with expression information for ~13,000 genes (Fig. S1C and Table S1). To assess global transcriptome patterns in the dataset, we implemented Pearson's correlation analysis, a pairwise measurement of linear correlation per section across the total transcriptome. Several blocks of continuous sections with high positive correlation of overall gene expression were observed (Fig. 1B). This indicates that specific molecular profiles based on explicit gene expression patterns subdivide the embryonic heart at this stage. In order to identify such gene clusters and elucidate underlying gene expression patterns, we performed a hierarchical clustering analysis. Robustly expressed genes (z-score >1.2, in 3 or more consecutive sections) were clustered according to their expression peak within the dataset. The cluster plot confirmed the presence of four large gene clusters with

region-specific expression, which likely corresponded to the outflow tract, ventricle, AV canal and atrium based on the genes present within these clusters (Fig. 1C).

To validate the presence of the above mentioned four cardiac sub-compartments and to identify the SA region where pacemaker cells reside in the tomo-seq data, we analyzed the expression of well-known cardiac genes. The total number of reads for a gene of interest was plotted against the consecutive section numbers and compared to its localized expression detected by whole mount in situ hybridization. Expression of *myosin light chain 7* (*myl7*) defining the boundaries of the myocardial tissue (Fig. 2A), indicated that all sections with exception of the first ten, were derived from myocardial tissue. The first 10 sections most likely contained the non-myocardial arterial pole. *Natriuretic peptide a* (*nppa*) expression is restricted to the working myocardium of the ventricle and atrium and was absent from the non-working myocardium of the outflow tract, AV canal and SA region (Fig. 2B). Together with the ventricle-specific expression of *ventricle myosin heavy chain* (*vmhc*) (Fig. 2C) and atrial-specific *myosin heavy chain 6* (*myh6*) (Fig. 2D) we concluded that the ventricle and the atrium were well separated in the *tomo*-seq data. To address whether genes that are expressed in the endocardial cushions, which give rise to the cardiac valves located in the outflow tract and in the AV canal, are present in the *tomo*-seq data we analyzed the expression of *hyaluronan synthase 2* (*has2*) (Fig. 2E), Indeed, *has2* was well detected in the sections assigned to the outflow tract and the AV canal. The non-working myocardium of the AV canal can be distinguished by the expression of *bone morphogenetic protein 4* (*bmp4*) and *T-box protein 2b* (*tbx2b*). Both genes showed a peak expression around section 25, indicating the position of the AV myocardium (Fig. 2F and G). Importantly, *bmp4* is also expressed in the SA region (Fig. 2F). In the *tomo*-seq data a clear expression peak was detected around section 34 (Fig. 2F), indicating the position of the SA region in the *tomo*-seq data. We superimposed the expression data of the known marker genes to identify the position of the cardiac sub-compartments in the *tomo*-seq data (Fig. 3). We directly compared the superimposed expression data with the previously identified gene clusters and concluded that positions of cardiac sub-compartments correlated well with the identified gene clusters. The SA region was only identified by the marker gene expression and not by the gene cluster analysis, most likely due to its small size in combination with the threshold settings of the gene cluster analysis.

In conclusion, we have generated a genome-wide transcriptome dataset with high spatial resolution. Furthermore, the dataset reveals five sub-compartments in the heart with distinct expression profiles.

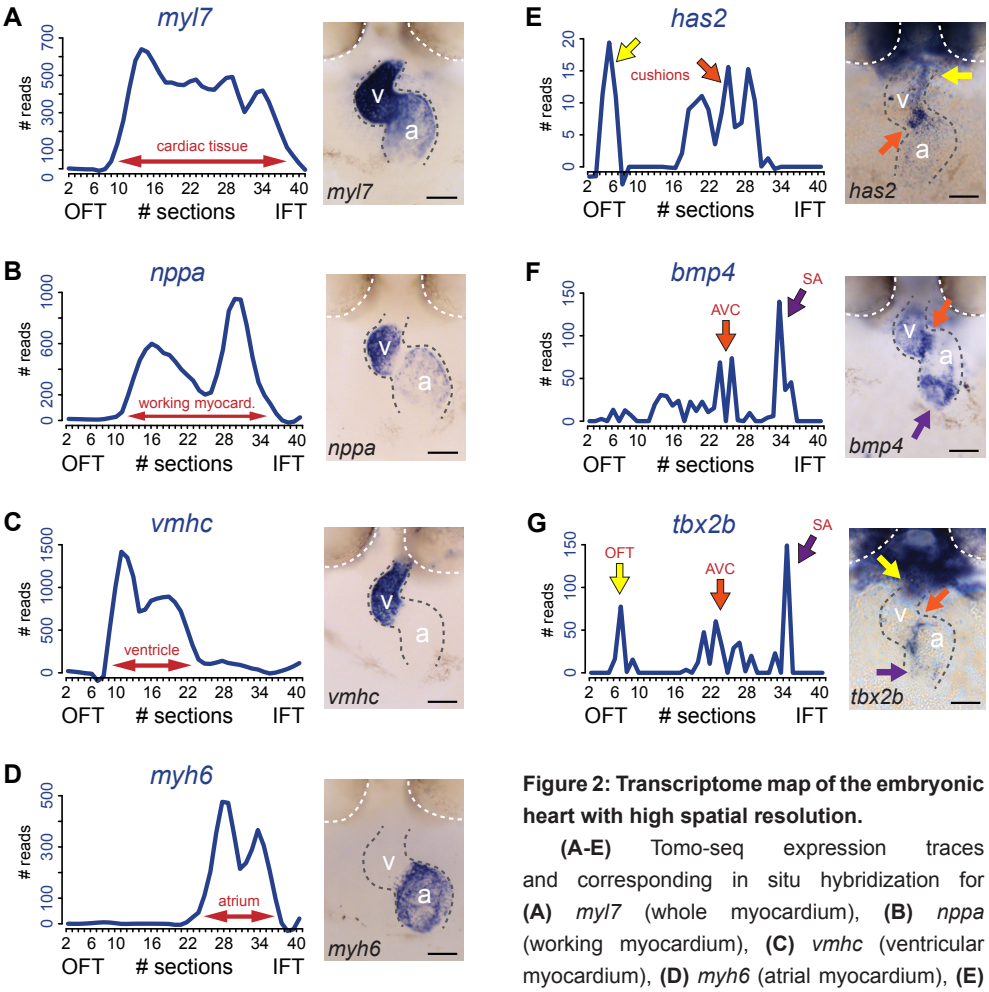

Figure 2: Transcriptome map of the embryonic heart with high spatial resolution.

(A-E) Tomo-seq expression traces and corresponding in situ hybridization for **(A)** *myl7* (whole myocardium), **(B)** *nppa* (working myocardium), **(C)** *vmhc* (ventricular myocardium), **(D)** *myh6* (atrial myocardium), **(E)** *has2* (endocardial cushions), **(F)** *bmp4* (AVC myocardium, orange arrow; IFT myocardium, purple arrow) and **(G)** *tbx2b* (OFT myocardium, yellow arrow, AVC myocardium, orange arrow; IFT myocardium, purple arrow). Anterior up. Gray dashed line outlines the heart. White dashed line outlines the eyes. A, atrium; V, ventricle; AVC: atrioventricular canal; IFT, inflow tract; OFT, outflow tract; SA, sinoatrial region. Scale bars represent 50µm.

Identification of differentially expressed genes

To identify molecular pathways that may be regulating development of the cardiac sub-compartments, we analyzed the sub-compartment-specific transcriptomes in more detail. The boundaries of the sub-compartments were set based on the gene cluster analysis and the mRNA-seq reads for known marker genes (Fig. 3). All genes were ranked according to the specificity of their expression level in the region of interest when compared with the rest of the dataset. With this approach, we identified

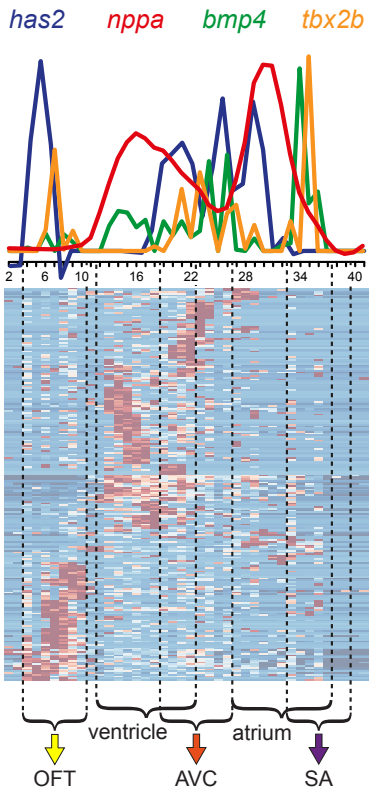

Figure 3: Differential gene expression reveals distinct sub-compartments within the heart.

Superimposed expression profiles of *has2*, *nppa*, *bmp4* and *tbx2b*. Expression peaks of the individual genes overlap with the position of the clusters (dashed lines). *has2* and *tbx2b* in the OFT (yellow arrow). *nppa* in the ventricle. *has2*, *bmp4* and *tbx2b* in the AVC (orange arrow). *nppa* in the atrium. *bmp4* and *tbx2b* in the SA region (purple arrow). OFT, outflow tract; AVC: atrioventricular canal; SA, sinoatrial region.

a total of 1,143 genes for which their expression was upregulated in one of the selected cardiac sub-compartments (ventricle, atrium, AV canal and sinoatrial region) (log2 FC > 2 and $p < 0.05$) (Fig. 4A-C and Table S2). This list of differentially expressed genes contained several genes for which the sub-compartment expression has been well described, such as *myh6* (atrium), *vmhc* and *vmhcl* (ventricle), *spp1* (AV valves), and *isl1, bmp4 and shox2* (sinoatrial region). Besides these few known sub-compartment specific marker genes, we identified many additional differentially expressed genes (99 genes for the atrium, 196 genes for the ventricle, 346 genes for the AV canal and 502 genes for the sinoatrial region). To validate the significance of the identified sub-compartment specific gene-expression profiles in the *tomo*-seq data, we performed in situ hybridization for selected genes. Using this approach, the sub-compartment specific gene expression profiles deduced from the *tomo*-seq data correlated well with the expression patterns obtained by in situ hybridizations (Fig. 4D-F and S2A-B).

We identified 99 genes with upregulated expression in the atrium and 196 genes with upregulated expression in the ventricle (Fig. 4A). Gene ontology analysis revealed enrichment in *oxygen transport* and *tricarboxylic acid cycle* genes in the ventricle, suggesting that already in the 2-day old ventricle metabolism is converting to aerobic oxidative phosphorylation to fulfill higher energy demands (Fig. S2C). Furthermore, several genes related to cardiac myopathies were found amongst the ventricle specific genes (e.g. *csrp3, rcan1a* (Fig. S2A), *tnnc2*, *myo1c* and *actn1*), indicating the value of the dataset for identifying potential disease-causing genes.

The AV canal region contains the AV myocardium and the endocardial cushions, forming the cardiac valves (Beis et al., 2005). We identified 346 differentially expressed genes in the AV canal, but gene-ontology analysis did not reveal any significant

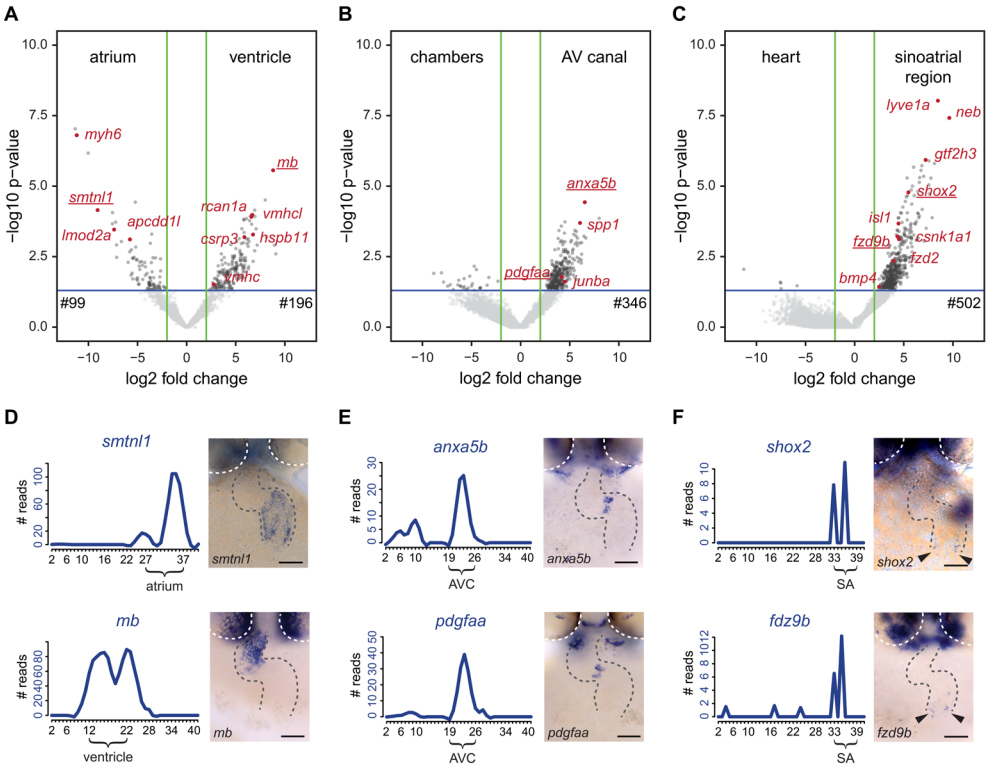

Figure 4: Differentially expressed genes in cardiac sub-compartments

(A-C) Volcano plots highlighting genes differentially expressed in the **(A)** atrium (n=99) and ventricle (n=196), **(B)** AV canal (n=346) and **(C)** sinoatrial region (n=502). Grey and red dots represent individual genes. Green lines indicate threshold of log2 fold change >2. Blue lines indicate threshold of *p*-value < 0,05. **(D-F)** Expression traces and in situ hybridization analysis for representative example genes (gene names underlined in volcano plots) significantly upregulated in **(D)** atrium (*smtnl1*) and ventricle (*mb*), **(E)** AV canal (*anxa5b* and *pdgfaa*) and in the sinoatrial region (*shox2* and *fzd9b*). Gray dashed line outlines the heart. White dashed line outlines the eyes. Anterior up. Scale bars represent 50µm. See also Figure S2 and Table S2.

enrichment for specific biological processes. In situ hybridization confirmed the strong expression of *annexin A*5 (*axna5b*) and *PDGF A* (*pdgfaa*) in the endocardial cushions. Both Annexin A5 and PDGF A have not been directly implicated in cardiac valve development, but PDGF A signaling plays numerous roles in organogenesis during embryo development by regulation of proliferation and directed cell migration (Hoch and Soriano, 2003).

The sinoatrial region contains the pacemaker and proepicardial cells. The majority (502) of the sub-compartment-specific upregulated genes was identified in this region. Gene ontology analysis revealed enrichment in *proepicardium development*

genes based on differential expression of *tbx5a*, *acvr1l* and *bmp4* in the sinoatrial region (Fig. S2E). In addition, several known regulators of pacemaker development (e.g. *isl1* and *shox2*) were identified in our analysis (Fig. 4C, F). Interestingly, *hippo signaling* genes were enriched in the gene ontology analysis. Indeed, the *tomo*-seq dataset contained several components of active hippo signaling, *sav1*, *stk3* and *lats1/2* that were differentially expressed in the sinoatrial region. Moreover, we noticed that several components of the Wnt-signaling pathway were amongst the genes enriched in the sinoatrial region, such as *casein kinase 1, alpha 1* (*csnk1a1*), *frizzled homolog 2* (*fzd2*) and *frizzled homolog 9b* (*fzd9b*) (Fig. 4C, F and S3). Finally, the differential gene expression analysis identified *lymphatic vessel endothelial hyaluronic receptor 1a* (*lyve1a*) as being upregulated in the sinoatrial region. The *lyve1* gene is a marker for lymphatic endothelium. Further factors associated with the lymphatic system were expressed in the sinoatrial region (*prox1a*, *prox1b*, *nr2f1a*, *nr2f2*, *elmo1* and *foxj2*), suggesting that, as in the mammalian heart, cardiac lymphatics can develop from the sinus venosus (Klotz et al., 2015).
In conclusion, the *tomo*-seq dataset reveals cardiac sub-compartment specific transcriptomes and has the potential to identify novel pathways that regulate the development or function of specific domains and structures within the heart.

Wnt/β-catenin signaling activity in pacemaker cells

Since there is very little known about the regulation of pacemaker development we focused our attention on the transcriptome of the sinoatrial region. As mentioned above, several genes that encode for Wnt signaling pathway components were enriched in the sinoatrial region. Wnt ligands bind to Frizzled (Fzd) receptors to activate intracellular β-catenin signaling, which plays multiple roles during cardiac development (reviewed in (Gessert and Kuhl, 2010)). Depending on the developmental stage, Wnt/β-catenin signaling has either positive or negative effects on cardiomyocyte differentiation (Tzahor, 2007, Gessert and Kuhl, 2010, Ueno et al., 2007). In addition, Wnt/β-catenin signaling in the atrioventricular (AV) canal induces the formation of endocardial cushions, giving rise to the AV valves, and the electrophysiological properties of the AV canal myocardium by slowing down electrical conductivity (Hurlstone et al., 2003, Verhoeven et al., 2011, Gillers et al., 2015). Even though Wnt/β-catenin signaling has been studied extensively, a role in pacemaker development has not been reported.
Expression of the Wnt receptor *fzd9b* was detected in sections 33-39 and whole mount in situ hybridization confirmed its expression in the sinoatrial region (Fig. 4F). In addition, expression of the Wnt inhibitor *apcdd1l* was observed in the atrium, but its expression was absent from sections 33-39, defining the sinoatrial region (Fig. S2B). From these results, we hypothesized that Wnt signaling is locally activated in

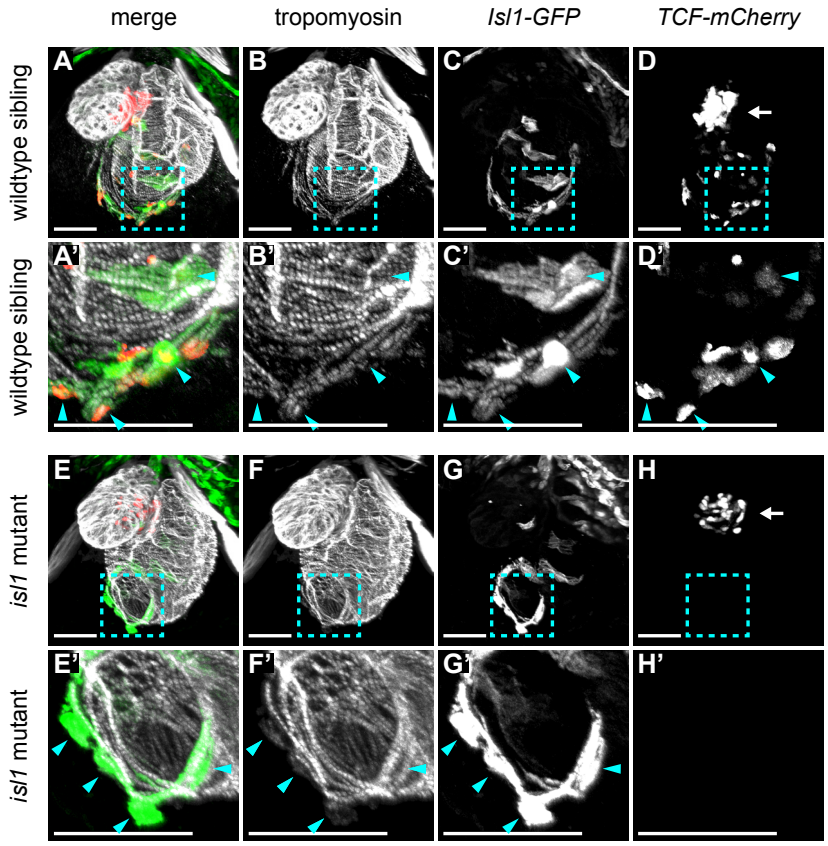

Figure 5: Wnt/β-catenin signaling in cardiac pacemaker cells

3D reconstructions of confocal scans from whole mount embryos containing the *tg(7xTCFXla.Siam:nlsmCherry)* (reporting Wnt/β-catenin activity in red) and the *tg(Isl1:GFF;UAS:GFP)* (reporting isl1 expression and marking pacemaker cells in green) and stained for tropomyosin (myocardium in white). Anterior is up and posterior is down. Wildtype sibling **(A-D')** and *isl1*^{K88X} mutant **(E-H')** embryos at 3 dpf. The blue dashed line boxes in **A-D** and **E-H** indicate the sinoatrial region shown enlarged in **A'-D'** and **E'-H'**, respectively. In wildtype hearts, Isl^{+} pacemaker cells (blue arrowheads) co-expressed TCF-mCherry. In Isl1$^{-/-}$ mutants, no TCF-mCherry expression was observed in the Isl1^{+} pacemaker cells (blue arrowheads). TCF-mCherry expression was also detected in the AV canal of wildtype (D) and Isl1$^{-/-}$ mutants (H) (arrows). Scale bars represent 50μm. See also Figure S3.

the sinoatrial region. To test this further, we analyzed a Wnt-reporter line containing a transgene with 7 repeats of a TCF-binding site upstream of mCherry (Moro et al., 2012). To identify the Isl1^{+} pacemaker cells, we made use of a transgenic *tg(Isl1:GFF;UAS:GFP)* line, further referred to as Isl1:GFP. Corroborating the hypothesis that Wnt/β-catenin signaling is activated in the sinoatrial junction, we observed cells that co-expressed both the *TCF:mCherry* reporter as well as the

Isl1:GFP reporter in the sinoatrial region (Fig. 5A-D'). In addition, TCF-mCherry positive cells were also located in the AV canal, a cardiac sub-domain in which Wnt-signaling plays a known role (Gillers et al., 2015, Hurlstone et al., 2003, Verhoeven et al., 2011) (Fig. 5C). Thus, Wnt-signaling is activated in the Isl1^{+} cardiac pacemaker cells. In both zebrafish and mouse embryos lacking functional Isl1, a progressive failure of pacemaker function leads to severe bradycardia and arrhythmia (de Pater et al., 2009, Tessadori et al., 2012, Liang et al., 2015). Isl1-GFP+ cells were still present in the sinoatrial region of isl1 mutants (Fig.5A-B' and E-F'), suggesting that pacemaker cell specification still occurs in the absence of Isl1, but that these cells fail to differentiate into functional pacemaker cells. To determine whether Wnt-signaling requires Isl1, we also crossed the TCF-Cherry reporter into the isl1 mutants. Interestingly, Wnt/β-catenin activity was lost specifically in the Isl1-GFP^{+} cells of the *isl1* mutant embryos, while it was still detectable in the AV canal (Fig. 5C,C',G and G'). These results reveal that in developing pacemaker cells active Wnt/β-catenin signaling depends on Isl1 activity.

Loss of Wnt/β-catenin signaling affects autonomic control of heart rate

To assess the role of canonical Wnt signaling in pacemaker cells we used a previously reported TetON system, in which Wnt/β-catenin signaling can be inhibited by the inducible and tissue-specific overexpression of its endogenous inhibitor Axin1 (Knopf et al., 2010). Overexpression of Axin1 stabilizes the β-catenin destruction complex, resulting in the inhibition of canonical Wnt signaling (Nakamura et al., 1998). Since cardiac specification and differentiation is regulated by Wnt/ β-catenin signaling at various stages during development (Ueno et al., 2007), it was important to block Wnt/β-catenin in a tissue-specific and temporally controlled manner. In the TetON system, Axin1 overexpression can be driven by the myocardial *myl7* gene promoter to restrict expression to the heart (Knopf et al., 2010). Since pacemaker cells also express the *myl7* gene, we reasoned that the TetON system could be used to inhibit Wnt signaling in the myocardium including the pacemaker cells without affecting embryo development in general. As a functional read-out for pacemaker function, we analyzed heart rates of control and Axin1 overexpressing embryos by high-speed video imaging and image analysis at 3 dpf (Fig. 6A). Surprisingly and in contrast to the decreased heart rates observed in Isl1$^{-/-}$ mutants (Tessadori et al., 2012, de Pater et al., 2009), inhibiting Wnt/β-catenin signaling by induction of Axin1 expression in the myocardium significantly increased cardiac contraction rates at 3 dpf (Fig. 6B, C). Despite the 10-15% increase in heart rate, the beating pattern was still regular (see suppl. movies S1 and S2, and Fig. S4). To determine at which point in development active Wnt signaling is required to regulate heart rate, we induced Axin1 expression at different time points and measured the effect on heart rate at

3 dpf. Only Axin1 overexpression specifically between 36 hpf and 52 hpf, when the *TCF:mCherry* reported active Wnt signaling in the pacemaker cells, significantly increased heart rate (Fig. 6D).

We have previously observed similarly high heart rates in zebrafish embryos treated with chemical compounds stimulating the sympathetic nervous system (e.g. isoproterenol) (Lodder et al., 2016). We therefore hypothesized that the observed increase in heart rate could be related to impaired control of the autonomic nervous system. To address this, we first induced Axin1 overexpression, followed by incubation of the embryos with either carbachol, a parasympathetic agonist, or isoproterenol, a sympathetic agonist (Hsieh and Liao, 2002, Dlugos and Rabin, 2010). While control embryos showed a significant reduction in heart rate by 37 bpm (from 181 ± 3,5 bpm to 145 ± 8,3 bpm) after addition of carbachol, the reduction in heart rate was abolished in Axin1 overexpressing embryos (heart rate reduced by 2 bpm from 196 ± 2 bpm to 194 ± 5,7 bpm) (Fig. 6E). Despite their already high heart rate, the Axin1-overexpressing embryos still responded to isoproterenol by increasing their heart rate by a further +17 bpm ± 8,1 bpm (Fig. 6E). This resulted in extreme heart rates of up to 266 bpm in some of the embryos with ectopic Axin1 expression and incubated

Figure 6: Wnt/β-catenin signaling regulates parasympathetic control of heart rate.

(A) Experimental timeline. Embryos with the ubiquitous *tg(TETRE:Mmu.Axin1-YFP)*^{tud1} and cardiomyocyte-specific *tg(myl7:TETAM2-2A-mCherry)*^{ulm8} transgenes were incubated with doxycycline (25 µg/mL) plus dexamethasone (100µM) to induce cardiomyocyte specific Axin1-YFP expression. Axin1-YFP was induced at different time points and the heart rate was measured at 3 dpf by high-speed video imaging and image analysis. **(B)** Atrial kymographs from a representative mCherry^{-}/YFP^{-} sibling control and an embryo with Axin1-YFP overexpression (Axin1^{+}). Kymographs span 2.8s. Note the shorter period per full heartbeat (indicated by white dotted lines) in the Axin1 expressing embryo. Movies are available as suppl. movies S1 and S2, respectively. **(C)** Result of heart rate analysis on sibling and Axin1^{+} embryos, showing a significant increase in heart rate in Axin1^{+} embryos. **(D)** Relative changes in heart rate measured at 3 dpf after induction of Axin1 expression at various time points. ∆heart rate was calculated by using the heart rates measured in the Axin1^{+} group and the control group using the following formula: (Axin1-YFP^{+} - mCherry^{-}/YFP^{-}) / (mCherry^{-}/YFP^{-}) x 100%. Induction of Axin1-YFP expression between 32 hpf and 56 hpf resulted in increased heart rates at 3 dpf. See also supplementary movies S1 and S2. n= 7-37 embryos measured per condition. Column bar graph plotting mean with SEM. **(E)** Heart rates at 3 dpf of control (mCherry^{-}/YFP^{-}) or Axin1-YFP^{+} embryos at baseline or after treatment with the parasympathetic agonist carbachol or the sympathetic agonist isoproterenol. (n=14-32 embryos) **(F)** Proposed model for Isl1/Wnt function in cardiac pacemaker cells. Isl1 is a central factor in pacemaker cell development. Isl1 expression is restricted to pacemaker cells in which it is required to establish the rhythmic cycle of membrane depolarizations and heart contractions and the activation of Wnt/β-catenin signaling. Wnt/β-catenin signaling is required to establish M2 cholinergic receptor signaling, which allows parasympathetic signals (e.g. acetylcholine) to adjust the rate of rhythmic membrane depolarizations and heart contractions. Statistical significance *p<0.05; **p<0.01; ***p<0.001; ****p<0.0001. See also Figure S4 and S5 and Movies S1 and S2.

with isoproterenol. Together, these results indicate that Wnt/β-catenin signaling in the heart regulates the parasympathetic, but not the sympathetic control of heart rate. *Muscarinic cholinergic receptor 2a* (*chrm2a*) encoding for the muscarinic M2 receptor responsible for parasympathetic regulation of the heart rate was expressed in the sinoatrial region of the 2 and 3 dpf heart (Fig. S5A, B). However, overexpression of Axin1 had no effect on the expression of *chrm2a* (Fig S5C), indicating that Wnt/β-catenin works downstream of M2 receptor signaling.

Together, our results reveal a new role for Wnt/β-catenin signaling in the autonomic control of heart rate by regulating the response of pacemaker cells to parasympathetic stimuli (Fig. 6F).

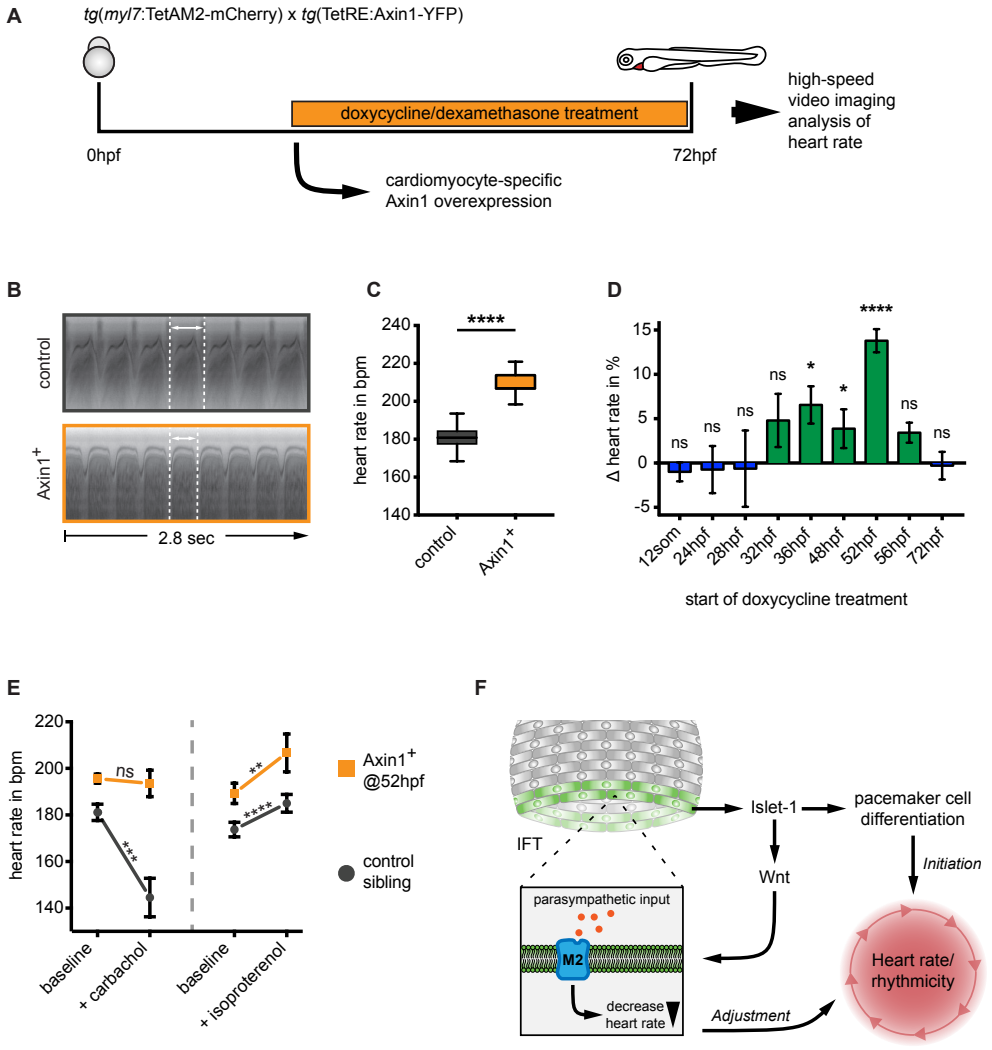

DISCUSSION

Recently, transcriptome maps with spatial resolution were made of the murine heart (DeLaughter et al., 2016, Li et al., 2016). These maps were made by combining microdissection of embryonic hearts with single-cell mRNA-seq. Although these transcriptome maps contain single cell expression data, the microdissection limited their spatial resolution. In addition, rare cell types may have been missed since not all cells within the heart were sequenced. In comparison, the *tomo*-seq transcriptome map was made by sectioning the entire heart in cryosections of 10 µm thickness. The high resolution and inclusion of all cardiac cells using the *tomo*-seq method likely explains why we were able to identify more differentially expressed genes even in a rare cell type such as the pacemaker cells. We established a comprehensive transcriptome map that includes the expression patterns of all genes expressed in the 2 day old zebrafish heart. The 502 genes differentially expressed in the sinoatrial region encompass many uncharacterized ones, indicating the potential value of this dataset for revealing new pathways that regulate pacemaker development. A limitation of the *tomo*-seq transcriptome map is that the gene expression information is not cell-type specific, which can be resolved by additional in situ hybridizations or combining *tomo*-seq with single-cell mRNA sequencing.

Wnt/β-catenin signaling in the AV canal regulates the expression of *bmp4* and *tbx2* (Verhoeven et al., 2011). Although *bmp4* and *tbx2* are also expressed in the sinoatrial region, this expression does not depend on Wnt/β-catenin signaling ((Verhoeven et al., 2011) and data not shown). We found that Isl1 is required for the activation of Wnt/β-catenin signaling in the sinoatrial region (Fig 5). Since isl1 is not expressed in the AV canal (Hami et al., 2011, Tessadori et al., 2012), and since we observed active Wnt/β-catenin signaling in the AV canal of *isl1*$^{-/-}$ mutants (Fig. 5G), we conclude that Wnt/β-catenin signaling plays different roles in the AV canal and sinoatrial region.

We found that Wnt/β-catenin signaling activity is required between 36hpf and 52hpf to reduce the heart rate at 3dpf (Fig. 6D). This was unexpected since *isl1*$^{-/-}$ mutant hearts have a severely reduced heart rate (de Pater et al., 2009, Tessadori et al., 2012). To explain these seemingly contradicting observations we propose a model in which Isl1 has two separate functions: 1) Isl1 regulates the expression of factors that are essential to drive the rhythmic membrane depolarizations, which is specific for pacemaker cells and absent from atrial cardiomyocytes. Without Isl1 the heart beat is maintained at low frequency since embryonic cardiomyocytes are able to spontaneously depolarize their membrane and contract, explaining the low beating frequency observed in isl1$^{-/-}$ mutants (de Pater et al., 2009, Tessadori et al., 2012). When the cardiomyocytes mature, and lose their ability to spontaneously contract, the heartbeat of isl1$^{-/-}$ mutants stops since the rhythmic membrane depolarizations were

not established. 2) Isl1 induces Wnt/β-catenin signaling in the pacemaker cells to establish parasympathetic control of the rhythmic membrane depolarizations. Since parasympathetic input through acetylcholine and muscarinic cholinergic receptors (mAChRs) decreases the heart rate, an increase in heart rate was observed after inhibiting Wnt/β-catenin signaling. In addition, we observed that carbachol, an acetylcholine agonist, was unable to reduce heart rate in embryos in which Wnt/β-catenin signaling was inhibited, indicating regulation at the level of the receptor or of downstream signaling. The M2 mAChR is expressed in the zebrafish heart from 30 hpf onwards and by 3dpf the autonomic response is mature (Hsieh and Liao, 2002, Dlugos and Rabin, 2010, Shin et al., 2010). Expression of the M2 mAChR was not affected by inhibiting Wnt/β-catenin signaling (Fig. S5), indicating that Wnt/β-catenin signaling either effects M2 receptor activity or affects the signaling pathway downstream of the M2 receptor.

In summary, the spatially-resolved transcriptome map of the embryonic heart provides an unprecedented opportunity to uncover novel mechanisms of cardiac development. The here identified Wnt-dependent mechanism to establish autonomous control of heart rate could be beneficial to ongoing efforts in creating biological pacemakers, which currently lack parasympathetic control (Protze et al., 2017).

METHODS

CONTACT FOR REAGENT AND RESOURCE SHARING

Further information and requests for reagents may be directed to, and will be fulfilled by the Lead Contact, Dr. Jeroen Bakkers, j.bakkers@hubrecht.eu.

EXPERIMENTAL MODEL AND SUBJECT DETAILS

Zebrafish

Fish used in this study were kept in standard conditions as previously described (Westerfield, 1995). Tupfel long fin (TL) wildtype, *isl1K88X (isl1$^{sa29/sa29}$)* (de Pater et al., 2009) mutant and *tg(myl7:EGFP)^{twu26}* (Huang et al., 2003) transgenic zebrafish lines were available from ZIRC. The TetON lines, ubiquitously expressed *tg(TETRE:Mmu.Axin1-YFP)^{tud1}* and cardiomyocyte-specific *tg(myl7:TETAM2-2A-mCherry)^{ulm8}* were received from the Weidinger lab (Ulm University, Germany) and crossed to obtain double transgenic embryos for wnt knockdown experiments. The Islet-1 reporter line *tg(Isl1:GFF;UAS:GFP)^{hu10018tg}* is an independent allele of a previously published line (Tessadori et al., 2012). Details on the generation of the transgenic line in *tg(UAS:GFP)* embryos (Asakawa et al., 2008) are given below. The *tg(7xTCF-nlsmCherry)* wnt-signaling reporter line was established in a TL wildtype background using the pDEST-7xTCF-nlsmCHERRY-polyA construct (Moro et al., 2012) received from the Smith lab (IMB, Brisbane, Australia). All studies involving vertebrate animals were performed with institutional approval in compliance with institutional ethical guidelines.

METHOD DETAILS

Tomo-sequencing

TL wildtype hearts were manually dissected from live 2-day-old zebrafish embryos. The heart tube was quickly transferred to Jung tissue freezing medium (Leica), carefully straightened and frozen on dry ice. The heart samples were cryo-sectioned in anterior to posterior direction with a thickness of 10µm per section. Total RNA was isolated using Trizol (Ambion). An ERCC RNA spike-in mix (Ambion) was added for normalization. The sections were processed individually, barcoded and processed for RNA sequencing as previously described in detail (Kruse et al., 2016, Junker et al., 2014). Illumina sequencing libraries were generated and sequenced using the NextSeq platform.

Data analysis

Independent tomo-seq datasets were established for 3 wildtype hearts. Based on statistical parameters (total read count, mappability of raw reads, tissue orientation

and spatial separation of the two main chambers) and expression peaks for known cardiac genes, the most robust heart sample (heart #1) was chosen for further detailed analysis. All 3 datasets can be accessed via the tomo-seq website (http://zebrafish.genomes.nl/tomoseq/Burkhard2017/). The raw data is accessible under GSE104057.

Bioinformatical analyses were performed with R software (R Core Team, 2013) using custom-written code (see source code file). The individual gene read counts were first normalized against the total counts per section before re-normalization to the median of the total reads per section. Thus, ensuring rough equivalence between read count numbers and original number of mapped raw reads. In addition, expression reads were normalized to the total spike-in read count to limit technical bias. The number of sequencing reads mapped for individual genes were plotted per section. LOESS (locally weighted scatterplot smoothening) with a smoothening parameter (span) of α=0.2 (Fig. 4) or α=0.3 (Fig. 2,3) was applied.

For Pearson's correlation analysis, all genes expressed at >4 reads in >1 section were selected prior to total-read-normalization. Based on the log2-fold-change (zlfc) of the *Z* score of all genes, correlation was calculated across the transcriptome for each pairwise combination of sections. Hierarchical clustering analysis on the entire dataset (after *Z* score transformation) was performed on all genes with a peak in >3 consecutive sections (*Z* score > 1.2). Comparative analysis of regional gene expression profiles was done using the EdgeR package (Robinson et al., 2010). Regions of interest were determined by expression of known cardiac marker genes. Genes significantly upregulated in ROI (log2 fold change >2; p-value < 0.05) were retrieved from the dataset and used for GO term enrichment analysis using the DAVID functional annotation tool (Huang da et al., 2009b, Huang da et al., 2009a).

In-situ hybridization

For in-situ hybridization (ISH) TL wildtype embryos were fixed in 4% PFA-PBS overnight and dehydrated in methanol. ISH on 2-3dpf embryos was carried out as previously described (Westerfield, 1995).

Generation of the Islet-1 transgenic line

The *tg(Isl1:GFF^{hu10018tg})* line was generated essentially as described previously (Tessadori et al., 2012, Bussmann and Schulte-Merker, 2011). An iTOL2_amp cassette for pTarBAC was inserted in the vector sequence of bacterial artificial chromosome (BAC) CH211-219F7, containing the full *isl1* locus. An expression cassette containing the GalFF gene (Asakawa et al., 2008) and kanamycin resistance gene was integrated at the ATG site of the 1st exon of the isl1 gene. Primers used were (in lower case sequence homologous to BAC): isl1_Gal4FF_F

5'-gggccttctgtccggttttaaaagtggacctaacac
cgccttactttcttaccATGAAGCTACTGT-CTTCTATCGAAC-3' and isl1_KanR_R
5'-aaataaacaataaagcttaacttactttcggtggatcccccatgtctccTCAGAAGAACTCGTC
AAGAAGGCG-3'. Red/ET recombination was done following the manufacturer's protocol (Gene Bridges) with minor modifications. BAC-DNA isolation was carried out using a Midiprep kit (Life Technologies). 300 ng/µl of BAC-DNA was injected in *tg(UAS:GFP*^{nkuasgfp1aTg}) embryos (Asakawa et al., 2008) in combination with 25ng Tol2 mRNA. To establish the stable transgenic line, healthy embryos displaying robust isl1-specific fluorescence were selected and grown to adulthood.

Immunohistochemistry and image processing

3dpf TL wildtype embryos were fixed in 2% PFA-PBS overnight. Immunohistochemistry was carried out as previously described (de Pater et al., 2009). The primary antibodies used were chicken αGFP (Aves Labs, RRID: AB_2307313, 1:500), rabbit αDsRed (Clontech, AB_10013483, 1:200) and mouse αTropomyosin (Sigma, AB_261817, 1:200). All immunohistochemistry images are 3D reconstructions of confocal scans. Image processing was done using the Imaris data visualization software (Bitplane). For image clarity, non-cardiac expression of the TCF-mCherry reporter line was removed (Fig.5).

Drug treatments in zebrafish embryos

Doxycycline (Sigma, D9891) was dissolved in 50% EtOH, kept as a 50mg/ml stock solution and stored at -20°C in the dark. Dexamethasone (Sigma, D1756) was dissolved in 100% EtOH, kept as a 10 mg/ml stock solution and stored at -20°C in the dark. For induction of the TetON system, we used a final concentration of 25µg/ml of doxycycline and 100µM dexamethasone diluted in E3 medium. Embryos were treated in 6cm dishes with a maximum of 30 embryos and kept at 28°C in the dark during the drug incubation. Efficient induction was confirmed by cardiomyocytes-specific YFP expression immediately prior to the heart rate analysis.
Carbamoylcholine chloride (*Carbachol*, Sigma, C4382) was dissolved in mQ water at a stock concentration of 50mM. Isoprenaline hydrochloride (*Isoproterenol*, Sigma, I5627) was dissolved in mQ water at a stock concentration of 50mM. Stock solutions were kept at -20°C for up to one week. A final concentration of 500µM Carbachol or 100µM Isoproterenol was used in 12 ml E3 medium.

High-speed imaging and analysis

Embryos were mounted in 0.25% agarose (Life Technologies BV) prepared in E3 medium with 16mg/ml tricaine. Recording of embryonic hearts were performed with a high-speed CCD camera and HoKaWo Image acquisition module (Hamamatsu

Photonics) at 150fps on a brightfield microscope (Leica). The temperature was kept at 28.5°C throughout the heart rate measurements using a controlled temperature chamber. For the carbachol/isoproterenol experiments, embryos were imaged before drug addition and after 30min drug incubation to calculate relative change in heart rate. Image analysis was carried out with ImageJ (http://rsbweb.nih.gov/ij/). Statistical analysis and drawing of the box-whisker plot were carried out GraphPad Prism7 (GraphPad software).

QUANTIFICATION AND STATISTICAL ANALYSIS

Bioinformatic analyses

Sequencing reads obtained from the paired-end Illumina sequencing were mapped to the zebrafish genome (Ensembl genome assembly Zv9) as described previously (Junker et al., 2014). All sequencing data analysis including normalization, single gene expression analysis, identification of expression patterns and clustering was performed in R (R Core Team, 2013) using custom-written code (Supplementary Methods) as well as publicly available packages (EdgeR).

The heart rate analyses were performed in ImageJ by manual measurement of each cardiac cycle. Box-whisker plots, outlier removal and statistical analysis was done in GraphPad Prism7 (GraphPad software). Further statistical details of experiments can be found in the figure legends.

DATA AND SOFTWARE AVAILABILITY

Software

All software used in this study was obtained from publicly or commercially available resources. Please refer to key resources table for more details.

Data resources

The processed tomo-seq dataset used is publicly available via the website: http://zebrafish.genomes.nl/tomoseq/Burkhard2017/

The raw data can be retrieved from the GEO database (GSE104057).

AUTHOR CONTRIBUTIONS

SB and JB designed the study. SB performed all experiments and data analysis. SB and JB wrote the manuscript.

ACKNOWLEDGEMENTS

We thank Utrecht Sequencing Facility for providing the sequencing service and data. Utrecht Sequencing Facility is subsidized by the University Medical Center Utrecht, Hubrecht Institute and Utrecht University. We thank Fabian Kruse for bioinformatics support, Federico Tessadori for help with the BAC transgenesis, Kelly Smith for help with the *tg(7xTCF-nlsmCherry)* analysis, the Hubrecht Imaging Facility for microscopy support and Life Science Editors for editing support. This work was supported by the ZonMW grant 40-00812-98-12086.

SUPPLEMENTARY FIGURES

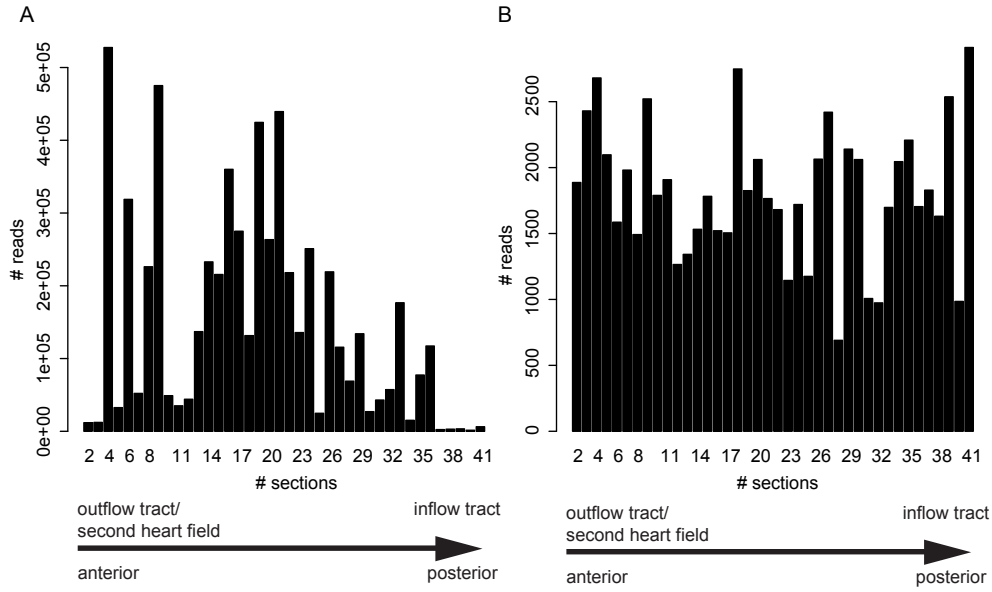

C

number of total reads:	6082553
number of total spike-in reads:	133885
total number of mapped genes:	13165

Figure S1: Tomo-seq statistics for the analyzed 2 dpf dataset.

(A) Total raw RNA-seq reads of the 2dpf heart sample. Plotted are the total reads per 10µm section. Sections #2 - #41 contained the tissue sample. **(B)** Total spike-in reads plotted per section. Spike-in expression per section was used for data normalization. **(C)** Basic statistics of RNA-seq results.

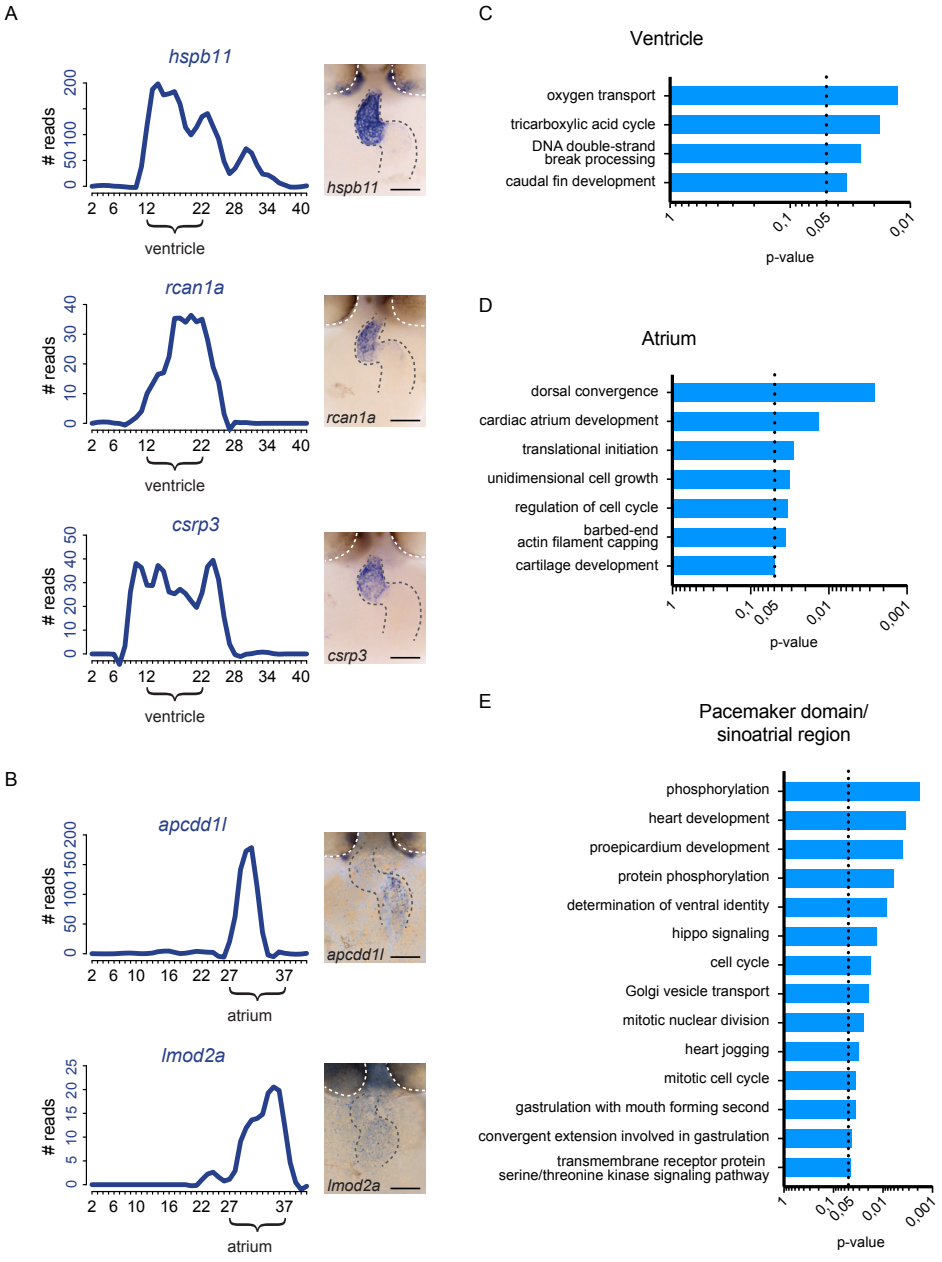

Figure S2: Identification of region-specific gene expression patterns.

(A-B) Additional gene expression plot and ISH analysis for representative example genes significantly upregulated in the ventricle (*hspb11, rcan1a, csrp3*) and atrium (*apcdd1l, lmod2a*). Gray dashed line: location of the heart. White dashed line outlines the eyes. Anterior to the top. **(C-E)** GO term enrichment for genes significantly enriched in the ventricle **(C)**, atrium **(D)** and pacemaker domain **(E)**. p-value < 0.05. Scale bars represent 50µm.

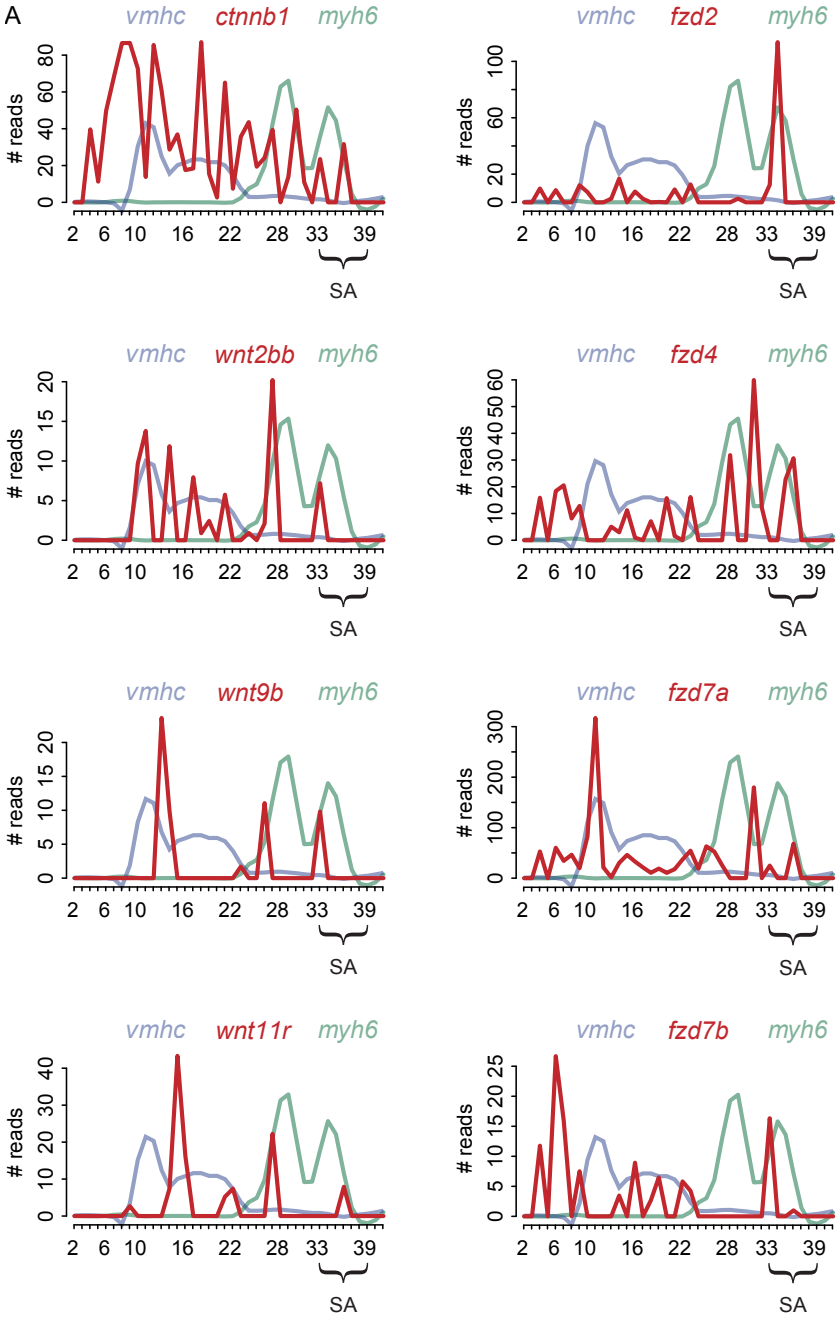

Figure S3: Expression profiles of Wnt-signaling components.

(A) RNA expression plots of Wnt-signaling components expressed in the pacemaker domain (dark red). Superimposed expression profiles of ventricular marker gene *vmhc* (light blue) and atrial marker gene *myh6* (light green) outline the position of the two chambers. SA, sinoatrial region.

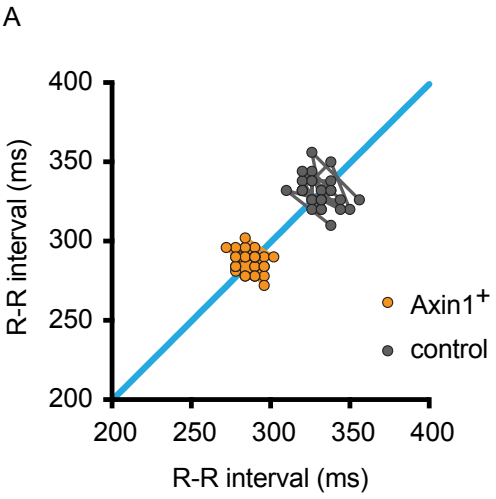

Figure S4: Heart rate variability in Axin1^{+} embryonic hearts.

(A) Plot showing heart rate variability (HRV). HRV was plotted as the time interval between successive heart contractions (R-R interval). The time intervals where measured in the kymographs shown in Figure 5B. Wildtype sibling in gray, Axin1^{+} embryo in orange. R-R interval in the Axin1^{+} embryo is decreased (corresponding to increased heart rate) but remains regular.

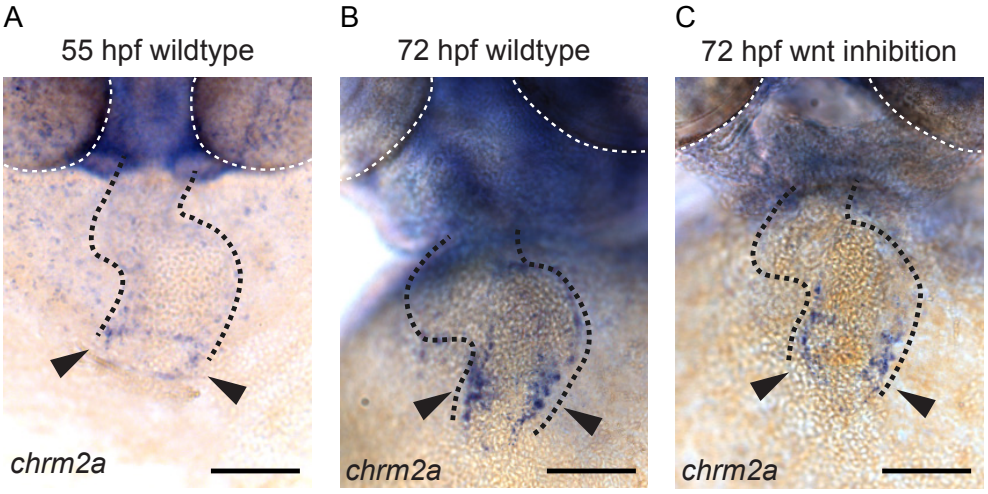

Figure S5: M2 muscarinic receptor is expressed at the venous pole.

(A-B) In-situ hybridization for the *muscarinic 2a cholinergic receptor* (*chrm2a*) in wildtype embryos at 55 hpf **(A)** and 72hpf **(B)**. **(C)** ISH for *chrm2a* at 72 hpf in Axin1-YFP^{+} embryo (Wnt inhibition started at 52 hpf). Arrowheads indicate expression at the venous pole. Gray dashed line: location of the heart; white dashed line: location of the eyes. Anterior up. Scale bars represent 50µm.

REFERENCES

ARRENBERG, A. B., STAINIER, D. Y., BAIER, H. & HUISKEN, J. 2010. Optogenetic control of cardiac function. *Science,* 330**,** 971-4.

ASAKAWA, K., SUSTER, M. L., MIZUSAWA, K., NAGAYOSHI, S., KOTANI, T., URASAKI, A., KISHIMOTO, Y., HIBI, M. & KAWAKAMI, K. 2008. Genetic dissection of neural circuits by Tol2 transposon-mediated Gal4 gene and enhancer trapping in zebrafish. *Proc Natl Acad Sci U S A,* 105**,** 1255-60.

BAKKER, M. L., CHRISTOFFELS, V. M. & MOORMAN, A. F. 2010. The cardiac pacemaker and conduction system develops from embryonic myocardium that retains its primitive phenotype. *J Cardiovasc Pharmacol,* 56**,** 6-15.

BEIS, D., BARTMAN, T., JIN, S. W., SCOTT, I. C., D'AMICO, L. A., OBER, E. A., VERKADE, H., FRANTSVE, J., FIELD, H. A., WEHMAN, A., BAIER, H., TALLAFUSS, A., BALLY-CUIF, L., CHEN, J. N., STAINIER, D. Y. & JUNGBLUT, B. 2005. Genetic and cellular analyses of zebrafish atrioventricular cushion and valve development. *Development,* 132**,** 4193-204.

BUSSMANN, J. & SCHULTE-MERKER, S. 2011. Rapid BAC selection for tol2-mediated transgenesis in zebrafish. *Development,* 138**,** 4327-32.

DE PATER, E., CLIJSTERS, L., MARQUES, S. R., LIN, Y. F., GARAVITO-AGUILAR, Z. V., YELON, D. & BAKKERS, J. 2009. Distinct phases of cardiomyocyte differentiation regulate growth of the zebrafish heart. *Development,* 136**,** 1633-41.

DELAUGHTER, D. M., BICK, A. G., WAKIMOTO, H., MCKEAN, D., GORHAM, J. M., KATHIRIYA, I. S., HINSON, J. T., HOMSY, J., GRAY, J., PU, W., BRUNEAU, B. G., SEIDMAN, J. G. & SEIDMAN, C. E. 2016. Single-Cell Resolution of Temporal Gene Expression during Heart Development. *Dev Cell,* 39**,** 480-490.

DLUGOS, C. A. & RABIN, R. A. 2010. Structural and functional effects of developmental exposure to ethanol on the zebrafish heart. *Alcohol Clin Exp Res,* 34**,** 1013-21.

DOBRZYNSKI, H., BOYETT, M. R. & ANDERSON, R. H. 2007. New insights into pacemaker activity: promoting understanding of sick sinus syndrome. *Circulation,* 115**,** 1921-32.

ESPINOZA-LEWIS, R. A., LIU, H., SUN, C., CHEN, C., JIAO, K. & CHEN, Y. 2011. Ectopic expression of Nkx2.5 suppresses the formation of the sinoatrial node in mice. *Dev Biol,* 356**,** 359-69.

GESSERT, S. & KUHL, M. 2010. The multiple phases and faces of wnt signaling during cardiac differentiation and development. *Circ Res,* 107**,** 186-99.

GILLERS, B. S., CHIPLUNKAR, A., ALY, H., VALENTA, T., BASLER, K., CHRISTOFFELS, V. M., EFIMOV, I. R., BOUKENS, B. J. & RENTSCHLER, S. 2015. Canonical wnt signaling regulates atrioventricular junction programming and electrophysiological properties. *Circ Res,* 116**,** 398-406.

GORDAN, R., GWATHMEY, J. K. & XIE, L. H. 2015. Autonomic and endocrine control of cardiovascular function. *World J Cardiol,* 7**,** 204-14.

HAMI, D., GRIMES, A. C., TSAI, H. J. & KIRBY, M. L. 2011. Zebrafish cardiac development requires a conserved secondary heart field. *Development,* 138**,** 2389-98.

HASHIMSHONY, T., SENDEROVICH, N., AVITAL, G., KLOCHENDLER, A., DE LEEUW, Y., ANAVY, L., GENNERT, D., LI, S., LIVAK, K. J., ROZENBLATT-ROSEN, O., DOR, Y., REGEV, A. & YANAI, I. 2016. CEL-Seq2: sensitive highly-multiplexed single-cell RNA-Seq. *Genome Biol,* 17**,** 77.

HOCH, R. V. & SORIANO, P. 2003. Roles of PDGF in animal development. *Development,* 130**,** 4769-84.

HSIEH, D. J. & LIAO, C. F. 2002. Zebrafish M2 muscarinic acetylcholine receptor: cloning, pharmacological characterization, expression patterns and roles in embryonic bradycardia. *Br J Pharmacol,* 137**,** 782-92.

HUANG, C. J., TU, C. T., HSIAO, C. D., HSIEH, F. J. & TSAI, H. J. 2003. Germ-line transmission of a myocardium-specific GFP transgene reveals critical regulatory elements in the cardiac myosin light chain 2 promoter of zebrafish. *Dev Dyn,* 228**,** 30-40.

HUANG DA, W., SHERMAN, B. T. & LEMPICKI, R. A. 2009a. Bioinformatics enrichment tools: paths toward the comprehensive functional analysis of large gene lists. *Nucleic Acids Res,* 37**,** 1-13.

HUANG DA, W., SHERMAN, B. T. & LEMPICKI, R. A. 2009b. Systematic and integrative analysis of large gene lists using DAVID bioinformatics resources. *Nat Protoc,* 4**,** 44-57.

HURLSTONE, A. F., HARAMIS, A. P., WIENHOLDS, E., BEGTHEL, H., KORVING, J., VAN EEDEN, F., CUPPEN, E., ZIVKOVIC, D., PLASTERK, R. H. & CLEVERS, H. 2003. The Wnt/beta-catenin pathway regulates cardiac valve formation. *Nature,* 425**,** 633-7.

JUNKER, J. P., NOEL, E. S., GURYEV, V., PETERSON, K. A., SHAH, G., HUISKEN, J., MCMAHON, A. P., BEREZIKOV, E., BAKKERS, J. & VAN OUDENAARDEN, A. 2014. Genome-wide RNA Tomography in the zebrafish embryo. *Cell,* 159**,** 662-75.

KLOTZ, L., NORMAN, S., VIEIRA, J. M., MASTERS, M., ROHLING, M., DUBE, K. N., BOLLINI, S., MATSUZAKI, F., CARR, C. A. & RILEY, P. R. 2015. Cardiac lymphatics are heterogeneous in origin and respond to injury. *Nature,* 522**,** 62-7.

KNOPF, F., SCHNABEL, K., HAASE, C., PFEIFER, K., ANASTASSIADIS, K. & WEIDINGER, G. 2010. Dually inducible TetON systems for tissue-specific conditional gene expression in zebrafish. *Proc Natl Acad Sci U S A,* 107**,** 19933-8.

KRUSE, F., JUNKER, J. P., VAN OUDENAARDEN, A. & BAKKERS, J. 2016. Tomo-seq: A method to obtain genome-wide expression data with spatial resolution. *Methods Cell Biol,* 135**,** 299-307.

LAKATTA, E. G., MALTSEV, V. A. & VINOGRADOVA, T. M. 2010. A coupled SYSTEM of intracellular Ca2+ clocks and surface membrane voltage clocks controls the timekeeping mechanism of the heart's pacemaker. *Circ Res,* 106**,** 659-73.

LEE, J. H., DAUGHARTHY, E. R., SCHEIMAN, J., KALHOR, R., YANG, J. L., FERRANTE, T. C., TERRY, R., JEANTY, S. S., LI, C., AMAMOTO, R., PETERS, D. T., TURCZYK, B. M., MARBLESTONE, A. H., INVERSO, S. A., BERNARD, A., MALI, P., RIOS, X., AACH, J. & CHURCH, G. M. 2014. Highly multiplexed subcellular RNA sequencing in situ. *Science,* 343**,** 1360-3.

LI, G., XU, A., SIM, S., PRIEST, J. R., TIAN, X., KHAN, T., QUERTERMOUS, T., ZHOU, B., TSAO, P. S., QUAKE, S. R. & WU, S. M. 2016. Transcriptomic Profiling Maps Anatomically Patterned Subpopulations among Single Embryonic Cardiac Cells. *Dev Cell,* 39**,** 491-507.

LIANG, X., ZHANG, Q., CATTANEO, P., ZHUANG, S., GONG, X., SPANN, N. J., JIANG, C., CAO, X., ZHAO, X., ZHANG, X., BU, L., WANG, G., CHEN, H. S., ZHUANG, T., YAN, J., GENG, P., LUO, L., BANERJEE, I., CHEN, Y., GLASS, C. K., ZAMBON, A. C., CHEN, J., SUN, Y. & EVANS, S. M. 2015. Transcription factor ISL1 is essential for pacemaker development and function. *J Clin Invest,* 125**,** 3256-68.

LODDER, E. M., DE NITTIS, P., KOOPMAN, C. D., WISZNIEWSKI, W., MOURA DE SOUZA, C. F., LAHROUCHI, N., GUEX, N., NAPOLIONI, V., TESSADORI, F., BEEKMAN, L., NANNENBERG, E. A., BOUALLA, L., BLOM, N. A., DE GRAAFF, W., KAMERMANS, M., COCCIADIFERRO, D., MALERBA, N., MANDRIANI, B., COBAN AKDEMIR, Z. H., FISH, R. J., ELDOMERY, M. K., RATBI, I., WILDE, A. A., DE BOER, T., SIMONDS, W. F., NEERMAN-ARBEZ, M., SUTTON, V. R., KOK, F., LUPSKI, J. R., REYMOND, A., BEZZINA, C. R., BAKKERS, J. & MERLA, G. 2016. GNB5 Mutations Cause an Autosomal-Recessive Multisystem Syndrome with Sinus Bradycardia and Cognitive Disability. *Am J Hum Genet,* 99**,** 786.

MOMMERSTEEG, M. T., HOOGAARS, W. M., PRALL, O. W., DE GIER-DE VRIES, C., WIESE, C., CLOUT, D. E., PAPAIOANNOU, V. E., BROWN, N. A., HARVEY, R. P., MOORMAN, A. F. & CHRISTOFFELS, V. M. 2007. Molecular pathway for the localized formation of the sinoatrial node. *Circ Res,* 100**,** 354-62.

MORO, E., OZHAN-KIZIL, G., MONGERA, A., BEIS, D., WIERZBICKI, C., YOUNG, R. M., BOURNELE, D., DOMENICHINI, A., VALDIVIA, L. E., LUM, L., CHEN, C., AMATRUDA, J. F., TISO, N., WEIDINGER, G. & ARGENTON, F. 2012. In vivo Wnt signaling tracing through a transgenic biosensor fish reveals novel activity domains. *Dev Biol,* 366**,** 327-40.

NAKAMURA, T., HAMADA, F., ISHIDATE, T., ANAI, K., KAWAHARA, K., TOYOSHIMA, K. & AKIYAMA, T. 1998. Axin, an inhibitor of the Wnt signalling pathway, interacts with beta-catenin, GSK-3beta and APC and reduces the beta-catenin level. *Genes Cells,* 3**,** 395-403.

PROTZE, S. I., LIU, J., NUSSINOVITCH, U., OHANA, L., BACKX, P. H., GEPSTEIN, L. & KELLER, G. M. 2017. Sinoatrial node cardiomyocytes derived from human pluripotent cells function as a biological pacemaker. *Nat Biotechnol,* 35**,** 56-68.

ROBINSON, M. D., MCCARTHY, D. J. & SMYTH, G. K. 2010. edgeR: a Bioconductor package for differential expression analysis of digital gene expression data. *Bioinformatics,* 26**,** 139-40.

ROSEN, M. R., ROBINSON, R. B., BRINK, P. R. & COHEN, I. S. 2011. The road to biological pacing. *Nat Rev Cardiol*.

SHIN, J. T., POMERANTSEV, E. V., MABLY, J. D. & MACRAE, C. A. 2010. High-resolution cardiovascular function confirms functional orthology of myocardial contractility pathways in zebrafish. *Physiol Genomics,* 42**,** 300-9.

SUN, C., YU, D., YE, W., LIU, C., GU, S., SINSHEIMER, N. R., SONG, Z., LI, X., CHEN, C., SONG, Y., WANG, S., SCHRADER, L. & CHEN, Y. 2015. The short stature homeobox 2 (Shox2)-bone morphogenetic protein (BMP) pathway regulates dorsal mesenchymal protrusion development and its temporary function as a pacemaker during cardiogenesis. *J Biol Chem,* 290**,** 2007-23.

TESSADORI, F., VAN WEERD, J. H., BURKHARD, S. B., VERKERK, A. O., DE PATER, E., BOUKENS, B. J., VINK, A., CHRISTOFFELS, V. M. & BAKKERS, J. 2012. Identification and functional characterization of cardiac pacemaker cells in zebrafish. *PLoS One,* 7**,** e47644.

TZAHOR, E. 2007. Wnt/beta-catenin signaling and cardiogenesis: timing does matter. *Dev Cell,* 13**,** 10-3.

UENO, S., WEIDINGER, G., OSUGI, T., KOHN, A. D., GOLOB, J. L., PABON, L., REINECKE, H., MOON, R. T. & MURRY, C. E. 2007. Biphasic role for Wnt/beta-catenin signaling in cardiac specification in zebrafish and embryonic stem cells. *Proc Natl Acad Sci U S A,* 104**,** 9685-90.

VERHOEVEN, M. C., HAASE, C., CHRISTOFFELS, V. M., WEIDINGER, G. & BAKKERS, J. 2011. Wnt signaling regulates atrioventricular canal formation upstream of BMP and Tbx2. *Birth Defects Res A Clin Mol Teratol,* 91**,** 435-40.

WESTERFIELD, M. 1995. A Guide for the Laboratory Use of Zebrafish (Danio rerio). *The Zebrafish Book.* 3rd ed. Eugene, OR: University of Oregon Press.

WIESE, C., GRIESKAMP, T., AIRIK, R., MOMMERSTEEG, M. T., GARDIWAL, A., DE GIER-DE VRIES, C., SCHUSTER-GOSSLER, K., MOORMAN, A. F., KISPERT, A. & CHRISTOFFELS, V. M. 2009. Formation of the sinus node head and differentiation of sinus node myocardium are independently regulated by Tbx18 and Tbx3. *Circ Res,* 104**,** 388-97.

WOLF, C. M. & BERUL, C. I. 2006. Inherited conduction system abnormalities--one group of diseases, many genes. *J Cardiovasc Electrophysiol,* 17**,** 446-55.

WU, C. C., KRUSE, F., VASUDEVARAO, M. D., JUNKER, J. P., ZEBROWSKI, D. C., FISCHER, K., NOEL, E. S., GRUN, D., BEREZIKOV, E., ENGEL, F. B., VAN OUDENAARDEN, A., WEIDINGER, G. & BAKKERS, J. 2016. Spatially Resolved Genome-wide Transcriptional Profiling Identifies BMP Signaling as Essential Regulator of Zebrafish Cardiomyocyte Regeneration. *Dev Cell,* 36**,** 36-49.

YE, W., WANG, J., SONG, Y., YU, D., SUN, C., LIU, C., CHEN, F., ZHANG, Y., WANG, F., HARVEY, R. P., SCHRADER, L., MARTIN, J. F. & CHEN, Y. 2015. A common Shox2-Nkx2-5 antagonistic mechanism primes the pacemaker cell fate in the pulmonary vein myocardium and sinoatrial node. *Development,* 142**,** 2521-32.

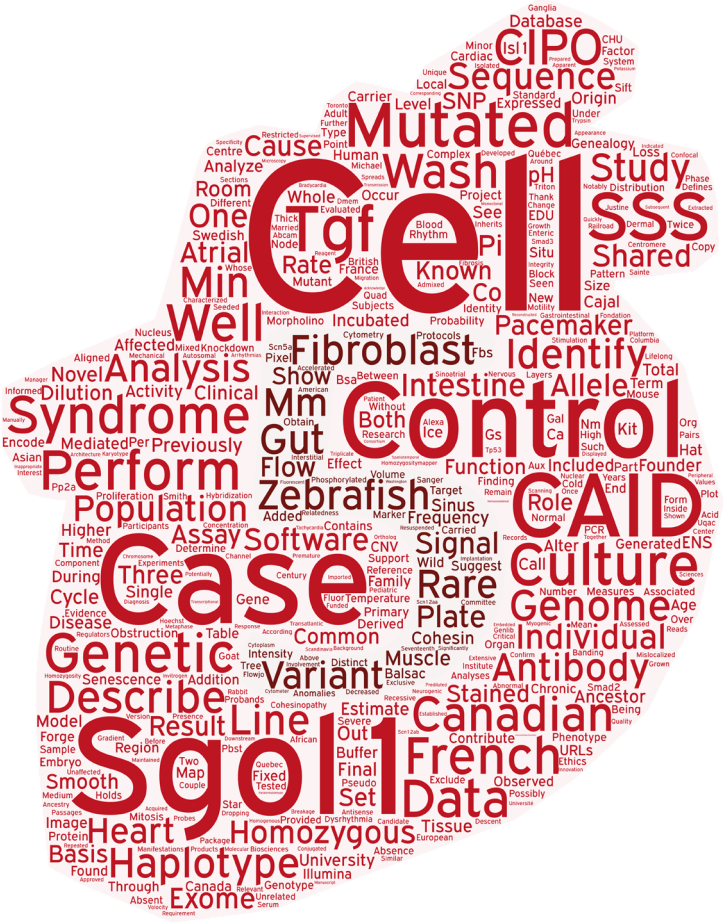
Cell
Sgol1
Control
Case
Mutated
Wash
Cgf
Data
Canadian
French
Genetic
Describe
Variant
Antibody
Individual
Culture
Genome
CAID
CIPO
Sequence
Study
Sss
Shared
Fibroblast
Identify
Pacemaker
Intestine
Allele
Analysis
Syndrome
Perform
Zebrafish
Population
Assay
Software
Signal
Rare
Plate
Function
Role
Gut
Mm
Min
Well
Line
Result
Haplotype
Heart
Homozygous
Tissue
Exome
Stained
Ancestor
Common
Cohesin
Muscle
Balsac
Estimate
Buffer
Final
Set
Pseudo
Fixed
Tested
Map
Couple
Two
Region
Forge
Model
Smooth
Holds
Image
Protein
Basis
Found
Through
Canada
Absent
Unrelated
Genotype
Illumina
University
Provided
Dysrhythmia
Absence
European
Descent
Contribute
Phenotype
URLs
Ethics
Observed
Possibly
Exclude
Pbst
Probands
Cohesinopathy
Severe
Out
African
Quebec
Star
Dropping
Antisense
Candidate
Similar
Packaged
Biosciences
Conjugated
Manifestations
Products
Velocity
Requirement
Serum
Relevant
Approved
Acquired
Probes
Mitosis
Maintained
Unaffected
Passages
Medium
Ancestry
Embryo
Sample
Gradient
Version
Presence
Baltoria
Homozygosity
Senescence
Addition
Obstruction
Disease
Evidence
Cycle
During
Component
Time
Higher
Participants
Concentration
Proliferation
Smith
Hybridization
Pp2a
Asian
Encode
Mediated
Per
Previously
Dilution
Activity
Clinical
Novel
Aligned
Affected
Nucleus
Mixed
Knockdown
Autosomal
Arrhythmias
Scn5a
Pixel
Show
Bsa
Between
Accelerand
American
Obtain
Gut
Flow
Effect
Interstitial
Tropical
Phosphorylated
Volume
Sanger
Target
Added
Relatedness
Marker
Contains
Frequency
Sinus
Normal
Carried
Wild
Suggest
Reference
Family
Fluor
Temperature
Primary
Derived
Cohesin
Plate
Organ
Genib
Critical
Mean
Number
Measures
Associated
Age
Over
Reads
Alter
Call
Generated
ENS
PCR
Records
Finding
Remain
Nuclear
Cold
Once
Years
End
Included
Part
Founder
Aux
Tp53
Distress
Org
Pairs
Hat
Kit
Nm
High
Such
Gal
Ca
Gs
Ice
Alexa
Both
Research
Without
Obtain
Intestinal
Between
Nervous
Layers
Total
Term
Mouse
Lifelong
Columbia
Platform
Stimulation
Fbs
Protocols
Cytometry
Probability
Incubated
Morpholino
Interaction
Seeded
Characterized
Quad
Subjects
Identity
Admixed
Mandible
Whose
Mutant
Rate
France
British
Known
Co
Pi
Blood
Rhythm
Project
See
Inherits
Occur
Whole
Thick
Married
Abcam
Node
Dmem
Evaluated
Swedish
Atrial
One
Room
Different
Sections
Analyze
Cause
Restricted
Centre
Human
Michael
Spreads
Complex
Developed
Québec
Around
pH
Triton
Thank
Change
EDU
Growth
Enteric
Smad3
Situ
Integrity
Block
Seen
New
Motility
Size
Pattern
Sainte
Cajal
Gastrointestinal
Fondation
Stimulation
Lifelong
Columbia
Platform
Total
Term
Mouse
Org
Pairs
Hat
Kit
Nm
High
Such
Gal
Ca
Gs
Ice
Alexa
Both
Research
Without
Obtain
Intestinal
Between
Nervous
Layers
Allele
Intestine
Show
Bsa
Pixel
Scn5a
Fbs
Protocols
Cytometry
Probability
Incubated
Morpholino
Interaction
Seeded
Characterized
Quad
Subjects
Identity
Admixed
Mandible
Whose
Mutant
Rate
France
British
Known
Co
Pi
Blood
Rhythm
Project
See
Inherits
Occur
Whole
Thick
Married
Abcam
Node
Dmem
Evaluated
Swedish
Atrial
One
Room
Different
Sections
Analyze
Cause
Restricted
Centre
Human
Michael
Spreads
Complex
Developed
Québec
Around
pH
Triton
Thank
Change
EDU
Growth
Enteric
Smad3
Situ
Integrity
Block
Seen
New
Motility
Size
Pattern
Sainte
Cajal
Gastrointestinal
Fondation
Shared
Centromere
Copy
Twice
Dermal
Railroad
Quickly
Justine
Consonant
Extracted
Sss
Study
Distribution
Notably
Loss
Confocal
Phase
Defines
Sss
Shared
Centromere
Copy
Twice
Dermal
Railroad
Quickly
Justine
Consonant
Extracted
Study
Distribution
Notably
Loss
Confocal
Phase
Defines
CIPO
Isl1
Database
Minor
Cardiac
CHU
Factor
System
Potassium
Sequence
Unique
Isolated
Local
Sift
Carrier
Level
SNP
Expressed
Origin
Standard
Under
Trypsin
Appearance
Mutated
Toronto
Adult
Further
Type
Point
Genealogy
Evaluated
Confocal
Wash
Complex
Developed
Québec
Around
Cell
Ganglia
Control
Case
Sgol1
Data
Canadian
French
Genetic
Describe
Variant
Antibody
Individual
Culture
Genome
CAID
Syndrome
Perform
Zebrafish
Population
Assay
Software
Signal
Rare
Plate
Function
Role
Gut
Mm
Min
Well
Line
Result
Haplotype
Heart
Homozygous
Tissue
Exome
Stained
Ancestor
Common
Cohesin
Muscle
Balsac
Estimate
Buffer
Final
Set
Pseudo
Fixed
Tested
Map
Couple
Two
Region
Forge
Model
Smooth
Holds
Image
Protein
Basis
Found
Through
Canada
Absent
Unrelated
Genotype
Illumina
University
Provided
Dysrhythmia
Absence
European
Descent
Contribute
Phenotype
URLs
Ethics
Observed
Possibly
Exclude
Pbst
Probands
Cohesinopathy
Severe
Out
African
Quebec
Star
Dropping
Antisense
Candidate
Similar
Packaged
Biosciences
Conjugated
Manifestations
Products
Velocity
Requirement
Serum
Relevant
Approved
Acquired
Probes
Mitosis
Maintained
Unaffected
Passages
Medium
Ancestry
Embryo
Sample
Gradient
Version
Presence
Baltoria
Homozygosity
Senescence
Addition
Obstruction
Disease
Evidence
Cycle
During
Component
Time
Higher
Participants
Concentration
Proliferation
Smith
Hybridization
Pp2a
Asian
Encode
Mediated
Per
Previously
Dilution
Activity
Clinical
Novel
Aligned
Affected
Nucleus
Mixed
Knockdown
Autosomal
Arrhythmias
Scn5a
Pixel
Show
Bsa
Between
Accelerand
American
Obtain
Gut
Flow
Effect
Interstitial
Tropical
Phosphorylated
Volume
Sanger
Target
Added
Relatedness
Marker
Contains
Frequency
Sinus
Normal
Carried
Wild
Suggest
Reference
Family
Fluor
Temperature
Primary
Derived
Cohesin
Plate
Organ
Genib
Critical
Mean
Number
Measures
Associated
Age
Over
Reads
Alter
Call
Generated
ENS
PCR
Records
Finding
Remain
Nuclear
Cold
Once
Years
End
Included
Part
Founder
Aux
Tp53
Distress
Org
Pairs
Hat
Kit
Nm
High
Such
Gal
Ca
Gs
Ice
Alexa
Both
Research
Without
Obtain
Intestinal
Between
Nervous
Layers
Allele
Intestine
Show
Bsa
Pixel
Scn5a
Fbs
Protocols
Cytometry
Probability
Incubated
Morpholino
Interaction
Seeded
Characterized
Quad
Subjects
Identity
Admixed
Mandible
Whose
Mutant
Rate
France
British
Known
Co
Pi
Blood
Rhythm
Project
See
Inherits
Occur
Whole
Thick
Married
Abcam
Node
Dmem
Evaluated
Swedish
Atrial
One
Room
Different
Sections
Analyze
Cause
Restricted
Centre
Human
Michael
Spreads
Complex
Developed
Québec
Around
pH
Triton
Thank
Change
EDU
Growth
Enteric
Smad3
Situ
Integrity
Block
Seen
New
Motility
Size
Pattern
Sainte
Cajal
Gastrointestinal
Fondation
Shared
Centromere
Copy
Twice
Dermal
Railroad
Quickly
Justine
Consonant
Extracted
Sss
Study
Distribution
Notably
Loss
Confocal
Phase
Defines
CIPO
Isl1
Database
Minor
Cardiac
CHU
Factor
System
Potassium
Sequence
Unique
Isolated
Local
Sift
Carrier
Level
SNP
Expressed
Origin
Standard
Under
Trypsin
Appearance
Mutated
Toronto
Adult
Further
Type
Point
Genealogy
Evaluated
Confocal

CHAPTER 5

Mutations in SGOL1 cause a novel cohesinopathy affecting heart and gut rhythm

Philippe Chetaille [1,14], Christoph Preuss [2,14], **Silja Burkhard** [3,14], Jean-Marc Côté [1], Christine Houde [1], Julie Castilloux [1], Jessica Piché [2], Natacha Gosset [2], Séverine Leclerc [2], Florian Wünnemann [2], Maryse Thibeault [2], Carmen Gagnon [2], Antonella Galli [4], Elizabeth Tuck [4], Gilles R Hickson [5], Nour El Amine [5], Ines Boufaied [5], Emmanuelle Lemyre [5], Pascal de Santa Barbara [6], Sandrine Faure [6], Anders Jonzon [7], Michel Cameron [2], Harry C Dietz [8], Elena Gallo-McFarlane [8], D Woodrow Benson [9], Claudia Moreau [5], Damian Labuda [5], FORGE Canada Consortium [10], Shing H Zhan [11], Yaoqing Shen [11], Michèle Jomphe [12], Steven J M Jones [11], Jeroen Bakkers [3] & Gregor Andelfinger [2,5,13]

[1] Department of Pediatrics, Centre Mère Enfants Soleil, Centre Hospitalier del'Université (CHU) de Québec, Quebec City, Quebec, Canada.
[2] Cardiovascular Genetics, Department of Pediatrics, Centre Hospitalier Universitaire Sainte-Justine Research Centre, Université de Montréal, Montreal, Quebec, Canada.
[3] Hubrecht Institute, Royal Netherlands Academy of Arts and Sciences (KNAW) and University Medical Center Utrecht, Utrecht, the Netherlands.
[4] Wellcome Trust Sanger Institute, Wellcome Trust Genome Campus, Hinxton, UK.
[5] Department of Pediatrics, Université de Montréal, Montreal, Quebec, Canada.

[6] INSERM U1046, Montpellier, France.
[7] Department of Women's and Children's Health, Section for Pediatrics, Astrid Lindgren's Children's Hospital, Uppsala University, Uppsala, Sweden.
[8] Howard Hughes Medical Institute, Johns Hopkins University School of Medicine, Baltimore, Maryland, USA.
[9] Department of Pediatrics, Medical College of Wisconsin, Milwaukee, Wisconsin, USA.
[10] Membership of the Steering Committee for the Consortium is given in the Acknowledgments.
[11] Michael Smith Genome Sciences Centre, BC Cancer Agency, Vancouver, British Columbia, Canada.
[12] Projet BALSAC, Université du Québec à Chicoutimi, Chicoutimi, Quebec, Canada.
[13] Department of Biochemistry, Université de Montréal, Montreal, Quebec, Canada.

[14] These authors contributed equally to this work.

Nature Genetics **46**, 1245-1249 (2014)

ABSTRACT

The pacemaking activity of specialized tissues in the heart and gut results in lifelong rhythmic contractions. Here we describe a new syndrome characterized by Chronic Atrial and Intestinal Dysrhythmia, termed CAID syndrome, in 16 French Canadians and 1 Swede. We show that a single shared homozygous founder mutation in *SGOL1*, a component of the cohesin complex, causes CAID syndrome. Cultured dermal fibroblasts from affected individuals showed accelerated cell cycle progression, a higher rate of senescence and enhanced activation of TGF-β signaling. Karyotypes showed the typical railroad appearance of a centromeric cohesion defect. Tissues derived from affected individuals displayed pathological changes in both the enteric nervous system and smooth muscle. Morpholino-induced knockdown of *sgol1* in zebrafish recapitulated the abnormalities seen in humans with CAID syndrome. Our findings identify CAID syndrome as a novel generalized dysrhythmia, suggesting a new role for *SGOL1* and the cohesin complex in mediating the integrity of human cardiac and gut rhythm.

INTRODUCTION

Disturbances of pacemaker activity in the heart and gut can have varied clinical manifestations. Dysregulation of the cardiac sinus node results in sick sinus syndrome (SSS), the most common cause of pacemaker implantation (Rodriguez and Schocken, 1990). SSS is rare in children and is characterized by persistently decreased heart rhythm, episodes of sinoatrial block and/or chronotropic incompetence. In the gut, pacemaking is mediated through the network of interstitial cells of Cajal and the autonomous enteric nervous system (ENS). Chronic intestinal pseudo-obstruction (CIPO) is a rare and severe disorder of gastrointestinal motility in which intestinal obstruction occurs in the absence of a mechanical obstacle. Several studies identified genetic risk factors for SSS (Benson et al., 2003, Holm et al., 2011, Laish-Farkash et al., 2010, Milanesi et al., 2006, Mohler et al., 2003, Mohler et al., 2004, Schulze-Bahr et al., 2003) and CIPO (Deglincerti et al., 2007, Gargiulo et al., 2007), but in most cases the genetic causes remain enigmatic.

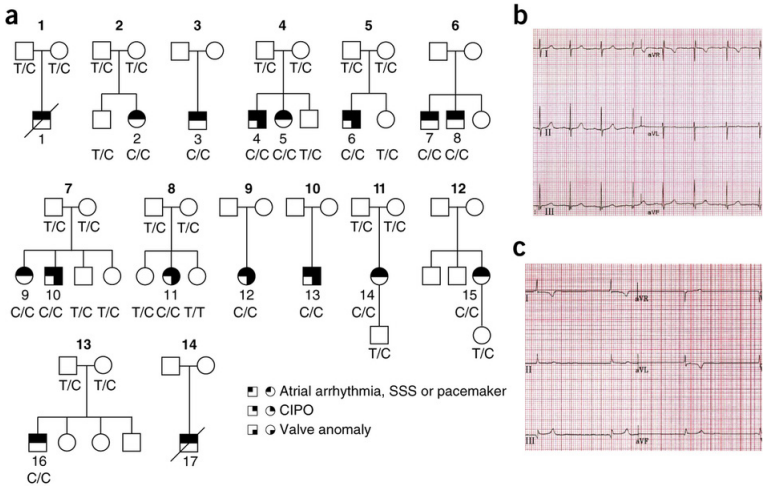

Figure 1: Synopsis of families and electrocardiographic features

(a) Pedigrees of the CAID syndrome cohort. Wild-type (T/T), heterozygous (T/C) and homozygous (C/C) mutation status are shown. Family and subject numbers refer to those used in the text and Supplementary Table 2. In family 1, in which the index case was deceased without any available biological material, we found both parents to be heterozygous for the CAID-linked mutation in SGOL1. **(b,c)** Evolution of clinical electrocardiographic findings in a CAID case, showing normal sinus rhythm at 3 years of age **(b)** and sinus node dysfunction with junctional escape rhythm (40 beats per minute) at 19 years of age **(c)**. I, II, III, aVR, aVL and aVF denote corresponding peripheral leads.

RESULTS

We identified 17 subjects in whom SSS and CIPO co-occurred during the first four decades of life (Fig. 1a). Distinctive clinical features included atrial dysrhythmias, SSS and valve anomalies, as well as a requirement for pacemaker implantation and total parenteral nutrition (Fig. 1b,c and Supplementary Tables 1 and 2). In different individuals with CAID, CIPO was found to be of neurogenic or myogenic origin (Supplementary Fig. 1). No case had clinical evidence of other congenital anomalies or manifestations of known cohesinopathies. Family evaluation suggested inheritance in an autosomal recessive manner, prompting us to perform whole-exome sequencing of three unrelated probands. We identified only one homozygous pathogenic variant shared by all probands, namely, c.67A>G, n.367–2014T>C, in *SGOL1* (rs199815268), which was predicted to encode a damaging change, p.Lys23Glu, at a highly conserved residue (Supplementary Fig. 2a–c and Supplementary Table 3). The mutation was extremely rare (minor allele frequency (MAF) < 1%) in public databases (Siva, 2008) (see URLs) and was absent in 360 French-Canadian control exomes. We confirmed the homozygous mutation by Sanger sequencing in all 14 surviving French-Canadian cases and the 1 Swedish case (Fig. 1a). The mutation was absent from 11 isolated pediatric SSS cases without CIPO and 43 isolated pediatric CIPO cases without SSS.

To genetically fine map the disease-causing haplotype and exclude the presence of copy number variants (CNVs), we performed Illumina HumanOmni5-Quad genotyping for 13 cases and 3 unaffected family members. Homozygosity mapping with PLINK and HomozygosityMapper (Purcell et al., 2007, Seelow et al., 2009) (see URLs) identified a single 1.4-Mb region between SNPs rs2929378 and rs442920 harboring *SGOL1* that was identical in all the cases (Supplementary Fig. 3). Further haplotype analysis identified a rare 700-kb disease-associated haplotype shared by the Swedish and French-Canadian cases lacking rare CNVs. Genealogy and genetic analyses excluded any direct relatedness for the Swedish and French-Canadian individuals (PLINK pi-hat < 0.2; *F* inbreeding coefficient -0.1 -0). Our population genetic analysis determined that the rare disease-causing haplotype was of northern European origin and demonstrated the absence of tagging SNPs for this haplotype in Asian, African and admixed American populations (Supplementary Fig. 4). Reconstitution of ascending genealogies from the BALSAC population database (Bouchard et al., 1989) for 8 French-Canadian cases identified 64 common ancestors married in the seventeenth century in France or in Quebec City. Identity-by-descent analysis supported the observation that all the French-Canadian CAID cases derived from the eastern part of Quebec and shared a common ancestral haplotype for *SGOL1*, whose age was estimated at 13 ± 4 generations. Allele

dropping analysis identified a founder couple, married in France in 1620, whose likelihood of being the mutation carriers exceeded that for other founders by a factor of >100 (Supplementary Fig. 5a,b). The haplotype sharing between the Swedish and French-Canadian cases (Supplementary Fig. 5c) suggests that they have common ancestry at about 30 generations, or 900 years, ago (Thompson, 2013). Taken together, our analyses support the association of *SGOL1* with the disease and suggest a transatlantic founder effect in the seventeenth century when Nouvelle France was settled.

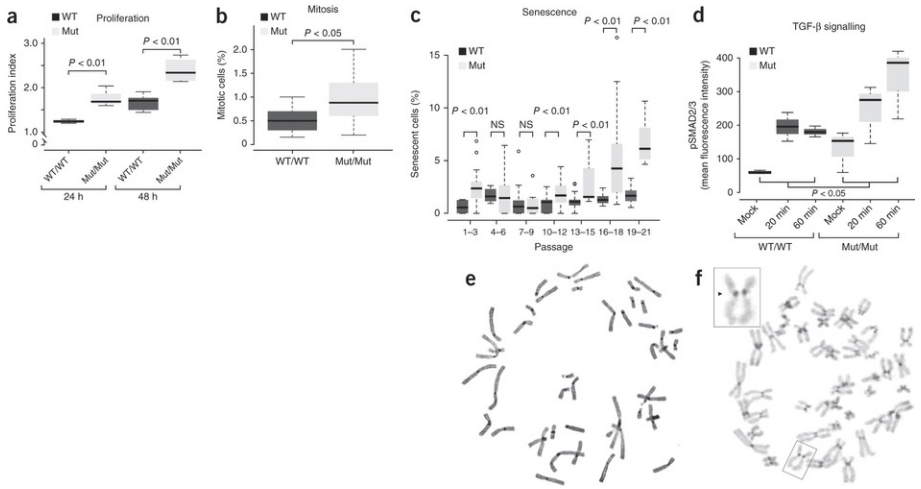

Figure 2: Cellular phenotypes of CAID

Experiments were performed in quadruplicate in three different cell lines for each individual with wild-type *SGOL1* (WT) or homozygous for the *SGOL1* mutation encoding p.Lys23Glu (Mut). **(a)** Primary fibroblasts from homozygous carriers of the SGOL1 mutation encoding p.Lys23Glu show significantly higher proliferation indices at 24 and 48 h of growth in culture. Shown is the fold increase relative to baseline values: 24 h, normal versus case, 1.26 versus 1.72, Wilcoxon rank-sum test, $P < 0.01$; 48 h, normal versus case, 1.72 versus 2.24, Wilcoxon rank-sum test, $P < 0.01$. Error bars, s.d. **(b)** The percentage of cells in mitosis is significantly higher in cells from CAID cases relative to controls as determined by FACS analysis (0.5% versus 1%, Wilcoxon rank-sum text, $P < 0.05$). Error bars, s.d. **(c)** Senescence is accelerated in mutant versus wild-type fibroblasts over time as measured by the senescence-associated (SA)-β-gal assay. The boxes represent the interquartile range of the data, and the whiskers indicate the upper and lower quartiles. The thick line represents the median. Error bars, s.d. Statistical significance was estimated by Wilcoxon rank-sum test. NS, not significant. **(d)** Phosphorylation of SMAD2 and SMAD3 (pSMAD2/3) is significantly increased at baseline and after stimulation with TGF-β1 in mutant versus wild-type cell lines. Error bars, s.d. **(e,f)** C banding of a metaphase spread in cells from a wild-type control **(e)** versus a CAID case **(f)** shows a centromeric cohesion defect in the cells from the case. Inset, enlarged chromosome from the boxed region highlighting the heterochromatic repulsion (arrowhead) observed in CAID.

Because of the known involvement of *SGOL1* in cell division, we studied cell cycling parameters in primary fibroblast cultures from three homozygous carriers of the *SGOL1* mutation encoding p.Lys23Glu. These fibroblasts exhibited significantly faster cell proliferation ($P < 0.01$) due to a higher percentage of cells in M phase ($P < 0.05$), as determined by intracellular flow cytometry, than corresponding cells from healthy controls (Fig. 2a,b). Over time, the rate of senescence was higher in mutant versus control cell lines (Fig. 2c). In control fibroblast cell lines, the SGOL1 protein was restricted almost exclusively to the nucleus, where it formed a distinct punctate pattern. In contrast, the mutated SGOL1 protein showed a homogenous distribution inside the nucleus of case-derived fibroblasts as well as the cytoplasm (Supplementary Fig. 6). This altered organization of nuclear SGOL1 was also apparent in quantitative analysis of the signal intensities for nuclei (Supplementary Fig. 7). During mitosis, the mutant form of SGOL1 was localized in an ordered fashion around the centromeres but displayed a rather homogenous cytoplasmic localization pattern (Supplementary Fig. 6). Because transforming growth factor (TGF)-β signaling is a known mitogenic cascade with clinical relevance to arrhythmias, we assayed the behavior of fibroblasts in response to TGF-β stimulation (Gramley et al., 2010). In comparison to wild-type fibroblast cell cultures, cell lines homozygously expressing mutant SGOL1 had higher baseline levels of phosphorylation of SMAD2 and SMAD3 (SMAD2/3), which constitute a critical downstream mediator of the TGF-β signaling pathway. These fibroblasts also showed higher levels of phosphorylated SMAD2/3 in response to TGF-β1 stimulation (Fig. 2d). On the basis of the known function of SGOL1, we assumed that there might be a potentially informative karyotype in the metaphase spreads of chromosomes from cases. Indeed, C banding identified heterochromatin repulsion at the centromere (resulting in a railroad track appearance) without signs of aneuploidy, fostering the diagnosis of a novel cohesinopathy (Fig. 2e,f).

In normal tissues, *SGOL1* is ubiquitously expressed in the intestinal wall, including in smooth muscle and the ENS (Supplementary Fig. 8). CAID cases showed characteristic anomalies in the ENS, which controls gastrointestinal reflexes. We found both hypoplastic ganglia and mislocalization of ganglia and Cajal cells in the circular and longitudinal smooth muscle layers, reminiscent of the phenotypes described in mouse models with altered Shh gradients (Fu et al., 2004, Sukegawa et al., 2000) (Fig. 3a,b). Compatible with the increased TGF-β signaling seen in cell culture, we found abundant T cells in the intestinal smooth muscle layers (Fig. 3c). Furthermore, thinning of smooth muscle layers, fragmentation of the smooth muscle fiber architecture and extensive fibrosis, a hallmark of chronic TGF-β activation, were observed (Fig. 3d,e). Together, these data suggest that both neuromuscular alterations contribute to the CAID syndrome.

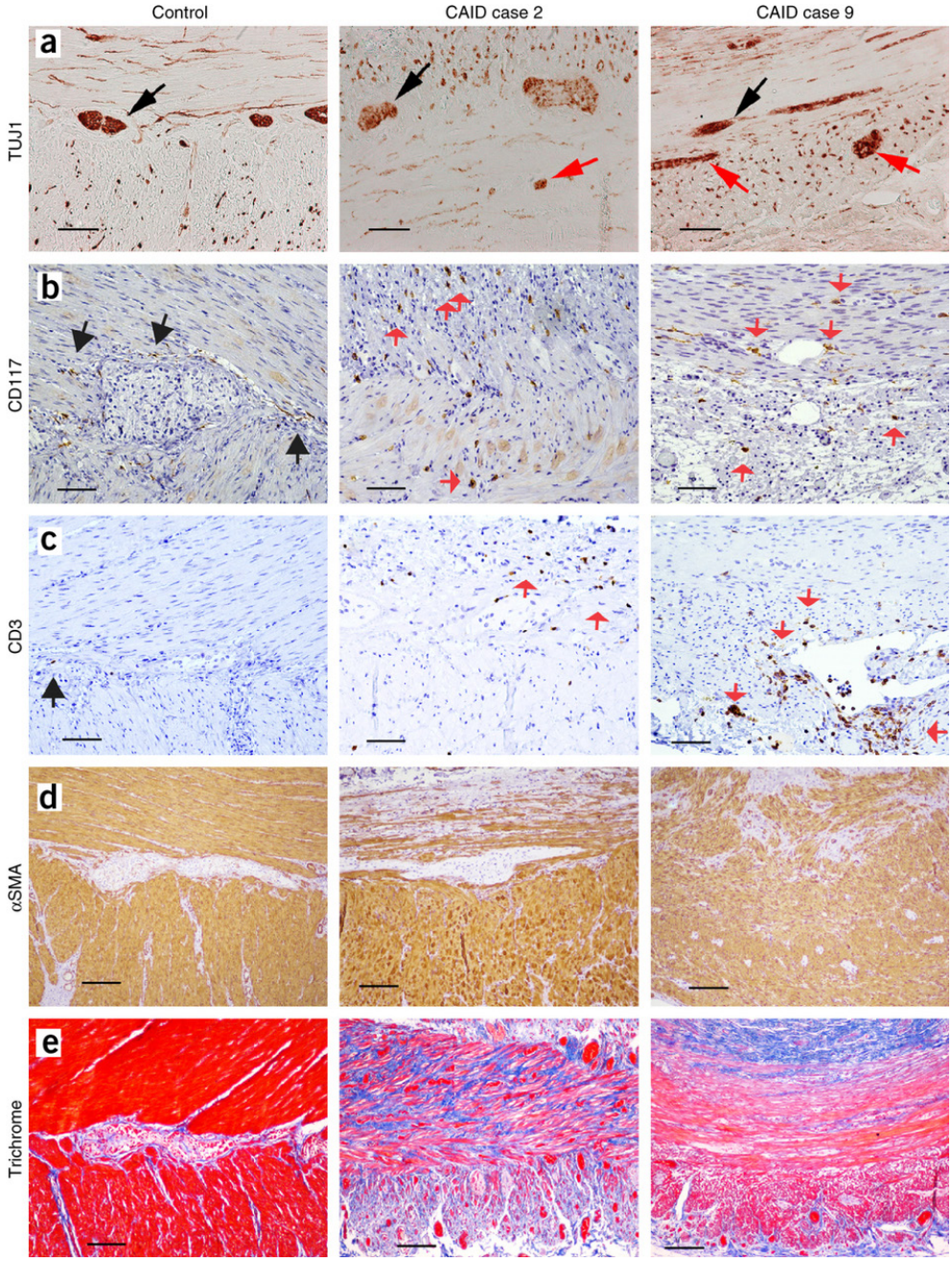
Control
CAID case 2
CAID case 9
a
TUJ1
b
CD117
c
CD3
d
αSMA
e
Trichrome

Figure 3: Synopsis of the gastrointestinal histology of CAID.

Full-thickness biopsies from a wild-type control and two individuals with CAID. All biopsies are oriented to show the circular muscular layer on top and the longitudinal layer on the bottom. **(a–e)** Staining was performed for TUJ1 (neuron-specific βIII tubulin, a neuronal marker expressed in intestinal ganglial cells) **(a)**, CD117 (c-KIT, a marker of Cajal cells) **(b)**, CD3 (a marker of mature lymphocytes) **(c)**, αSMA (α smooth muscle actin, a smooth muscle cell marker) **(d)** and Trichrome-Masson (distinguishes cells (red) from surrounding connective tissue (blue)) **(e)**. **(a)** In addition to the presence of normal intestinal ganglia (black arrows), smaller ganglia mislocalized into the longitudinal smooth muscle layer are seen in CAID cases (red arrows). **(b)** Whereas Cajal cells are localized in a perigangliar fashion in wild-type cells (black arrows), they are seen abundantly within the circular and longitudinal smooth muscle layers in CAID (red arrows). **(c)** Mature lymphocytes abundantly invade the smooth muscle layers in CAID (red arrows) in comparison to wild-type tissue (black arrow). **(d)** αSMA staining demonstrates the presence of the two smooth muscle layers but also indicates vacuolization and disruption of the fiber architecture of smooth muscles previously reported in individuals with CIPO. **(e)** This disruption of wall architecture is further confirmed by Trichrome-Masson staining, which also documents extensive fibrotic remodeling of the intestinal wall. Scale bars, 100 μm **(a–c)** and 200 μm **(d,e)**.

To illustrate the role of *sgol1* during heart and gut development, we established a zebrafish model. We observed a distinct spatiotemporal expression pattern for zebrafish *sgol1* in developing heart and gut (Fig. 4a–d,f). Notably, a strong and discrete expression signal was found at the level of the sinus venosus from which the pacemaker tissue arises, in a mutually exclusive pattern with *nppa*, a marker of terminal cardiomyocyte differentiation (Fig. 4c–f) (Tessadori et al., 2012). Morpholino-mediated knockdown of *sgol1* significantly decreased heart rate in zebrafish ($P < 0.0001$), with an effect size similar to the knockdown of known conduction and pacemaker regulators such as *scn12a* (the zebrafish ortholog of *SCN5A*) and *isl1* (Fig. 4g and Supplementary Fig. 9) (de Pater et al., 2009, Benson et al., 2003).

All the affected individuals described in this study shared a unique combination of cardiac arrhythmias and intestinal pseudo-obstruction that defines a novel cohesinopathy syndrome we have termed CAID. Several lines of genetic and functional evidence show that a single homozygous mutation in *SGOL1* predisposes to this generalized co-occurring cardiac and intestinal rhythm phenotype. This mutation arose recently on a rare haplotype in the European population, with an estimated age of 900 years. The identification of a Swedish case sharing an extended haplotype with the French-Canadian cases highlights the possibility that migration might have had an important role in disease etiology. Linking the geographical gradient of the *SGOL1* haplotype (Supplementary Fig. 4) and the known migration routes of Vikings in the twelfth century from Scandinavia to Normandy supports the idea of a transatlantic founder effect originating in Scandinavia.

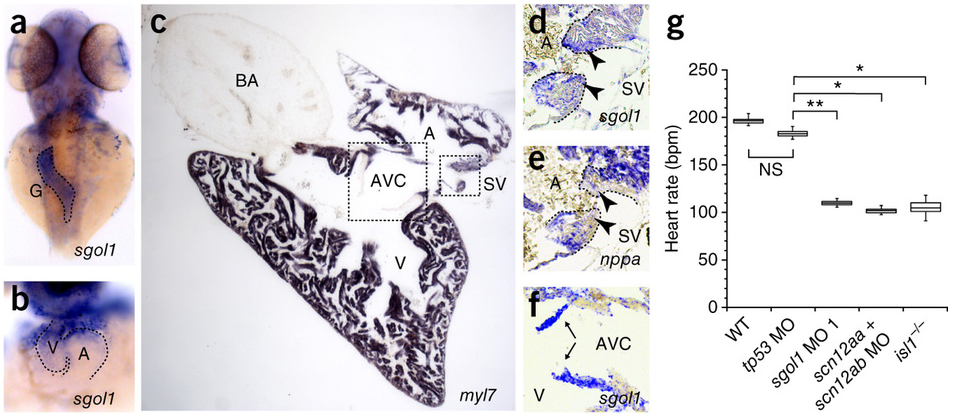

Figure 4: Spatiotemporal expression and function of sgol1 in zebrafish

(a,b) *In situ* hybridization for *sgol1* on wild-type zebrafish embryos (3 days post-fertilization (d.p.f.)). **(a)** Dorsal view; *sgol1* expression marks the intestinal bulb and intestine (dotted line). **(b)** Ventral view; *sgol1* expression in the embryonic heart (dotted line). **(c)** Labeling with the myocardial marker *myl7* delineates the myocardium; boxed areas indicate the magnified regions shown in d–f. **(d–f)** Section *in situ* hybridization on adult wild-type zebrafish hearts. **(d,e)** Expression of *sgol1* at the base of the venous valves (demarcated area) in the sinoatrial region **(d)**. Expression of *nppa* in the sinoatrial region **(e)**. Arrowheads indicate *nppa*-negative cells located at the base of the venous valves. **(f)** *sgol1* expression in the atrioventricular valves (arrows). **(g)** Analysis of heart rate by high-speed video imaging. Box-whisker plots show the heart rate with the indicated morpholino injections (n = 15 embryos per group). Significance was determined by Student's t test: *P < 0.05, **P < 0.01, NS P > 0.05. A, atrium; AVC, atrioventricular canal; BA, bulbus arteriosus; G, gut; SV, sinus venosus; V, ventricle; bpm, beats per minute.

5

DISCUSSION

We propose that the mutated SGOL1 protein results in loss of cohesin protection, accelerating cell cycling and senescence and thereby replicating the bradycardia-tachycardia syndrome usually observed in elderly individuals. Our novel syndrome falls under the umbrella term cohesinopathy, which includes phenotypically diverse entities such as premature ovarian failure (*STAG3*), Cornelia de Lange syndrome (*NIPBL*, *RAD21*, *SMC1* and *HDAC8*), Warsaw breakage syndrome (*DDX11*), Nijmegen breakage syndrome (*NBS1*) and Roberts syndrome (*ESCO2*), which all result from mutations in cohesin components (Caburet et al., 2014, Deardorff et al., 2012a, Deardorff et al., 2012b, Gillis et al., 2004, Kline et al., 2007, Musio et al., 2006, van der Lelij et al., 2010). The unique CAID phenotype raises the possibility that both loss-of-function and gain-of-function effects co-occur. The disruption of the known interaction between SGOL1 and PP2A (Yamagishi et al., 2008) might result in loss of separase inhibition at the nuclear level, whereas mislocalization of SGOL1 in the cytosol during interphase might alter PP2A-mediated ion channel regulation

(Heijman et al., 2013). We hypothesize that spatiotemporally restricted expression of *SGOL1* during embryogenesis or the restricted requirement for *SGOL1* in adult pacemakers might confer the target organ specificity observed in CAID syndrome.
The involvement of SGOL1 in the cohesin complex could entail consequences for long-range transcriptional regulation (Schmidt et al., 2010, Deardorff et al., 2012a), possibly interfering with the expression of gene products associated with SSS or CIPO (Benson et al., 2003, Gargiulo et al., 2007, Holm et al., 2011, Laish-Farkash et al., 2010, Mohler et al., 2004). Notably, the histological findings in individuals with CAID might point to an interaction of both developmental (mislocalized, abnormal ganglia) and acquired (destruction of smooth muscle architecture, fibrosis) phenotypes. Thus, in addition to acting through TGF-β signaling, a non-canonical role for SGOL1 and the cohesin complex in maintaining shared transcriptional modules of the sinoatrial node in the heart and Cajal cells in the gut is an intriguing possibility. In conclusion, the findings in this study support a hitherto unsuspected role for SGOL1 in the lifelong integrity of human pacemaker activity.

METHODS

STUDY SUBJECTS

The ethical committees at all participating institutions approved the study, and all participants gave informed consent. Cases were ascertained through participating centers and underwent repeated clinical, electrocardiographic, echocardiographic and gastrointestinal assessments as part of their routine medical management. The diagnostic criterion for SSS was chronic, inappropriate sinus bradycardia associated with inappropriate junctional rhythm, sinus pauses and atrial dysrhythmias (frequent atrial premature, atrial tachycardia, atrial flutter and atrial fibrillation). A diagnosis of CIPO was made on the basis of mechanical obstruction of the intestine in the absence of an anatomical cause and evidence of impaired motility. Full-thickness biopsy material for two CAID cases and an unaffected control was available after surgery. Distribution of phenotypes in the CIPO validation cohort (total $n = 43$) was as follows: neurogenic, $n = 10$; myogenic, $n = 4$; mixed origin, $n = 2$; uncertain origin, $n = 27$.

GENETIC ANALYSES

Whole-exome sequencing.

DNA was extracted from peripheral blood using the Qiagen Gentra PureGene Blood kit. We performed whole-exome sequencing on three cases (subjects 2, 8 and 12; Fig. 1) from apparently unrelated families to identify the causative mutation, under the hypothesis that CAID was an autosomal recessive trait caused by a rare allele with a heterozygous frequency of <1%. The FORGE Canada team at the Michael Smith Genome Sciences Centre (Vancouver, British Columbia, Canada) used standard protocols for the Agilent SureSelect 50Mb exome enrichment kit with subsequent 100-bp paired-end sequencing on the Illumina HiSeq 2000 platform. Reads remaining after quality control were aligned to the reference human genome (hg18) using the Burrows-Wheeler Aligner, and variants were called using SAMtools 0.1.13 utilities (Li et al., 2009, Li and Durbin, 2009). At least 96% of the targeted exomes were covered by 20-fold for each sample. Only variants (single-nucleotide variants and small insertion-deletions (indels)) inside protein-coding regions defined by Ensembl release 54 gene models were retained for downstream analysis (Flicek et al., 2012). To obtain a tractable set of potentially causative candidates, we correlated variants with the dbSNP 129 and 130 databases, the 1000 Genomes Project database (Siva, 2008), an in-house database of normal germline variants developed at the Michael Smith Genome Sciences Centre and a similar database at the CHU Sainte-Justine Research Center that contains data from 360 French-Canadian subjects without a history of SSS or CIPO. Variant positions were annotated with reference to Build 36

of the NCBI genome assembly and sequences NM_001199252 and NP_001186184.

SGOL1 mutation genotyping.

We performed PCR-based bidirectional Sanger sequencing to confirm the *SGOL1* mutations detected by whole-exome sequencing as well as to screen additional probands with either CAID or SSS alone. For dideoxy sequencing of *SGOL1*, PCR amplification products were bidirectionally sequenced using BigDye 3.1 chemistry on an ABI 3130xl Genetic Analyzer (Applied Biosystems). Primer sequences are provided in Supplementary Table 4a. Sequencing traces were aligned to the genomic reference sequence using Lasergene SeqMan Pro software (DNASTAR).

High-density genotyping.

SNP data were generated at the McGill Genome Innovation Centre. Hybridization and laser scanning of Illumina HumanOmni5-Quad arrays with a mean call rate of 99.8% was performed according to the specifications of the manufacturer, with subsequent analysis on the GenomeStudio platform (Illumina). To perform homozygosity mapping, we analyzed SNP haplotype data for homozygous regions with HomozygosityMapper and PLINK (Purcell et al., 2007, Seelow et al., 2009). Genetic quality control included identity-by-descent testing and principal-components analyses. Relatedness testing was performed with PLINK, reporting pairs of individuals with genome identity (PLINK pi-hat) > 0.2 as being closely related or cryptic duplicates. Haplotypes and their frequencies were estimated using PLINK and the Haploview algorithm for populations from the HapMap phase 3 and 1000 Genomes Project data sets (Siva, 2008, International HapMap, 2003, Gabriel et al., 2002). The populations in these data sets included ones of African, admixed American, East Asian, South Asian and European ancestry. In addition, allele frequencies from Alfred were used to obtain accurate and well-defined estimates of the frequency distributions of variants across multiple populations (Rajeevan et al., 2007). The haplotype age for the French-Canadian founder population was estimated on the basis of haplotype alignments and a demographic model that was described previously (Labuda et al., 1996, Labuda et al., 1997), which takes population growth into account. CNV calls were generated with the PennCNV and CNVtools software package, using the log R ratio (LRR) and B allele frequency (BAF) measures automatically computed by the BeadStudio software (Illumina) (Glessner et al., 2013, Subirana et al., 2011).

Genealogy reconstruction.

Genealogies were reconstructed through the BALSAC Project at the Université du Québec in Chicoutimi, which holds an electronic database of the vital records for the

French-Canadian population since 1608 (Bouchard et al., 1989). The gene dropping method (Maccluer et al., 1986) implemented in the R GenLib software package (see URLs) was used to estimate the genetic contribution of each common ancestor to *SGOL1* mutation carriers and 228 unrelated controls. For each common ancestor, the probability of allele transmission was determined on the basis of known genealogies. Permutations were repeated 100 million times for each candidate ancestor, and the allele transmission probability was assessed on the basis of the assumption that each affected individual inherits two copies of the allele and the allele is absent in controls. The final probability for each common ancestor was obtained by multiplying the probabilities across all affected individuals and controls. The probability of ancestor *i* being the most likely common ancestor was given on the basis of the observed genetic information *G* that was estimated as the denominator sums of all the probabilities over all candidate ancestors.

CELL CULTURE ASSAYS

All cell cultures were routinely tested for the absence of mycoplasma infection. All assays were carried out between passages 3 and 12, with a matched number of passages in each assay.

Proliferation assays.

Primary dermal fibroblasts from normal controls and homozygous carriers of the *SGOL1* mutation encoding p.Lys23Glu were cultured in DMEM culture medium in the presence of 10% FBS and seeded at 4,000 cells/well in a 96-well plate in triplicate in three sets of plates. Cell proliferation was evaluated using WST-1 reagent (Roche) according to the manufacturer's instructions. The day after seeding, WST-1 was added to one set of plates to determine the background control. The other plates were maintained in culture for 24 and 48 h, and WST-1 was added at the end of each culture period. Proliferation was assessed by measuring the absorbance of the samples relative to the background controls at 440 nm.

Cell cycling and mitosis.

To analyze cell cycling and mitosis, fibroblasts were cultured as described above and then washed with PBS and fixed with cold 70% ethanol for 1 h on ice. After fixation, cells were resuspended in PBS with 0.5% Triton X-100 and incubated at room temperature for 30 min. Cells were washed in PBS and incubated with Alexa Fluor 488–conjugated antibody to phosphorylated histone H3 (Cell Signaling Technology; 1:20 dilution in PBS with 1% BSA; 16-h incubation). Cells were washed and resuspended in PBS containing 150 µg of RNase A (Fermentas) and 7.5 µg of propidium iodide and incubated for 30 min at room temperature. Fluorescence

was measured using a flow cytometer (BD Biosciences FACS Fortessa) and FlowJo software (Tree Star). Three cell lines were studied for each genotype in triplicate, with a minimum of 100,000 total events.

Immunofluorescence microscopy.

Fibroblasts were cultured on poly-L-lysine–coated coverslips in 12-well plates and fixed for 5 min in 4% paraformaldehyde in PBS, permeabilized in PBS containing 0,25% Triton X-100 (PBST buffer), blocked for 1 h at room temperature in PBST buffer containing 5% goat serum and incubated overnight at 4 °C with primary antibody (1:90 dilution; mouse antibody to Sgol1, Abcam, ab58023). Cells were washed three times for 5 min per wash with PBS and incubated for 1 h at room temperature with Alexa Fluor 488–conjugated goat anti-rabbit secondary antibody (1:1,000 dilution; Molecular Probes/Invitrogen). Hoechst 33258 (1:500 dilution) was added for the final 5 min before cells were washed with PBS and mounted in ProLong antifade reagent (Molecular Probes/Invitrogen). Images were acquired with Volocity version 6.0 software (Improvision/PerkinElmer) controlling an Ultraview Vox spinning-disc confocal system (PerkinElmer), employing a CSU-X1 scanning unit (Yokogawa) and an Orca-R2 charge-coupled device camera (Hamamatsu) fitted to a Leica DMI6000B inverted microscope equipped with a 1.4-NA Plan Apochromat 100× oil immersion objective.

Image analysis.

Images were exported from Volocity as “item as tiff” files and imported into ImageJ software (version 1.47). Using single confocal sections, regions of interest were manually drawn around each nucleus (using the Hoechst channel), and SGOL1 pixel intensity values were extracted using the Sixteenbit Histogram extension plug-in. Pixel intensity values were plotted as a function of their frequencies (normalized by pixel numbers) using Prism software (GraphPad). SGOL1 intensity distributions are shown as the mean frequencies (± s.e.m.) for a total of 12 cells from 3 different homozygous cases or wild-type controls. The corresponding background distribution represents the data from similarly sized regions of interest selected from cell-free areas of the images.

Senescence assays.

Senescence was measured with SA-β-gal staining at pH 5.5 using previously published protocols (Itahana et al., 2007). Briefly, 40,000 fibroblasts/well were seeded and grown in 6-well plates as described above and were analyzed at the indicated passages. All assays were performed in quadruplicate in three different cell lines for each wild-type control and homozygous carrier of the *SGOL1* mutation

encoding p.Lys23Glu. After the aspiration of medium, cells were washed twice with PBS, fixed with 4% formaldehyde (Sigma) for 5 min at room temperature, washed twice with 2 ml of PBS and incubated for 16 h in a 37 °C chamber with staining solution at pH 5.5 (final concentrations: citric acid, 20 mM; phosphate, 40 mM; potassium ferricyanide, 5 mM; potassium ferrocyanide, 5 mM; NaCl, 150 mM; $MgCl_2$, 2 mM; X-gal in dimethylformamide, 1 mg/ml). Stained cells were counted manually for 200 cells, and numbers were documented digitally.

Flow cytometric TGF-β assays.

Fibroblasts were grown to approximately 80% confluence in DMEM supplemented with 10% FBS in a 6-well plate. Cultures were then starved in 2% serum for 24 h before stimulation with vehicle or 10 ng/ml TGF-β1 (R&D) for the indicated times. At each time point, cells were quickly lifted from the plates by adding trypsin and pipetting forcefully with a P1000 pipette; signaling was stopped by quickly mixing one volume of cells plus trypsin with one volume of 4% paraformaldehyde (EMS) in PBS. Cells were fixed for 10 min at 37 °C, washed once in PBS containing 0.5% BSA (flow cytometry staining buffer), and resuspended and incubated for 30 min in ice-cold 90% methanol. Cells were then washed once with flow cytometry staining buffer and stained at room temperature for 1 h with phycoerythrin-conjugated antibody to phosphorylated Smad2 and Smad3 (clone O72-670, BD Biosciences) by adding 5 µl of antibody to 1 × 10^6 cells in a 100-µl volume. Unbound antibody was removed by washing the cells twice in flow cytometry staining buffer. Stained cell suspensions were analyzed on a BD FACSVerse flow cytometer (BD Biosciences). Results were evaluated, including median fluorescent intensity calculation, using FlowJo software (Tree Star).

C banding.

Metaphase chromosome spreads were prepared from peripheral blood samples, and Giemsa C banding was performed using standard cytogenetic protocols.

IMMUNOHISTOCHEMISTRY ON INTESTINAL SECTIONS

Paraffin-embedded sections (8-µm thick) were immunostained as previously described (Notarnicola et al., 2012, Rouleau et al., 2009). Antigen retrieval was achieved by heating at 98 °C for 20 min in 1 mM citrate (pH 6.0). For SGOL1 immunostaining, a mouse monoclonal antibody (ab58023, Abcam) was used at a 1:200 dilution as the primary antibody. In addition, antibodies to the neuronal marker TUJ1 (MMS-435P, mouse monoclonal antibody, Covance; 1:400 dilution), the TMEM16A marker for interstitial cells of Cajal (ab53212, rabbit polyclonal antibody, Abcam; 1:200 dilution), αSMA (IR611, Dako; prediluted), CD117 (A4502, Dako; 1:500 dilution) and CD3

(IR503, Dako; prediluted) were used. Trichrome-Masson staining was performed according to standard protocols (AR173, Dako). Immunohistochemistry control experiments were performed by excluding the primary antibody (data not shown).

ZEBRAFISH STUDIES

Zebrafish husbandry and in situ hybridization.

The fish used in this study were kept under standard conditions as previously described (Westerfield, 1995). All zebrafish work conformed to ethical guidelines and was approved by the relevant local ethics committees at the University of Utrecht. The *isl1*-mutant line isl1K88X SA0029 has been described previously (de Pater et al., 2009). *In situ* hybridization on zebrafish embryos was carried out as previously described (Thisse and Thisse, 2008). *In situ* hybridization on adult heart tissue was carried out as previously described with minor modifications (Moorman et al., 2001). The sample size was not predetermined.

Heart rate measurements.

Embryos at 3 d.p.f. were embedded in 0.25% agarose prepared in E3 embryonic medium with 16 mg/ml 3-aminobenzoic acid ethyl ester. Heartbeat was imaged using high-speed video recording at 28 °C and analyzed as previously described (Tessadori et al., 2012). Statistical analysis and drawing of the box-whisker plot were carried out in Excel 2007 (Microsoft).

Antisense morpholino-mediated knockdown.

Antisense morpholinos targeting *sgol1* were used at a final concentration of 500 μM in a volume of 1 nl per embryo and injected into embryos at the one-cell stage (Supplementary Table 4b). Antisense morpholinos targeting the zebrafish *SCN5A* orthologs *scn12aa* and *scn12ab* and *tp53* have been described previously and were used at final concentrations of 200 μM for *scn12aa* and 100 μM for *scn12ab* and *tp53* (Chopra et al., 2010). Uninjected embryos from the same egg lay were used as controls for all experiments.

URLS

HomozygosityMapper, http://www.homozygositymapper.org/; PLINK, http://pngu.mgh.harvard.edu/~purcell/plink/; BALSAC, http://balsac.uqac.ca/; Exome Variant Server (EVS), http://evs.gs.washington.edu/EVS/; SIFT, http://sift.jcvi.org/; SeattleSeq, http://snp.gs.washington.edu/; R GenLib software package, http://balsac.uqac.ca/english/acces-aux-donnees-2/service-aux-chercheurs/.

ACKNOWLEDGEMENTS

We are deeply indebted to all participating families and patients. We thank L. Gosselin, L. L'Écuyer, M.-F. Boudreault, C. Faure, F. LeDeist, L. D'Aoust and the McGill Genome Québec Innovation Centre (D. Vincent) for expert assistance. We gratefully acknowledge the contribution of all referring physicians and supporting staff to this project. We would like to thank J. Marcadier (clinical coordinator) and C. Beaulieu (project manager) for their contributions to the infrastructure of the FORGE Canada Consortium. The FORGE (Finding of Rare Disease Genes) Consortium Steering Committee includes Kym Boycott (University of Ottawa), Jan Friedman (University of British Columbia), Jacques Michaud (Université de Montréal), François Bernier (University of Calgary), Michael Brudno (University of Toronto), Bridget Fernandez (Memorial University), Bartha Knoppers (McGill University) and Steve Scherer (University of Toronto). FORGE Canada was funded by the Canadian government through Genome Canada, the Canadian Institutes of Health Research and the Ontario Genomics Institute (OGI-049). Additional funding was provided by Génome Québec, Genome British Columbia, Foundation Nussia and André Aisenstadt, La Fondation du Grand défi Pierre Lavoie, Fondation CHU Sainte-Justine, Fondation Leducq, Association des Pseudo Obstructions Intestinales Chroniques (France), the Netherlands Organization for Scientific Research (NWO) and ZonMw (91212086). G.A. holds a Senior Scholarship from the Fonds de Recherche du Québec–Santé and holds the Banque Nationale Research Chair in Cardiovascular Genetics. We thank G. Rouleau for sharing whole-exome data for control purposes and M. Samuels for critical reading of the manuscript.

CONTRIBUTIONS

P.C., J.-M.C. and G.A. identified the novel CAID syndrome in the families. Functional experiments were performed by F.W., N.G., J.P., S.L., C.G., E.L., I.B., J.B., S.B., A.G., E.T., S.F., M.C., N.E.A., E.G.-M., S.H.Z., Y.S., M.J. and S.J.M.J. Further patient recruitment and enrollment was performed by P.C., J.-M.C., C.H., J.C., A.J., P.d.S.B., M.T., D.W.B. and G.A. C.P. performed and supervised the genotyping and the haplotype and population genetic analysis. G.R.H., G.A., J.P. and N.E.A. performed confocal microscopy for the cell lines and analyzed the data. S.B. and J.B. established the zebrafish model. C.G., J.P. and E.G.-M. performed the functional cell line experiments. Genealogical analysis was provided by M.J., D.L. and C.M. H.C.D. provided advice on the analysis of the functional data derived from the cell lines. P.C., C.P., J.B., S.J.M.J. and G.A. wrote the manuscript with contributions and input from all authors. G.A. designed and supervised the study.

SUPPLEMENTARY FIGURES

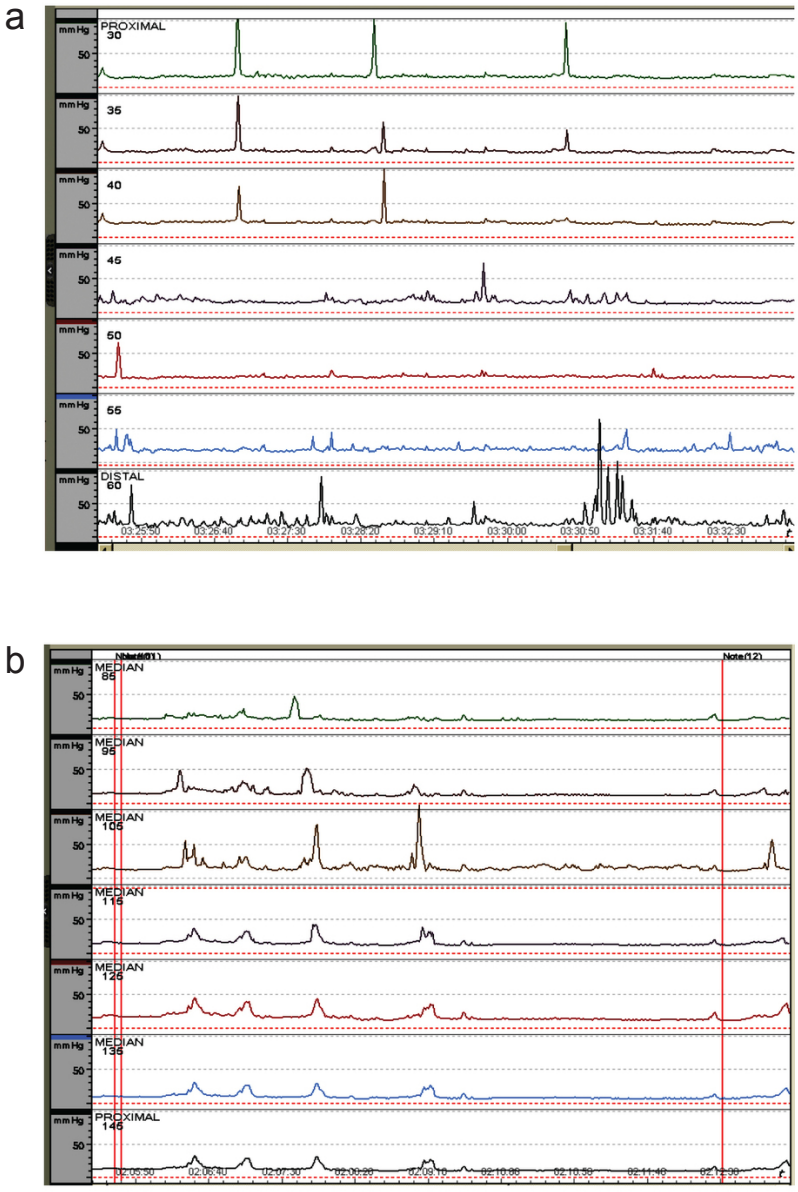

Figure S1: Representative manometries in two CAID patients.

(a) Antroduodenal manometry showing visceral neuropathy with abnormal response (normal amplitude, no phase III–like contractions) to IV erythromycin (antrum, channels 1–3; duodenum, channels 4 and 5; jejunum, channels 6 and 7). **(b)** Colonic manometry showing visceral myopathy with low-amplitude propagated contractions after stimulation (intracolonic bisacodyl) (right colon, channels 1 and 2; transverse, channels 3 and 4; sigmoid rectum, channels 5–7).

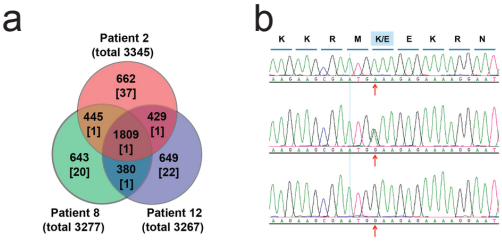

c

Shugoshin-like 1									
Human (NP_001186181)	K	K	R	M	K	E	K	R	N
CAID mutant	K	K	R	M	E	E	K	R	N
Macaque (XP_001089281)	K	K	R	M	K	E	K	R	N
Mouse (NP_082508)	K	N	R	M	K	E	K	R	N
Frog (NP_001090071)	K	E	R	M	K	E	K	R	I
Zebrafish (NP_001074089)	K	E	K	M	K	E	K	R	N

Figure S2: Results of sequencing.

(a) Venn diagram indicating the number of genes with homozygous nonsynonymous variants in three sequenced patients. In parentheses are the numbers of genes after filtering for rare alleles (MAF < 1%). **(b)** Examples of Sanger sequencing results for the screening of the exon 1 c.67A>G mutation (red arrow) showing the wild-type allele (top), a heterozygous parent (middle) and a homozygous CAID patient (bottom). One-letter amino acid code is used for the translation of individual codons. **(c)** The lysine (K) at position 23 is highly conserved in all vertebrates.

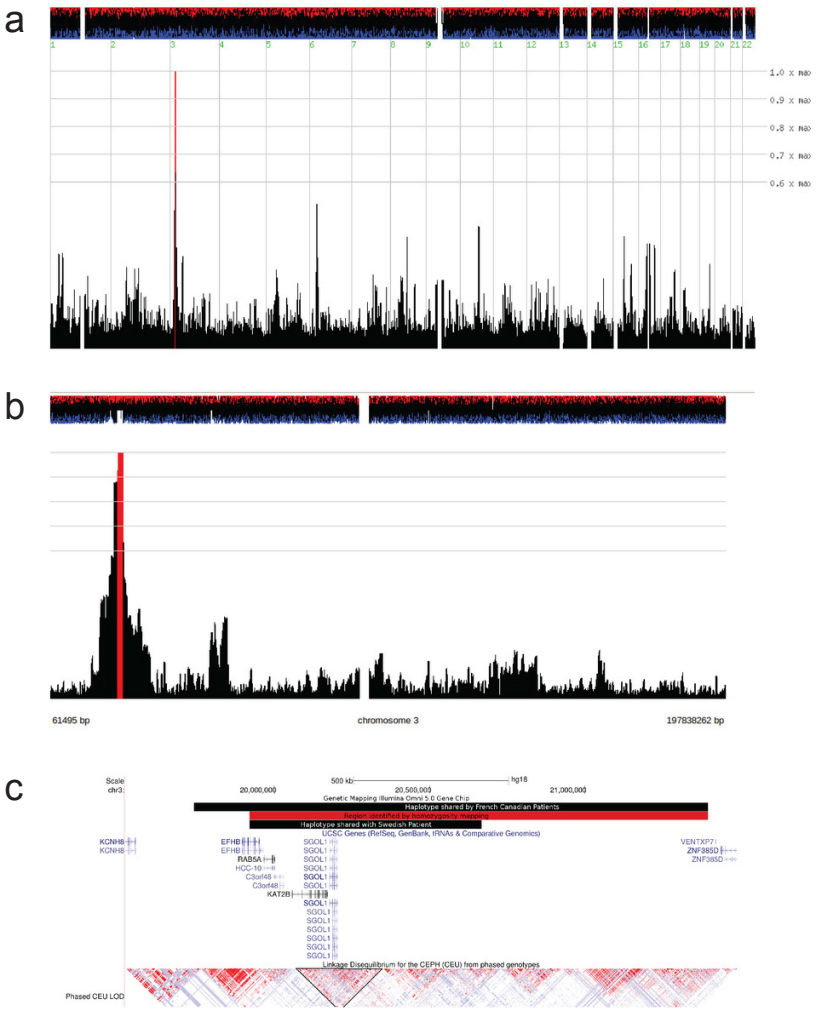

Figure S3: Results from homozygosity and haplotype mapping.

The results from homozygosity mapping1 in 12 French-Canadian CAID patients, 3 unaffected family members (family 4) and the Swedish patient are displayed. **(a,b)** Graphic depiction of homozygosity scores **(a)** across the genome and **(b)** for chromosome 3 providing mapping evidence for the *SGOL1* locus in CAID. **(c)** Reconstruction of the founder haplotype in the *SGOL1* region based on the largest window of consecutive homozygous variant calls obtained from high-density genotyping. The haplotype is displayed on the UCSC Genome Browser, showing that a 650-kb interval overlapping the *SGOL1* locus is identical by descent. Graphic depiction of haplotypes on the UCSC Genome Browser for the region between 20 Mb and 20.65 Mb on chromosome 3 harboring the following four genes: *SGOL1*, *RAB5A*, *C3orf48* and *PCAF*.

Figure S4: Haplotype gradients.

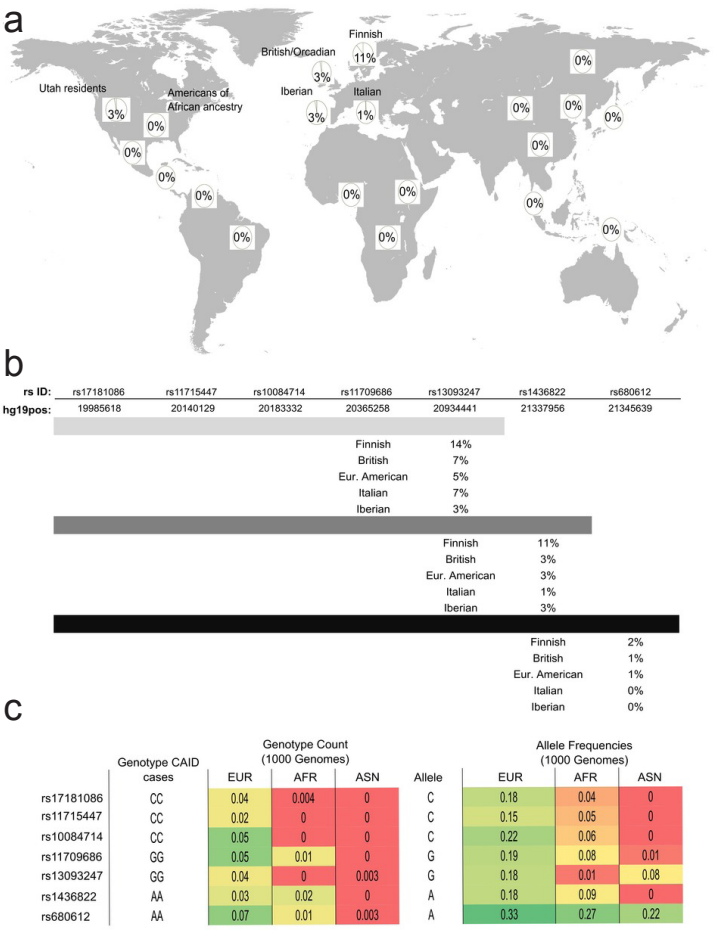

	Genotype CAID cases	Genotype Count (1000 Genomes) EUR	AFR	ASN	Allele	Allele Frequencies (1000 Genomes) EUR	AFR	ASN
rs17181086	CC	0.04	0.004	0	C	0.18	0.04	0
rs11715447	CC	0.02	0	0	C	0.15	0.05	0
rs10084714	CC	0.05	0	0	C	0.22	0.06	0
rs11709686	GG	0.05	0.01	0	G	0.19	0.08	0.01
rs13093247	GG	0.04	0	0.003	G	0.18	0.01	0.08
rs1436822	AA	0.03	0.02	0	A	0.18	0.09	0
rs680612	AA	0.07	0.01	0.003	A	0.33	0.27	0.22

(a) The distribution of haplotype frequencies across a world map highlights the absence of the disease-associated haplotype outside of Europe and North America. The haplotype gradients follow a migration pattern from northern European populations across the Atlantic. **(b)** For simplicity, a set of seven rare tagging SNPs for three haplotype combinations of different length is shown. Recombination breaks down the haplotypes over time within a population2. The presence of the longest haplotype in northern European populations and in North America combined with the absence of this haplotype in southern Europeans undermines the idea of a transatlantic founder effect. **(c)** Overview of allele frequencies and genotype counts for the rare tagging SNPs from the 1000 Genomes Project panel. Colors highlight the higher frequencies of variants in the European population compared to the Asian and African populations.

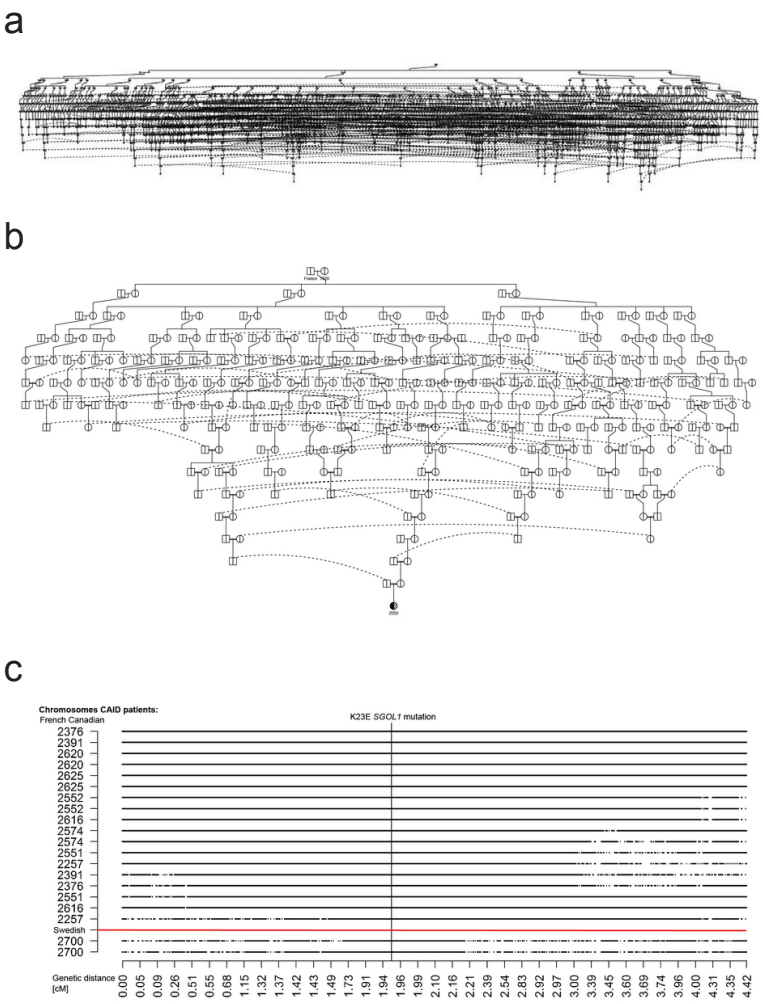

Figure S5: Genealogical analysis.

(a) The genealogy of the French-Canadian CAID patients linking all of them to their most likely founder couple married in France in 1620. **(b)** The corresponding genealogy of only one of the patients, illustrating details of the familial relationships along generations. The proposed founder couple is more than 100 times more likely to be the founder than other potential founders (posterior probability P = 0.993, estimated by gene dropping). Duplicated individuals are indicated by dashed lines. **(c)** Haplotype alignment. A schematic representation of the haplotypes around the CAID mutation (vertical line) found in nine patients, each representing an independent nuclear family, compared with two haplotypes for the Swedish patient. The consensus haplotype is represented by a solid line that is interrupted by empty spaces representing recombination break points. Notably, the Swedish patient shares about 0.5 cM with the Quebec haplotypes. We estimated the age of the founder haplotype to be between 9 and 17 generations, given proportions of 78% and 50% for the non-recombined mutation-carrying haplotypes at lengths of 0.28 and 0.41 cM, respectively. This is in line with the genealogical evidence pointing to the founder couple arriving in Nouvelle France around 1620 (ref. 3).

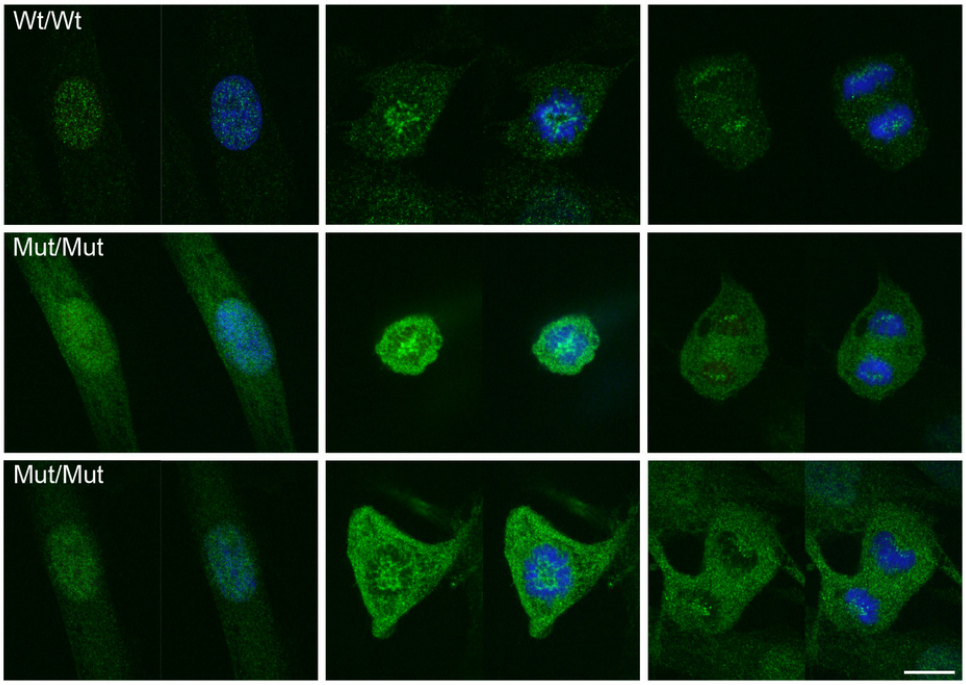

Figure S6: Confocal analysis of SGOL1 during mitosis.

Comparison of a control wild-type cell line and two cell lines homozygous for the SGOL1 K23E mutant is shown. SGOL1 K23E localizes correctly to the centromeric regions during pro-metaphase and anaphase but retains an abnormal cytosolic localization pattern. Left: green, SGOL1 staining. Right: green and blue, SGOL1 plus Hoechst. Scale bar, 10 µm.

Figure S7: Quantitative analysis of confocal microscopy.

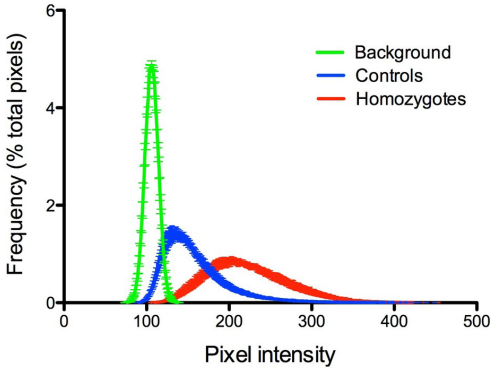

Quantitative analysis of the distribution of nuclear SGOL1 pixel intensities reveals altered SGOL1 organization in fibroblasts from homozygous CAID patients (red) compared to controls (blue). Data are the mean ± s.e.m. from 12 cells from 3 individuals per genotype. In control nuclei, the distribution partially overlaps that of adjacent cell-free regions (background, green), reflecting nuclear domains of negligible SGOL1 signal intensity among domains of higher intensity. In patient nuclei, the SGOL1 (K23E) intensity distribution does not overlap the background, showing that, in fibroblasts from three different patients, nuclear SGOL1 is reproducibly delocalized compared to three different controls, consistent with the more diffuse staining patterns observed.

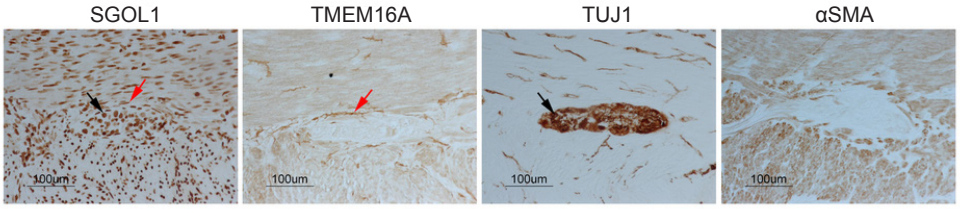

Figure S8: SGOL1 expression in normal human colon.

Quantitative analysis of the distribution of nuclear SGOL1 pixel intensities reveals altered SGOL1 organization in fibroblasts from homozygous CAID patients (red) compared to controls (blue). Data are the mean ± s.e.m. from 12 cells from 3 individuals per genotype. In control nuclei, the distribution partially overlaps that of adjacent cell-free regions (background, green), reflecting nuclear domains of negligible SGOL1 signal intensity among domains of higher intensity. In patient nuclei, the SGOL1 (K23E) intensity distribution does not overlap the background, showing that, in fibroblasts from three different patients, nuclear SGOL1 is reproducibly delocalized compared to three different controls, consistent with the more diffuse staining patterns observed.

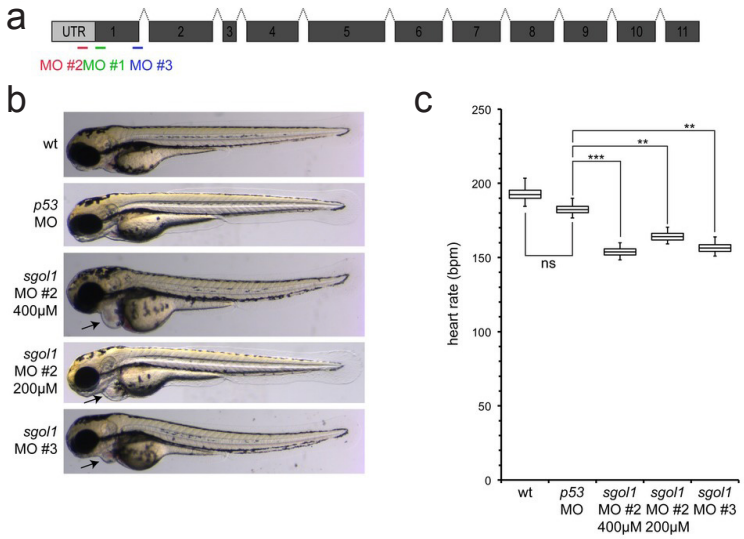

Figure S9: Antisense morpholino knockdown of *sgol1* analyzed at 3 d.p.f.

(a) Schematic of the morpholino target site location in the *sgol1* gene transcript. **(b)** Representative images of control and sgol1 morpholino-injected embryos (3 d.p.f.). Arrows point to cardiac edema. **(c)** Analysis of cardiac cycle length by high-speed video imaging (n = 15 per group). **P* < 0.05, ***P* < 0.01.

REFERENCES

BENSON, D. W., WANG, D. W., DYMENT, M., KNILANS, T. K., FISH, F. A., STRIEPER, M. J., RHODES, T. H. & GEORGE, A. L., JR. 2003. Congenital sick sinus syndrome caused by recessive mutations in the cardiac sodium channel gene (SCN5A). *J Clin Invest,* 112**,** 1019-28.

BOUCHARD, G., ROY, R., CASGRAIN, B. & HUBERT, M. 1989. [Population files and database management: the BALSAC database and the INGRES/INGRID system]. *Hist Mes,* 4**,** 39-57.

CABURET, S., ARBOLEDA, V. A., LLANO, E., OVERBEEK, P. A., BARBERO, J. L., OKA, K., HARRISON, W., VAIMAN, D., BEN-NERIAH, Z., GARCIA-TUNON, I., FELLOUS, M., PENDAS, A. M., VEITIA, R. A. & VILAIN, E. 2014. Mutant cohesin in premature ovarian failure. *N Engl J Med,* 370**,** 943-9.

CHOPRA, S. S., STROUD, D. M., WATANABE, H., BENNETT, J. S., BURNS, C. G., WELLS, K. S., YANG, T., ZHONG, T. P. & RODEN, D. M. 2010. Voltage-gated sodium channels are required for heart development in zebrafish. *Circ Res,* 106**,** 1342-50.

DE PATER, E., CLIJSTERS, L., MARQUES, S. R., LIN, Y. F., GARAVITO-AGUILAR, Z. V., YELON, D. & BAKKERS, J. 2009. Distinct phases of cardiomyocyte differentiation regulate growth of the zebrafish heart. *Development,* 136**,** 1633-41.

DEARDORFF, M. A., BANDO, M., NAKATO, R., WATRIN, E., ITOH, T., MINAMINO, M., SAITOH, K., KOMATA, M., KATOU, Y., CLARK, D., COLE, K. E., DE BAERE, E., DECROOS, C., DI DONATO, N., ERNST, S., FRANCEY, L. J., GYFTODIMOU, Y., HIRASHIMA, K., HULLINGS, M., ISHIKAWA, Y., JAULIN, C., KAUR, M., KIYONO, T., LOMBARDI, P. M., MAGNAGHI-JAULIN, L., MORTIER, G. R., NOZAKI, N., PETERSEN, M. B., SEIMIYA, H., SIU, V. M., SUZUKI, Y., TAKAGAKI, K., WILDE, J. J., WILLEMS, P. J., PRIGENT, C., GILLESSEN-KAESBACH, G., CHRISTIANSON, D. W., KAISER, F. J., JACKSON, L. G., HIROTA, T., KRANTZ, I. D. & SHIRAHIGE, K. 2012a. HDAC8 mutations in Cornelia de Lange syndrome affect the cohesin acetylation cycle. *Nature,* 489**,** 313-7.

DEARDORFF, M. A., WILDE, J. J., ALBRECHT, M., DICKINSON, E., TENNSTEDT, S., BRAUNHOLZ, D., MONNICH, M., YAN, Y., XU, W., GIL-RODRIGUEZ, M. C., CLARK, D., HAKONARSON, H., HALBACH, S., MICHELIS, L. D., RAMPURIA, A., ROSSIER, E., SPRANGER, S., VAN MALDERGEM, L., LYNCH, S. A., GILLESSEN-KAESBACH, G., LUDECKE, H. J., RAMSAY, R. G., MCKAY, M. J., KRANTZ, I. D., XU, H., HORSFIELD, J. A. & KAISER, F. J. 2012b. RAD21 mutations cause a human cohesinopathy. *Am J Hum Genet,* 90**,** 1014-27.

DEGLINCERTI, A., DE GIORGIO, R., CEFLE, K., DEVOTO, M., PIPPUCCI, T., CASTEGNARO, G., PANZA, E., BARBARA, G., COGLIANDRO, R. F., MUNGAN, Z., PALANDUZ, S., CORINALDESI, R., ROMEO, G., SERI, M. & STANGHELLINI, V. 2007. A novel locus for syndromic chronic idiopathic intestinal pseudo-obstruction maps to chromosome 8q23-q24. *Eur J Hum Genet,* 15**,** 889-97.

FLICEK, P., AMODE, M. R., BARRELL, D., BEAL, K., BRENT, S., CARVALHO-SILVA, D., CLAPHAM, P., COATES, G., FAIRLEY, S., FITZGERALD, S., GIL, L., GORDON, L., HENDRIX, M., HOURLIER, T., JOHNSON, N., KAHARI, A. K., KEEFE, D., KEENAN, S., KINSELLA, R., KOMOROWSKA, M., KOSCIELNY, G., KULESHA, E., LARSSON, P., LONGDEN, I., MCLAREN, W., MUFFATO, M., OVERDUIN, B., PIGNATELLI, M., PRITCHARD, B., RIAT, H. S., RITCHIE, G. R., RUFFIER, M., SCHUSTER, M., SOBRAL, D., TANG, Y. A., TAYLOR, K., TREVANION, S., VANDROVCOVA, J., WHITE, S., WILSON, M., WILDER, S. P., AKEN, B. L., BIRNEY, E., CUNNINGHAM, F., DUNHAM, I., DURBIN, R., FERNANDEZ-SUAREZ, X. M., HARROW, J., HERRERO, J., HUBBARD, T. J., PARKER, A., PROCTOR, G., SPUDICH, G., VOGEL, J., YATES, A., ZADISSA, A. & SEARLE, S. M. 2012. Ensembl 2012. *Nucleic Acids Res,* 40**,** D84-90.

FU, M., LUI, V. C., SHAM, M. H., PACHNIS, V. & TAM, P. K. 2004. Sonic hedgehog regulates the proliferation, differentiation, and migration of enteric neural crest cells in gut. *J Cell Biol,* 166**,** 673-84.

GABRIEL, S. B., SCHAFFNER, S. F., NGUYEN, H., MOORE, J. M., ROY, J., BLUMENSTIEL, B., HIGGINS, J., DEFELICE, M., LOCHNER, A., FAGGART, M., LIU-CORDERO, S. N., ROTIMI, C., ADEYEMO, A., COOPER, R., WARD, R., LANDER, E. S., DALY, M. J. & ALTSHULER, D. 2002. The structure of haplotype blocks in the human genome. *Science,* 296**,** 2225-9.

GARGIULO, A., AURICCHIO, R., BARONE, M. V., COTUGNO, G., REARDON, W., MILLA, P. J., BALLABIO, A., CICCODICOLA, A. & AURICCHIO, A. 2007. Filamin A is mutated in X-linked chronic idiopathic intestinal pseudo-obstruction with central nervous system involvement. *Am J Hum Genet,* 80**,** 751-8.

GILLIS, L. A., MCCALLUM, J., KAUR, M., DESCIPIO, C., YAEGER, D., MARIANI, A., KLINE, A. D., LI, H. H., DEVOTO, M., JACKSON, L. G. & KRANTZ, I. D. 2004. NIPBL mutational analysis in 120 individuals with Cornelia de Lange syndrome and evaluation of genotype-phenotype correlations. *Am J Hum Genet,* 75**,** 610-23.

GLESSNER, J. T., LI, J. & HAKONARSON, H. 2013. ParseCNV integrative copy number variation association software with quality tracking. *Nucleic Acids Res,* 41**,** e64.

GRAMLEY, F., LORENZEN, J., KOELLENSPERGER, E., KETTERING, K., WEISS, C. & MUNZEL, T. 2010. Atrial fibrosis and atrial fibrillation: the role of the TGF-beta1 signaling pathway. *Int J Cardiol,* 143**,** 405-13.

HEIJMAN, J., DEWENTER, M., EL-ARMOUCHE, A. & DOBREV, D. 2013. Function and regulation of serine/threonine phosphatases in the healthy and diseased heart. *J Mol Cell Cardiol,* 64**,** 90-8.

HOLM, H., GUDBJARTSSON, D. F., SULEM, P., MASSON, G., HELGADOTTIR, H. T., ZANON, C., MAGNUSSON, O. T., HELGASON, A., SAEMUNDSDOTTIR, J., GYLFASON, A., STEFANSDOTTIR, H., GRETARSDOTTIR, S., MATTHIASSON, S. E., THORGEIRSSON, G. M., JONASDOTTIR, A., SIGURDSSON, A., STEFANSSON, H., WERGE, T., RAFNAR, T., KIEMENEY, L. A., PARVEZ, B., MUHAMMAD, R., RODEN, D. M., DARBAR, D., THORLEIFSSON, G., WALTERS, G. B., KONG, A., THORSTEINSDOTTIR, U., ARNAR, D. O. & STEFANSSON, K. 2011. A rare variant in MYH6 is associated with high risk of sick sinus syndrome. *Nat Genet,* 43**,** 316-20.

INTERNATIONAL HAPMAP, C. 2003. The International HapMap Project. *Nature,* 426**,** 789-96.

ITAHANA, K., CAMPISI, J. & DIMRI, G. P. 2007. Methods to detect biomarkers of cellular senescence: the senescence-associated beta-galactosidase assay. *Methods Mol Biol,* 371**,** 21-31.

KLINE, A. D., KRANTZ, I. D., SOMMER, A., KLIEWER, M., JACKSON, L. G., FITZPATRICK, D. R., LEVIN, A. V. & SELICORNI, A. 2007. Cornelia de Lange syndrome: clinical review, diagnostic and scoring systems, and anticipatory guidance. *Am J Med Genet A,* 143A**,** 1287-96.

LABUDA, D., ZIETKIEWICZ, E. & LABUDA, M. 1997. The genetic clock and the age of the founder effect in growing populations: a lesson from French Canadians and Ashkenazim. *Am J Hum Genet,* 61**,** 768-71.

LABUDA, M., LABUDA, D., KORAB-LASKOWSKA, M., COLE, D. E., ZIETKIEWICZ, E., WEISSENBACH, J., POPOWSKA, E., PRONICKA, E., ROOT, A. W. & GLORIEUX, F. H. 1996. Linkage disequilibrium analysis in young populations: pseudo-vitamin D-deficiency rickets and the founder effect in French Canadians. *Am J Hum Genet,* 59**,** 633-43.

LAISH-FARKASH, A., GLIKSON, M., BRASS, D., MAREK-YAGEL, D., PRAS, E., DASCAL, N., ANTZELEVITCH, C., NOF, E., REZNIK, H., ELDAR, M. & LURIA, D. 2010. A novel mutation in the HCN4 gene causes symptomatic sinus bradycardia in Moroccan Jews. *J Cardiovasc Electrophysiol,* 21**,** 1365-72.

LI, H. & DURBIN, R. 2009. Fast and accurate short read alignment with Burrows-Wheeler transform. *Bioinformatics,* 25**,** 1754-60.

LI, H., HANDSAKER, B., WYSOKER, A., FENNELL, T., RUAN, J., HOMER, N., MARTH, G., ABECASIS, G., DURBIN, R. & GENOME PROJECT DATA PROCESSING, S. 2009. The Sequence Alignment/Map format and SAMtools. *Bioinformatics,* 25**,** 2078-9.

MACCLUER, J. W., VANDEBERG, J. L., READ, B. & RYDER, O. A. 1986. Pedigree Analysis by Computer-Simulation. *Zoo Biology,* 5**,** 147-160.

MILANESI, R., BARUSCOTTI, M., GNECCHI-RUSCONE, T. & DIFRANCESCO, D. 2006. Familial sinus bradycardia associated with a mutation in the cardiac pacemaker channel. *N Engl J Med,* 354**,** 151-7.

MOHLER, P. J., SCHOTT, J. J., GRAMOLINI, A. O., DILLY, K. W., GUATIMOSIM, S., DUBELL, W. H., SONG, L. S., HAUROGNE, K., KYNDT, F., ALI, M. E., ROGERS, T. B., LEDERER, W. J., ESCANDE, D., LE MAREC, H. & BENNETT, V. 2003. Ankyrin-B mutation causes type 4 long-QT cardiac arrhythmia and sudden cardiac death. *Nature,* 421**,** 634-9.

MOHLER, P. J., SPLAWSKI, I., NAPOLITANO, C., BOTTELLI, G., SHARPE, L., TIMOTHY, K., PRIORI, S. G., KEATING, M. T. & BENNETT, V. 2004. A cardiac arrhythmia syndrome caused by loss of ankyrin-B function. *Proc Natl Acad Sci U S A,* 101**,** 9137-42.

MOORMAN, A. F., HOUWELING, A. C., DE BOER, P. A. & CHRISTOFFELS, V. M. 2001. Sensitive nonradioactive detection of mRNA in tissue sections: novel application of the whole-mount in situ hybridization protocol. *J Histochem Cytochem,* 49**,** 1-8.

MUSIO, A., SELICORNI, A., FOCARELLI, M. L., GERVASINI, C., MILANI, D., RUSSO, S., VEZZONI, P.

& LARIZZA, L. 2006. X-linked Cornelia de Lange syndrome owing to SMC1L1 mutations. *Nat Genet,* 38**,** 528-30.

NOTARNICOLA, C., ROULEAU, C., LE GUEN, L., VIRSOLVY, A., RICHARD, S., FAURE, S. & DE SANTA BARBARA, P. 2012. The RNA-binding protein RBPMS2 regulates development of gastrointestinal smooth muscle. *Gastroenterology,* 143**,** 687-97 e1-9.

PURCELL, S., NEALE, B., TODD-BROWN, K., THOMAS, L., FERREIRA, M. A., BENDER, D., MALLER, J., SKLAR, P., DE BAKKER, P. I., DALY, M. J. & SHAM, P. C. 2007. PLINK: a tool set for whole-genome association and population-based linkage analyses. *Am J Hum Genet,* 81**,** 559-75.

RAJEEVAN, H., CHEUNG, K. H., GADAGKAR, R., STEIN, S., SOUNDARARAJAN, U., KIDD, J. R., PAKSTIS, A. J., MILLER, P. L. & KIDD, K. K. 2007. ALFRED: an allele frequency database for microevolutionary studies. *Evol Bioinform Online,* 1**,** 1-10.

RODRIGUEZ, R. D. & SCHOCKEN, D. D. 1990. Update on sick sinus syndrome, a cardiac disorder of aging. *Geriatrics,* 45**,** 26-30, 33-6.

ROULEAU, C., MATECKI, S., KALFA, N., COSTES, V. & DE SANTA BARBARA, P. 2009. Activation of MAP kinase (ERK1/2) in human neonatal colonic enteric nervous system. *Neurogastroenterol Motil,* 21**,** 207-14.

SCHMIDT, D., SCHWALIE, P. C., ROSS-INNES, C. S., HURTADO, A., BROWN, G. D., CARROLL, J. S., FLICEK, P. & ODOM, D. T. 2010. A CTCF-independent role for cohesin in tissue-specific transcription. *Genome Res,* 20**,** 578-88.

SCHULZE-BAHR, E., NEU, A., FRIEDERICH, P., KAUPP, U. B., BREITHARDT, G., PONGS, O. & ISBRANDT, D. 2003. Pacemaker channel dysfunction in a patient with sinus node disease. *J Clin Invest,* 111**,** 1537-45.

SEELOW, D., SCHUELKE, M., HILDEBRANDT, F. & NURNBERG, P. 2009. HomozygosityMapper--an interactive approach to homozygosity mapping. *Nucleic Acids Res,* 37**,** W593-9.

SIVA, N. 2008. 1000 Genomes project. *Nat Biotechnol,* 26**,** 256.

SUBIRANA, I., DIAZ-URIARTE, R., LUCAS, G. & GONZALEZ, J. R. 2011. CNVassoc: Association analysis of CNV data using R. *BMC Med Genomics,* 4**,** 47.

SUKEGAWA, A., NARITA, T., KAMEDA, T., SAITOH, K., NOHNO, T., IBA, H., YASUGI, S. & FUKUDA, K. 2000. The concentric structure of the developing gut is regulated by Sonic hedgehog derived from endodermal epithelium. *Development,* 127**,** 1971-80.

TESSADORI, F., VAN WEERD, J. H., BURKHARD, S. B., VERKERK, A. O., DE PATER, E., BOUKENS, B. J., VINK, A., CHRISTOFFELS, V. M. & BAKKERS, J. 2012. Identification and functional characterization of cardiac pacemaker cells in zebrafish. *PLoS One,* 7**,** e47644.

THISSE, C. & THISSE, B. 2008. High-resolution in situ hybridization to whole-mount zebrafish embryos. *Nat Protoc,* 3**,** 59-69.

THOMPSON, E. A. 2013. Identity by descent: variation in meiosis, across genomes, and in populations. *Genetics,* 194**,** 301-26.

VAN DER LELIJ, P., CHRZANOWSKA, K. H., GODTHELP, B. C., ROOIMANS, M. A., OOSTRA, A. B., STUMM, M., ZDZIENICKA, M. Z., JOENJE, H. & DE WINTER, J. P. 2010. Warsaw breakage syndrome, a cohesinopathy associated with mutations in the XPD helicase family member DDX11/ChlR1. *Am J Hum Genet,* 86**,** 262-6.

WESTERFIELD, M. 1995. A Guide for the Laboratory Use of Zebrafish (Danio rerio). *The Zebrafish Book*. 3rd ed. Eugene, OR: University of Oregon Press.

YAMAGISHI, Y., SAKUNO, T., SHIMURA, M. & WATANABE, Y. 2008. Heterochromatin links to centromeric protection by recruiting shugoshin. *Nature,* 455**,** 251-5.

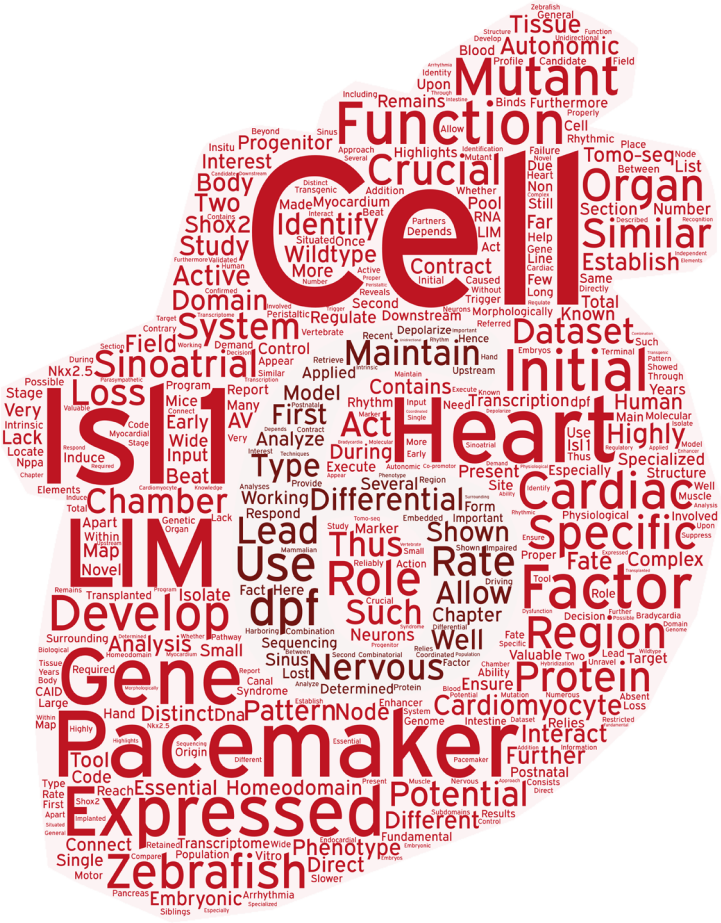
Cell
Heart
Pacemaker
Expressed
Zebrafish
Gene
Lim
Isl1
Develop
Factor
Function
Mutant
Organ
Tissue
Autonomic
Crucial
Identify
Similar
Initial
Dataset
Maintain
Sinoatrial
Loss
Chamber
Cardiac
Specific
Region
Protein
Nervous
Cardiomyocyte
Potential
Differentiation
Transcription
Progenitor
Myocardium
Wildtype
Contract
Regulate
Lead
Use
Role
Rate
Allow
Shown
Thus
Dpf
Shox2
Nkx2.5
Tbx5
Tomo-seq
Single-cell
Rna-seq

CHAPTER 6

General discussion

Silja Burkhard [1] and Jeroen Bakkers [1,2]

[1] Hubrecht Institute-KNAW and University Medical Center Utrecht, 3584 CT, Utrecht, The Netherlands.
[2] Department of Medical Physiology, Division of Heart and Lungs, University Medical Center Utrecht, 3584 CT Utrecht, The Netherlands.

During embryonic development, the heart is the first organ to develop. The fundamental function of the heart, to pump blood through the body is well conserved in the animal kingdom. Its mechanical activity relies upon contractile cardiac muscle cells. The cardiomyocytes act in a coordinated manner to achieve a wave of contraction to ensure unidirectional blood flow. In the simple linear heart tubes of invertebrates or early vertebrate embryos, cardiomyocyte contraction is sufficient to ensure the peristaltic heartbeat. In the morphologically more complex, chambered heart proper coordination of cardiac function relies on highly specialized cardiomyocytes, the pacemaker cells. Their intrinsic pacemaker potential enables them to rhythmically depolarize and trigger neighboring cardiomyocytes to contract and establish the basal heart rate.

The evolutionary appearance of complex organisms went hand in hand with the diversification of cell types. Highly specialized cells facilitate, control and direct the function of complex tissues and organs. They may stem from a completely different progenitor cell pool or even germ layer and reach their prospective location by migration. Nevertheless, many arise from the same common pool of progenitors as the tissue surrounding them. Their specialization is driven by differential gene expression. In the heart, the pacemaker cells are a small, highly specialized population of cardiomyocytes embedded in the myocardial wall that are crucial for cardiac function. Given the importance of cardiac function for any organism's survival, it is vital that the pacemaker cells execute their function properly. The failure of pacemaker cells to initiate or maintain proper heart beat frequency and regularity results in arrhythmia, an abnormal heart rhythm. In humans, arrhythmias caused by a malfunction of the sinus node pacemaker cells are grouped under the umbrella term sick sinus syndrome (SSS).

Zebrafish is one of the most widely used model organisms, especially in the field of embryogenesis and an excellent model to study cardiac development. Numerous discoveries initially made in zebrafish have highlighted fundamental aspects of vertebrate development that could be extrapolated to other organisms including humans. The physiological hallmarks of the zebrafish heart, such as heart rate, and electrophysiological parameters are very similar to their human counterparts. Here we made use of the zebrafish model to study the development and function of the cardiac pacemaker cells.

In **chapter 2** we report the initial molecular identification of the cardiac pacemaker cells in the zebrafish heart. The origin of cardiac contractions in the sinoatrial region of the zebrafish heart had been identified previously (Arrenberg et al., 2010) and the existence of a discrete pacemaker structure had been agreed upon. We identified expression of the LIM-homeodomain transcription factor Islet-1 as the first pacemaker

cell specific molecular marker in the zebrafish heart. The Isl1K88X mutant zebrafish displays a cardiac rhythm phenotype reminiscent of pacemaker failure (de Pater et al., 2009, Tessadori et al., 2012). At 2 dpf the mutant heart is beating significantly slower than in wildtype siblings. By 3 dpf the bradycardia worsens dramatically and the heart frequently stops for up to 20 seconds. The lack of Isl1 is lethal by 5 dpf. Thus, Isl1 is crucial for pacemaker cell function in zebrafish. In contrary to mice, who lack large parts of the heart, the Isl1 mutant zebrafish heart is morphologically normal. Either zebrafish are able to compensate for a loss of Isl1 activity during early heart development or the role of Isl1 in the zebrafish heart is limited to pacemaker development, explaining the highly specific mutant phenotype. SAN-specific knockout of Isl1 in mouse leads to bradycardia, similar to the phenotype in zebrafish mutants (Liang et al., 2015).

Isl1 is a transcription factor, well-known for its role in the development and function of endocrine cells in the pancreas and motor neurons in the spinal cord.

The Isl1 protein contains two major functional domains (Karlsson et al., 1990). The C-terminal homeodomain consists of a DNA binding motif present in many transcription factors. The homeodomain binds to the specific recognition site at the promotor of their target gene. A specific recognition site for Isl1 has not been identified yet. The N-terminal LIM domain consists of a tandem zinc finger domain structure mediating protein-protein interactions with other LIM-domain containing proteins (reviewed in (Hunter and Rhodes, 2005, Kadrmas and Beckerle, 2004)). Usually, several transcription factors and co-factors interact and form a complex at the promotor to regulate the expression of the targeted gene. This interaction between different LIM-homeodomain proteins is highly tissue and cell type specific. LIM-proteins are abundantly involved in tissue specification and patterning in progenitor cell populations during embryonic development. Depending on combinatorial expression of LIM-proteins and their co-factors, they activate distinct gene expression profiles driving the cell fate decision (Song et al., 2009, Ediger et al., 2014). Their role is especially well studied in neuronal development. The combinatorial expression of LIM-homeodomain transcription factors in specific neuronal subtypes has been referred to as the LIM-code. Isl1 is highly expressed in motor neurons and it has been shown that the interaction with LIM homeobox 3 (LHX3), another LIM-homeodomain protein, is essential for their development (Bhati et al., 2017). Little is known about the expression of other LIM-homeodomain proteins in the sinoatrial region of the heart. In zebrafish, there are more than 100 LIM-domain containing proteins. To identify potential interaction partners of Isl1 our tomo-seq dataset can help narrowing down the list of candidates to genes expressed sinoatrial region. We detected expression in the sinoatrial region for 36 LIM-domain-containing genes, pending further gene expression and functional analysis.

During early stages of heart development, Isl1 is expressed in cardiac progenitor cells in the second heart field. Once the progenitor cells differentiate into cardiomyocytes, expression of Isl1 is lost. Pacemaker cells are cardiomyocytes, originating from the second heart field. Whether the expression of Isl1 in pacemaker cells is maintained from progenitor cell stages or re-initiated later is unclear. Initially, all cardiomyocytes possess the potential to initiate action potentials independent of extracellular stimuli. Pacemaker cells become morphologically and functionally distinct from the surrounding myocardium. The identification of Isl1 as a molecular marker allowed us to isolate and analyze the pacemaker cells in detail. In fact, Isl1 has a crucial role in maintaining pacemaker cell function. Isl1 remains expressed in the adult pacemaker cells, highlighting that the role of Isl1 reaches beyond the initial cell fate decision. Contrary to the compact sinoatrial node structure harboring the pacemaker cells in the mammalian heart, zebrafish pacemaker cells form a ring around the sinoatrial junction, embedded at the base of the venous valves.
A central question remains: Are pacemaker cells actively triggered to execute a genetic pacemaker cell program and what is the initiating factor? Or are they prevented from differentiating further into working cardiomyocytes, retaining their initial pacemaker potential? Could Isl1 be the crucial factor in the cell fate decision? It will be interesting to analyze the $Isl1^{+}$ pacemaker cells in the $Isl1^{-/-}$ mutant. If Isl1 suppresses cardiomyocyte differentiation, mutant pacemaker cells might differentiate into chamber working cardiomyocytes. We showed an expansion of expression of *nppa*, a gene expressed in the chamber myocardium. Nkx2.5 is a crucial factor driving differentiation in chamber cardiomyocytes but is absent from the sinoatrial region. Isl1 and *nkx2.5* are considered the main cell fate and patterning factors in pacemaker cells and working cardiomyocytes. We speculate that a loss of Isl1 in the $Isl1^{-/-}$ mutant leads to ectopic expression of *nkx2.5* in the pacemaker cells, leading them to differentiate into working cardiomyocytes.

In **chapter 3** we showed that the pacemaker cells are still present in the heart of $Isl1^{-/-}$ embryos and that the total number of cardiomyocytes is unchanged. Thus, the bradycardia and arrhythmia phenotype is not due to a loss of the pacemaker cells but a deficiency in the initiation and maintenance of the pacemaker cell potential, placing Isl1 upstream of the “pacemaker gene program”. Two genes expressed in the sinoatrial region but absent in the chamber myocardium, *tbx2b* and *bmp4*, are lost specifically in the sinoatrial region of $Isl1^{-/-}$ embryonic hearts. Furthermore, expression of *nppa,* a gene specifically expressed in the working chamber myocardium was expanded posteriorly in the $Isl1^{-/-}$ mutant heart. We hypothesize that a loss of Isl1 expression in the pacemaker cells leads to differentiation into chamber cardiomyocytes and loss of pacemaker function. A similar essential requirement for maintaining postnatal

Isl1 expression to preserve the cell type specific function has been described in mammalian pancreatic b-cells. Specifically in the postnatal pancreas, Isl1 directly induced expression of Pdx1, a transcription factor essential for maintaining b-cell function. Loss of Isl1 in postnatal b-cells lead to impaired b-cell function without altering cell numbers (Ediger et al., 2014). Thus, a situation similar to the phenotype we observed in Isl1$^{-/-}$ pacemaker cells in the zebrafish. Hence, a general course of action of Isl1 to suppress further cellular differentiation and maintain the highly specialized cell function postnatally is not restricted to cardiac pacemaker cells. Thus far, only very few downstream targets of Isl1 have been identified in cardiac pacemaker cells. It remains to be determined whether Isl1 induces the expression of a yet unknown crucial pacemaker cell determinant.

In Isl1$^{-/-}$ embryonic hearts, the pacemaker cells appear morphologically similar to wildtype siblings. Total numbers and localization in the sinoatrial region resemble the wildtype situation as wells. Hence, Isl1 is not required for pacemaker cell specification but essential for pacemaker cell function. But how is Isl1 expression restricted to and regulated in pacemaker cells? Shox2 is an essential factor in the determination of sinoatrial node cell identity in mice, acting directly upstream of Isl1 (Hoffmann et al., 2013). In zebrafish *shox2* is expressed in the sinoatrial region. Furthermore, a knockdown of *shox2* leads to a slower heart rate (Hoffmann et al., 2013). It remains to be determined whether Shox2 might have a crucial role in zebrafish pacemaker cells by acting on or upstream of Isl1.

In recent years, increasing effort has been directed to the regulation of gene expression by non-coding elements such as enhancers. We have shown that expression of isl1 in embryonic pacemaker cells depends on regulatory elements situated within a 180kb stretch of genomic DNA downstream of the Isl1 locus. It has long been acknowledged that enhancer elements are involved in fine-tuning the spatio-temporal gene expression. However, it remains challenging to identify active enhancers acting on a gene of interest. Apart from the noticeable absence of Isl1-GFP in the pacemaker cells, the overall expression pattern of Isl1 in the two transgenic lines reveals several other distinct differences. This highlights the importance of the non-coding regulatory landscape on the expression of a gene and should not be left out of consideration when establishing transgenic reporter constructs.

The small number of pacemaker cells is the main impediment in applying any large-scale gene expression analysis. In **chapter 4** we applied the tomo-seq method on isolated embryonic hearts. By combination of cryo-sectioning and RNA sequencing, we have established a spatially resolved transcriptome map of the 2 dpf zebrafish heart. We could reliably locate the different anatomical domains of the developing heart by using expression patterns of known cardiac marker gene such as chamber-

specific myosins *vmhc* and *myh6*.
The sinoatrial region was identified by expression of *isl1*, *shox2* and other genes known to be expressed in the pacemaker domain. Tomo-seq allows us to retrieve genome-wide expression information without prior cell isolation. Furthermore, the entire transcriptome information is retained, allowing for unbiased gene expression analysis of a region of interest. The established transcriptome map provides the unique opportunity to elucidate the cardiac expression patterns of thousands of genes. Filtering the transcriptome dataset for genes with a similar expression pattern as a gene of interest is a valuable tool to identify possible genetic interaction partners. Furthermore, we were able to analyze the transcriptome of distinct subdomains within the heart, such as the chambers, AV canal and sinoatrial region. Gene expression enrichment analyses revealed novel pathways involved in the patterning of the subdomains. We retrieved multiple lists of candidate genes and validated their expression patterns by in-situ hybridization confirming the reliability of the dataset. On top of the 2 dpf wildtype dataset, a similar analysis of mutant hearts, such as the Isl1$^{-/-}$ mutant, would be a valuable addition, permitting genome-wide, comparative expression analyses.
Recently, numerous studies have used RNA sequencing techniques to analyze gene expression (DeLaughter et al., 2016, Li et al., 2016, Vedantham et al., 2015). Especially the single cell sequencing approaches might be a valuable addition to our tomo-seq dataset. However, they have so far only been applied for other organisms, not the zebrafish pacemaker cells. We used a section thickness of 10mm. Each section contains approximately 10 cells of the different cardiac cell types. Thus, we cannot distinguish between the e.g. myocardial or endocardial cells. This distinction requires additional experimental expression analysis, as shown for several candidate genes expressed in the AV canal sections. *pdgfaa* and *anxa5b* are expressed in the endocardial cushion and not in the myocardium as shown by in situ hybridization. Comparison of the tomo-seq dataset presented here with a single cell sequencing dataset on cardiomyocytes of the same stage would help in pinpointing the cell type identity and homogeneity.
Mechanistically, we uncovered and confirmed a novel role for the wnt/b-catenin signaling pathway in pacemaker cell function. More specifically in the ability of the cells to respond to input from the parasympathetic nervous system. The autonomic nervous system has a crucial role in controlling heart rate. While the rhythmic depolarization of the pacemaker cells dictate the baseline heart rate, it can vary greatly depending on the bodies physiological demand. Input from both the sympathetic and parasympathetic nervous system constantly controls and manipulates heart rate. Thus, apart from their ability to spontaneously and independently depolarize, pacemaker cells also need to connect to and communicate with the autonomic

nervous system. Knowledge of how pacemaker cells properly connect to the autonomic nervous system will be crucial for any therapeutic approach using in vitro engineered pacemaker cells to replace dysfunctional native pacemaker cells. Promising results from generating functional pacemaker cells from iPS cells or cardiac progenitors have shown that it is feasible to induce pacemaker potential in vitro (Protze et al., 2017, Zhang et al., 2017). These cells were able to function as pacemaker cells after implantation in pig or rat hearts. However, the measured heart rates were lower than in healthy hearts and they could not respond to the physiological demand of the body due to a lack of connection to the autonomic nervous system. For a biological pacemaker approach to be favorable over the current standard treatment using implanted electrical pacemakers, the ability to adapt and respond to the physiological demand of the body is essential. It has been shown that transplanted hearts are initially impaired in their response to autonomic input because the nervous connections have been severed. However, within the first 2 years post-transplantation the heart, including the sinus node is re-innervated by nerves from the autonomic nervous system, allowing direct regulation of the transplanted heart's function (Grupper et al., 2017). Thus, as long as transplanted pacemaker cells are able to respond to autonomic input, they are likely able to integrate in to the host autonomic nervous system - pacemaker structure. Further knowledge of how the connection with the autonomic nervous system is established and maintained in pacemaker cells will be beneficial for the generation of biological pacemakers.

The cardiac pacemaker cells are not the only cells harboring intrinsic pacemaker potential. The rhythmic peristaltic contractions of the muscle cells surrounding the intestine ensure a unidirectional passage of food through the digestive system. In **chapter 5** we introduced a novel human syndrome called Chronic Atrial and Intestinal Dysrhythmia (CAID) affecting heart and gut rhythm (Chetaille et al., 2014). CAID syndrome is a cohesinopathy and caused by a mutation in Shugoshin-like 1 (*sgol1*), a member of the cohesion complex. This collaborative study highlights an application of zebrafish as a model for functional validation of human phenotypes. Furthermore, the combination of specific pacemaker dysfunction phenotypes in two very different organs, the cardiovascular and intestinal systems, implies that basic functionality of pacemaker cells is similar.

Tomo-seq can be applied to any tissue of interest. The established 2 dpf wildtype dataset which apart from the direct analysis described in **chapter 4** may also serve as a reference to compare to mutant datasets. Similar gene expression maps of mutant hearts will allow us to assess the effect of single gene mutations on the

total transcriptome of the heart. Especially in combination with precise gene editing techniques such as CRISPR/Cas9, tomo-seq will be a valuable tool in the analysis of mutant phenotypes in and beyond the field of cardiac research.

Further analysis of the cardiac pacemaker cells and their development will certainly also benefit from single cell sequencing data on embryonic cardiomyocytes and isolated pacemaker cells. The fact that the Isl1^{+} pacemaker cells are still present in the Isl1$^{-/-}$ mutant heart and the possibility to visualize them in the transgenic reporter line will allow us to analyze their gene expression profile. Discrepancies in gene expression between wildtype and Isl1$^{-/-}$ pacemaker cells will indicate putative effectors downstream of Isl1. If our hypothesis is correct, and the Isl1$^{-/-}$ pacemaker cells fail to execute the pacemaker gene program downstream of Isl1, we might be able to unravel how Isl1 initiates/maintains the pacemaker potential in these cells.

In the last few years we gained insight into the function and regulation of Isl1. This will provide us with the tools needed and suggest possible strategies to further unravel how exactly a small population of cells manages to develop and maintain such a fundamentally important function; the beating heart that to keeps us alive. Yet, only once we know how something was built in the first place, will we ever be able to repair it.

REFERENCES

ARRENBERG, A. B., STAINIER, D. Y., BAIER, H. & HUISKEN, J. 2010. Optogenetic control of cardiac function. *Science,* 330**,** 971-4.

BHATI, M., LLAMOSAS, E., JACQUES, D. A., JEFFRIES, C. M., DASTMALCHI, S., RIPIN, N., NICHOLAS, H. R. & MATTHEWS, J. M. 2017. Interactions between LHX3- and ISL1-family LIM-homeodomain transcription factors are conserved in Caenorhabditis elegans. *Sci Rep,* 7**,** 4579.

CHETAILLE, P., PREUSS, C., BURKHARD, S., COTE, J. M., HOUDE, C., CASTILLOUX, J., PICHE, J., GOSSET, N., LECLERC, S., WUNNEMANN, F., THIBEAULT, M., GAGNON, C., GALLI, A., TUCK, E., HICKSON, G. R., EL AMINE, N., BOUFAIED, I., LEMYRE, E., DE SANTA BARBARA, P., FAURE, S., JONZON, A., CAMERON, M., DIETZ, H. C., GALLO-MCFARLANE, E., BENSON, D. W., MOREAU, C., LABUDA, D., CONSORTIUM, F. C., ZHAN, S. H., SHEN, Y., JOMPHE, M., JONES, S. J., BAKKERS, J. & ANDELFINGER, G. 2014. Mutations in SGOL1 cause a novel cohesinopathy affecting heart and gut rhythm. *Nat Genet,* 46**,** 1245-9.

DE PATER, E., CLIJSTERS, L., MARQUES, S. R., LIN, Y. F., GARAVITO-AGUILAR, Z. V., YELON, D. & BAKKERS, J. 2009. Distinct phases of cardiomyocyte differentiation regulate growth of the zebrafish heart. *Development,* 136**,** 1633-41.

DELAUGHTER, D. M., BICK, A. G., WAKIMOTO, H., MCKEAN, D., GORHAM, J. M., KATHIRIYA, I. S., HINSON, J. T., HOMSY, J., GRAY, J., PU, W., BRUNEAU, B. G., SEIDMAN, J. G. & SEIDMAN, C. E. 2016. Single-Cell Resolution of Temporal Gene Expression during Heart Development. *Dev Cell,* 39**,** 480-490.

EDIGER, B. N., DU, A., LIU, J., HUNTER, C. S., WALP, E. R., SCHUG, J., KAESTNER, K. H., STEIN, R., STOFFERS, D. A. & MAY, C. L. 2014. Islet-1 Is essential for pancreatic beta-cell function. *Diabetes,* 63**,** 4206-17.

GRUPPER, A., GEWIRTZ, H. & KUSHWAHA, S. 2017. Reinnervation post-Heart transplantation. *Eur Heart J*.

HOFFMANN, S., BERGER, I. M., GLASER, A., BACON, C., LI, L., GRETZ, N., STEINBEISSER, H., ROTTBAUER, W., JUST, S. & RAPPOLD, G. 2013. Islet1 is a direct transcriptional target of the homeodomain transcription factor Shox2 and rescues the Shox2-mediated bradycardia. *Basic Res Cardiol,* 108**,** 339.

HUNTER, C. S. & RHODES, S. J. 2005. LIM-homeodomain genes in mammalian development and human disease. *Mol Biol Rep,* 32**,** 67-77.

KADRMAS, J. L. & BECKERLE, M. C. 2004. The LIM domain: from the cytoskeleton to the nucleus. *Nat Rev Mol Cell Biol,* 5**,** 920-31.

KARLSSON, O., THOR, S., NORBERG, T., OHLSSON, H. & EDLUND, T. 1990. Insulin gene enhancer binding protein Isl-1 is a member of a novel class of proteins containing both a homeo- and a Cys-His domain. *Nature,* 344**,** 879-82.

LI, G., XU, A., SIM, S., PRIEST, J. R., TIAN, X., KHAN, T., QUERTERMOUS, T., ZHOU, B., TSAO, P. S., QUAKE, S. R. & WU, S. M. 2016. Transcriptomic Profiling Maps Anatomically Patterned Subpopulations among Single Embryonic Cardiac Cells. *Dev Cell,* 39**,** 491-507.

LIANG, X., ZHANG, Q., CATTANEO, P., ZHUANG, S., GONG, X., SPANN, N. J., JIANG, C., CAO, X., ZHAO, X., ZHANG, X., BU, L., WANG, G., CHEN, H. S., ZHUANG, T., YAN, J., GENG, P., LUO, L., BANERJEE, I., CHEN, Y., GLASS, C. K., ZAMBON, A. C., CHEN, J., SUN, Y. & EVANS, S. M. 2015. Transcription factor ISL1 is essential for pacemaker development and function. *J Clin Invest,* 125**,** 3256-68.

PROTZE, S. I., LIU, J., NUSSINOVITCH, U., OHANA, L., BACKX, P. H., GEPSTEIN, L. & KELLER, G. M. 2017. Sinoatrial node cardiomyocytes derived from human pluripotent cells function as a biological pacemaker. *Nat Biotechnol,* 35**,** 56-68.

SONG, M. R., SUN, Y., BRYSON, A., GILL, G. N., EVANS, S. M. & PFAFF, S. L. 2009. Islet-to-LMO stoichiometries control the function of transcription complexes that specify motor neuron and V2a interneuron identity. *Development,* 136**,** 2923-32.

TESSADORI, F., VAN WEERD, J. H., BURKHARD, S. B., VERKERK, A. O., DE PATER, E., BOUKENS, B. J., VINK, A., CHRISTOFFELS, V. M. & BAKKERS, J. 2012. Identification and functional characterization of cardiac pacemaker cells in zebrafish. *PLoS One,* 7**,** e47644.

VEDANTHAM, V., GALANG, G., EVANGELISTA, M., DEO, R. C. & SRIVASTAVA, D. 2015. RNA sequencing of mouse sinoatrial node reveals an upstream regulatory role for Islet-1 in cardiac pacemaker cells. *Circ Res,* 116**,** 797-803.

ZHANG, L., LI, X., YU, X., LI, Y., SUN, A., HUANG, C., XU, F., GUO, J., SUN, Y., ZHANG, X., YANG, X. & ZHANG, C. 2017. Construction of vascularized pacemaker tissues by seeding cardiac progenitor cells and endothelial progenitor cells into Matrigel. *Life Sci,* 179**,** 139-146.

6

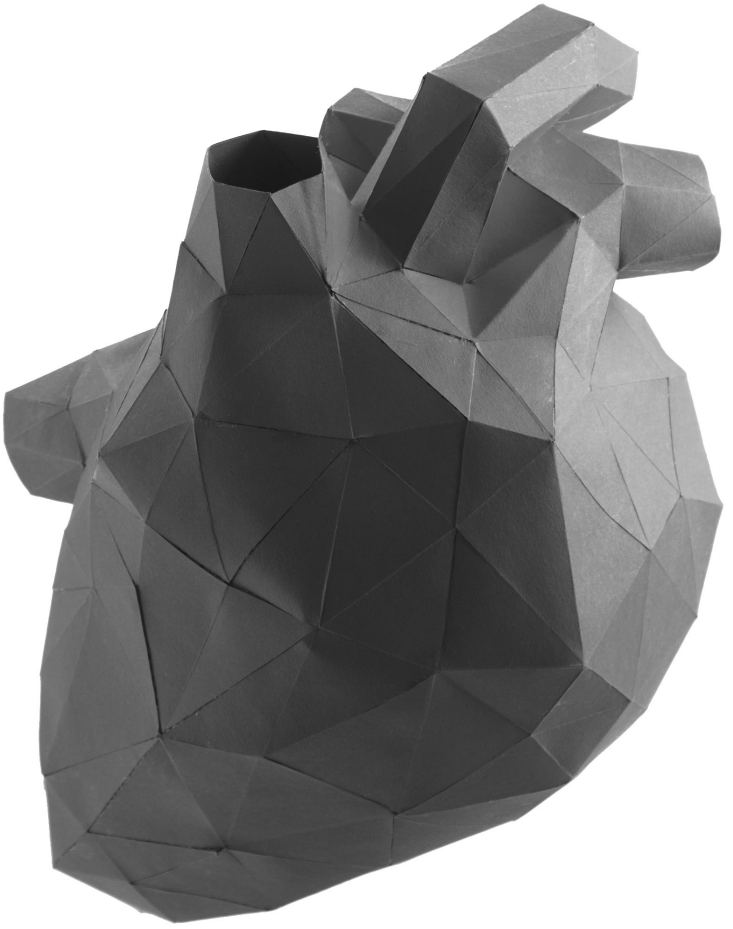

ADDENDUM

Nederlandse samenvatting

Deutsche Zusammenfassung

Acknowledgements

List of publications

Curriculum vitae

&

&

NEDERLANDSE SAMENVATTING

Een mensenhart klopt gemiddeld 90000 keer per dag. Met elke hartslag pompt het hart bloed door het lichaam om alle organen van zuurstof en voedingsstoffen te voorzien. Het hart vervult zijn rol continu en betrouwbaar, een heel leven lang. Het is zelfs zo dat onze definitie van het leven is gebaseerd op het kloppende hart.
Het hart zelf is een spier. Het bestaat uit vier holle kamers (twee boezems en twee hartkamers) waar het bloed doorheen gepompt kan worden. In vergelijking tot hun omgeving hebben de inactieve spiercellen een negatieve elektrische lading. Als gevolg van een elektrische prikkel, bijvoorbeeld vanuit het zenuwstelsel, reageren de spiercellen met een mechanische contractie. Dit betekent dat ze zichzelf samentrekken. Als dit gebeurt in het spierweefsel van bijvoorbeeld de biceps in de bovenarm, dan verkort de hele spier zich. De spier trekt dan aan de onderarm en zorgt ervoor dat de arm zich buigt bij de ellenboog. In het hart zorgt een zeer gecoördineerde spiercontractie voor een verkorting van de hartspierwand. Het bloed wordt hierdoor van de boezems naar de hartkamers gepompt en vervolgens door het hele lichaam. Maar in tegenstelling tot de skeletspieren is de hartspier niet afhankelijk van prikkels vanuit de hersenen om samen te trekken. Het hart vervult zijn rol compleet onafhankelijk. Het elektrische signaal van het hart start in de sinusknoop, die zich rechts bovenin de rechter boezemwand bevindt. De sinusknoop bestaat uit een groep gespecialiseerde cellen, de pacemakercellen van het hart.
De pacemakercellen zijn ook hartspiercellen, maar ze hebben de unieke eigenschap dat ze zelf elektrische prikkels kunnen produceren. Men denkt dat dit kan door speciale ion-kanalen en ion-pompen op het celoppervlak. De ritmisch geproduceerde elektrische prikkels worden vanuit de pacemakercellen doorgegeven aan de omliggende normale hartspiercellen. Dit zet ze aan om samen te trekken. Deze spiercontractie verplaatst zich vervolgens over het hele hart, wat ervoor zorgt dat het hart klopt. Eerst trekken de boezems samen, waarmee het bloed van de boezems naar de hartkamers gepompt wordt. Dan trekken de hartkamers samen, waarmee het bloed naar de longen en naar de rest van het lichaam gepompt wordt. De pacemakercellen bepalen het basis-hartritme. Afhankelijk van wat het lichaam nodig heeft, bijvoorbeeld meer zuurstof tijdens het sporten, kan de hartslagfrequentie worden aangepast. Verschillende zenuwuiteinden van het zogenaamde autonome zenuwstelsel bevinden zich rond de sinusknoop. Deze uiteinden geven signaalstoffen af die direct via de pacemakercellen de hartslagfrequentie kunnen beïnvloeden. In dit proefschrift hebben we de moleculaire basis en ontwikkeling van de pacemakercellen van het hart bestudeerd.
De pacemakercellen bevinden zich bij de ingang van het hart, waar de aders aangesloten zitten en het bloed het hart binnenstroomt. Deze locatie is goed

geconserveerd tussen mensen, veel zoogdieren en veel andere dieren. In hoofdstuk 1 geven we een overzicht van de evolutionaire oorsprong van de pacemakercellen. We kijken naar bekende (moleculaire) factoren in pacemakercelontwikkeling bij verschillende organismen. De fundamentele functie en regulatie van pacemakercellen vertoont ook grote gelijkenis tussen diverse groepen diersoorten.
Wij gebruiken de zebravis (Danio rerio) om hart- en pacemakercelontwikkeling te bestuderen. Zebravissen zijn kleine tropische zoetwatervissen en sinds 1980 is de zebravis een bekend modeldier voor het bestuderen van de ontwikkeling en genetica van gewervelde dieren. Ze zijn makkelijk om te houden in een laboratorium en produceren veel nakomelingen. Het zebravisembryo ontwikkelt zich binnen een paar dagen tot een compleet visje, buiten het lichaam van de moeder. Daarnaast zijn zebravisembryo's bijna geheel transparant. Hierdoor is het erg makkelijk om de vorm en de functie van organen, zoals het ontwikkelende hart, met eenvoudige instrumenten te bekijken. Ongeveer 2 dagen na bevruchting is het embryonale hart volledig functioneel. In tegenstelling tot het zoogdierhart dat uit 4 kamers bestaat, bestaat het zebravishart uit slechts 2 kamers: één boezem en één hartkamer. De boezem en de hartkamer worden gescheiden door hartkleppen. Er is al een ritmische hartslag in het embryonale hart. Deze hartslag begint bij de ingang van de boezem. De hartslagfrequentie is ongeveer 180-200 slagen per minuut.
In hoofdstuk 2 beschrijven we als eerste onderzoeksgroep de identificatie van de pacemakercellen in het zebravishart. We toonden aan dat één specifiek gen alleen actief is in de pacemakercellen, maar niet in de andere cellen van het hart. Om de activiteit van dit gen te visualiseren hebben we het gelabeld met een fluorescent eiwit. Wanneer het gen actief is, zorgt het fluorescente eiwit ervoor dat de hele cel groen licht geeft. Hiermee konden we de pacemakercellen herkennen en isoleren. Door de karakteristieke elektrische signalen van deze geïsoleerde cellen te meten, konden we bewijzen dat het inderdaad pacemakercellen waren. Ook konden we voor het eerst de structuur en locatie van de pacemakercellen in de zebravis aantonen. In tegenstelling tot het zoogdier hart, zitten de zebravispacemakercellen niet in een compacte sinusknoop, maar vormen ze een losse ring om de ingang de boezem. Het moet nog vastgesteld worden of deze ring een evolutionaire voorloper is van de compacte sinusknoop en of de ring ook in andere gewervelden voorkomt.
Het gen dat we geïdentificeerd hebben is Islet-1. Naast de pacemakercellen is het gen ook actief in specifieke andere delen van het lichaam. Het eiwit waarvoor Islet-1 codeert is een bekende transcriptie factor. Dit houdt in dat het andere genen activeert en beïnvloedt. Dat wordt voornamelijk bewerkstelligd door directe binding van het eiwit aan de DNA-streng. Elke cel wordt onder andere gekarakteriseerd door de genen die actief en inactief zijn. Dit betekent dat transcriptie factoren een erg speciale rol hebben. We tonen aan dat een defect in de Islet-1 gensequentie

resulteert in een verkeerd, inactief eiwit in de cel en een ernstige verstoring van het hartritme veroorzaakt. Zebravissen met deze Islet-1 mutatie hebben een sterke bradycardie, een zeer lage hartslag. De symptomen verergeren over de tijd en uiteindelijk zijn er periodes waarin het hart compleet stil ligt. We zagen pauzes in de hartslag die tot wel 20 seconden aanhielden. De embryo's overleven het tot 5 dagen na bevruchting. Het defect in hartslagfrequentie en het feit dat de activiteit van Islet-1 beperkt is tot specifieke cellen, toonde aan dat Islet-1 een essentiële rol heeft in de ontwikkeling van de pacemakercellen.

In hoofdstuk 3 hebben we de rol van Islet-1 verder geanalyseerd. We laten zien dat de pacemakercellen nog aanwezig zijn op de normale locatie, ondanks het verlies van Islet-1 functie. Dus het hartritmedefect dat we zagen, komt niet doordat de pacemakercellen verdwenen zijn. In plaats daarvan lijken de pacemakercellen niet in staat om hun functie vast te leggen en vast te houden. We hebben verschillende genen kunnen identificeren die niet geactiveerd worden wanneer Islet-1 afwezig is. Daarom nemen we aan dat die genen aangestuurd worden door Islet-1. Hun rol, en de rol van andere factoren, in de ontwikkeling van pacemakercellen moet nog onderzocht worden. Verder konden we aantonen dat het hart van de volwassen zebravis aangestuurd wordt door veel zenuwuiteinden. We nemen aan dat dit zenuwuiteinden zijn van het autonome zenuwstelsel.

In hoofdstuk 4 gebruiken we een recent ontwikkelde techniek waarmee het mogelijk is om de activiteit en locatie van alle genen in een weefsel te analyseren. Deze techniek staat bekend als tomo-sequencing (tomo-seq). Het weefsel of orgaan, in dit geval het hart van een zebravisembryo, wordt in hele dunne plakjes gesneden. De volgorde van de plakjes gemarkeerd, waardoor er geen ruimtelijke informatie verloren gaat en het mogelijk is om een virtuele reconstructie van het weefsel of orgaan te maken. Dit lijkt op de klassieke tomografie techniek. Vervolgens wordt het genetische materiaal uit de plakjes geïsoleerd en geanalyseerd. Hiermee kunnen we de activiteit van individuele genen bepalen. Als een gen actief is in een cel, worden er kopieën gemaakt van de DNA-sequentie van het gen. Deze kopieën, de zogenaamde boodschapper of messenger RNAs (mRNAs), kunnen worden vertaald in een eiwit. mRNAs bevatten het bouwplan van een specifiek eiwit. Ze zijn niet erg stabiel en worden binnen een korte tijd afgebroken. Als een mRNA aanwezig is in de cel, kun je dus concluderen dat de DNA-sequentie (het gen), waar het mRNA van gekopieerd is, actief is op dat moment. Daarnaast geeft de hoeveelheid mRNA een indicatie van hoeveel eiwit er nodig is in de cel. Belangrijke eiwitten worden vaak in grote hoeveelheden en in hoge frequentie aangemaakt en hun mRNA is vaak ook in grote hoeveelheden aanwezig. De som van al het mRNA dat wordt geproduceerd door de cel noemen we het transcriptoom. We hebben het aantal mRNAs in elk individueel plakje van het embryonaal hart kunnen vaststellen.

Twee dagen na bevruchting is het embryonale zebravishart een S-vormige buis. De ontwikkelende kamers kunnen al worden onderscheiden. Nadat we een hart hadden geïsoleerd uit een embryo, hebben we het in plakjes gesneden van het ene eind van de buis naar het andere eind van de buis. Omdat we de volgorde van de plakjes wisten, konden we de gen-activiteit koppelen aan een locatie in het hart. Daardoor konden we als eerste onderzoeksgroep een gedetailleerde kaart maken van de activiteit van alle genen in het embryonale zebravishart, met een hoge ruimtelijke resolutie. Dit bleek een erg goede bron van informatie te zijn om specifieke delen van het hart te kunnen analyseren. We konden bijvoorbeeld verschillende genen identificeren die alleen actief zijn in de boezem óf de hartkamer. Daarnaast konden we aantonen dat de belangrijke zogenaamde wnt signalering actief is in de pacemakercellen. Bij verdere analyse zijn we erachter gekomen dat deze wnt signalering nodig is voor de controle die het autonome zenuwstelsel heeft op de hartslag. Als de wnt signalering niet actief is, reageert het hart minder op het autonome zenuwstelsel. De hartslagfrequentie is dan permanent verhoogt.
In hoofdstuk 5 beschrijven we de ontdekking van een nieuw syndroom. Patiënten met het syndroom hebben symptomen die karakteristiek zijn voor defecte pacemakercellen. Dit syndroom, bekend als CAID (“Chronic Atrial and Intestinal Dysrhythmia”, of in het Nederlands “Chronische ritmestoornissen van hartboezem en darm”) werd voor het eerst ontdekt in een kleine groep patiënten in Canada. De patiënten hebben een erg lage en onregelmatige hartslag, en daarom is er een kunstmatige pacemaker bij hen geïmplanteerd. Daarnaast maken hun darmen weinig tot geen peristaltische bewegingen. Dit betekent dat er geen eten door de darmen vervoert kan worden en dat de patiënten permanent afhankelijk zijn van voeding via een infuus. Met behulp van een genetische analyse, konden we aantonen dat een kleine fout in de genetische sequentie van het SGOL1-gen het CAID syndroom veroorzaakt. De symptomen van de patiënten konden we ook zien in zebravissen waarbij het Sgol1-gen was uitgeschakeld, en we zagen dus een relatie tussen oorzaak en gevolg. Een combinatie van hart- en darmsymptomen lijkt in eerste instantie verassend, maar beide organen zijn functioneel afhankelijk van interne, onafhankelijke pacemaker systemen. De exacte rol en het precieze effect van Sgol1 blijven onduidelijk. Desondanks denken we dat Sgol1 direct de basisfunctie van pacemakercellen beïnvloedt en dat dit de reden is dat een genetisch defect in Sgol1 een effect heeft op hart- en darmfunctie.
In het laatste hoofdstuk, hoofdstuk 6, eindigen we met een algemene discussie. We discussiëren over de resultaten die we in dit proefschrift presenteren en we bekijken ze in een bredere context.

(Vertaald door Lotte Koopman & Melanie Laarman)

DEUTSCHE ZUSAMMENFASSUNG

Das Herz eines Menschen schlägt im Durchschnitt neunzigtausend Mal pro Tag. Mit jedem Herzschlag pumpt es Blut durch den Körper, um damit alle anderen Organe und Gewebe mit Sauerstoff und wichtigen Nährstoffen zu versorgen. Es erfüllt diese Rolle fortwährend und zuverlässig, ein Leben lang. Nicht zuletzt deshalb steht das schlagende Herz absolut zentral in unserer Definition von Leben.
Das Herz an sich ist ein Muskel. Es besteht aus vier hohlen Kammern, durch die das Blut gepumpt werden kann. Muskelzellen sind im Ruhezustand im Vergleich zu ihrer Umgebung elektrisch negativ aufgeladen. Verändert sich dieser Zustand nun durch ein elektrisches Signal von außen, zum Beispiel durch einen Impuls des Nervensystems, reagieren die Muskelzellen darauf mit einer mechanischen Kontraktion. Das heißt, sie ziehen sich zusammen. Geschieht dies beispielsweise im Muskelgewebe des Armbeugemuskels (Bizeps), so verkürzt sich der gesamte Muskel, übt Zug auf den Unterarm aus und beugt so den Arm am Ellenbogengelenk. Im Falle des Herzens ermöglicht eine hochgradig koordinierte Muskelkontraktion, dass sich die Wände des Herzens zusammenziehen und dadurch das Blut in einer Richtung von den Vorhöfen (Atria) in die Herzkammern (Ventrikel) und weiter in den Blutkreislauf gepumpt wird. Im Gegensatz zu den Muskeln des Bewegungsapparates im Rest des Körpers ist das Herz nicht von Signalen aus dem Gehirn oder Nervensystem abhängig und erfüllt seine Aufgabe völlig eigenständig. Das elektrische Signal im Herzen entspringt dem Sinusknoten, einer Ansammlung hochspezialisierter Zellen, den Herzschrittmacherzellen, eingebettet in der oberen Wand des rechten Vorhofs. Die Herzschrittmacherzellen sind ebenfalls muskulären Ursprungs und besitzen die einzigartige Fähigkeit, elektrische Impulse eigenständig zu erzeugen. Man geht davon aus, dass spezielle Ionenkanäle und –pumpen dafür verantwortlich sind. Die in gleichmäßigen Abständen erzeugten elektrischen Impulse werden von den Schrittmacherzellen an die sie umgebenden normalen Herzmuskelzellen weitergegeben und verursachen damit eine Kontraktion des Herzmuskelgewebes. Diese Kontraktion verbreitet sich wellenförmig weiter, zuerst über die beiden Vorhöfe und schließlich die beiden Herzkammern. Dadurch wird das Blut von den Vorhöfen in die Herzkammern und von dort weiter in den Lungen- beziehungsweise Blutkreislauf gepumpt. Die Herzschrittmacherzellen diktieren die grundlegende Herzfrequenz. Diese kann aber je nach Bedarf des Körpers, zum Beispiel während körperlicher Anstrengungen, angepasst werden. Im Bereich des Sinusknotens liegen eine Vielzahl von Nervenendigungen des vegetativen Nervensystems, welche Botenstoffe absondern, die die Aktivität der Schrittmacherzellen und somit die Herzfrequenz beeinflussen können. Gegenstand dieser Doktorarbeit war es, den embryonalen Ursprung und die molekularen Grundlagen der Entwicklung der

Herzschrittmacherzellen zu untersuchen.
Die Lage der Schrittmacherzellen am „Eingang“ des Herzens, in der Schnittstelle zwischen dem rechten Vorhof und den venösen Blutgefäßen, gleicht sich bei Menschen, anderen Säugetieren und vielen, zum Teil weitaus primitiveren Tierarten. In Kapitel 1 beschäftigen wir uns mit der evolutionären Geschichte der Herzschrittmacherzellen. Wir geben einen Überblick über wichtige Faktoren in ihrer Entwicklung in verschiedenen Organismen. Die grundlegende Arbeitsweise und Regulierung der Schrittmacherzellen zeigte hierbei ein hohes Maß an Übereinstimmung zwischen den teilweise höchst verschiedenen Tierarten.
Zur Erforschung der Herz- und Herzschrittmacherzellentwicklung verwendeten wir den Zebrabärbling (auch Zebrafisch, lat. *Danio rerio*). Dieser kleine, tropische Süßwasserfisch ist ein gut etablierter Modellorganismus und wird bereits seit den 1980er Jahren als Versuchstier in der Genetik und Entwicklungsbiologie eingesetzt. Ihre Haltung unter Laborbedingungen ist sehr einfach und sie produzieren eine hohe Anzahl an Nachkommen. Die Embryonen der Zebrabärblinge entwickeln sich innerhalb nur weniger Tage zur Selbstständigkeit. Sie befinden sich dabei in Eiern außerhalb des Körpers der Mutter und sind zu Beginn fast komplett transparent. Sie eignen sich also hervorragend dazu, die Entwicklung und Funktion der Organsysteme, inklusive des Herzens, mit einfachen Mitteln zu beobachten. Nur etwa zwei Tage nach der Befruchtung des Eies ist das Herz des Embryos bereits voll funktionsfähig. Im Gegensatz zum vierkammrigen Herzen der Säugetiere, besteht das Herz eines Zebrabärblings lediglich aus zwei Kammern, einem Vorhof und einer Herzkammer, getrennt durch die Herzklappen. Bereits in diesem frühen Stadium zeigen sich kontrollierte, rhythmische Kontraktionen, die von der Öffnung des Vorhofs ausgehen. Die Herzfrequenz beträgt in diesem Stadium etwa 180-200 Schläge pro Minute.
In Kapitel 2 beschreiben wir die erstmalige Identifikation der Herzschrittmacherzellen in Zebrabärblingen. Sie gelang durch die Entdeckung, dass ein bestimmtes Gen nur in den Schrittmacherzellen, nicht aber in anderen Zellen des Herzens aktiv ist. Um die Aktivität des Gens sichtbar zu machen, wurde es mit einem fluoreszierenden Protein versehen. Schaltet die Zelle nun das markierte Gen an, so sorgt das fluoreszierende Markerprotein dafür, dass sich die gesamte Zelle grün färbt und somit sichtbar wird. Wir konnten dadurch einzelne potentielle Herzschrittmacherzellen isolieren und mittels Analyse ihrer charakteristischen elektrischen Aktivität zweifelsfrei nachweisen, dass es sich um Herzschrittmacherzellen handelte. Es war uns dadurch erstmals möglich, die Struktur und Lage der Schrittmacherzellen in Zebrabärblingen zu charakterisieren. Im Gegensatz zum kompakten Sinusknoten im Säugetierherz, sind die Schrittmacherzellen des Zebrabärblings in einem Ring rund um den Eingang des Vorhofs angeordnet. Inwieweit dies auch auf andere Wirbeltiere zutrifft und

womöglich eine evolutionäre Vorstufe zum kompakten Sinusknoten darstellt, bleibt zu ermitteln.

In unserem Fall handelte es sich um das Gen Islet-1. Dieses ist neben den Herzschrittmacherzellen auch in anderen Teilen des Körpers aktiv und das von ihm produzierte Protein ist dafür bekannt, als Transkriptionsfaktor zu agieren. Das bedeutet, dass seine Aufgabe darin besteht, durch meist direkte Bindung an den DNA Strang, die Aktivität anderer Gene zu beeinflussen und sie einzuschalten. Eine jede Zelle wird auch dadurch charakterisiert, welche Gene ihres Genoms an- oder ausgeschaltet sind. Somit kommt Transkriptionsfaktoren eine besondere Aufgabe zu. Wir zeigen, dass ein Defekt in der Gensequenz des Islet-1 Gens und somit der Verlust des Islet-1 Proteins in der Zelle zu schwerwiegenden Defekten in der Herzfunktion führt. Das Herz dieser Zebrabärblingembryonen zeigt starke Symptome einer Bradykardie, also einer stark verminderten Herzfrequenz. Im Laufe der weiteren Entwicklung verschlimmern sich diese Symptome zusehends und es kommt phasenweise zum völligen Erliegen der Herzfunktion. Bis zu 20 Sekunden lange Pausen konnten beobachtet werden. Die Embryonen konnten maximal bis zu 5 Tage nach der Befruchtung überleben. Dieser funktionale Defekt und die lokale Aktivität von Islet-1 ließ uns zu der Schlussfolgerung kommen, dass Islet-1 eine essentielle Rolle in der Entwicklung der Herzschrittmacherzellen innehat. Es bleibt allerdings weiterhin unklar, wie genau der Verlust von Islet-1 diese schwerwiegenden Defekte im Herzen auslöst und welche Funktion es in den Schrittmacherzellen im Detail ausführt.

In Kapitel 3 vertiefen wir die Analyse der Rolle von Islet-1. Wir konnten zeigen, dass die Herzschrittmacherzellen trotz des Defektes in Islet-1 an der korrekten Stelle des Herzens anwesend sind. Das heißt, der funktionale Defekt, den wir beobachten konnten, geht nicht auf einen Verlust der Schrittmacherzellen an sich zurück, sondern vielmehr auf deren Unvermögen ihre normale Funktion auszuführen. Wir konnten daraufhin mehrere Gene identifizieren, die durch den Verlust von Islet-1 in den Schrittmacherzellen nicht eingeschaltet werden konnten. Es ist deshalb davon auszugehen, dass diese Gene unter der Kontrolle von Islet-1 stehen. Welche Rolle diese und weitere Faktoren in der Entwicklung der Herzschrittmacherzellen spielen, bleibt der Gegenstand aktueller Forschung. Ferner konnten wir zeigen, dass das ausgewachsene Herz des Zebrabärblings von unzähligen Nervensträngen durchzogen wird. Wir gehen davon aus, dass es sich hierbei um Nervenenden des vegetativen Nervensystems handelt.

In Kapitel 4 wenden wir uns einem, erst vor Kurzem entwickelten Verfahren zu, welches es uns erlaubt, die Aktivität aller Gene in einem Gewebe zu analysieren und räumlich zuzuordnen. Dieses Verfahren ist unter dem Namen Tomo-Sequenzierung (engl. *tomo-sequencing*, kurz *tomo-seq*) bekannt. Hierbei wird ein Organ oder

Gewebe, im vorliegenden Fall das embryonale Herz, mittels präziser Schnitte in einzelne hauchdünne Scheiben zerlegt, ohne dabei aber die Information der räumlichen Struktur zu verlieren. Dies ähnelt den Schnittbildern einer Tomografie. Anschließend wurde das genetische Material aus den einzelnen Gewebescheiben isoliert und analysiert. Hierbei kann die Aktivität einzelner Gene ermittelt werden. Ist ein Gen in einer Zelle aktiv, werden zur Proteinproduktion Abschriften der Gensequenz, sogenannte Boten-RNA Stränge produziert. Diese Boten-RNA Stränge enthalten die Bauanleitung des jeweiligen Proteins. Sie sind nicht sehr stabil und werden in der Zelle nach kurzer Zeit wieder abgebaut. Ist eine solche Boten-RNA also in der Zelle anwesend, deutet dies darauf hin, dass das betreffende Gen zurzeit angeschaltet und aktiv ist. Außerdem kann die Anzahl an Boten-RNA Strängen darauf hindeuten, wie sehr das zu produzierende Protein in der Zelle benötigt wird. Proteine, die für eine Zelle sehr wichtig sind, werden oft in sehr hoher Zahl und Frequenz produziert und ihre Boten-RNA ist ebenfalls in großer Menge vorhanden. Die Gesamtheit der in einer Zelle hergestellten Boten-RNA Stränge wird auch als das Transkriptom der Zelle bezeichnet. Wir konnten die Menge an Boten-RNA für jedes einzelne Gen des Genoms in jeder einzelnen Gewebescheibe ermitteln.

Zwei Tage nach der Befruchtung ist das Herz des Embryos eine s-förmige Röhre, an der man bereits die beiden Kammern erkennen kann. Nachdem wir das Herz aus dem Körper herausgetrennt hatten, wurde es von einem Ende der Röhre zum anderen in Scheiben geschnitten. Da die Reihenfolge der Gewebescheiben bekannt war, konnte die Information der Genaktivität problemlos räumlich zugeordnet werde. Dadurch war es uns möglich, erstmals eine detaillierte „Karte“ der lokalen Aktivität aller Gene des Genoms im embryonalen Herzen zu erstellen. Dies erwies sich als äußerst nützliche Ressource für die Analyse bestimmter Regionen des embryonalen Herzens. So konnten wir zum Beispiel mehrere Gene identifizieren, die nur in einer der sich entwickelnden Kammern aktiv waren. Darüber hinaus gelang es uns, das Transkriptom der Region, in der sich die Schrittmacherzellen befinden, genauer zu analysieren. Dabei konnten wir erstmals zeigen, dass ein wichtiger Signalweg (Wnt) in den Herzschrittmacherzellen aktiv ist. Durch weitere Analyse stellte sich heraus, dass dessen Aktivität nötig ist, um eine Kontrolle der Herzfrequenz durch das vegetative Nervensystem zu ermöglichen. Wird der Wnt Signalweg ausgeschaltet, kann das Herz nicht mehr durch das vegetative Nervensystem kontrolliert werden und die Herzfrequenz ist konstant erhöht.

In Kapitel 5 beschreiben wir die Entdeckung eines zuvor unbekannten Syndroms, welches mehrere Symptome, die charakteristisch für einen Defekt in den Schrittmacherzellen sind, vereint. Dieses unter dem Namen CAID (Abkürzung für engl. *Chronic Atrial and Intestinal Dysrhythmia*) beschriebene Syndrom wurde erstmals in einer kleinen Patientengruppe in Kanada identifiziert. Die Patienten

litten an einem stark verlangsamten und irregulären Herzschlag, was durch die Implantation eines künstlichen Herzschrittmachers behandelt wurde. Des Weiteren zeigte der Darm der Patienten keine oder eine zumindest stark verminderte Peristaltik. Das heißt, sie waren nicht in der Lage, Nahrung mittels Muskeltätigkeit durch den Darm zu transportieren, was eine lebenslange intravenöse Nährstoffversorgung erforderlich machte. Durch genetische Analyse konnte nachgewiesen werden, dass dem CAID Syndrom eine einzige Veränderung in der Sequenz des Gens SGOL1 zu Grunde liegt. Wir konnten diese Symptome durch gezieltes Inaktivieren von Sgol1 in Zebrabärblingen reproduzieren und somit den Kausalzusammenhang belegen. Auf den ersten Blick scheint eine Kombination aus funktionalem Herz- und Darmdefekt ungewöhnlich. Allerdings sind die Muskelbewegungen des Darms ebenfalls von eigenen Schrittmacherzellen abhängig und unterliegen nicht der willkürlichen Kontrolle des Gehirns. Die genaue Rolle und Wirkweise von Sgol1 bleibt bisher unklar. Wir spekulieren jedoch, dass es in Verbindung mit der grundlegenden Funktion der Schrittmacherzellen steht und ein Gendefekt sich daher sowohl auf Herz- als auch auf Darmschrittmacherzellen auswirkt.
Im abschließenden Kapitel 6 folgt eine allgemeine Diskussion der vorgestellten Forschungsergebnisse. Diese sollen hierbei in einem breiteren Kontext besprochen und bewertet werden.

ACKNOWLEDGEMENTS

„Was lange währt, wird endlich gut." – A German proverb roughly translating to: Sometimes it might take a while, but it will all be worth it in the end. Quite fitting I think. When I first moved to the Netherlands in 2009, I was planning to stay for just 2 years to earn my Master's degree. Thanks to this PhD-adventure, 2 turned into 8 and a half years. Over the years I had the pleasure to meet, work with and befriend lots of people. You have played a major part in turning these years into what they are – a fun and memorable part of my life. Thank. You. All!

Jeroen, who else to start these acknowledgments with? Thank you very much for letting me join your lab – repeatedly. For the guidance throughout my time in the lab, the constructive criticism and encouragement that helped me to always become a little better at what I'm doing. I remember how, when I was looking for a lab to do my Masters internship in before even setting foot into this country, I found your website and thought it sounds pretty cool what they are doing. This first impression proved to be just right. It's true that your door is always open for us, even though it sometimes takes 3-4 tries to actually find you. It's clearly not just science that's on your mind, but also what's in the best interest of each and every one in your lab and that makes for a truly great working atmosphere. Thank you!

I would like to thank all the members of my reading and defence committee for taking the time to assess my thesis. My two sidekicks on this special day, **Stefan** and **Sonja**, thank you for agreeing to be my paranimfen!

Over the years many people joined and left the Bakkers lab and there is really no specific order in thanking you other than chronology. You are all awesome! Often, we take it for granted how much fun we have and how easy it is to work together in the lab. If you spend as much time at work as we scientist often do, it is awesome that your colleagues are not "just" colleagues but actually friends. Maybe that's why so many of us stay much longer than initially planned ;)

Sonja, what would the Bakkers lab be without you? Chaos and anarchy (kind of), at least that's what happens when you go on holiday… You were the first person from the lab I met and initially even my supervisor when I was just a fresh young Masters student (yeah, a long time ago…). You introduced me to the zebrafish work and taught me many of the essential protocols I'm still using almost every week. It's no surprise I insisted to get the lab bench next to yours when we moved upstairs, clear advantage of location. I'm still amazed how you manage to know exactly where

everything is in the lab. We always have lots of fun in and outside of the lab. I still remember the hilarious lab trip to Germany for Fabian's wedding. Or the many lab uitjes and retreats (Pictionary!) we went on. I never really had to question myself who from the lab I want to ask to be my paranimf. Easy decision and I'm very glad you accepted and will be sitting right behind me when I defend this thesis.

Anne, even though it wasn't the initial match plan, you adopted me as your student during my first internship and it was so much fun! Thanks for introducing me to the importance of the vrijdagmiddagborrel. But oh my god all of those in situs… The grant I eventually got from the Graduate School to do my PhD was awarded mainly due to performance during the first internship and you had a great deal to do with that. In the end, our PhDs overlapped by exactly 2 weeks before you and Wanda moved to Australia. I wish you all the best!

Fede, that guy wearing pink shoes in a lab with 8 women – at least that was my initial impression when I first started… By now there is a much more even distribution, but you are still the best one to talk to about football, well, as long as it's not Italy vs. Germany ;). I was very fortunate to start my PhD at the time you were working on the Islet-1 story. Not just did I managed to sneak onto a paper very early on in my project but I also learned the painstaking process of publishing it. We got to set up the high-speed imaging (I'm still using your excel sheet!). Little did I know how much time I would be spending on counting kymographs over the next few years… I learned so much from you and I bet all your former students will agree that you are an exceptionally good supervisor and teacher. The lab is lucky to have you and with everyone eventually leaving you and Sonja are the backbone. And PS: your cocktails and Italian food are amazing! And I'll probably always have to think of you when they play Mister Bombastic.

Ina, at one point the Bakkers lab was half German, we really are everywhere... However, you did a much better job integrating here with Allard and your two Dutch kids. You were the lab's social butterfly, which was especially useful when the boss sent you and the two introverts to a conference in strange, strange America. We had the same opinion on sweatpants-Sunday, cause even though you are at work, it's still the weekend. You are still my hero for joining for another beer after actually breaking your hand at the Christmas party. But hey, 7 beers equal a meal, right?! I'll never forget the karaoke night with our incredibly German interpretation of "The Ring of Fire".

Emma, our time in the Bakkers lab only overlapped for a short time during my internship. But you started the Isl1 project and your PhD thesis is the one I consulted by far the most. **Kelly**, you also left the lab shortly after I started my internship. But I still remember (and use) the trick you told me to stay awake during your after-lunch dip in meetings (grocery shopping list!). **Marah**, also a lab member during my

internship days. I remember you being constantly busy mapping mutants. Oh and of course how you managed to “drive” home a traffic cone under your car.

Emily, what can I say, you are a great friend and a great scientist. When we first met you were a starting postdoc and I was a first year Master student. Now I’m defending my thesis and you are a PI with your own lab and maybe even part of my defence committee. Though I still mostly remember you for your postdoc years ;) Working hard but always up for a Friday beer (vier uur – bier uur!) and a likeminded partner in crime for anything borrel-related. The bike shed pool borrel, the pizza plus ice cream evening, photocopying faces - just to name a few… I always got good advice from you and I’m glad you were around for most of my PhD. I enjoyed the discussions we had, about anything, from science to politics to Wayne Rooney’s hair transplant. When you left us, the lab not only lost its delightful British touch but also the main organiser of Bakkers lab social events. You were always all for people coming over for spontaneous drinks and parties. Even though someone ended up stealing your cat’s toys… (Sorry!!). I’m glad you found your place in Sheffield and that your own lab is running well. I’m sure it’ll just get better and better in the future. I hope I get to visit you there again soon, for a pint, some cheesy chips and of course to say hello to Suffie ;)

Fabian, you were the first one to join the lab after I started. After having been the only PhD student (who can imagine that now) and alone with the postdocs, it was really nice to have someone to share the joy and pain of PhD-ing with. Plus, being infinitely more organized, you saved me from missing CSnD program deadlines more than once. Thanks for being the German stereotype when I wasn’t ;) But hey in the end I think I even saw you dance once… I wish you, Elli and Antonia all the best, in Munich or somewhere else, I’m very sure you’ll find your place. Aber es bleibt dabei: Fassenacht >>> Karneval!

Mel, you never had it easy working on brain-stuff in a heart-stuff lab. But you taught us a lot about aneurysms and the fact that there is such a thing as a brain bank. If something is important to you, like the environment and sustainability, you (and Jelle) go for it and that passion is quite inspiring. You make sure people around you are happy, by baking amazing cookies or sneaky cuddles. The latter exponentially increasing in frequency with each beer. We share an affection for Brezeln and what could be better than that. I hope I’ll get to come back for your defence soon. Good luck with finishing your book, I’m sure you’ll do a great job. And thanks for the Dutch translation support, I literally couldn’t have done it without you.

Lotte, probably one of the most organized people I know. Your desk is a stark contrast to mine, well, everyone else’s really. FYI, I know it’s you who keeps moving my E3 bottle back to my lab bench every time… You have become the Bakkers group’s master of high-speed imaging (joy!) and gave all of us trust issues with your

Photoshop skills. I'm very glad we got to share an office after moving to the 2nd floor. Until recently you were the only Dutchie in our office and had to patiently explain and translate a lot for us. Thank you for saving me from having to trust google translate with my Dutch summary. I can't believe it's already been almost 4 years and you are also planning and starting to write your book now. I wish you all the best and lots of patience finishing up those last experiments. And I'm sorry for all the blasphemy, I just can't help it sometimes. Still friends, right?

Sven or Sveni, I can't believe I'm saying it, but I'll for sure miss your man-jokes. So predictable and just slightly creepy. And of course, the lunch time discussions about cars, (bad) music, ginger babies and mankinis… By now I've even given up on convincing you that I don't actually like Scooter. Someone just made that up (cheers, Em). Well, so be it, I'm still glad we have our own Bakkers group DJ around. We once did the R-course together, but your learning curve was clearly steeper than mine. So, thanks for all the R support, much needed and appreciated! By now you are almost the only one in the group flying the flag for truly fundamental research in developmental biology. Good luck with all these exploding 2-cell stage embryos and tomo-seq adventures. I'm already looking forward to your PhD graduation, can we touch your hair again?

Laurence, you are such a good addition to our lab and of course the girls' office. So many good laughs! But also in a strictly scientific way, it was great for me to finally have someone working on the same topic. We had many good discussions and got to share the frustration of non-working antibodies and shitty in-situ probes. Apart from that we share a, let's say limited appreciation for the Dutch weather (moved here by choice, moved here by choice…). Also, my knowledge of French swear words has increased enormously and who knows when that might come in handy, merci beaucoup! You always volunteered your place for Bakkers lab parties and there surely were some memorable evenings. Plus, you got the whole lab to get into yoga, who would have thought…? You are just super fun to be around and an endless source of entertainment, sometimes more, sometimes less intentionally. I'll definitely miss that. Stay awesome and thanks for being the backup ;)

Dennis, you are so full of enthusiasm for your project or anything sciency. When you started you were kind of like an excited puppy and you had enough plans for about 5 PhD projects. You didn't let all the grumpy old lab members kill that enthusiasm and I hope you never lose your passion for science. Though I'm glad you lost the Justin Bieber hair cut ;) Good luck analysing the one million tomo-seq experiments you did. Just never ever forget the cookies for lab meeting again!

Sarah, I'd say you are just about the right amount of crazy, a perfect fit for our office. Thanks (mostly) to you we really live up to our reputation - "there is always chocolate/cookies/candy in the girls' office!". And I'm not complaining. Thanks for

being an endless source of cat memes whenever someone needs some cheering up. Please keep it up! You took over the sgol1 project from me just when it started to get really complicated. But I'm sure you'll make it work, just don't stress yourself out too much. See I didn't even make a joke about your height, because that would have been too obvious, eh?

Phong, the best Australian accent around! I'm still not entirely sure what you are exactly up to in the lab… What was that enormous tub of liquid silicon for?? I always got good input from you during meetings and discussions. You lived up to your reputation as a great scientist, but your "performance" at the Oktoberfest proved you are also just human… I hope someday you'll catch them all! And I hope you manage to see all the castles of Europe during your time here. Let me know if you are ever in the neighbourhood, I'll buy you a pastry, or six.

Yeszamin, you only joined the Bakkers lab recently and secured the last spot in the infamous girls' (a.k.a. cat) office. Even though it means I now have to contain my chaos on just one desk, I'm glad we are desk-neighbours. You clearly are a very lively addition and just about the most direct person I have met so far. Your impact in the lab is already clear, our fish have never been this organized. It does indeed make our work a lot easier.

Hessel, at present the lab youngster, I'm glad you liked your internship so much that you decided to stay for the big adventure. Outplaying everyone at bubble football was a good start I guess. Good luck with your PhD. I'm sure at some point your fish will actually survive the cryo injury ;)

Over the years quite a few students have been part of the Bakkers group during their internship. I got to supervise four of them during their research projects. **Babette**, **Lynn**, **Reijer** and **Morgan** thanks for all your enthusiasm and all the work you did. I also learned a lot about myself being on the side of the supervisor but above all it was a lot of fun. And **Reijer**, thanks for the awkward turtle move, it still lives on in the lab…

Back in the day, for the first half of my PhD, the Bakkers lab was at home on the first floor. We got to share our office and lab space with the ever-growing van Rheenen lab. **Eve**, **Anoek**, **Saskia**, **Laila**, **Anko**, **Sander**, **Arianna**, **Danielle**, **Carrie**, even though our office clearly wasn't made for 9 people it was a delight to have you as neighbours. Luckily Romke could ensure us that there was enough oxygen in the room even when the temperature was closing in on 30°C. Ever since moving one floor up we have a lot more space, no one talks about tumors anymore and we have even more candy in the office now. Nevertheless, I'm glad I didn't miss out on the Bakkers-van Rheenen group friendship/rivalry (we won the bowling!!). Except of course for that fridge, nobody will miss that nasty fridge. To those still around, good luck at the NKI, a sad loss for the Hubrecht.

Moving to the second floor didn't just give us more office and lab space, we also got lovely new neighbours. With the den Hertog lab we share the love-hate relationship with the zebrafish. Especially, **Alex**, **Miriam**, **Jelmer**, **Sasja**, **Maja** and **Petra** it's great to have you around, in and outside of the institute. Clearly, we have more in common than just fish ;). I wish you all the best with your projects and always lots of eggs! Alex, when we first met you had a completely scratched face and the infamous goatee. I'm glad you managed to overcome both. As I write this your PhD defence is exactly one week away and I'm sure you'll do great. I'm looking forward to the party, beer-commander-style!

During the first year of my PhD I joined the PV and it was one of the best decisions. I got to know lots of people around the institute and of course had lots of fun organising borrels, parties and so on. **Anoek**, **Joppe**, **Roel**, **Manda** and **Wensi,** cheers to the glorious PV of 2012, to great borrels and after-borrel beers at the Cambridge bar, to star-gazing on top of the bike shed and to zebrafish embryo-shaped salads. It was a great year. Last fossil out!

The Hubrecht has been a great place to work for the past few years. **Britta**, **Alex**, **Dorien**, **Eirinn**, **Frans-Paul**, **Maaike**, **Tamara**, **Petra**, **Paul**, **Geert**, **Annabel**, **Kay**, **Chloé**, **Leon**, **Rob, Anna, Ismaël** and many more. Thank you for all the borrel fun, chats at the coffee machine and general gezelligheid!

A big thank you to all the people "behind the scenes" who keep the institute running smoothly. Particularly the guys from the Civiele dienst and IT as well as the ladies at the reception, especially **Thea**. Thank you **Anko** for solving all of our microscope problems. **Mark**, **Erma**, **Rob**, **Luuk**, **Bert** and the other animal care takers who take excellent care of our precious fish, thank you! The final months of a PhD comes with a sharp increase in bureaucracy and lots of paper work, thank you **Litha** for helping me navigate through it and ensuring neither me nor Jeroen miss any deadlines.

The PhD-life can be great fun but also full of frustration. I'm glad I got to be part of a very likeminded "support group". **Suzanne**, **Joppe**, **Bilge** and **Inge** our regular evenings of dinner and beers to share each other's agony and annoyance with failed experiments, endless weekend work and not-so-helpful supervisors were (and still are!) a very welcome relief from day-to-day PhD life. It really helps to put things into perspective when you hear that everyone else is dealing with the same, or worse shit. Now that we have all graduated, or are at least close to it, I really hope we can keep our group alive, even across borders!

Starting a PhD also came with the pleasant introduction of a regular salary. **Suzanne** and **Elke**, our first salary party was hands down the best way to invest a month worth of work! Even though that place we rented was sliiiightly shady. Our chaotically awesome trips to Berlin and New York were an absolute highlight too. We all need more boozy milkshakes in our lives! Elke, by some funny coincidence you moved to

my old hometown to finish your PhD. We should have some wine (or IMB vrijmibo) in Mainz again soon. Suzanne, partner in crime during all those CSnD Master classes and retreats, you know what I mean. You also introduced me to so many Dutch things. To name a few: Koninginnedag (still have the cat mask), dodgy music (camping disco anyone?), Ekko parties (ze collapsing German speaking) and I even ended up cheering on the Dutch football team – in a very orange shirt (whoa!). We started our PhDs on the same day, so soon it'll be time for a last salary party, right?! Maybe with that strange Dutch liquor that colours your tongue purple, I vaguely remember this… Good luck to the both of you finishing your PhDs. I'm looking forward to the celebrations!
Sofia, I think you are my oldest friend here in the Netherlands. We are the last survivors of the UU Summer School '09 group. Ever since that first Dutch class we have kept in touch and I hope that won't change. Thanks for being a perfect tour guide around Porto, so many amazing pastries! Both of us stayed here a lot longer than we first planned but I guess it has definitely paid off. I hope to see you again soon for a coffee and a chat!
Lisa and **Yustin**, thanks for being such nice flat mates in the early times of my Dutch adventure.

Danke auch an meine Familie und Freunde zuhause in Deutschland. Zwar sehe ich die meisten von euch nur noch an Weihnachten, runden Geburtstagen oder zu den alljährlichen Weinfesten, aber es ist immer wieder ein sehr willkommener Grund für Kurzurlaube in der Heimat.
Julia, **Hannah** und **Jasmin**, danke dass ihr es mir nie übelnehmt, dass ich mich erst ins Ausland verdrücke und dann auch noch ewig nicht melde. Ich hoffe wir sehen uns in Zukunft wieder regelmäßiger!

Stefan, Stevie, Herr Ingenieur, ich bin froh und stolz dich als immer fröhlichen kleinen Bruder zu haben und dass du mich bei meiner Verteidigung als einer meiner Paranimfen unterstützt. Jetzt wohne ich schon so lange nicht mehr in der Heimat, da ist es besonders schön wenn sich jemand immer so von Herzen freut wenn man mal zu Besuch kommt. Das gilt natürlich auch für dich **Ina**, bist du doch aus unserer Familie auch nicht mehr wegzudenken. Vielen Dank für das professionelle Fotoshooting für mein Coverfoto. Es schmückt meine Doktorarbeit doch ausgesprochen gut.

Zu guter Letzt **Mama** und **Papa**, ihr beiden seid für mich die besten Vorbilder, Unterstützer und Ratgeber die ich mir hätte wünschen können. Mein Interesse an Naturwissenschaften war sicher in jeglicher Hinsicht keine Überraschung, wollte ich doch schon immer am liebsten mit allerlei Getier, dem Mikroskop oder meinem

Chemiebaukasten spielen. Dass ich jetzt (auch) zum Doktor werde ist dann doch auch irgendwie eure Schuld ;). Es ist definitiv viel Wahres dran, dass nur wer sich starken und sicheren Wurzeln gewiss ist, wirklich frei in die Welt hinausfliegen kann. Euer liebevoller und entspannter Erziehungsstil hat einen Großteil dazu beigetragen und ich komme immer gerne nachhause. Danke, dass ihr mir oft mehr zu- und vertraut als ich mir selbst. Danke, dass ihr mich oft einfach mal machen lasst und immer der wohlbehütete Heimathafen seid. Auch wenn das bedeutet, dass ich ans andere Ende der Welt ziehe, oder eben nur ins unbekannte Nachbarland. Papa, du bist mir ein Vorbild darin, das Leben und sich selbst nicht immer zu ernst, sondern optimistisch und mit einer ordentlichen Portion Humor zu nehmen. Dabei aber auch die eigenen Prinzipien nicht allzu schnell über Bord zu werfen. Mama, du zeigst mir, dass es auch Realismus und Hartnäckigkeit braucht um erfolgreich zum Ziel zu kommen. Danke für alles!

„Im Grunde sind es immer die Verbindungen mit Menschen, die dem Leben seinen Wert geben.“
(Wilhelm von Humboldt)

Silja

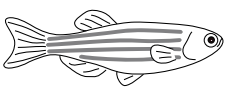

&

LIST OF PUBLICATIONS

Burkhard, S.*, Garric, L.*, & Bakkers, J. (2017) Islet-1 regulation in pacemaker cell development and function.
In preparation

Burkhard, S. & Bakkers, J. (2017) Spatially resolved RNA-sequencing of the embryonic heart identifies a role for Wnt/β-catenin signaling in autonomic control of heart rate.
submitted

Burkhard, S., van Eif, V., Garric, L., Christoffels, V. M., & Bakkers, J. (2017) On the Evolution of the Cardiac Pacemaker*. J. Cardiovasc. Dev. Dis.* 2017, 4(2), 4.

Chetaille, P.*, Preuss, C.*, **Burkhard, S.***, Cote, J. M., Houde, C., Castilloux, J., Piche, J., Gosset, N., Leclerc, S., Wunnemann, F., Thibeault, M., Gagnon, C., Galli, A., Tuck, E., Hickson, G. R., El Amine, N., Boufaied, I., Lemyre, E., de Santa Barbara, P., Faure, S., Jonzon, A., Cameron, M., Dietz, H. C., Gallo-McFarlane, E., Benson, D. W., Moreau, C., Labuda, D., FORGE CANADA Consortium, Zhan, S. H., Shen, Y., Jomphe, M., Jones, S. J., Bakkers, J. & Andelfinger, G. (2014). Mutations in SGOL1 cause a novel cohesinopathy affecting heart and gut rhythm. *Nat Genet*, 46(11), 1245-1249.

Tessadori, F., van Weerd, J. H.*, **Burkhard, S. B.***, Verkerk, A. O., de Pater, E., Boukens, B. J., Vink, A., Christoffels, V. M., & Bakkers, J. (2012). Identification and functional characterization of cardiac pacemaker cells in zebrafish. *PLoS One*, 7(10), e47644.

Lagendijk, A. K., Goumans, M. J., **Burkhard, S. B.**, & Bakkers, J. (2011). MicroRNA-23 restricts cardiac valve formation by inhibiting Has2 and extracellular hyaluronic acid production. *Circ Res*, 109(6), 649-657.

Rathke, C., Barckmann, B., **Burkhard, S.**, Jayaramaiah-Raja, S., Roote, J., & Renkawitz-Pohl, R. (2010). Distinct functions of Mst77F and protamines in nuclear shaping and chromatin condensation during Drosophila spermiogenesis. *Eur J Cell Biol*, 89(4), 326-338.

** Equal contribution*

&

CURRICULUM VITAE

Silja Burkhard was born on the 4th of March 1986 in Mainz, Germany. She grew up in Monsheim, a small town in the countryside of southern Rhine-Hesse. After receiving her high school diploma (Abitur) from the Elisabeth-Langgässer-Gymnasium in Alzey in 2005, she decided to study biology at the Philipps-University in Marburg. She wrote her bachelor thesis in the lab of Prof. Renkawitz-Pohl working on drosophila spermatogenesis. In the Summer of 2008, she moved to Dunedin on the southern island of New Zealand to study Anatomy and Structural Biology at the University of Otago. She graduated with a Postgraduate Diploma in Science in July 2009. Soon after, Silja decided to move to the Netherlands and enrol in the “Cancer, Stem cells and Developmental Biology” Master’s program at Utrecht University. She spent her major research internship in the lab of Jeroen Bakkers at the Hubrecht Institute where she was working on the role of microRNAs in zebrafish heart development. For the minor internship, she joined the lab of Jacqueline Jacobs at the Netherlands Cancer Institute (NKI) in Amsterdam. After receiving her Master’s degree (*cum laude*) in November 2011 she decided to return to the Bakkers lab to start her PhD working on the development of the cardiac pacemaker cells in zebrafish. The results of this research are described in this thesis.